University of Novi Sad
FACULTY OF TECHNICAL SCIENCES
DEPARTMENT OF PRODUCTION ENGINEERING
21000 NOVI SAD, Trg Dositeja Obradovica 6, SERBIA

UDK 621 ISSN 1821-4932

JOURNAL OF

PRODUCTION ENGINEERING

Volume 18 Number 1

Novi Sad, June 2015

Journal of Production Engineering, Vol.18 (2015), Number 1

Publisher: FACULTY OF TECHNICAL SCIENCES
DEPARTMENT OF PRODUCTION ENGINEERING
21000 NOVI SAD, Trg Dositeja Obradovica 6
SERBIA

Editor-in-chief: *Dr.* Pavel Kovač, *Professor, Serbia*

Reviewers:
Dr. Janko HODOLIČ, *Professor, Serbia*
Dr. Marin GOSTIMIROVIĆ, *Professor, Serbia*
Dr. František HOLEŠOVSKY, *Professor, Czech Republic*
Dr. Dušan JEŠIĆ, *MTM Academia, Serbia*
Dr. Janez KOPAČ, *Professor, Slovenia*
Dr. Pavel KOVAČ, *Professor, Serbia*
Dr. Mikolaj KUZINOVSKI, *Professor, Macedonia*
Dr. Ildiko MANKOVA, *Professor, Slovak Republic*
Dr Snežana RADONJIĆ, *Professor, Serbia*
Dr. Branko ŠKORIĆ, *Professor, Serbia*
Dr. Ljubomir ŠOOŠ, *Professor., Slovak Republic*
Dr. Wojciech ZEBALA, *Professor, Poland*
Dr. Miodrag HADŽISTEVIĆ, *Professor, Serbia*
Dr. Milenko SEKULIĆ, *Assoc. Professor, Serbia*
Dr. Slobodan TABAKOVIĆ, *Assoc. Professor, Serbia*

Technical treatment and design: *M.Sc.* Borislav Savković, *Assistant*

Manuscript submitted for publication: June 30, 2015.
Printing: 1st
Circulation: 300 copies

CIP classification:

CIP – Катаголизација у публикацији
Библиотека Матице српске, Нови Сад

621

JOURNAL of Production Engineering / editor in chief Pavel Kovač. – Vol. 12, No. 1 (2009)- . – Novi Sad : Faculty of Technical Sciences, Department for Production Engineering, 2009-. – 30 cm

Dva puta godišnje (2012-). Je nastavak: Časopis proizvodno mašinstvo = ISSN
0354-6446
ISSN 1821-4932

Printing by: FTN, Graphic Center ***GRID,*** *Novi Sad*

ISSN: 1821-4932

INTERNATIONAL EDITORIAL BOARD

Dr. Joze BALIĆ, *Professor, Slovenia*
Dr. Marian BORZAN, *Professor, Romania*
Dr. Konstantin BOUZAKIS, *Professor, Greece*
Dr. Miran BREZOČNIK, *Professor, Slovenia*
Dr. Ilija ĆOSIĆ, *Professor, Serbia*
Dr. Pantelija DAKIĆ, *Professor, Bosnia and Herzegovina*
Dr. Numan DURAKBASA, *Professor, Austria*
Dr. Katarina GERIĆ, *Professor, Serbia*
Dr. Marin GOSTIMIROVIĆ, *Professor, Serbia*
Dr. Janko HODOLIČ, *Professor, Serbia*
Dr. František HOLEŠOVSKY, *Professor, Czech Republic*
Dr. Juliana JAVOROVA, *Professor, Bulgaria*
Dr. Vid JOVIŠEVIĆ, *Professor, Bosnia and Herzegovina*
Dr. Janez KOPAČ, *Professor, Slovenia*
Dr. Borut KOSEC, *Professor, Slovenia*
Dr. Mikolaj KUZINOVSKI, *Professor, Macedonia*
Dr. Miodrag LAZIĆ, *Professor, Serbia*
Dr. Stanislav LEGUTKO, *Professor, Poland*
Dr. Chusak LIMSAKUL, *Professor, Thailand*
Dr. Vidosav MAJSTOROVIĆ, *Professor, Serbia*
Dr. Ildiko MANKOVA, *Professor, Slovak Republic*
Dr. Miroslav RADOVANOVIĆ, *Professor, Serbia*
Dr. Mirko SOKOVIĆ, *Professor, Slovenia*
Dr. Antun STOIĆ, *Professor, Croatia*
Dr. Peter SUGAR, *Professor, Slovak Republic*
Dr. Katica ŠIMUNOVIĆ, *Professor, Croatia*
Dr. Branko ŠKORIĆ, *Professor, Serbia*
Dr. Ljubomir ŠOOŠ, *Professor, Slovak Republic*
Dr. Ljubodrag TANOVIĆ, *Professor, Serbia*
Dr. Wiktor TARANENKO, *Professor, Ukraine*
Dr. Marian TOLNAY, *Professor, Slovak Republic*
Dr. Gyula VARGA, *Professor, Hungary*
Dr. Milan ZELJKOVIĆ, *Professor, Serbia*
Dr. Miodrag HADŽISTEVIĆ, *Professor, Serbia*
Dr. Igor BUDAK, *Assoc. Professor, Serbia*
Dr. Ognjan LUŽANIN, *Assoc. Professor, Serbia*
Dr. Milenko SEKULIĆ, *Assoc. Professor, Serbia*
Dr. Slobodan TABAKOVIĆ, *Assoc.Professor, Serbia*
Dr. Đorđe VUKELIĆ, *Assoc. Professor, Serbia*
Dr. Aco ANTIĆ, *Assist. Professor, Serbia*
Dr. Sebastian BALOŠ, *Assist. Professor, Serbia*
Dr. Arkadiusz GOLA, *Assist. Professor, Poland*
Dr. Dejan LUKIĆ, *Assist. Professor, Serbia*
Dr. Mijodrag MILOŠEVIĆ, *Assist. Professor, Serbia*

Editorial

The ***Journal of Production Engineering*** *dates back to 1984, when the first issue of the* ***Proceedings of the Institute of Production Engineering*** *was published in order to present its accomplishments. In 1994, after a decade of successful publication, the Proceedings changed the name into Production Engineering, with a basic idea of becoming a Yugoslav journal which publishes original scientific papers in this area.*

In 2009 year, our Journal finally acquires its present title - ***Journal of Production Engineering****. To meet the Ministry requirements for becoming an international journal, a new international editorial board was formed of renowned domestic and foreign scientists, refereeing is now international, while the papers are published exclusively in English. From the year 2011 Journal is in the data base COBISS and KoBSON presented.*

The Journal is distributed to a large number of recipients home and abroad, and is also open to foreign authors. In this way we wanted to heighten the quality of papers and at the same time alleviate the lack of reputable international and domestic journals in this area.

In this journal are published, reviewed papers from International Conference "ETIKUM 2015" which was in Novi Sad, Serbia and certain number of new scientific papers as well.

Editor in Chief

Professor Pavel Kovač, PhD,

Journal of Production Engineering
Vol.18 No.1

Contents

ORIGINAL SCIENTIFIC PAPER

Journal of Production Engineering
Vol.18 No.1
JPE (2015) Vol.18 (1) Original Scientific Paper
K.Vijaya Kumar, N.Ramanaiah, N. Bhargava Rama Mohan Rao,
B.Srinivasa Prasad.

MICROSTRUCTURAL AND MECHANICAL PROPERTIES OF SHIELDED METAL ARC WELDED JOINTS

Received: 27 May 2015 / Accepted: 25 June 2015

Abstract: *Experiments have been carried out to investigate the characterization, micro hardness and impression creep on SMAW SA 516 GR 70 steel plates for the samples. The specimen was prepared by slicing the weldment into a single specimen which contains three zones (PM, HAZ and FZ). The cross-section of the specimen is 35 mm x 15 mm sample was investigated for all the above experiments. Impression creep behavior of samples was studied using tungsten carbide indenter at various stress levels in different temperatures ranges. From the creep profiles the steady state creep rates (ε_s) were calculated. Further stress exponent and activation energy values were determined. Creep rates for PM, HAZ and FZ are compared. Results on impression creep behavior suggest that creep resistance of fusion zone is superior to those for PM and HAZ at all stress levels in any temperature of testing. It is observed that creep rate measurement over the weldment. Dislocation creep mechanism seems to be dominating the impression creep process under the conditions of present investigation.*
Key words: *Creep, shielded metal arc welding, micro hardness.*

Mikrostrukturna i mehanička svojstva zavarenih spojeva. *Eksperimenti su sprovedeni da bi se istražila karakterizacija, mikro tvrdoća i otisak puzanja na uzorcima od čeličnih ploča oznake SMAW SA 516 GR 70. Uzorak je pripremljen obradom zavarenog spoja koji sadrži tri zone (AM, ZUT i FZ). Poprečni presek ispitivanog uzorka u svim eksperimentima je (35 x 15)mm. Ispitivanje uzorka na otisak puzanja izvršeno je koristeći volframkarbid utiskivač na različitim nivoima pri različitim temperaturama. Izračunata su stabilna stanja profila puzanja (ε_s). Određene su vrednosti eksponenta puzanja i energije aktivacije. Upoređene su stope puzanja za PM, ZUT i FZ. Pri ispitivanju otiska puzanja rezultati pokazuju da je otpor u zoni vara superioran u odnosu na PP i ZUT na svim nivoima pri bilo kojoj temperaturi testiranja. Merenje stope puzanja izvršeno je preko zavarenih spojeva. U ovom istraživanju pri ispitivanju otiska puzanja dominira dislokacija mehanizma puzanja.*
Ključne reči: *Puzanje, zavareni spoj, mikro tvrdoća.*

1. INTRODUCTION

Low carbon steel of SA 516 GR 70 is being widely used as a major structural material for boiler plates in view of its good high temperature mechanical properties and adequate weld ability [1]. These steels owing to their excellent high temperature mechanical properties, find wide applications as piping and super heater tube material in steam generating plants [2].

The duplex microstructure consisting of ferrite and pearlite phases transforms to carbides and brittle inter-metallic phases [3]. Consequently, the creep properties of the weld metal would be significantly influenced by the kinetics as well as the nature of the products of this transformation which in turn strongly depend on the chemical composition of the deposit [4].This investigation is aimed at understanding the characterization, mechanical properties like micro hardness and creep behavior of SA 516 GR 70 alloy shielded metal arc welds.

Impression creep technique is a modified indentation creep test wherein the conical or ball indenter is replaced by a cylindrical, flat bottomed punch [5]. The usefulness of this technique, pioneered by Prof. Li, is illustrated by application to a variety of problems [6]. High temperature creep behavior of a number of metals and alloys, particularly estimation of the thermal activation parameters aiding the identification of the rate controlling mechanisms of creep, has been investigated.

This test offers several advantages over the conventional creep testing. It is the most suitable method to study the creep behavior of welded portion; a small process zones HAZ [7]. It takes the shorter duration for test, and small quantity of the testing material. The temperature and stress dependency of creep rate could be obtained on a single sample. The test can be carried out with a constant stress at constant load. Utilizing the impression creep test, the creep behavior of individual zones in steel weldment has been examined. Experiments have been carried out to investigate the indentation (impression) creep on SMAW welded SA 516 GR 70. Samples were selected from the plates which had been SMAW. Impression creep behavior of samples was studied using tungsten carbide indenter at various stress levels and various temperatures. From the creep profiles steady state creep rates (ε_s)are calculated. Further stress exponent and activation energy values are also determined. Creep rates for three regions are compared.

2. MATERIAL AND EXPERIMENTAL DETAILS

2.1 Material Composition

The SA 516 GR 70 steel plates are used in this investigation to produce the weldment's in five different layers. The specifications of the plate of SA 516 GR 70 are 325 mm x 293 mm x 12 mm and the nominal chemical specification of SA 516 GR 70 steel plate is; C: 0.27%, Mg: 0.79-1.30%, Ph :0.035%, S: 0.035% and Si-0.20-04%.

2.2 Shielded Metal Arc welding unit

Welded joints of SA 516 GR 70 with a thickness of 12 mm. Butt type of joint were prepared by using SMAW technique (Fig.1). The welding parameters are shown in Table 1.

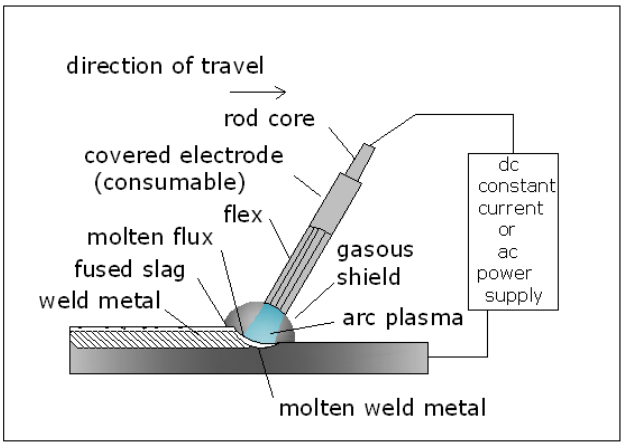

Fig. 1. Schematic drawing of Shielded Metal Arc Welding Unit

2.4 Length of HAZ for Welded Plate

The weld samples contain three zones i.e. parent material (PM), heat affected zone (HAZ) and fusion zone (FZ). But, visual observation is not sufficient to predict the actual length of HAZ. So, length of HAZ is calculated through theoretical correlations and shown in Table 2 for all the conditions.

$$H_{net} = \frac{\eta \cdot E \cdot I}{V} \tag{1}$$

$$\frac{1}{T_p - T_o} = \frac{4.13 \cdot \rho_{cp} Y_t}{N_{net}} + \frac{1}{T_m - T_o} \tag{2}$$

2.5 Sample Preparation

Samples for various tests were taken from parent metal (PM), heat affected zone (HAZ) and fusion zone of welded steels. Specimen of size 35mm x 12 mm were cut from the welded steels as presented in the schematic diagram presented in Figure 2.

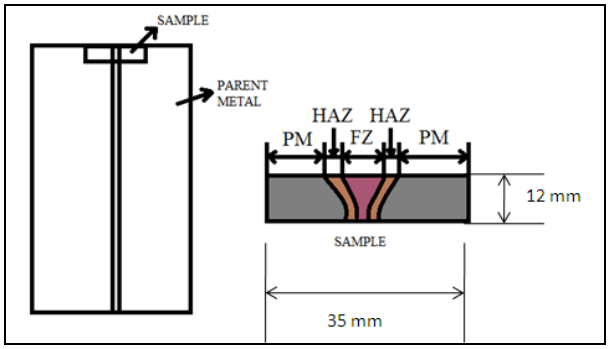

Fig. 2. Schematic diagrams for the cutting plane of the welded sample

Run	Process	Size of Filler Metal	Current (A)	Voltage (V)	Type of current/Polarity	Wire feed/ speed mm/min	Heat input (kJ/mm)
LAYER 1	SMAW	2.50	73-82	22-24	DCEP	95	1.01
LAYER 2	SMAW	3.15	118-123	18-20	DCEP	196	1.01
LAYER 3	SMAW	4.00	163-166	16-19	DCEP	205	0.76
LAYER 4	SMAW	3.15	145-148	20-22	DCEP	190	0.91
LAYER 5	SMAW	3.15	142-148	20-24	DCEP	196	0.86

Table 1. Experimental conditions for SMAW process

Layer	Wire feed speed mm/sec	H_{net} J/mm	HAZ (Y) mm
Layer 1	1.58	1015.3	2.67
Layer 2	3.27	630.13	1.58
Layer 3	3.41	759.78	1.91
Layer 4	3.17	873.45	2.19
Layer 4	3.25	811.8	2.04
Layer 5	3.27	877.9	2.20

Table 2. Length of HAZ for different layers

2.6 Micro-structural Studies

The cut samples are polished using surface grinding machine and then mechanically ground polished using 1/0, 2/0, 3/0, 4/0 grade papers. Next these samples are polished on a disc polishing machine by using diamond paste as abrasive medium until a flat and scratch-free mirror-like finish was obtained. To reveal the micro-structure, the sections were etched in 3% nital solution, rinsed in deionized water, and dried with drier.

2.6.1 Optical metallographic

Polished Samples were taken for microscopic examination and photomicrographs were taken with the help of standard metallurgical optical microscope and digital image recorder at appropriate magnification.

2.6.2 Scanning electron microscopy (SEM)

Micro structures of the polished sample were studied using SEM* on the PM, HAZ and FZ. Secondary electron images were recorded with appropriate magnification.

2.7 Micro hardness

Micro hardness measurements were made on welded specimens using Knoop micro hardness equipment. Measurements were taken for each condition at five different lengths along the weld with a load of 100 kgf.

2.8 Impression creep studies

Specimen cut from the different zones are grounded parallel using cylindrical grinding machine and etched to reveal the various zones. Photograph of such a specimen is presented in Figure 3.

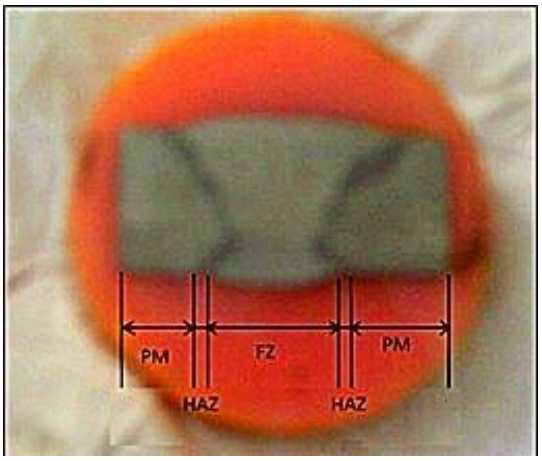

Fig. 3. Specimen Prepared for Impression Creep Test

2.8.1 Impression creep testing apparatus

The schematic line diagram of the creep machine set up used in the present study is shown in Figure 4. In this machine compression load is applied to the sample by means of a cage set up as shown in Figure 5. The cage consists of two rectangular components R_1, and R_2. R_1 is fixed to the base plate and R_2 to the pull rod which is connected to the lever arm. When load is applied R1 will remain stationary, R_2 will move up. As a result, the indenter fixed to the top plate of R_1will remains stationary whereas the bottom plate of R_2 containing the specimen will be pulled up which results in the impression of the indenter on the specimen.

Since the experimental work is at both room temperature and high temperature, the specimen cage must be made from a material capable of withstanding high temperature and must undergo zero deformation at the testing temperature throughout the testing period. The material which meets requirement of a specimen cage is Nimonic 90 (Methane grade super Ni 90) cold rolled and annealed 14 mm rods procured from Mishra Dhatu Nigam Limited, Hyderabad.

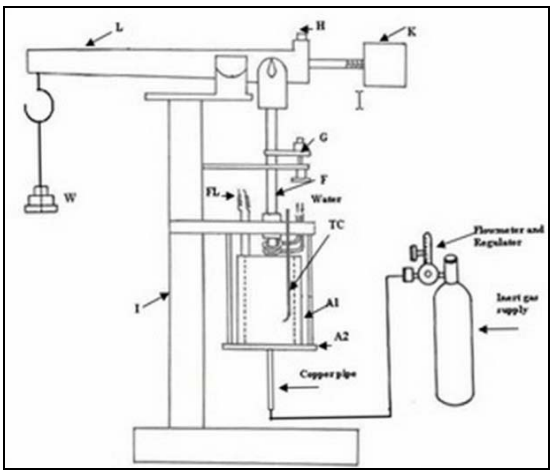

Fig. 4. The schematic line diagram of the impression creep setup (A_1- Furnace, A_2- Specimen cage, F - Pull rod, G - LVDT transducer, H- Spirit level, I- I beam frame, K- Balancing weight, L - Lever arm, W - Weight, TC - Thermocouple, FL - Furnace leads)

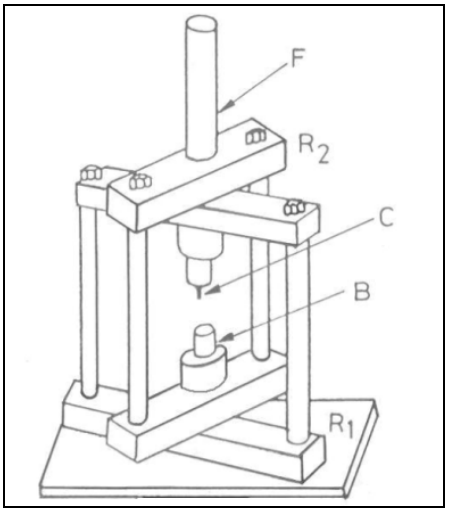

Fig. 5. Specimen cage setup (F- Full Rod, C- Indenter, B-Specimen)

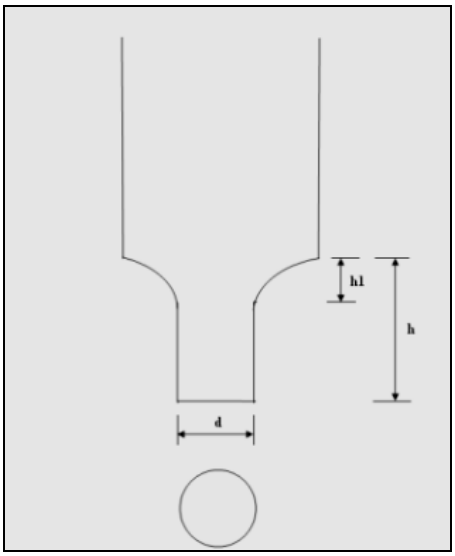

Fig. 6. Dimensions of the tungsten carbide indenter (d = 2 mm h = 1.967 mm h_1= 1.127 mm, Area of the base is 3.1416 mm^2)

The pull rod connected to the cage is also connected to the lever arm (L). These two parts of the pull rod are held together by a stainless steel block. The precise alignment of the pull rod and the specimen cage is very important to obtain good results. A platform is attached to the upper pull rod which presses against the transducer and measures the displacement. A horizontal 25mm thick steel plate is supported by means of two vertical channels. A 12.5mm thick stainless steel plate is supported from the above steel plate by means of four steel rods. The specimen cage is fixed to the stainless steel plate. A furnace also rests over it for high temperature creep testing. The dimensions of the tungsten carbide indenter used in the present work are shown in Figure 6.

Fig. 7. Impression creep setup used in the present work

2.8.2 Impression creep testing

The specimens, prepared as mentioned above, were polished by standard metallographic techniques and were tested for parallelism of faces before introducing into the specimen cage of the machine. The specimen (B) kept in one part of the super alloy cage (A_2) as shown in Figure 3 and the other part of the cage contains the cylindrical indenter (C) of diameter 2 mm made of tungsten carbide (its axis coinciding with the axis of the pull rod). Using the balancing weight (K) and the spirit level (H) the lever was initially kept horizontal. Now the specimen was made to touch the indenter. The load was applied gradually at the other end of the lever which was dipped in machine oil in order to avoid damping.

The indenter displacement could be measured with an accuracy of 1 micron. The readings are noted for every 1 minute until the steady state was reached. The creep testing was done on three zones of specimen with different loads and different temperatures.

3. RESULTS AND DISCUSSIONS

Figures 8 and 9 shows the banded structure of ferrite (white region) and pearlite (black region). This chapter includes results obtained from optical microscope, SEM on unpeened and laser peened samples. Microhardness and creep test results are tabulated and plotted.

3.1 Microstructures

Micro-structural features of SA 516 GR 70 grade steels in Parent, Heat affected and Fusion regions of the welds are recorded using optical and scanning electron microscopes and presented in Figures 8a to 8c and 9a to 9c.

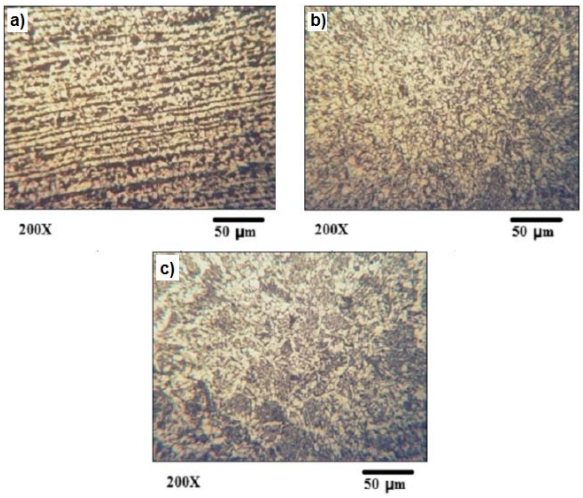

Fig. 8. Optical photomicrograph. **a)** PM (SA 516 GR 70); **b)** FZ (SA 516 GR 70), etchant Nital 3 %; **c)** HAZ (SA 516 GR 70), etchant Nital 3 %;

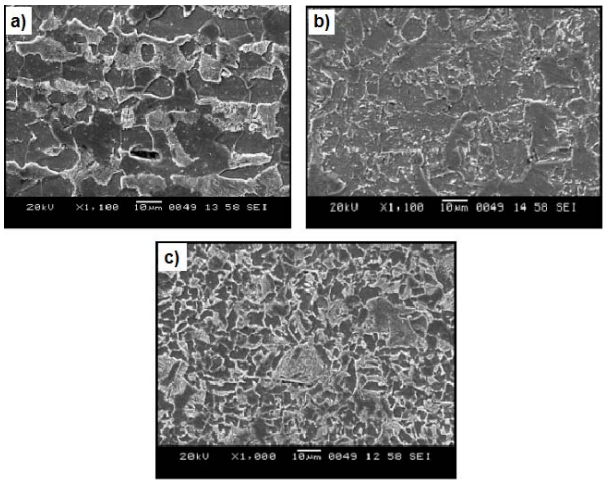

Fig. 9. Microstrucrures of SA 516 GR 70: a) PM; b) FZ; c) HAZ

Following observations can be made on Photomicrographs:

(i) Parent metal consists of banded ferritic and pearlitic structure. Pearlite content is around 30 %.

(ii) Fusion zone consists of very fine ferrite and pearlite, well distributed throughout, banded structure disappears.

(iii) Heat affected zone consists of fine ferrite and pearlite. Ferrite is seen surrounding the pearlitic region as in the case of steel containing more than 0.45 % Carbon.

(iv) Martensitic or bainitic are not observed in HAZ zone.

3.2 Micro hardness results for welded material

Hardness results of individual zones of steel material are given in Table 3. Hardness profile over the weldment steel material is presented in Figure 10.

Zones	Hardness (HV)
Parent Metal	165
Heat Affected Zone	183
Fusion Zone	188

Table 3. Micro hardness results for unpeened and peened welded material

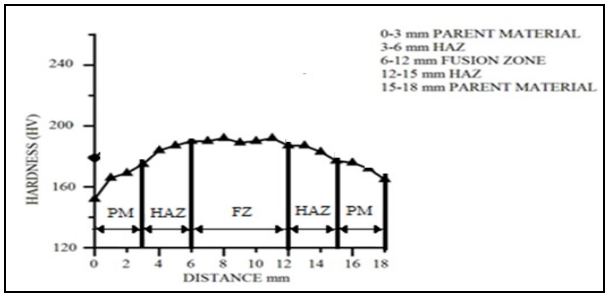

Fig. 10. Micro Hardness Profile for PM,HAZ,FZ regions

Parent metal is supposed to show a constant hardness. The area where hardness is changing may be regarded as HAZ.

Following points are revealed by the values presented in Table 3 and Hardness profile in Figure 9c:

(i) Fusion zone records highest hardness, followed by heat affected zone and parent metal.

(ii) Contrary to expectation highest hardness is not recorded by HAZ.

(iii) Hardness varies from 165 – 187 VHN in welded material.

3.3 Steady state creep test results

Steady state creep test was performed at 10 kg and 12 kg loads for different temperatures and for different zones. The results of the test are tabulated in Table 4.

Creep rate measurement over the weldment successful. Following observations can be made on the Table 4.

(i) Fusion zone records the lowest steady state creep rate, followed by heat affected zone and parent metal under all the conditions of load and temperatures of testing.

3.3.1 Activation energy

Activation energy was calculated at 10 kg and 12 kg loads for different temperatures and for PM, HAZ, FZ regions. The results of the test are tabulated in Table 5. For all the zones, Activation energy increases as the temperature increases. Activation energy is in the range of 20 – 46 for 10 kg load, and 15 – 41 for 12 kg load.

Temperatures	Steady State Creep Rate values / min ($\epsilon \times 10^{-3}$)					
	Parent Material		Heat Affected Zone		Fusion Zone	
	10 kg load	12 kg load	10 kg load	12 kg load	10 kg load	12 kg load
Room Temperature	0.0138	-	0.0018	0.005	0.0009	0.0020
100	0.1000	-	0.0167	0.050	0.0111	0.0416
200	0.4160	-	0.3300	0.833	0.2700	0.5000

Table 4. Steady State creep rate at 10 kg and 12 kg loads at different temperatures and for PM,HAZ,FZ Regions

Load (kg)	Zones	Parent Metal		Heat Affected Zone		Fusion Zone	
	Temperature (°C)	RT – 100	100 - 200	RT - 100	100 - 200	RT - 100	100 - 200
10	Activation Energy Q kJ/mol	26.95	20.45	30.31	42.81	34.18	45.80
12	Activation Energy Q kJ/mol	15.03	17.22	31.33	40.36	41.30	35.68

Table 5. Activation energy values 10 kg and 12 kg loads at different temperaturesand for different zones

3.3.2 Stress exponent values

Temperature	Stress exponent values 'n'	
	Fusion Zone	Heat Affected Zone
RT	4.38	5.67
100	7.33	6.05
200	3.40	5.14

Table 6. Stress exponent values

4. RESULTS AND DISCUSSIONS

Welding is the joining process involving high thermal input. The thermal effect creates distinctly three microstructural zones, viz: fusion zone (FZ), heat affected zone (HAZ) and parent metal (PM). The spread of the fusion and heat affected zone depends on the process of welding. With the present process of

shielded metal arc welding (SMAW) the width of fusion zone is around 6 mm. Heat transfer equation is used to find out the thickness HAZ and it is found that it extends by 2-3 mm. The calculation of thickness of heat affected zone is given in the appendix. Impression creep testing is one of the convenient methods for mechanical characterization of the micro regions like fusion zone and heat affected zones, at room temperature and higher temperature. Further, values of steady state creep rates can be used to find out the activation energy (Q*) which reveals the mechanism of creep.

The laser treatment on the surface of the weldment is expected to induce the residual compressive stresses and its mechanical properties, including creep. Further, three regions with different micro-structural features are expected to respond differently to the laser treatment. Hence, laser beam of power 50 mJ is scanned over the welded plates in single and double rows. However, it is found that surface of weldment got damage due to the action of laser. The initiation of cracks in the laser affected area is clear from the SEM photomicrograph presented in figures 8a to 9c.

4.1 Details of microstructure

Following are the observations for sample:

(i) Parent metal consists of banded ferritic and pearlitic structure. Pearlite content is around 30 %. As the base metal was cold rolled, banded ferritic and micro-structural characteristics of three zones have been investigated by optical microscope and scanning electron microscopy (SEM) for samples pearlitic structure was found.
(ii) Fusion zone consists of very fine ferrite and pearlite, well distributed throughout. Banded structure disappears as it reaches austeniting temperature.
(iii) Heat affected zone consists of fine ferrite and pearlite. Ferrite is seen surrounding the pearlitic region as in the case of steel containing more than 0.45 % Carbon.
(iv) For low carbon steels, the nose in the TTT diagram will be nearer to the y axis. As the percentage of carbon increases, nose pushes to the right of the TTT diagram. As the distance of nose from y axis increases, there is a chance of formation of martensite or bainite. So, martensitic or bainitic are not observed in HAZ zone the hardness value is in the range of 165 – 188 VHN.

5. CONCLUSIONS

Based on the present investigation following conclusions have been arrived at. The activation energy in the range of 15 – 46 kJ/mol and stress exponent values in the range of 3.4 – 7.33 suggest that the dominant mechanism is dislocation creep. Hardness value is more in Fusion zone compare to Parent and Heat Affected zones.

REFERENCES

[1] Andrews, E. W., Huang, J. S. and Gibson L. J.: Actamater, 47 (1999) 2927-2935.
[2] Spigarelli, S., European Aluminium Association (1999).
[3] Wadsworth, J., Ruano, O.A., and Sherby, O.D.: Metallurgical and Materials Transactions, 33A (2002) 219-229.
[4] Burton, B.: In Diffusional Creep of Polycrystalline Material*s*, TransTech Pub, Aedermannsdorf, Switzerland, (1977).
[5] Poirer, J.P.: Creep of Crystals, Cambridge University Press, Cambridge United Kingdom, (1985).
[6] Liming Ke, Chunping Huang, Li Xing, Kehui Huang.: Al–Ni intermetallic composites produced in situ by friction stir processing. Journal of Alloys and Compounds, 503, (2010) 494-499.
[7] D. Yadav, R. Bauri. Processing, microstructure and mechanical properties of nickel particles embedded aluminium matrix composite. Materials Science and Engineering A 528 (2011) 1326–1333.

Author: **Assistant Professor K.Vijaya Kumar, Ph.D. N.Ramanaiah, N. Bhargava Rama Mohan Rao, B. Srinivasa Prasad.** Dept. Mech, GITAM University, Visakhapatnam 530045, Phone:+919652805628
E-mail: kvzaymtech@gmail.com

Journal of Production Engineering
Vol.18 No.1
JPE (2015) Vol.18 (1) Original Scientific Paper
Vasilko, K.

METAL OF THE FUTURE – TITANIUM AND THE PROBLEMS OF ITS MANUFACTURING

Received: 20 April 2015 / Accepted: 16 May 2015

Abstract: *Titanium is considered to be the metal of the 21st century [1]. Metal, which would have small volume density (at least 2-3 times smaller than iron), plasticity, workability, high rigidity, resistance and life span, has long been desired. It has also been required no to lose those characteristics when exposed to air, river and sea water, not to be soluble in acid or potash. At the same time it has been required to be of sufficient content in earth crust. Titanium is such a material. Thanks to its specific characteristics its application has been spreading into many areas, such as medicine (implants), space (material for space technology) [2], chemical facilities, ships for sea transport (resistance to acids and salts), buckles for mountain climbers (low density and high rigidity), etc. Titanium mechanic characteristics, however, lead to new problems in technological manufacturing. It is necessary to apply a considerably different approach to its manufacturing. Titanium and its alloys behave in a specific way during manufacturing and it is necessary to know and use this behaviour for an effective production of parts.*
Key words: *machining, titanium alloys, turning, grinding*

Metal budućnosti - Titanijum i problemi njegove obradivosti. *Titanium se smatra metalom 21. veka [1]. Metal, koji ima malu specifičnu gustinu (barem 2-3 puta manju od gvožđa), plastičnost, obradljivost, veliku čvrstoću, otpornost i radni vek, je kao takav odavno poželjan. Neki od zahteva vezanih za osobine su da zadrže te karakteristike usled izlaganja vazduhu, rečnoj i morskoj vodi, i da nisu razgradive u kiselinama i potaši. Istovremeno je zatraženo da ga bude dovoljno sadržanog u zemljinoj kori. Titanium je takav materijal. Zahvaljujući svojim specifičnim karakteristikama njegova primena se proširira u mnoge oblasti, kao što je medicina (implanti), svemir (materijalno za svemirske tehnologije) [2], hemijska postrojenja, brodovi za pomorski saobraćaj (otpornost na kiseline i soli), kopče za alpiniste (niska gustina i visoka krutost), itd. Titaniumove mehaničke karakteristike međutim, dovode do novih problema u tehnologiji proizvodnje. Potrebno je primeniti značajno drugačiji pristup za njegovu proizvodnju. Titanijum i njegove legure se ponašaju na specifičan način u toku proizvodnje i neophodno je znati i koristiti ove ponašanje za efikasnu proizvodnju delova.*
Ključne reči: *mašinska obrada, legure titanijuma, struganje, brušenje*

1. INTRODUCTION - Titanium features

In Mendeleev periodic table titanium has serial number 22. Its neutral atom consists of the nucleus including 22 protons and a set of 22 electrons. The number of neutrons is about 24-28. Therefore also the number of titanium isotopes can be different. Some metals can be added to titanium, which increase its durability to tenths or hundreds times. These are for instance Zr, Ha, Ta, W. By adding 20-30% of Mo, a corrosion stability of gold can be achieved in titanium. Titanium is hard to smelt. The temperature of clean titanium smelting is the highest of all construction metals: 1668^0C. Titanium toughness is high [3]. This is the reason why it resists cavitation very well, for example. It is a suitable material for ship screw-propeller. It possesses a special feature – shape memory. In an alloy with other metals, for instance nickle, it remembers the shape of the part which has been produced at certain temperature. For instance, if the material is hot-turned into the shape of a spring, when it is heated to the temperature at which it was produced, it returns to its original shape. This is used in space (opening of aerials folded before), medicine (a wire, which turns into a coil, is directed into constricted blood wessel, where it spreads and extends it). Titanium has small heat conductivity (λ =0,071 J.cm^{-1}.s^{-1}.^{0}C^{-1}), which is three times smaller than that of iron [4]. At room temperature, the coefficient of linear heat conductivity is $8{,}5.10^{-6}.^0$C^{-1}. At room temperature, its electric conductivity is $42{,}1.10^{-6}$ Ω.cm. It is a typical paramagnet. However, it also has some negative features. It has tendency to self-ignition, it is combustible in some cases. It can self-ignite also without heat supply in a form of fine chip or powder. Titanium maintains its mechanic features up to high temperatures ($400\text{-}500^0$C). It is not disrupted up to the temperature of -235^0C. It belongs to light metals. Its density is 4,517 g.cm^{-3}. Therefore it is 1.4 times heavier than aluminium and 1.5 lighter than iron. However, it exceeds them by rigidity. It absorbs gases at higher temperatures, mainly oxygen and nitroggen, by which its plasticity decreases and its rigidity and firmness rises (used for gas turbine blades) [3]. Pure titanium is tough, rigid, ductile, plastic metal. Its *HB* is about 1000 MN.m^{-2}, E = 108 tis.MN.m^{-2}, R_e = 250 MN.m^{-2}. It has the highest friction coefficient among all metals therefore it is not suitable for parts which are in friction contact with other parts (slips, friction bearings).

2. PROBLEMS WITH MACHINING TITANIUM

Machining is complicated due to high friction coefficient of titanium. Titanium sticks to tool working areas. Practically there does not occur slipping of the chip along the tool face. The area of contact of the chip with tool face is very small. Great pressures and temperatures are created on this area. Heat discharge is complicated due to titanium small heat conductivity. By sticking of titanium elements on the tool, its geometry changes and it quickly loses its machinability. Diamond, which has the smallest friction coefficient, is a suitable tool material.

Titanium and its alloys belong among materials that are difficult to machine. Machining character differs from machining other metal materials. Tool durability is very low as a consequence of cutting wedge deformation and increasing cutting edge rounding. Heat concentrates into a narrow area in tool cutting wedge as titanium heat conductivity prevents heat off-take into the chip and workpiece. On the other hand, cutting forces and performance consumed are considerably smaller than during steel machining. The problem is that the chip is not compact, but it consists of elements which are created as a result of high friction coefficient between the tool and cut materials [5], [6], [7]. The chip does not leave along the tool face, but upwards and creates segments as a consequence of periodic slips in material (Fig. 1).

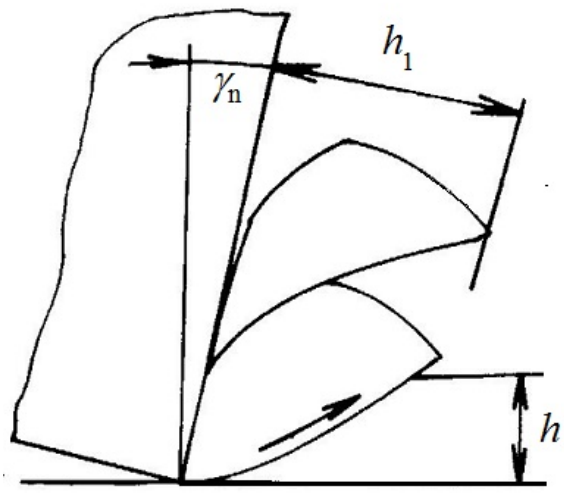

Fig. 1. Mechanism of chip creation during titanium machining

Gradual compression of creating chip segment pushes the segment upwards. The contact between created segment and the new one gradually moves as a result of segment alignment from the side of the tool. Chip movement speed along the tool face is equal to the speed of chip element compression. As the slip has been created and it spreads fast, it moves the creating element in the direction of slip area. Basically it must speed up element movement. This cycle part, which is marked by segment movement along the tool face, has periodic brakings which possesses a special feature, minimal force is necessary for segment compression.

In Fig. 2 there is a photograph of the chip under spacing microscope.

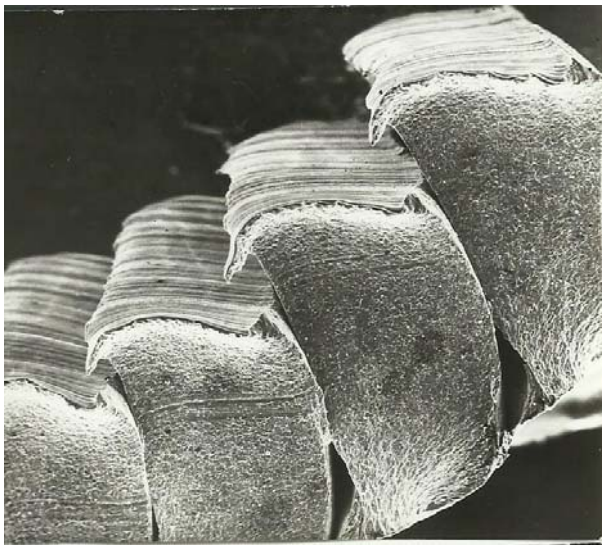

Fig. 2. Photograph of titanium chip under spacing microscope

It can be seen that plastic deformation intensity in the chip is visibly variable. An undeformed structure is located in the center of elements, a periodic adiabatic slip occurs between elements. Chips segmentation is probably related to instabile deformation character, which is conditioned by mutual influence of two mechanisms:

- rigidity decrease under the influence of heating by friction and deformation
- deformation reinforcement

Creating strips of concentrated slip is connected with bad material heat conductivity. Heat energy concentrates into a strip. Observation of chip creation by a speed camera has shown alternating braking of the chip, the reason of which can be welded connection of tool and the chip. This eplains high intensity of tool wear.

There is a considerable slip on segement borders. A visible deformation can be seen at the back side of the chip which used to be a transfer workpiece area. The fact, that there are no problems with chip shaping during titanium machining is a positive aspect, the chip is elementary, little compact and falls apart at the impact with an obstruction. Chip shaper on the tool is not necessary. Self-excited tool oscillation is the result of the above described chip creating mechanism.

The order of the phenomena at segment chip creation can be divided into two stages.

- The first stage is marked by plastic instability which leads to location of the deformation along the slip area. This area starts at cutting edge and first it is oriented in the direction of cutting speed vector, then it bends upwards where it crosses with cut surface. Slip disruption of the chip occurs at its outer side in the form of fissures and inner side in the form of deformed strips.
- In the second stage, gradual smoothing (smooothing out of semi-wedge) of the incliend side of

chip segment oriented towards cut material as a result of tool shifting occurs. Chip thickness approximately equals the thickness of cut-off layer.

This has lead many authors to a wrong conclusion that there is a large limit angle of primary plastic deformation during titanium machining. It means that chip compression should equal 1, which does not correspond with the laws of plastic deformation (volume conservation law). The use of term „slide angle“ does not suit the case. Deformation process in this narrow strip is very probably an adiabatic slip. The disruption occurs as a result of compression from surrounding metal layers (case of area deformation). There is some free and not fixed material alongside the chip (area tension state), which allows the segment to spread and create fissures.

In this connection there occurs a question how to consider chip creation parameter in this case. Chip thickness cannot be identified by geometric measurement (h_t from Fig.1 is only a limit chip width). It is necessary to use the following procedure. Trapped chip of certain lenght is considered and mean chip compression is calculated for known cut material density from the equation:

$$k = \frac{100.m_t}{l_t.\gamma.S} \qquad (1)$$

where:
m_t is chip weight, lenght l_t, g
S – cross section area cut (a_pxf), mm^2
l_t – lenght of trapped chip, mm

2.1 Some experimental results

As it has been presented, cutting forces are considerably smaller than at machining steel in spite of higher titanium rigidity. In Fig. 3 there is an experimental dependence of cutting forces on cutting speed for both materials.

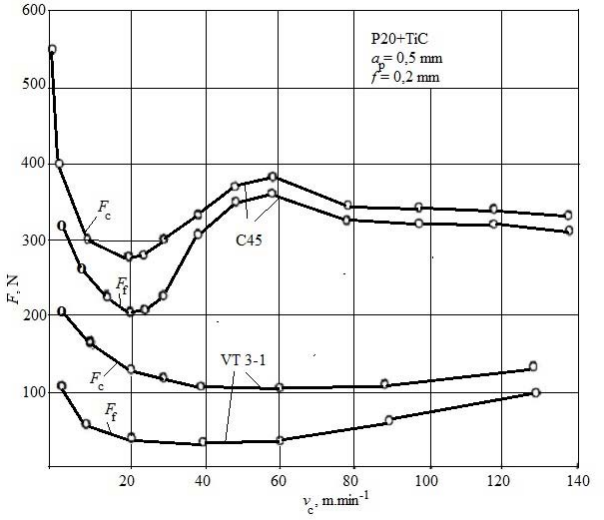

Fig. 3. Experimental dependence of cutting forces F_c and F_f on cutting speed at machining steel C45 and titanium alloy VT 3-1

While for steel it is possible to identify of minimum force, at cutting speed 20 m.min^{-1} and maximum at cutting speed cca 60 m.min^{-1}, titanium behaves completely differently. Cutting force continually decreases up to 60 m.min^{-1}, (which can be considered to be a limit one at machining titanium), then it increases.

Specific mechanic features of titanium condition also the mechanism of tool wear [8]. In Fig. 4 there are experimental curves of dependences of tool wear on the back on machining time and cuttting speed, obtained during turning titanium alloy VT 3-1 by a tool made of sintered carbid P20 with TiC coating.

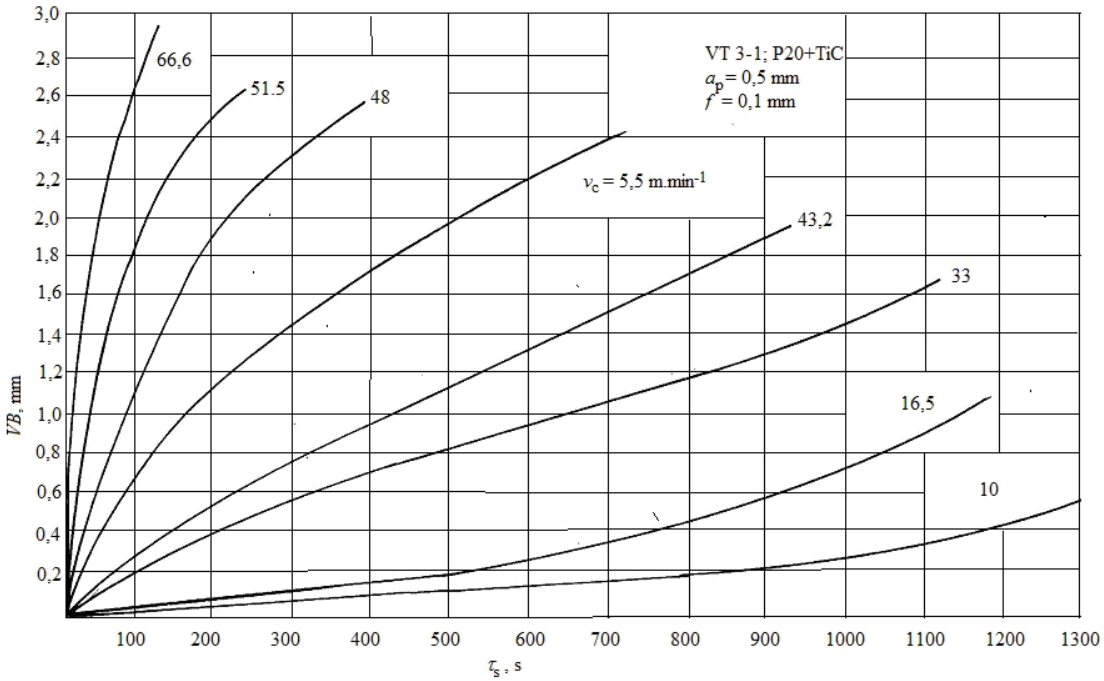

Fig. 4. Experimental curves of dependence VB-τ_s

It can be seen that with rising cutting speed, tool wear intensity sharply increases. It can be seen more visibly on dependence T-v_c, obtained from Fig. 4 for blunting criterion VB_k = 0.8 mm, in Fig. 5.

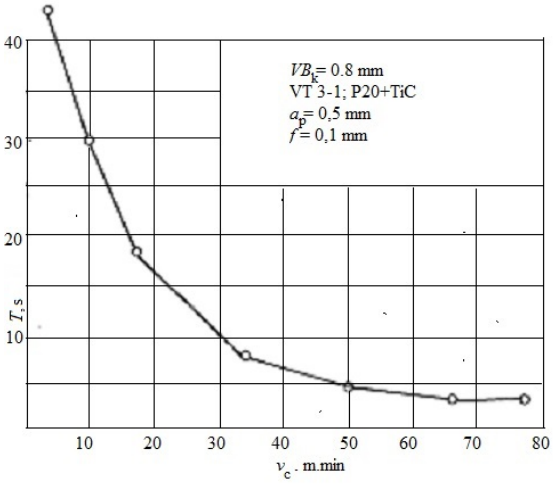

Fig. 5. Experimental dependence of tool durability on cutting speed

It is a typical hyperbolic dependence, it documents considerably lower tool durability than at cutting steel in whole range of cutting speeds. Inadequacy of higher cutting speed than 50 m.min^{-1} follows this fact. General principle for selecting cutting speed can be presented:

$v_{cti} = 0{,}1.v_{cFe}$ for the same cutting material.

One of the important parameters of titanium machining is the quality of machined surface [9], [10]. In Fig. 6 there is an experimental dependence *Rz-f* diagrammme for machining with a classical tool with rounded cutting wedge with radius r_ε = 0.4 mm and a special tool with linear cutting edge. Considering the cutting edge rounding, for the first curve, *Rz* increase is observed after decreasing the shift under 0.1 mm. It is caused by the compression of cut material under the tool cutting wedge. To remove this problem, a tool with the following geometry has been used: $\gamma_n = 0^0$; $\lambda_s = \pm 45^0$; $\varkappa_r = 0^0$.

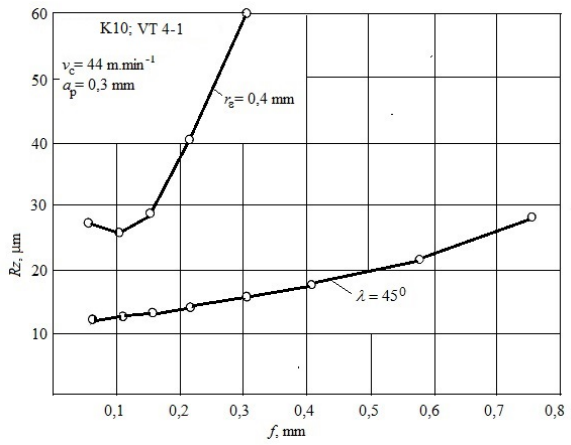

Fig. 6. Experimental curves of dependence Rz – f obtained during turning titanium alloy with a classical tool with tip rounding radius and tool with linear cutting edge

Considering titanium alloy plasticity, it is suitable to create conditions for a free cut [7] during turning. Therefore a tool with linear cutting edge with inclination angle λ_s = - 45^0 (Fig. 7) has been used in the second phase for linear turning.

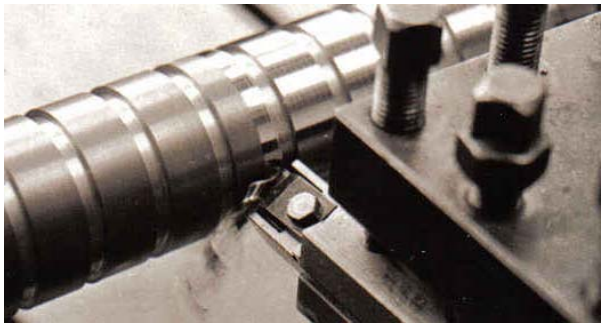

Fig. 7. Turning with a tool with linear cutting edge

Visible improvement of the quality of machined surface of the workpiece can be seen. Visually, mirror shine can be seen, it means a very good quality of machined surface.

A dependence of *Rz* on cutting speed has an interesting course (Fig. 8).

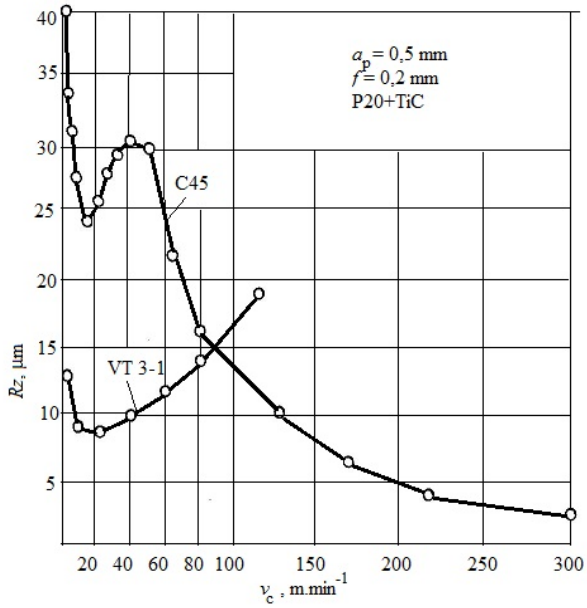

Fig. 8. Experimental dependence of the highest point of uneveness of machined surface on cutting speed for turning steel C45 and titanium alloy r_ε = 0.8 mm

The dependence has the opposite course in comparison with turning steel. It continually grows worse with the growth of cutting speed *Rz* above 20 m.min^{-1} *Rz* when turning titanium. Cutting speed higher than 60 m.min^{-1} is not suitable for machining titanium. The experimenta could have been held for only a few seconds during higher cutting speeds. Similraly to steel, at cutting speeds ≤ 20 m.min^{-1} *Rz* increases as a result of compression of material under the rounded cutting wedge. In whole range of cutting speeds up to 60 m.min^{-1} , the quality of machined

titanium surface is considerably higher than for steel.

Cutting threads is the critical operation of titanium turning. Considering titanium memory and limited minimal thickness of cut-off layer, serial taps cannot be used. Tap seizure occurs, mainly when the work is interrupted (material tries to return to its original dimension). Threads can be successfully cut with a machine tap, quickly, with full gear and suitable cutting oil.

High friction coefficient of titanium with tool material has lead to the idea to apply ultrasound oscillation on the tool. The results are very interesting and documented, Fig. 9 and 10.

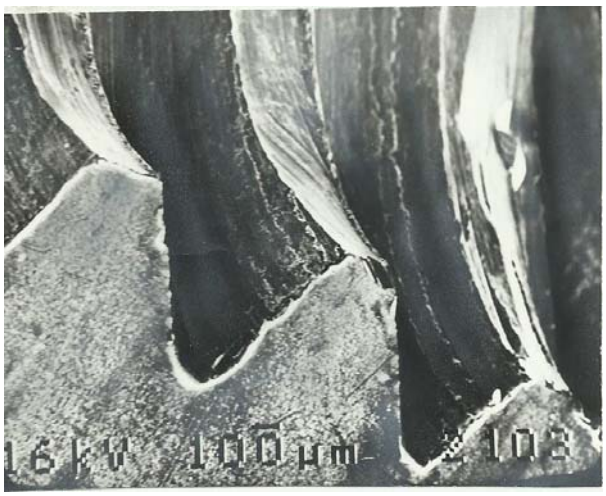

Fig. 9. View of thread cut by a classical tap under scale microscope

Fig. 10. View of thread made by a tap oscillated by ultrasound

The difference is sharp. As it can be seen, the thread sides do not have microuneveness caused by the tool back friction with transfer workpiece area.

Other problems occur during grinding. It is well-known that titanium cannot stand small thickness of cut-off layer which is created during grinding [5], [11]. There occurs a danger from ignition [12], [13]. In Fig. 11 there is a metallographic cut of the place of chip creation during grinding with Al_2O_3 tool. Creating chip possesses fibre-like structure. There occurs friction between titanium in the chip and titanium in the workpiece. These are exceptionally difficult machining conditions. The solution lies in the application of diamond grinding abrasion wheels or cubic nitride of boron. Diamond, as it is known, has a very small friction coefficient and in contact with titanium, favourable conditions for chip creation occur.

Fig. 11. Metallographic cut of chip creation during gridning titanium alloy VT 6 with Al_2O_3 tool

3. CONCLUSION

It is obvious that the application of titanium and its alloys will have spread to different applications in mechanical enginerring, chemmical, food-processing, air and cosmetic industries [14], [15]. Therefore knowing the conditions of economical turning of this material has high importance. Physical and mechanical as well as chemical features of titanium predestinate it for light and firm constructions. However, it causes considerable difficulties in its technological manufacturing. Mainly its high rigidity causes that higher cutting speeds cannot be applied. Low heat conductivity causes that during machining, heat is not lead into the chip and workpiece. It concentrates in cutting wedge and causes its degradation after short machining. It is important for the cutting wedge to remain sharp with minimal cutting edge rounding radius. This is the reason why cutting edge durability effectiveness is considerably lower than for machining steel. Exceptionally high friction coefficient of titanium with any other metal, it means tool material, causes problems in chip creation and machined surface. Due to adhesive connection it is not possible to use cutting tools which contain titanium. The chip does not slide along the tool face but leaves under the angle of slide deformation limit ϕ in the form of little compact elements. This is why knowledge about creating a chip from machining steel cannot be used for machining titanium.

4. REFERENCES

[1] ZUBKOV, I, B.: *Kozmičeskij metal*. Moskva: Nauka. 1987, 128 s.

[2] BOYER, P, R.: An averview on the use of titanium in the aerospace industry. *Material*

Science and Engineering, 1976. A. Vol. 213, pp. 103-114

[3] GLAZUNOV, S, G., MOJSEJEV, V, N.: *Metalurgija titana*. Moskva, Mašinostrojenije, 1974

[4] WAISS, I., SEMIATIN, S, L.: Thermomechanical processing of beta titanium. *Science and Engineering*, 1998, Vol. 243, pp. 46-65

[5] GENTE, A., HOFMEISTER, H, W., EVANS, C, J.: Chip Formation in Machining Ti6Al4V at extremely High Cutting Speeds. *Annals of the CIRP*, Vol 50/1/2001, pp. 49-54

[6] KOMANDURI, R.: Some Classification on the Mechanics of Chip Formation of Titanium Alloys. In: 2nd Int. *Conference on High Speed Machining*. Darmstadt, 1999, pp. 21-28

[7] ORTMAN, R.: Drehbearbeitung der Titanlegierung TiAl6V4, mit Werkzeugen ans den Schnellarbeitstahl S10-43-10. *KEM 1974*, Nr. 4

[8] KOVAČ, P. et al.:The role of Material Qality Control in modern Manufacturing. *Journal of Production Engineering*, Vol. 17. No. 2, 2014, pp. 63-66

[9] BUMBALEK, B., BUMBALEK, Z.: Surface Layer Properties of Titanium Alloys Ti16A14V, Ti7A13, 3MoO3Si ofter Milling and Grinding Operation and Their Influence on the Fatique. *Manufacturing Technology*, 2008, Vol VIII, pp 40-46

[10] CZAN, A. et al.: Studying og Cutting Zone When Finishing Titanium Alloy Application of Multificaction Measuring System. *Manufacturing Technology*. December 2013, Vol. 13, No.4, ISSN 1213-2489

[11] VASILKO, K.: *Obrábanie titánu a jeho zliatin*. FVT TU v Košiciach, 2001, ISBN 80-7099 683-8

[12] KREIS, K.. Verschleissursachen beim Drehen von Titanwerkstoffen. *VDI.Zeitschrift*, 116, 1974, s. 57-57

[13] KARASEVSKAYA, O. P. et al.: Deformation behovior of beta titanium alloys, *Materials Science and Engineering*, 2003, Vol. 354, pp. 121-123. Titanium a technical guide

[14] KÖNIG, W., SCRODER, K, H.: Stirnfräsen von Titanwerkstoffen. *Industrie Anzeiger*, 1975, Nr. 77, s. 1657-1661

[15] NOVAKOVA, L., HOMOLA, P., KAFKA, V.: Microstructure Analysis of Titanium Alloys after Deformation by means of Asymmetric Ineremental Sheet Forming. *Manufacturing* Technology, 2012, No. 13, Vol 12, pp. 201-206

***Authors*: Dr.h.c. prof. Ing. Karol Vasilko, DrSc.,**
Technical University of Košice, Faculty of Manufacturing Technologies, 080 01 Prešov, Bayerova 1, Slovakia. E-mail: karol.vasilko@tuke.sk;

Journal of Production Engineering
Vol.18 No.1
JPE (2015) Vol.18 (1) Original Scientific Paper
Todić, A., Pejović, B., Kovač, P., Ješić, D., Savković, B.

IMPROVE OF TOUGHNESS AND HARDNESS OF HIGH ALLOYED STEEL BY VANADIUM AND APPROPRIATE HEAT TREATMENT

Received: 12 January 2015 / Accepted: 30 March 2015

Abstract: *Characteristics of air hardening steel are high hardness and low impact toughness. In order to increase the impact toughness while retaining replace with the high hardness value is the alloying of Cr-Mo steel with vanadium and application of appropriate heat treatment. Vanadium formed V_6C_5 carbides that block the growth of austenitic dendrites and structure makes fine-grained. Vanadium which forms V_6C_5 carbides is partly distributed between present phases in the steel, carbide $(Cr,Fe)_7C3$ and austenite. Also, the presence of vanadium can enable the formation of $(Cr,Fe)_{23}C6$ carbide and its precipitation in austenite during the cooling process. In local areas around fine carbide particles, austenite is transformed into martensite. In other words vanadium reduces the amount of remained austenite and so improves hardenability of the Cr-Mo steel.*
Key words: *Vanadium, Impact Toughness, Hardness, Microstructure*

Poboljšanje čvrstoće i tvrdoće visoko legiranih čelika pomoću vanadijuma i odgovarajuće termičke obrade. *Karakteristike čelika ojačanog na vazduhu su visoka tvrdoća i niska udarna žilavost. U cilju povećanja udarne žilavosti da bi se zadržala visoka tvrdoća primenjuje se legiranje Cr-Mo čelika sa vanadijumom i odgovarajuća termička obrada.Vanadijum koji formira V_6C_5 karbide je delimično raspoređen između prisutnih faza u čeliku, karbida $(Cr,Fe)_7C3$ i austenita. Takođe prisustvo vanadijuma može da spreči nastanak $(Cr,Fe)_{23}C6$ i njegovu precipijaciju u austenitu za vreme procesa hlađenja. U okolini finih čestica karbida austenit se transformiše u martenzit. Drugim rečima vanadijum redukuje količinu zaostalog austenita i na taj način povećava tvrdoću Cr-Mo čelika.*
Ključne reči: *vanadijum, udarna žilavost, tvrdoća, mikrostruktura*

1. INTRODUCTION

The cast microstructure of high alloyed Cr-Mo steel consists of primary austenite dendrites, which can be partially or completely transformed. It is expected that with the increasing of the vanadium content, the alloy hardness and wear resistance decreases, and the impact toughness increases.

The basic problem with these steels is low impact toughness. Until very recently, the solution to increase the impact toughness was sought in getting of the complete martensite structure, that can be achieved by quenching of steel from the temperature of about 1000°C.

In recent years, the research goes in the direction of investigation of the influence of alloying elements such as molybdenum, manganese and particularly vanadium [1, 2, 3].

Vanadium affects the crystallization process, as it moves the liquid and solid lines toward higher temperatures.

In this paper, the research focus is set to study the influence of vanadium on the structure, hardness and toughness of the Cr-Mo steel.

1.1. The influence of chemical composition on structure and properties of Cr-Mo steel

Effect of Chromium

Chromium reacts with carbon to form hard wear resistant carbides, prevents the transformation of austenite to perlite during cooling of castings and affects the structure of the steel metal matrix by closing of γ area in the phase diagram [4].

Carbides Cr_7C_3 type and $Cr_{23}C_6$ can be alloy with iron to form the interstitial phases $(Cr,Fe)_7C_3$ and $(Cr,Fe)_{23}C_6$. Best toughness and hardness have the structures containing carbide $(Cr,Fe)_7C_3$, which is formed in steel containing more than 6% of chromium. With the increase of chromium content eutectic point is shifted to lower concentrations of carbon. However, chromium does not increase hardenability but combined with higher carbon content increases the depth of the quenched layer.

Effect of Vanadium

Vanadium affects the solidification process of these alloys by narrowing of the temperature interval of crystallization. Namely, the crystals of V_6C_5 carbides are formed during the separation of primary austenite from the solution, blocking further growth of austenite dendrites and support the production of fine grained structures [5].

Besides it forms added, V_6C_5 carbides, similar to the molybdenum, vanadium, is partly distributed between present phases in the steel; carbide $(Cr,Fe)_7C_3$ and austenite.

The presence of vanadium enables the formation of $(Cr,Fe)_{23}C_6$ carbide and its precipitation in austenite

during the cooling process. In local areas around fine carbide particles, austenite is transformed into martensite. In other words, vanadium reduces remained austenite and improves steel air-hardening. Vanadium concentration over 2.5% significantly improves the impact toughness.

Effect of microstructure on the steel properties

The microstructure determines the two most important characteristics of the wear-resistant material, hardness and toughness. Customizing content and arrangement of the phases and micro-constituents, present in the structure of steel, is possible to obtain the maximum value of hardness and toughness, or the optimal combination of these characteristics [6].

In terms of structure, this type of steel belongs to the ledeburitic steels. Because of dendritic segregation, crystallization of the ledeburitic steel starts with the separation of primary austenite crystals that containing less carbon, chromium and molybdenum than in the melt. Ledeburit is distributed as a network around the primary austenite crystals. After the solidification of ledeburit, shape, size and distribution of the proeutectic carbide cannot be changed by heat treatment, and solidification process is of essential importance for the steel properties[7, 8].

At high-alloyed ledeburit, austenitic phase has a higher growth rate, so that the austenite formed a wrapper around carbide fibers and this structure result in higher chromium steel strength and toughness, compared to unalloyed or low alloyed ledeburitic micro-constituent.

Precipitation of secondary carbides, mostly $(Cr, Fe)_{23}C_6$, from austenite grains takes place during slow cooling or subsequent annealing [6]. At the very beginning, the precipitate is very fine and oriented along the border with eutectic $(Cr, Fe)_7C_3$ carbide and around the austenite grains boundaries.

The process of precipitation of secondary carbides reduces the chromium and carbon content in the metal matrix so that a higher percentage of austenite will be transformed to martensite. Such a phenomenon of secondary carbides has dual positive effect as follows: hard, fine dispersed phase is formed and the amount of residual austenite is reduced [9, 10, 11].

2. DESCRIPTION OF THE EXPERIMENT

For melting of the steel, induction furnace added of 250 kg capacity, was used. The samples for the experiments were cast into the sand molds. Molds are made according to the patterns that have the shape and dimensions in accordance to the impact toughness and hardness test standards. Castings were heat treated by hardening in controlled air flow and subsequent tempering. The tempering was done at two temperatures as follows:

- low temperature tempering at 250°C, which removes micro-stresses, improves toughness and ductility of steel, compared to the hardened state, but keeps high strength and toughness that is required of wear resistant castings and
- medium temperature tempering at 400°C, which, also removes micro-stresses, but leads to the formation of bainitic structure, and therefore increase the impact toughness of steel.

Predicted chemical composition of the steel for this type of test was: C=2,2%, Cr=12%, Mo=1.2%, while the vanadium changed as follows: for the first series 0,5%V, second 1% V , third 2% V and for the fourth series vanadium was 3%. The chemical composition of samples I, II, III and IV series are in the Table 1.

Serial Number	Mark	Chemical Composition				
		C (%)	Cr (%)	Mo (%)	S (%)	V (%)
1	I	2,17	11,12	1,1	0,03	0,45
2	II	2,19	11,01	1,12	0,03	0,91
3	III	2,15	11,59	1,09	0,03	1,96
4	IV	2,11	11,52	1,01	0,03	2,80

Table 1. Chemical Composition of the Samples

Surface of the samples, immediately after casting and heat treatment, is very rough so it was necessary to clean up cast samples and machined it to the standard test dimensions. Mechanical processing should be done with permanent cooling in order to avoid any change in the microstructure.

For testing of the impact toughness samples 55 mm long and 10x10 mm cross section were prepared. Testing of impact toughness was performed using computerized pendulum *Schenck-Trebel 150/300J*. Pendulum computerization includes connecting of the force meter, detector of the fracture time and deformation gauge through the amplifier with an oscilloscope. As the fracture of the samples caused by impact is a very short phenomenon (since 0.5 to 8 ms), the role of the oscilloscope is to make the signal visible. Oscilloscope is then connected to a computer for processing signals obtained in the measurement.

For the purposes of hardness testing the samples of similar size as the impact toughness tests are made. Because of the relatively high hardness of the material, hardness testing was done by Rockwell C method on the *Vexus SHR-150M device*.

Analysis of the microstructure was performed under a light microscope *Olympus GX41* that was equipped with software for image processing and phase analysis and on SEM microscope *JEOL JSM-6610LV*. Preparation of samples was carried out using standard metallographic procedure.

3. RESULTS AND DISCUSSION

3.1. Effect of vanadium on the hardness

Hardness testing was performed on six points of the sample so that the mean values for the relevant value was taken.

Results of hardness testing are shown in Table 2. From the table it can be seen that with increasing vanadium content in the alloy, hardness decreases, respectively, and more intensive when the samples were tempered at the temperature of 400°C. When the tempering temperature was 250°C decrease in hardness

is less severe, as seen in Figure 1. However, hardness remained at a relatively high level and the decrease of hardness is acceptable.

Serial Number	Sample Mark	Hardness (HRC)	
		250°C	400°C
1	I	63,00	62,25
2	II	60,30	60,50
3	III	60,10	58,50
4	IV	58,90	57,20

Table 2. The values of hardness

This reduction in hardness undoubtedly entails increasing of impact toughness.

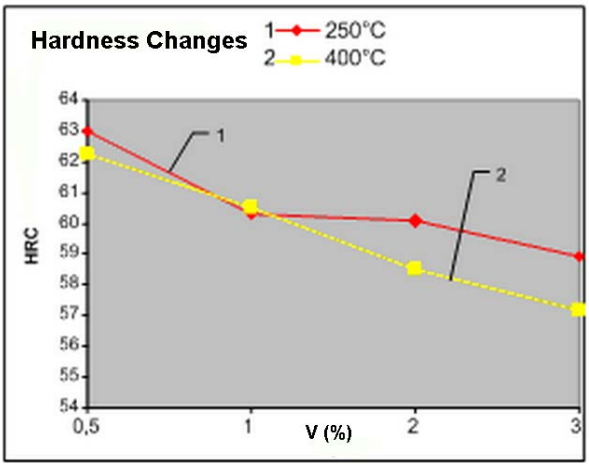

Fig. 1. Diagram of Hardness Changes

3.2. Effect of vanadium on the impact toughness

Impact toughness testing was performed on three samples from each series. The mean value of toughness measurements was taken as authoritative. Table 3 presents the results of impact toughness.

From the table it can be seen that with increasing of vanadium content increases the impact toughness values, especially at the samples from the fourth series (mark IV) containing 3% V.

Serial Number	Sample Mark	Toughness (J/cm^2)	
		250°C	400°C
1	I	2,37	5,45
2	II	4,50	5,55
3	III	6,45	6,96
4	IV	7,15	8,71

Table 3. The values of impact toughness

From the table it can be seen that with increasing of vanadium content increases the impact toughness values, especially at the samples from the fourth series (mark IV) containing 3% V.

Increasing of impact toughness is more noticeable for the samples tempered at temperature of 400°C than for samples tempered at 250°C (Fig. 2). Increasing of impact toughness is significant, while the hardness remained on satisfactory high level.

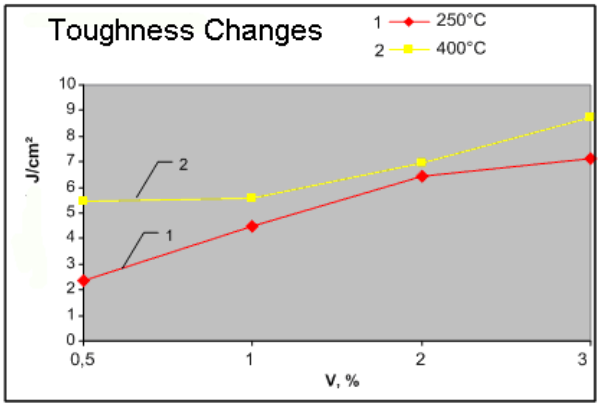

Fig. 2. Diagram of Toughness Changes

3.3. Effect of vanadium on the structure

With increasing of vanadium content, the radial distribution of $(Cr, Fe)_7C_3$ carbides becomes a dominant but the proportion of long directed lamellas and plates do not change.

Vanadium is soluble in both, eutectic carbide and austenite. In alloys containing 2-3% of vanadium, austenite, is largely transformed to bainite during cooling. In the structure also present added in a small amount of martensite, mainly along the border with eutectic carbide.

Figure 3 shows the structure of the sample made under a light microscope, while Figure 4 shows micrographs of the structures made on SEM. In order to determine the chemical composition of the present phases, the EDS analysis was performed.

From the SEM micrographs it is evident that the metal matrix of the alloy is immersed with fine carbides of alloying elements. A carbide network has a rounded shape with a small amount of carbide rods. Locations where an EDS analysis was done are marked with the counts 1 to 4. Count 1 is a point on the carbide grains dispersed in metal matrix, while points since 2 to 4 refer to the points in carbide network.

The analysis in count 1 added which relates to the carbides of metal matrix, shows that the carbides contain 24% of carbon, 10% of chromium, 81% of iron, 0.21% of vanadium and a small amount of manganese that could not be precisely determined. However, carbon content is close to his stechiometric content in Fe_3C carbide, indicating the possibility that the carbides type M_3C are formed in the metal matrix. EDS analysis shows that in the crystal lattice of this carbide a small number of iron atoms are replaced by atoms of chromium and manganese. Manganese builds Mn_3C carbide that is similar to Fe_3C. It has orthorhombic lattice and is most likely that the carbide $(Fe, Mn)_3C$ is precipitated in a steel metal matrix.

Counts 2, 3 and 4 refer to the eutectic carbide network and EDS analysis shows that these are the M_7C_3 type carbides.

Table 4 presents the chemical composition of the tested phases in weight percentages, while Table 5 shows the chemical composition of the tested phases in atomic percentages.

On the figure 5 and 6 the chemical spectar done by EDS analysis was shown.

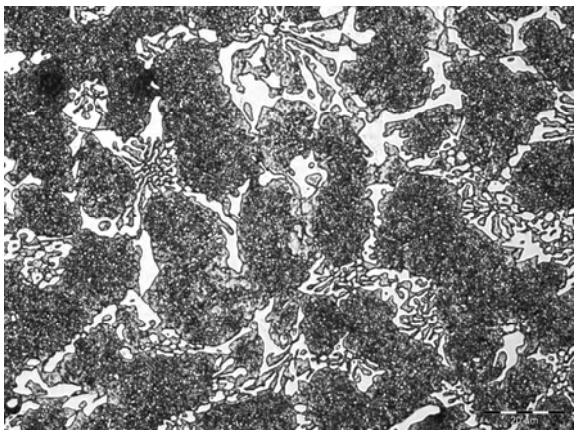

Fig. 3. The Structure of the Sample made by Light Microscopy

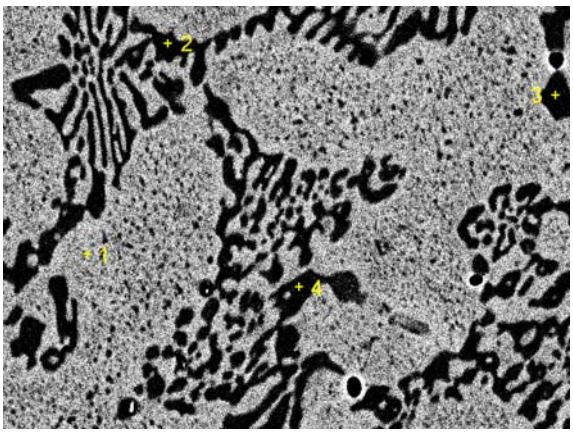

Fig. 4. SEM Micrograph of the Sample

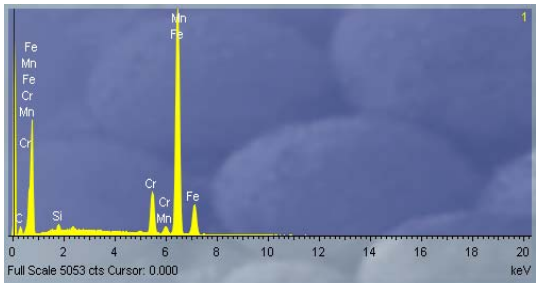

Fig. 5. EDS Spectrum at Point 1

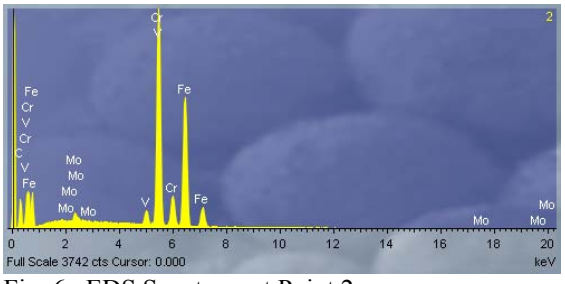

Fig. 6. EDS Spectrum at Point 2

Samples	Elements Content (weight %)							
	C	Si	V	Cr	Fe	Ni	Mo	Total
Count 1	7,24	0,63	0,21	9,99	81,04	0,00	0,87	100,00
Count 2	13,07	0,00	2,42	42,50	40,69	0,00	1,33	100,00
Count 3	12,21	0,00	2,23	42,43	41,00	0,00	2,12	100,00
Count 4	13,25	0,00	2,47	42,16	40,07	0,00	2,06	100,00

Table 4. Chemical composition of the tested samples in weight percentage

Series of samples	Elements Content (atomic %)						
	C	Si	V	Cr	Fe	Ni	Mo
Count 1	22,72	1,21	0,22	7,94	67,46	0,00	0,44
Count 2	40,94	0,00	1,72	29,90	26,79	0,00	0,66
Count 3	42,77	0,00	1,67	29,38	25,49	0,00	0,69
Count 4	42,40	0,00	1,63	29,77	25,44	0,00	0,77

Table 5 Chemical composition of the tested samples in atomic percentages

Based on the SEM micrograph, EDS analysis in figure 5 and 6 and data that are given in Tables 4 and 5 it can be concluded that the structure consists of bainitic metal matrix with a small amount of martensite and retained austenite and carbide phase, type $(Cr,Fe)_7C_3$.

4. POTENTIAL OF APPLICATION

This type of steel, because of its high hardness and satisfactory impact toughness, and therefore high wear resistance, can have a wide application area.

Parts and components that are exposed to abrasive, impact-fatigue or combined wear are used in mining, metallurgy, engineering constructions, paper industry, mechanical engineering, etc. Assortment of these parts are: parts of mining machinery (excavator teeth and tooth covers, crusher plates for stone coal and ore minerals, mills hammers, plates and linings, separation grates, etc.). In addition, this material can be used for making bunkers lining for abrasive materials, sand blasting shovels, mud pumps housing, molds for briquetting of coal and steel turnings, tanks and transporters caterpillars, and many other parts. Mills hammers and jaw crushers plates are exposed to abrasive wear combined with the high compressive stress and impulse impact loads. Therefore, the materials used to manufacture these parts should, in addition to hardness, have a good impact toughness.

5. CONCLUSION

In this paper, the influence of vanadium on the microstructure, hardness and toughness of the steel with 2.2% of carbon, 12% of chromium and 2.0% of molybdenum was discussed. Generally, with increasing vanadium content, the structure becomes finer affecting the mechanical properties of the steel i.e. the hardness and impact toughness. Vanadium content in the steel added was varied: as first series added is 0,5%V, for the second series is 1%V, for the third series is 2%V and for the fourth series is 3%. All 20 samples were casted. The chemical compositions the samples of I, II, III and IV are showed in Table 1.

Vanadium content higher than 3% have a negative influence on the properties of steel (significant decrease in hardness) and therefore the research with a higher percentage of vanadium were not included.

It can be seen that an increase of vanadium has a positive effect on the structure and the properties of materials. Testing samples of Series I showed high hardness while the impact toughness is extremely small. Samples of the Series II showed a slight reduction in hardness while the impact toughness is greater than the toughness of Series I. Hardness of the samples of Series III follows this trend and is slightly lower than the Series I and II, while the impact toughness slightly increased compared to Series I, and for Series II. Series IV showed the best properties. Hardness is reduced compared to Series III but is still satisfactory, while the increasing added the impact strength is significant.

It is well known that these materials have extremely high hardness but their impact toughness is very small, so their use is limited. From this research added can be concluded that the composition of the steel with 3% of vanadium have impact strength which is, for this type of material added is extremely high, while the hardness decreased slightly but remained at an acceptable level. These mechanical properties enable new applications of steel with chemical composition corresponding to Series IV.

6. REFERENCES

[1] Vodopivec F., Šuštatrčić B., Vojvodić T. J., Kosec G., Charpy notch toughness and hardness of reheated martensite and lower bainite, Metalurgija, vol. 49, no. 3, 2010, p.149-154.

[2] Wang Y., He D., Yu C., Jiang J., Effect of vanadium on the Properties of Fe-Cr-C Hard facing Alloy, Hanjie Xuebao, Transaction of the China Welding Institution, vol. 31, no. 5, 2010, p.61-64.

[3] Radović N., Koprivica A., Glišić D., Fadel A., Drobnjak Đ., Influence of Cr, Mn and Mo on the Structure and Properties of V Micro- alloyed Medium Carbon Forging Steels, MjoM-Journal of Metalurgy, vol .16, no. 1, 2010, p.1-9.

[4] Schuman H., Metallography, translated from German, Faculty of Technology and Metallurgy, Belgrade, 1989.

[5] Radulović M., Fiest M., Peev K., Effect of Rare Earth Elements on Micro-structure and Properties of High Chromium White Iron, Materials Science and Technology, 1994, vol. 10, no. 12, 1057-62 CODEN: MSCTEP; ISSN: 0267-0836.

[6] Baker T.N., Processes, microstructure and properties of vanadium microalloyed steels, Materials Science and Technology, vol. 25, no. 9, 2009, p.1083-1107.

[7] Golubovic D., Kovac P., Savkovic B., Jesic D., Gostimirovic M.: Testing the tribological characteristics of nodular cast iron austempered by a conventional and an isothermal procedure, Materiali in tehnologije, Vol 48, No 2, pp. 293-298, 2014.

[8] Kovac, P., Gostimirovic, M., Sekulic, M., Savkovic, B., A review of research related to advancing manufacturing technology, Journal of Production engineering, Vol 12, Novi Sad 2009.

[9] Yang F., Haisheng S., Junfei F., Zhou X., An investigation of secondary carbides in the spray-formed, high alloyed Vanadis 4 stell during tempering, Elsevier, Materials characterization, vol 59, 2008, p. 883-889.

[10] Todić A. Čikara D., Todić T., Čamagić I., Influence of Vanadium on Mechanical Characteristics of Air-Hardening Steels, FME Transactions, vol. 39 no. 2, 2011 p.49-54.

[11] Ješić, D., Pulić, J., Kovač, P., Savković, B., Kulundžić, N., Application of Nodular Castings in the Modern Industry of Tribo- Mechanical Systems Today and Tomorrow, Journal of Production Engineering, Volume 17 (1), 2014, pp 55-58

Authors: **Assist. Todić Aleksandar M.Sc.[1], Prof. Pejović Branko PhD[1],, Prof. Kovac Pavel PhD[2], Prof. Ješić Dusan PhD[3], Assist. Savkovic Borislav, M.Sc.[2].**

E-mail: branko.pejovic@pr.ac.rs

[1]University of Pristina, Faculty of Technical Sciences, Kneza Milosa 7., 38220 Kosovska Mitrovica, Serbia

[2]University of Novi Sad, Faculty of Technical Sciences, Institute for Production Engineering, Trg Dositeja Obradovica 6, 21000 Novi Sad, Serbia, Phone.: +381 21 450-366, Fax: +381 21 454-495.

E-mail: pkovac@uns.ac.rs, savkovic@uns.ac.rs

[3]Tribotehnik, Croatia, Titov trg 6/4, 51000 Rijeka

***Note*: This paper presents a part of researching at the CEEPUS project and Project number TR 35015.**

Journal of Production Engineering
Vol.18 No.1
JPE (2015) Vol.18 (1) Original Scientific Paper
Adekunle, A. S. Adedayo, S. M. Ohijeagbon, I. O. Olusegun, H. D.

CHIP MORPHOLOGY AND BEHAVIOUR OF TOOL TEMPERATURE DURING TURNING OF AISI 301 USING DIFFERENT BIODEGRADABLE OILS

Received: 19 February 2015 / Accepted: 25 April 2015

Abstract: *In this study, vegetable oil was investigated for use as coolant in the turning process of mild steel using carbide cutting tool at different spindle speed and depth of cut. The result showed that the cooling ability of palm kernel oil was better than that of Jatropha oil but closer to that of soluble oil coolant which extracted heat faster from the cutting zone. The surface finish produced using vegetable oil coolants was far better compared to that of soluble oil, also Jatropha oil gave better surface finish compared to other coolants; the chips formed by vegetable oils were continuous and more ductile in nature than that produced by soluble oil coolants. Vegetable oil can be used as alternative coolant to the conventional soluble oil.*
Key words: *Jatropha oil, palm kernel oil, coolant, AISI 301, turning process*

Morfologija strugotine i ponašanje temperature alata tokom struganja čelika AISI 301 korišćenjem različitih biorazgradivih ulja. *U okviru ovog rada je ispitivana mogućnost korišćenja biljnih ulja kao sredstva za hlađenje i podmazivanje pri procesu rezanja čelika AISI 301 karbidnim alatom pri različitim brzinama obrade i dubine rezanja. Došlo se do zaključka da je sposobnost hlađenja uljem od palminih koštica bolja od Jatropho ulja i bliža je rastvorljivim uljima koji su imali mnogo bolju sposobnost hlađenja. Završna obrada pri korišćenju biljnog ulja, kao sredstva za hlađenje, je mnogo bolja u odnosu na rastvorljivo ulje, dok Jatropha ulje daje bolju završnu obradu u odnosu na ostale rashladne tečnosti. Formirana strugotina kod biljnih ulja je neprekidna i elastičnija nego kod rastvorljivih ulja. Biljno ulje se može koristiti kao alternativno sredstvo za hlađenje pri konvencionalnim obradama.*
Ključne reči: *Jatropha ulje, ulje palminih koščica, tečnost za hlađenje i podmazivanje, čelik AISI 301, struganje*

1. INTRODUCTION

The introduction of vegetable oil based coolant in machining applications has made it possible to achieve large increase in overall performance. About two-thirds of all coolant applications involve mineral oil-based products, about one third of the applications use synthetic products, and just a few percent of the applications use vegetable oil based coolant [1]. Mineral oil based coolants are used during machining for various reasons such as improving tool life, reducing work-piece thermal deformation and improving surface finish, but it is not biodegradable nor hazardous to human health but causes environmental pollution and also incurs a major portion of the total manufacturing costs for waste treatment. [2, 3. 4]. The growing demand for biodegradable materials has opened an avenue for using vegetable oils as an alternative to conventional soluble oil coolants. Measurements made during metal cutting show that 97% of the energy expended in cutting metals is converted into heat [5]. When left uncontrolled in the absence of a coolant, it may result in the following: cutting tool losing its hardness, increase in thermal deformation of work piece, heat build-up in the work piece makes control of size tolerances impossible and could result in decolouration. To avoid the situation mentioned above, coolant must be employed when machining. Recent development in metal coolants industries has helped in the machining of difficult-to-cut materials e.g. stainless steels and composites materials. The key limitations in the machining of these materials include friction, vibration, energy consumption and the temperature at the cutting zone [6]. Invariably, all these cause tool wear. Therefore, coolants are used to annul the negative effect of heat and friction, improve surface finish, provide boundary lubrication between chips and tools and flush away chips in the cutting area [7]. For a typical machining operation, the coolant's and heat transfer performance properties are crucial in achieving a successful result. To reduce the heat generated during machining, it is important to provide the means of controlling its development and minimizing its detrimental effects on the cutting process [8,9]. Using vegetable oil technology as coolant has been shown to deliver considerable advancements in productivity and longer tool life. Likewise, vegetable oil-based coolants during machining can achieve surface finishes and dimensional tolerances with comfortable margins, yielding a process capability that makes for consistent, eventful machining with opportunities for increased production rates [10]. Newer vegetable-based green coolants can offer as much lubricity as standard oil-based products, but the coolants tend to cost more, often up to double the price of oil-based lubricants [11, 12].

Turning is a most commonly used machining process in manufacturing. Therefore, favourable selection of cutting parameters to satisfy profitable objective within the constraints of turning operations is a very important task [13,14]. A significant number of studies

have investigated the general effects of the speed, feed, and depth of cut on the turning process [15, 16]. Swarup and Pradip [17] worked on surface quality during high speed machining using karanja oil and neem oil as eco-friendly cutting fluid. Their performances were compared with that of conventional soluble oil. The study showed that surface roughness was much better using vegetable oil based cutting fluid with increasing rate of feed or depth of cut variation compared to dry machining or machining with conventional cutting fluid. But cooling capacity slightly deteriorated for vegetable oil based cutting fluids than conventional cutting fluid. Ulrich [18] work showed that new water based grinding fluid formulation was able to meet both the performance and environmental requirements for grinding. The new fluid concept consisting of a high concentration (up to 40%) of sulfonate vegetable oil in water was proposed and tested. In this way it was possible to combine high lubricity, better heat conductivity and good environmental properties in one fluid. Moreover, Wisley et al. [19] in his research work "vegetable oil-based coolants improve cutting performance" showed that vegetable oil technology gave considerable advancements in productivity and longer tool life. Using vegetable oil-based coolants during machining achieved surface finishes and dimensional tolerances with comfortable margins, yielding a process capability that made for consistent, uneventful machining with opportunities for increased production rates. Abhang and Hameedullah [20] in their work tagged "Chip-Tool Interface Temperature Prediction Model for Turning Process", showed that sunflower oil a vegetable based coolant reduced surface roughness and cutting forces better than other mineral based oil used.

This work is aimed at investigating the possibility of using palmkernel oil and Jatropha oil as an alternative coolant to soluble oil during continuous turning process of AISI 301 on a lathe machine by determining: the temperature generated at the cutting zone when different oils are used as coolant at different cutting speeds and depth of cut on the work piece, the effect of oil coolants on the chips morphology in the range of cutting speeds from 80 rpm to 260 rpm and the effect of coolants on the surface finish of the work piece after turning operation.

2. MATERIAL AND METHOD

Mild steel with chemical composition shown in Table1 was used for the experiment. The tool material used was a round half carbide cutting tool soldered on a mild steel holder. The mild steel holder was bored through and tapped at a point very close to cutting edge of the carbide tool before soldering. A thermocouple of 0-600^{o}C was tightly screwed into the tapped hole until the tip of the thermocouple made a direct contact with the carbide tool. Unrefined vegetable oils of groundnut oil and melon oil were used as alternative coolants to the conventional soluble oil during machining. The vegetable oils were obtained from the south-western region of Nigeria, while the mild steel was obtained from Federated Steel Limited, Otta, Ogun State, Nigeria. The major test parameter used to investigate the performance of the vegetable oil as cutting fluid were temperature at cutting zone, spindle speed and chip thickness. Mild steel bar of diameter 35mm and length 120mm was prepared for machining using conventional soluble oil, palmkernel oil and Jatropha oil as coolants. During machining, various spindle speeds of 80, 108, 190 and 260 rpm were investigated at depths of cut of 0.4, 0.6, 0.8, 1.0 and 1.2 mm. The temperature of heat generated between the surface of work piece and the carbide tool was captured during turning operation using a 3 channel SD card data lodger thermometer monitor of model number MTM-380SD connected via the thermocouple at a time interval of 5 seconds Figure 1.

Fig. 1. Experimental setup

During machining, coolants were applied using dripping method at a constant rate of 0.28cm^3/s. Maximum temperature for each reading was taken, while the chips morphology were analyzed in the range of cutting speeds from 80 rpm to 260 rpm and various depth of cut . The work piece was then removed and labelled against the spindle speed and the specific coolant used. The procedure highlighted above was used for dry cut, conventional soluble oil, palmkernel oil and Jatropha oil in order to compare the effectiveness of the coolants. The deformed chip thickness was measured by micrometer. The composition of the base metal was determined using an Atomic Absorption Spectrometer. The tests carried out on the mild steel metal showed the following percentage composition as given in Table 1.

Components	Fe	C	Si	Mn
Composition (wt%)	99.200	0.131	0.140	0.347
Components	Ni	Cu	Al	Ti
Composition (wt%)	0.004	0.038	0.004	0.016
Components	P	Cr	Co	Sn
Composition (wt%)	0.015	0.013	0.001	0.001

Table 1. Chemical composition of the mild steel used

3. RESULTS AND DISCUSSION

The result obtained showed that temperature at the cutting zone increased with increase in depth of cut and spindle speed irrespective of the coolant used, Figure 2 to Figure 4.

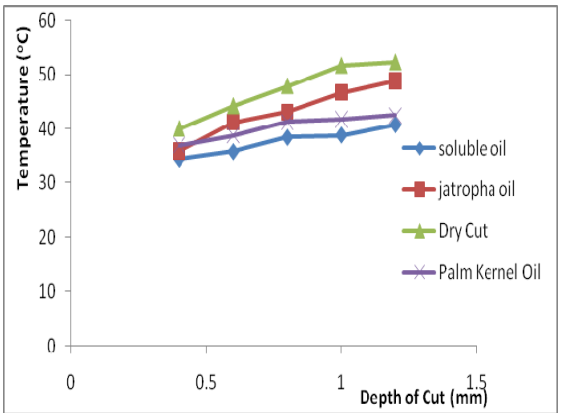

Fig. 2. Temperature variation at spindle speed of 80 rpm

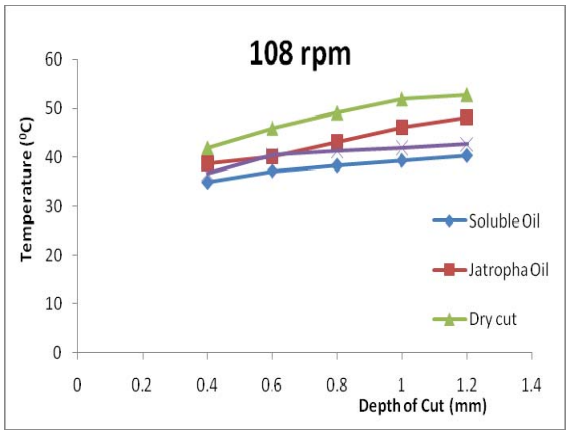

Fig. 3. Temperature variation at spindle speed of 108 rpm

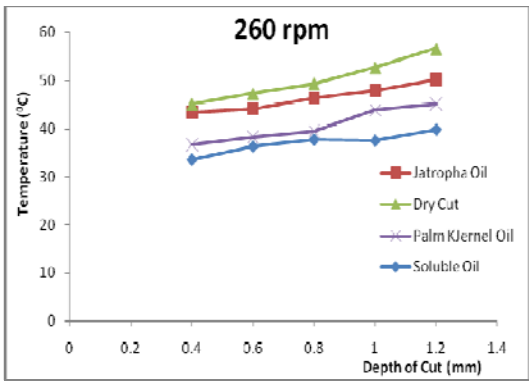

Fig. 4. Temperature variation at spindle speed of 260 rpm

The temperature generated in dry cut machining was higher at all speeds however, soluble oil removed heat better than all other coolants at low, medium and high spindle speeds of 80, 108, 260 rpm respectively. At lower spindle speeds, palm kernel oil absorbed heat better than jatropha oil; the amount of heat absorbed by palm kernel was almost the same as soluble oil; indicating that the property of palm kernel oil was similar to that of soluble oil at 80rpm and 108rpm. At higher spindle speed and higher depth of cut, the property of palm kernel oil changed and its performance declined with increase in depth of cut as shown in Figure 4. which gave rise to higher temperature. Surface roughness examination showed that vegetable oil coolants gave better surface finish than soluble oil coolant. However, jatropha oil gave the best surface finish on the work piece.

It is observed from Fig 5- Fig 8 that the nature of chips obtained are different forms of continuous and discontinuous chips. The chips formed in dry machining are snarled ribbon, snarled washer, snarled tubular and long ribbon at spindle speed of 80, 108, 190 and 260 rpm respectively. Snarled tubular and long ribbon chips are obtained at moderate cutting speed, feed rate and high depth of cut. The burnt, discontinuous and black coloured chips obtained in dry machining indicates the temperature developed in cutting zone is high. Using palmkernel oil and Jatropha oil as coolant most of the chips obtained are snarled ribbon and snarled helical washer at low cutting speeds Fig 5 and Fig 6.

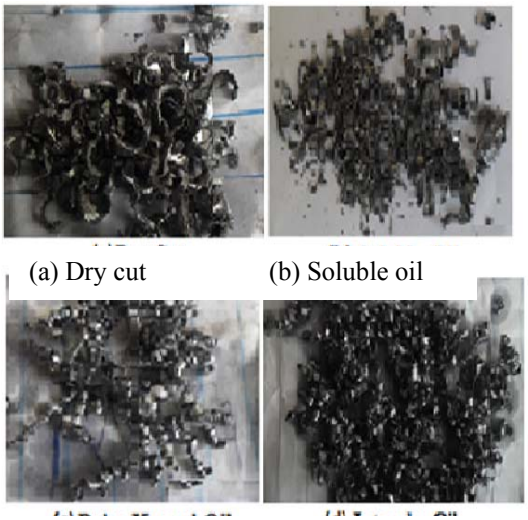

(a) Dry cut (b) Soluble oil

(c) Palm Kernel oil (d) Jatropha oil

Fig. 5. Chips formation at spindle speed of 80 rpm

(a) Dry cut (b) Soluble oil

(c) Palm Kernel oil (d) Jaropha oil

Fig. 6. Chips formation at spindle speed of 108 rpm

Long helical washer and long tubular chips are obtained at cutting spindle speed of 190 rpm and moderate depth of cut Fig 7. At high cutting spindle speed of 260 rpm snarled conical helical and long tubular chips are obtained for palmkernel and Jatropha oil respectively Fig 8.

(a) Dry cut (b) Soluble oil

(c) Palmkernel oil (d) Jaropha oil

Fig. 7. Chips formation at spindle speed of 190 rpm

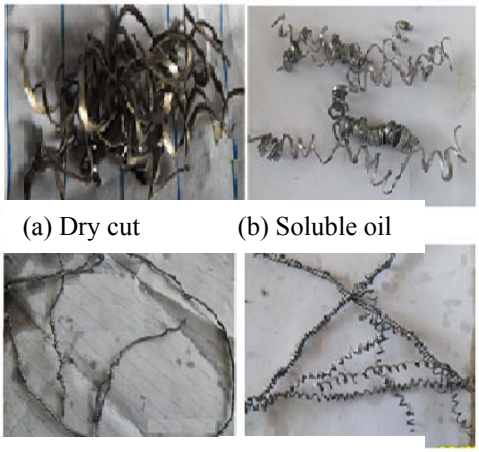

(a) Dry cut (b) Soluble oil

(c)Palmkernel oil (d) Jatropha oil

Fig. 8. Chips formation at spindle speed of 260 rpm

The different chips formed was due to different cutting conditions; different normal and frictional forces at tool and chip interface and also different coefficient of friction developed at chip and tool interface under different machining environmental conditions. Physical observation showed that the back surface of chips for dry cut and soluble oil is rough which was as a result of high surface roughness on machined surface. But the back surface of chips obtained using palmkernel oil and Jatropha oil as coolant appeared much brighter and smoother, which indicates that the surface roughness on machined surface is less. The deformed chip thickness measured by micrometer was as shown in Table 2 and the result indicated that the chips thickness increases as depth of cut increases irrespective of the cutting fluid used. Jatropha oil as coolant caused oxidation on the work piece surfaces which may be attributed to its high percentage moisture content.

Coolant	Spindle speed rpm	Dept of cut (mm)	Chips thickness (mm)
Dry cut	80	0.4	0.125
	80	0.8	0.132
	80	1.2	0.157
	108	0.4	0.138
	108	0.8	0.144
	108	1.2	0.167
	260	0.4	0.158
	260	0.8	0.166
	260	1.2	0.172
Soluble oil	80	0.4	0.125
	80	0.8	0.131
	80	1.2	0.155
	108	0.4	0.137
	108	0.8	0.144
	108	1.2	0.166
	260	0.4	0.158
	260	0.8	0.166
	260	1.2	0.171
Palmkernel oil	80	0.4	0.125
	80	0.8	0.132
	80	1.2	0.157
	108	0.4	0.138
	108	0.8	0.144
	108	1.2	0.167
	260	0.4	0.158
	260	0.8	0.165
	260	1.2	0.172
Jatropha oil	80	0.4	0.125
	80	0.8	0.132
	80	1.2	0.157
	108	0.4	0.138
	108	0.8	0.144
	108	1.2	0.167
	260	0.4	0.158
	260	0.8	0.166
	260	1.2	0.172

Table 2. Measured chip thnikness for different coolant

4. CONCLUSION

The cooling ability of palm kernel oil was better than that of jatropha oil and closer to that of soluble oil coolant which absorbed heats the most from the cutting zone. The good cooling ability of palm kernel oil over jatropha oil may be attributed to its higher kinematic viscosity. Surface roughness examination of the machined surfaces revealed that the surface finish produced using vegetable oil coolants was better compared to that of soluble oil; however, jatropha oil gave better surface finish than the other coolants used. The chips formed by vegetable oils were continuous and more ductile in nature than that produced by soluble oil coolants and dry cut machining. The continuity or discontinuity of chips solely depend on the spindle speed and the lubricity of the oil used in machining. During machining, vegetable oil coolants produced less wear on the cutting tool compared to soluble oil as coolant thereby prolonging the tool life. Also the volume of vegetable oil used in cooling was

less than that of conventional coolant which was in the ratio 2:3. The cooling capacity of conventional oil was better than that of raw vegetable oil coolants, but vegetable oils could be used as alternative coolant during machining for longer tool life, better surface finish, minimum volume expended and continuous chip flow.

5. ACKNOWLEDGEMENT

Our sincere appreciation goes to Mr V. O. Ayegbusi, J. T. Oloruntoba, S. F. Olorunshola and Mr S. Arinde
for their understanding and assistance in making these work a success.

6. REFERENCES

[1] Bashi, S. M., Abdullahi U. U., Robia, Y., Amir N. *Use of natural vegetable oil as alternative Dielectric transformer coolants*. International Journal of Engineers, Malaysia, Vol. 67(2), pp 1-9, 2006.

[2] Salete, M. A., João, F. G.O. *Vegetable based cutting fluid – an environmental alternative to grinding process* pp1, 2008, Accessed Nov., 2012 from www.notox.com.br/pdf/artigol01.pdf

[3] Emel, K.M., Huseyin, C., Babur O., Erhan, D. *Performance analysis of developed vegetable-Based coolant by D-optimal design in turning process*. International Journal of Computer Integrated Manufacturing, Vol. 25(12), 2012.

[4] Wilson, M. *Insulating Liquids:Their Uses, Manufacture and Properties*, Stevenage, U.K: Peregrinus. 1980.

[5] Olusegun Adegbuyi P., Lawal G., Oluseye O.,Odunaiya G. *Analysing the effect of cutting fluids on the mechanical properties of mild steel in a turning operation*, American Journal of Scientific and Industrial Research, Vol 2(1), pp 1-10, 2011.

[6] Kramar, D., Sredanović, B., Globočki - Lakić, G., Kopač, J. *Contribution to universal Machinability definition*, Journal of Production Engineering, Vol. 15(2), 2012.

[7] Blaser, S. *Vegetable oil-based coolants improve cutting performance*, 2002. www.blaser.com/download/Dec02.pdf, Accessed on 12th November, 2012.

[8] Jeffrey B. D and Timothy, G. G. *An environmental analysis of machining*, ASME International Mechanical Engineering Congress and RD&D Expo November 13-19, 2004.

[9] Mangesh, R. Phate, Tatwawadi, V.H. *Ann based model for prediction of human energy in convenctional machining of nonferrous material from indian industry prospective*, Vol. 17(1), pp 1-6, 2014.

[10] Hamdan, A., Fadzil, M., Abou-El-Hossein, K.A., Hamdi, M. *Performance evaluation of different types of cutting fluid in the machining of AISI 01 Hardened Steel using Pulsed Jet minimal quantity lubrication system*, pp1-8, 2008.

[11] Patric, W. *Green coolant technologies advance*, Journal of Society of Manufacturing Engineers. 2012. http://www.sme.org. Checked on August 13th 2013.

[12] Ojolo, S.J., Amuda, M.O.H., Ogunmola O.Y., Ononiwu, C.U. *Experimental determination of the effect of some straight biological oils on cutting force during cylindrical turning*, Materia (Rio de Janeiro) vol.13(4), 2008, *On-line version.Accessed November 2012.*

[13] Tanveer, H. B. and Imtiaz, A**.** *Optimization of cutting parameters in turning process*, Journal of Production Engineering, Vol. 16(2), 2012.

[14] Atul, K. Sudhir, K. and Rohit, G. *Statistical modeling of surface roughness in turning Process*, International Journal of Engineering Science and Technology (IJEST) Vol. 3(5), pp 4246-4252, 2011.

[15] Komanduri, R. And Brown, R. H. *The mechanics of chip segmentation in machining*, Journal of Engineering for Industry, Vol. 103, pp: 33-51, 1981.

[16] Iwona, P., Christina, B., Hamid, R. K. and Peter, M. *Mathematical model of micro turning process*, International Journal of Advanced Manufacturing Technology, pp. 33–40, 2009.

[17] Swarup, P. and Pradip, K. P. *Study of surface quality during high speed machining using Eco-friendly cutting Fluid*, http://www.mechin.com/journal/archive/20011 checked on 3rd June 2013.

[18] Ulrich, K. *Vegetable oil-based coolants improve cutting performance*, Journal of cutting fluids, htt://www.blaser.com/download/Dec02.pdf, 2002, Checked on August 9th 2013.

[19] Wisley, F. S., Álisson, R. M. and Anselmo, E. D. *Application of cutting fluids in machining processes,* Journal of the Brazilian Society of Mechanical Sciences vol.23, 2001, http://www.scielo.br/scielo.php?pid accessed on 13th November, 2012.

[20] Abhang, L. B and Hameedullah, M.: *Chip-tool interface temperature prediction model for turning process*, International Journal of Engineering Science and Technology, Vol. 2(4), 385-386, 2010.

Authors: **Lecturer. Dr. Adebayo S. Adekunle,** University of Ilorin, Department of Mechanical Engineering, P.M.B. 1515, Ilorin, Nigeria. Phone: 2348033591465, e-mail: adekunlebayor@gmail.com
Associate Professor. Dr. Segun M. Adedayo, University of Ilorin, Department of Mechanical Engineering, P.M.B.1515, Ilorin, Nigeria. Phone: 234-8033821984, e-mail: amsegun@unilorin.edu.ng
Senior Lecturer. Dr. Idehai O. Ohijeagbon, University of Ilorin, Department of Mechanical Engineering, P.M.B.1515, Ilorin, Nigeria. Phone: 234-7030092411, e-mail: idehaiohi@yahoo.com
Professor. Prof. Henry D. Olusegun, Federal University of Technology Minna, Department of Mechanical Engineering, Minna, Nigeria, e-mail: olusegunhenry@yahoo.com

Journal of Production Engineering
Vol.18 No.1
JPE (2015) Vol.18 (1) Original Scientific Paper
Lanc, Z., Zeljković, M., Štrbac, B., Živković, A., Drstvenšek, I., Hadžistević, M.

THE DETERMINATION OF THE EMISSIVITY OF ALUMINUM ALLOY AW 6082 USING INFRARED THERMOGRAPHY

Received: 26 May 2015 / Accepted: 30 June 2015

Abstract: *The emissivity of a given surface is the measure of its ability to emit radiation energy in comparison to a blackbody at the same temperature. The emissivity of an object depends primarily on the type of material and its surface properties. In this paper we propose to investigate the influence of temperature and surface roughness on emissivity of 4 diffrent samples of aluminum alloy AW 6082 using infrared thermography. The results show that emissivity of mentioned alloy decreases with increasing temperature in range between 50 and 200°C and also manly decreases with increas of surface roughness in the wavelength range between 8 and 14 µm.*
Key words: *emissivity, infrared thermography, AW 6082*

Određivanje koeficijenta emisivnosti aluminijumske legure AW 6082 korišćenjem infracrvene termografije. *Emisivnost posmatrane površine predstavlja meru njene sposobnosti da emituje toplotu u poređenju sa crnim telom pri istoj temperaturi. Emisivnost tela najviše zavisi od vrste materijala i njenih površinskih svojstava. U okviru ovog rada predložena je mogućnost određivanja uticaja temperature i površinske hrapavosti na emisivnost 4 različita uzorka aluminijumske legure AW 6082 uz pomoć infracrvene termografije. Rezultati pokazuju da emisivnost pomenute legure opada sa porastom temperature u opsegu od 50 do 200°C i takođe uglavnom opada sa povećanjem površinske hrapavosti u opsegu talasnih dužina između 8 i 14 µm.*
Ključne reči: *emisivnost, infracrvena termografija, AW 6082*

1. INTRODUCTION

Most processes in aluminum industry (e.g., rolling, forging, extrusion, etc.) are highly temperature-dependent. During extrusion, for example, accurate temperature measurements are necessary during melting, casting, heating of billets, and profile pressing in order to achieve the desired microstructure and product quality. Accurate and precise determination of the alloy temperature has a strong bearing on both process control and final product quality. Achieving a superior microstructure and mechanical properties, and hence the aforementioned desired attributes, relies heavily on the ability to accurately measure alloy temperature at virtually every stage of an aluminum fabrication process. Therefore, accurate temperature determination and control are of paramount importance in the quest for superior alloys, lower cost and reduced waste [1, 2].

In the aluminum industry different types of temperature sensors are used, including direct contact probes and radiation thermometers. While they are still widely used, direct contact thermocouples and thermisters can mar the aluminum surface, besides being difficult to implement with parts in fast transit (e.g. extrusions), where the fast transit of extruded parts often reduces the accuracy of contact sensors to no better than 10 K. These situations require the use of noncontact infrared thermography for temperature measurement [3].

The infrared thermography represents a non-contact temperature measurement method, which allows monitoring of thermal phenomena on the surface in real time. This method is suitable for industrial process control, due to the ability to perform spatial and temporal thermal analysis of the observed surface [4].

One of the most efficient devices for contactless temperature measurement is certainly infrared or thermovision camera. Thermal imaging camera records the intensity of the infrared radiation emitted by the real body according to its own temperature and emissivity. The blackbody is an ideal emitter, meaning that no surface can emit more radiation than a blackbody at the same temperature. Therefore the blackbody represents a reference in describing emission from a real surface. We define emissivity as the ratio of the radiation emitted by the surface to the radiation emitted by a blackbody at the same temperature [5]. The emissivity is crucial for thermographic measurements, since without knowing the emissivity of the object it is not possible to determine the true value of its temperature.

The emissivity of aluminum depends on many factors, such as the chemical composition of the alloy, surface finish quality, heating time, temperature, emission angle and wavelength of the radiation [6]. In general, metals have low emissivity and is therefore difficult to correctly determine their temperature using infrared technique.

Because the emissivity of metals depends on the surface roughness and the temperature at which the measurement is performed, many authors have tried to determine the relationship between emissivity and the parameters mentioned above.

Wen and Mudawar have done several cases where they showed that the emissivity of 4 different

aluminum alloys: AW 1100, AW 7150, AW 7075 and AW 2024 manly decreases appreciably between 2.05 and 3.5 μm, and increases slightly between 3.5 and 4.72 μm. Authors also showed that emissivity decrease between 600 i 700 K and rises between 700 i 800 K, while, generally speaking, emissivity increases with the increase of surface roughness [1,3].

Albatici and others have proposed a novel instrumentation called The Infrared Thermovision Technique Emissometer (ITT-emissometer), for the measurement of thermal emissivity of aluminum at temperatures of 100, 175 and 250°C. The resulting value were 0.368, 0.416 and 0.418, respectively [7]. Valiorgue and others have made a calibration device for determining emissivity, which used thermal imaging camera to determine emission curve for steel 316L. It is shown that emissivity of the steel increases between 100 and 200°C, after which it decreases to about 400°C [8].

The aim of this paper is to experimentally determine the emissivity of aluminum alloy AW 6082 using infrared camera for different values of the surface quality and temperature of the 4 aluminum workpiece.

2. EXPERIMENTAL METHODS

In this study four aluminum workpiece made of alloy AW 6082 with different surface roughness were examined. Each workpiece is individually heated in a furnace at 4 different temperatures. The value of the heating temperature was monitored on-line by means of three thermocouples that were attached to the front and back side of the workpiece.

During the heating time furnace door were closed. After reaching the aforementioned temperature, the oven door were opened, and thermovision camera had recorded the intensity of the infrared radiation emitted by the observed sample.

Obtained thermographic images were analyzed in the software *Guide IrAnalyser*, in which by setting the coefficient of emissivity from 0 to 1 temperature of workpiece changes until it reaches value shown by thermocouple on a front side of observed sample.

2.1 Experimental setup

During the experiment, aluminum samples were heated up in furnance in front of which was set a thermal camera at a distance of 1 m. The samples were individually tested. Each sample is placed vertically within the furnace, so that the heating is carried out evenly from all sides. The sample temperature was measured by a thermocouple type K, which were derived through a manhole furnace to manually contact thermometer *PCE - T395*.

Two thermocouples were attached on the back side of the workpiece by two metal plates and screws, so that thermocouple beads are equidistant from the center of the sample, on the left and right side. The third thermocouple was placed on the front, right side of the sample and its contact with the workpiece was secured with live rubber.

Experimental setup is shown in Fig. 1. Because of the the appearance of reflection due to the furnace heater radiation and possibility of getting the error in the result of measurement, the furnace is coated within with a black sheet which represented a simulation of a black body.

Fig. 1. Experimental setup

Emissivity tests have been performed using a thermal camera *ThermoPro*^{TM} *TP8S*, with a spectral sensitivity of 8/14 μm (infrared thermal wavelength range) and field of view: 30.1 × 21.6° (320 × 240 pixels).

2.2 Aluminum specimens

Aluminium alloy 6082 is a medium strength alloy with excellent corrosion resistance. It has the highest strength of the 6000 series alloys. This alloy is also known as a structural alloy and in a plate form is most commonly used for machining. Chemical composition of the AW 6082 is given in Table 1.

Si	Fe	Cu	Mn	Mg	Zn	Ti	Cr
0.7			0.4	0.6			
1.3	0.5	0.1	1.0	1.2	0.2	0.1	0.25

Table 1. Chemically composition of AW 6082

Square samples 150 mm × 150 mm with a 10 mm thickness have been prepared. To investigate the effects of surface roughness, the samples were treated with two different surface finishes: grinding and milling. One aluminum sample was processed by grinding machine, while the rest of the samples were processed by milling machine.

Machining process	Roughness Ra [μm]	Sample label
Grinding	1.07	G. 1
Milling I	1.55	M. 1
Milling II	1.25	M. 2
Milling III	1.77	M. 3

Table 2. Characteristics of the sample

The average surface roughness (R_a) was selected as a characteristic of surface finish for each sample and it was measured with the use of contact profilometer. Arithmetic average roughness, or R_a, represents arithmetic average height of roughness-component irregularities (peak heights and valleys) from the mean line, measured within the sampling length, L.

R_a was measured on nine points uniformly distributed on the front side of aluminum workpiece. Obtained values are given in Table 1.

2.3 Experimental procedure

During the experiment each of the 4 aluminum samples was heated separately in furnace to a temperature slightly above the desired value. Once the sample temperature reached steady state, both the intensity and temperature data were recorded by the infrared camera. This procedure was repeated for each sample at temperatures of 50, 100, 150 and 200°C.

Concurrently, the sample temperature was monitored online by the thermocouple with the aid of a digit thermometer. Before taking the thermographic picture of the observed sample a non-uniformity calibration was performed on camera. Non-uniformity calibration allows the automatic adjustment of the camera's detector to ensure normalization and sharpness of the image.

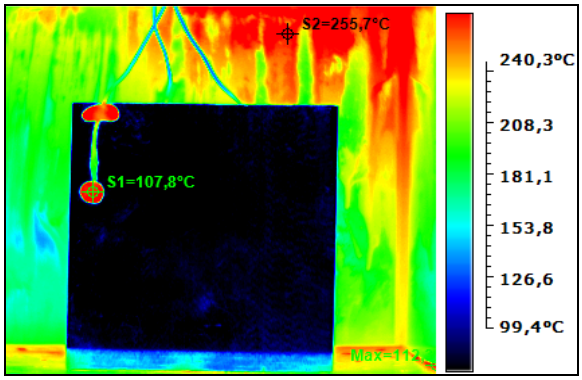

Fig. 2. Thermogram of G.1 sample at 100°C

As mentioned before, thermovision camera can detect infrared radiation emitted by an object. The images they produce are called thermograms. False colours are added to a thermogram to give an indication of how hot each object in the image is, where the hottest parts are coloured white, yellow or red and the coldest parts are coloured purple, dark blue or black. In the thermogram shown on Fig. 2, the walls of the furnace are the hottest parts and the aluminum sample are much colder.

3. RESULTS AND DISCUSSION

3.1 Temperature effects

Aluminum alloys represent serious challenges to the implementation of infrared thermography because of their complex spectral emissivity behavior. As we can see from Table 3. emissivity of the samples varies within certain limits with rising temperature.

T [°C]	ε (G.1)	ε (M.1)	ε (M.2)	ε (M.3)
50	0.19	0.16	0.25	0.12
100	0.18	0.15	0.17	0.09
150	0.16	0.14	0.11	0.08
200	0.15	0.12	0.10	0.07

Table 3. Emissivity of the samples at different temperatures

Fig. 3 represents emissivity distributions for $8 < \lambda < 14$ μm for AL 6082 samples with different surface finishes at 50, 100, 150 i 200°C. The emissivity of aluminum samples generally decreases between 50 i 200°C, for all 4 aluminum samples, contrary to the trend of increasing emissivity with increasing temperature for most metallic surfaces.

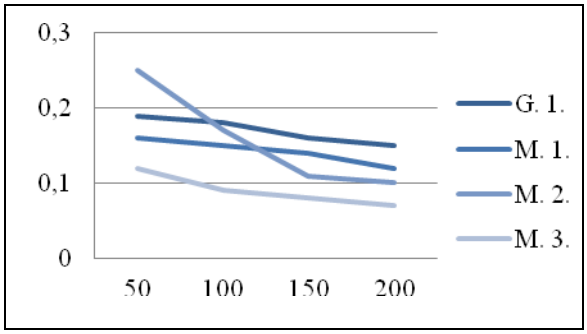

Fig. 3. Temperature effects

Fig. 3 also shows that the highest emissivity was measured at 50°C for the G.1 sample (ε = 0.25), while the lowest emissivity was measured at 200°C for the M.3 sample (ε = 0.07).

3.2 Effects of surface roughness

Fig. 4 compare the measured emissivity values at 50, 100, 150 and 200°C for the aluminum samples and it shows general similarities among the emissivity spectra.

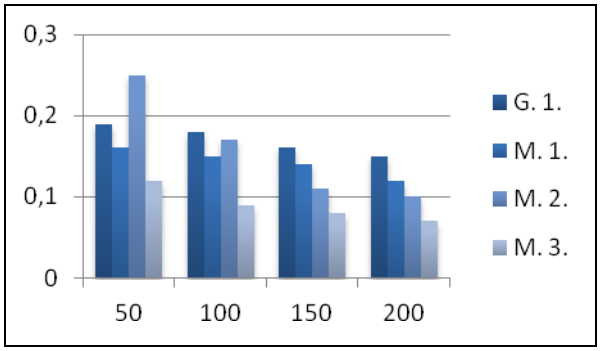

Fig. 4. Effects of surface roughness

At 50 and 100°C, the emissivity is highest for M.2 sample, while the M.3 has the lowest one. The emissivity variations are less pronounced at 150 and 200°C. For all four temperatures, the M.3 sample does not exhibit the expected trend for most metallic surfaces in the infrared range of monotonically decreasing emissivity with increasing temperature.

4. CONCLUSION

This study explored the relationship between the emissivity of aluminum alloy surface roughness and temperature. Based on the presented results, it is concluded that the emissivity of AW 6082 aluminum alloys decreases with increasing temperature in the temperature range from 50 to 200°C and decreases with increasing roughness from 1.07 to 1.77 μm in the spectral range from 8 to 14μm. The values of the emissivity are in the range from 0.07 to 0.3, which is in good correlation with the results of other authors [1,2].

Because of its complex emission behavior, determining the temperature of aluminum with the aim of infrared thermography can be problematic. Given the fact that we can not find the table for the emissivity of aluminum depending on the temperature, roughness and types of alloys in the literature, the issue can become more complicated.

In addition to the above, during thermography tests it must be taken in consideration the influence of other heat sources, because aluminum is highly reflective material. These parazite radiation can lead to significant errors in the measurement.

Therefore in future research, the authors will try to determine the emissivity of different aluminum alloys using thermal imaging tecnique at higher temperatures and more severe controlled laboratory conditions, in order to minimize the impact of the surrounding heat sources. One of the suggestions for further investigations is to use samples of smaller size, in order to acheveing highly uniform temperature of the sample.

5. REFERENCES

[1] Wen, C., Mudawar I.: *Emissivity characteristics of roughened aluminum alloy surfaces and assessment of multispectral radiation thermometry (MRT) emissivity models,* International Journal of Heat and Mass Transfer, Vol. 47, p.p. 3591-3605, avgust 2004.

[2] Wen, C., Mudawar I.: *Emissivity characteristics of polished aluminum alloy surfaces and assessment of multispectral radiation thermometry (MRT) emissivity models*, International Journal of Heat and Mass Transfer, Vol. 48, p.p. 1316-1329, mart, 2005.

[3] Wen, C., Mudawar I.: *Modeling the effects of surface roughness on the emissivity of aluminum alloys*, International Journal of Heat and Mass Transfer, Vol. 49, p.p. 4279-4289, novembar, 2006.

[4] Iniewski, K.: *Smart Sensors for Industrial Applications*, CRC Press, Boca Raton, 2013.

[5] Incropera, F., Dewitt, D.: *Fundamentals of Heath and Mass Transfer*, John Wiley and Sons, New York, 2002.

[6] Bently, E.: *Temperature and Humidity Measurement*, Springer Science & Business Media, Lindfield, 1998.

[7] Albatici, R., Passerini, F., Tonelli, A., Gialanellac, S.: *Assessment of the thermal emissivity value of building materials using an infrared thermovision technique emissometer*, Energy and Buildings, Vol. 66, p.p. 33-40, juli, 2013.

[8] Valiorgue, F., Brosse, A., Naisson, P., Rech, J., Hamdi, H., Bergheau, J.: *Emissivity calibration for temperatures measurement using thermography in the context of machining*, Applied Thermal Engineering, Vol. 58, p.p. 321-326, april, 2013.

Autori: **M.Sc. Zorana Lanc, M.Sc. Branko Štrbac, prof. dr Miodrag Hadžistević, prof. dr Milan Zeljković, doc. dr Aleksandar Živković.** Univerzitet Novi Sad, Fakultet Tehničkih Nauka, Institut za Proizvodno mašinstvo, Trg Dositeja Obradovića 6, 21000 Novi Sad, Serbia, Tel: +381 21 485 2306, Fax: +381 21 454-495.

e-mail: zoranalanc@uns.ac.rs; strbacb@uns.ac.rs miodrags@uns.ac.rs; milanz@uns.ac.rs acoz@uns.ac.rs

Prof. dr Igor Drstvenšek, Univerzitet u Mariboru, Strojnički fakultet, Smetanova 17, SI- 2000 Maribor, Slovenija, Tel: +386 2 220 75 93.

e-mail: drsti@uni-mb.si

Journal of Production Engineering
Vol.18 No.1
JPE (2015) Vol.18 (1) Original Scientific Paper
Gostimirović, M., Kovač, P., Radovanović, M., Madić, M., Krajny, Z.

MODULAR DESIGN OF UNCONVENTIONAL CUTTING MACHINE TOOLS

Received: 20 January 2015 / Accepted: 28 March 2015

Abstract: *Modular design provides development and implementation in different stages of the products during the whole life cycle. In this paper, based on the principle of modular design, an unconventional cutting machine concept is presented. The modular design strategy of the unconventional machine includes water jet, laser beam and plasma arc cutting. The developed modular system of the unconventional cutting machine and its modules are illustrated as an example. The result is a competitive cutting machine which gives a sustainable market solution and answering customer requirements for various options with reduced expenses of the manufacturing.*
Key words: *unconventional machining processes, cutting, modular design*

Modularni dizajn nekonvencionalnih mašina za sečenje. *Modularni dizajn omogućava razvoj i izgradnju različitih faza proizvoda tokom celog životnog ciklusa. U ovom radu je prikazan koncept nekonvencionalne mašine za sečenje koristeći osnovne principe modularnog dizajna. Strategija modularnog dizajna nekonvencionalne mašine obuhvata obradu sečenjem vodenim mlazom, laserom i plazmom. Primer razvijenog modularnog sistema nekonvencionalne mašine za sečenje je prikazan sa osnovim modulima. Rezultat je konkurentna mašina za sečenje koja daje održivo tržišno rešenje i odgovara na različite zahteve kupaca sa smanjenim troškovima proizvodnje.*
Ključne reči: *nekonvencionalni postupci obrade, sečenje, modularni dizajn*

1. INTRODUCTION

Today's manufacturing is facing ever-growing requests on a daily basis. System flexibility, productivity, quality, reliability and cost savings of manufacturing are the most vital requests facing the market-oriented company. If manufacturing firms are to meet these high market requests, the imperative is to adopt new production methods.

Modular design method is one of the significant solutions to realize modern product solutions. The concept was first presented by Star in 1965 [1], where the use of modular product in manufacturing processes was proposed. This is an issue that was constantly investigated and today modular design concept has been presented in many fields of design and manufacturing.

In this work is presented investigation of the modular design of machine tools for unconventional machining processes in terms of cutting operations. The objective of this research is to investigate development trends of the modular design of unconventional machines for Water Jet Cutting (WJC), Laser Beam Cutting (LBC) and Plasma Arc Cutting (PAC)

.

2. MODULAR DESIGN

Modular design is simple, flexible and reliable construction method, which modernized production by introducing more efficient ways to build the products, especially those with many complex parts and assemblies. The modular design is a new trend of designing complex systems as a series of standalone objects. Each of these can be built by themselves and stand on their own until the system is ready to accept them. It involves separating a product into definable smaller units.

2.1 Benefits of the modular design

Modular design has many benefits. The modular design is economical because it allows production of safe parts which find their way into a strong market requests. Also, there is efficiency in production. The modular design means that it is now possible design and manufacturing implemented in parallel. This means that building the product is just a series of finished modules that come together to become a unity.

Besides reduction in cost of development, design and manufacturing, modular design offers other benefits such as adding new solution by merely plugging in a new module, reusable parts and assemblies, transparency and manageability of modules etc. An especially benefits of the modular design are standardization of components and processes.

2.2 Modular design of machine tools

Modern manufacturing systems are leading to considerable changes in the way of design and manufacture of machine tools. Bases to this change are the adoption of modular methods of machine tool construction. The benefits include shortening machine design time, improved machine reliability, reduced construction costs and simplifying service. Furthermore, modular machine tool construction is increasingly becoming an important mean of flexible manufacturing automation.

Engineering research and development into the modular design for machine tools was first launched by Koenigsberger in 1968 [2] and since then these technologies have been further advanced. Thereby, the modular principle into machine tools design has not been sufficiently studied so far in the academic sphere

but has already been developed on the basis of long standing practical experience. Various examples of modular machine design have been seen in modern manufacturing systems like machining centres, transfer lines and flexible manufacturing systems. The developing history of the modular design for machine tools can be found in [3].

In order to improve manufacturing efficiency, methods of designing machine tools must be simple and practical. In this context, it is suitable to use modular design of machine tools, in which manufacturing consists of components and controllable processes. In machine tools analysis, a module is understood as a group of elements of the system which may be used autonomously or in combination with other modules. The use of the modular design concept allows the machine tool system to be regarded as consisting of a number of modules. Thereby, modules are subsystems that functionally and structurally are independent and perform controllable executive motion in manufacturing [4-6].

3. UNCONVENTIONAL CUTTING TECHNIQUES

There can be little doubt that production technologies will remain important in today's manufacturing industry. Especially important are material cutting operations as the integral part of manufacturing and assembly processes [7-10].

Modern world largely implements cutting operations which are supported by novel technologies, which are based on completely new machining principles. These manufacturing processes are defined as a group of methods that remove the material by various techniques involving mechanical and thermal energy, but do not use a cutting tools as it needs to be used for traditional manufacturing processes. Among them are extracted unconventional technologies which produce precise and high-quality cuts on all sorts of materials: difficult to machine materials, very fragile materials, complex-shaped parts, etc. In the first place [11-13], they are Water Jet Cutting (WJC), Laser Beam Cutting (LBC) and Plasma Arc Cutting (PAC).

Observed unconventional methods of cutting utilize high-power kinetic or thermal energy of the working flow (water jet, laser beam or plasma arc) to remove the material. The basic principle of the unconventional cutting techniques is shown in Fig. 1.

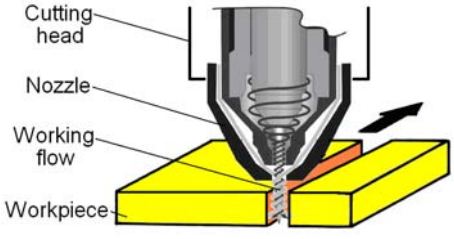

Fig.1. Principle of the unconventional cutting method

These machines have a similar structure, designed for processing a wide variety of plate materials. Basic structure of the unconventional cutting machine consists: base of the machine tool, working table, extraction system, motion system, drive, cutting head and nozzle, energy source and controller unit.

In this paper will not be considered which of these three unconventional techniques is best suited for cutting materials. These techniques and their comparisons are illustrated in Fig. 2, where are seen cutting area and some of the differences between them.

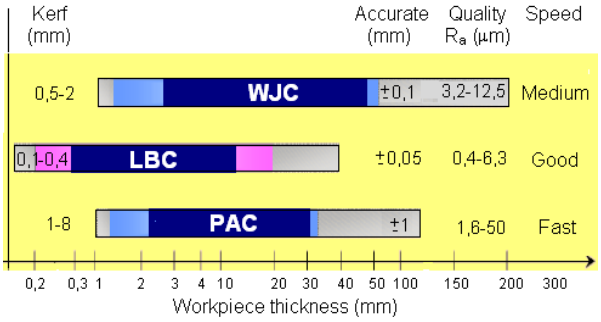

Fig.2. Comparison of unconventional cutting methods

3.1 Water Jet Cutting

Most theories explain water jet cutting as a form of micro erosion used material. Through a small orifice in the nozzle extreme pressure of the accelerated pure water or together with abrasive particles, in a small area of the workpiece develops small cracks. Water extremely high pressures and impact of abrasives in the following stream cause the mall crack to propagate until the material is processed.

Water jet machining is in use more than half century. Due to the uniqueness of water jet cutting, there are many applications where it is more useful and economical than standard machining processes. Pure water jet cutting is used mostly to cut softer materials such as wood, plastics and aluminium. Together with abrasive means this method is successfully used for cutting strength materials such as steel, ceramic and composite material.

3.2 Laser Beam Cutting

Laser beam cutting is a thermal process that utilizes a high energy of light beam to melt and vaporize material particles on the surface of the workpiece. Advantage of laser beam cutting are: no limit cutting of hard and fragile materials, cost effective and flexible process, high accuracy parts, narrow heat affected zone, no tool wear, etc.

This process is used widely for cutting, drilling, welding and marking of metallic and non-metallic materials. Laser beam cutting is being used extensively in the mechanical, electronic and automotive industries.

3.3 Plasma Arc Cutting

Plasma arc cutting is a thermal material removal process via the heat generated from an ionized gas, which is produced by applying an electric current. The plasma arc cutting has always been seen as an alternative to the oxy-fuel process. Plasma arc cutting is characterized: low capital cost, high speed of cutting, increased quality of the cut, low finishing costs, mobility, cutting of all positions, etc.

Plasma arc cutting is used for industrial production cutting of all materials. This process is chiefly used for cutting bulky sections of electrically conducive materials. Plasma is the fastest cutting process on carbon steel, aluminium or stainless steel.

4. MODULARITY OF THE UNCONVENTIONAL CUTTING MACHINE

The modular design for unconventional machine tools is the real example for mode of complex technical systems standardization. This means composition of great number of common modules, produced from standard or non-standard elements composed in a functional composition of complex unconventional machines. Efficiency and reliability of the modular design of these machines allows designing complex modules from different elements which are checked in design and technology meaning.

4.1 Modular strategy for design

In industrial practice a variety of unconventional cutting machines exist, yielding a number of different technical, technological and economical levels. As with any purchase, the wants and needs must be weighed well. Closely examining machine needs can minimize unnecessary expenditures.

There are different criteria for classification of unconventional cutting machines. Selection of these machine tools includes: power, size of the work area, number of cutting heads, level of controlled axles, etc.

These requirements most effectively modular design strategy implement. The modular system offers optimum technology of design for different types of the unconventional cutting machine, while having to meet the specific conditions of the cutting process. All requirements have to be covered with detailed analysis of various options, combined with extensive engineering expertise.

Due to the specifics of each of the unconventional processes, there are elements, objects and systems that are common, as well as those that are unique to a given case. The main composition of the modular system of unconventional cutting machine is shown in Fig. 3.

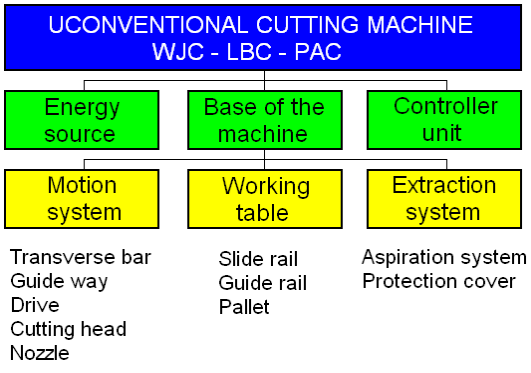

Fig.3. Modular system composition

4.2 Modular conception

Because of high price of unconventional cutting machines and specific production conditions, modular design is one of the significant solutions to implement these machines. This modular design is complicated, but flexible and considerably cheaper.

The developed standard variant of the modular design of unconventional cutting machine is illustrated in Fig. 4.

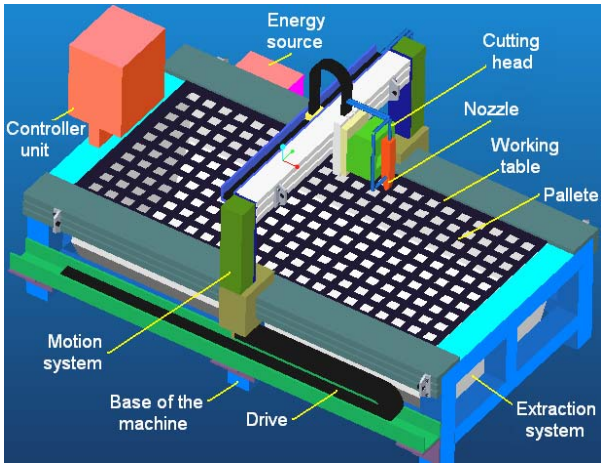

Fig.4. Modular design of the unconventional machine

If customer designs unconventional cutting machine, manufacturer can produce part of equipment or to order it from another supplier. For most of the production conditions it is possible to produce basic parts of machine tools structure. Energy source, drive system, control unit and nozzle are usually ordered from specialized producer of equipment parts.

The unconventional machine structure is usually produced according to own flexible system needs. Shown in Fig. 5 is upgradeable bed of the machine tool with slide and guide rails. The scalable modular motion system is shown in Fig. 6.

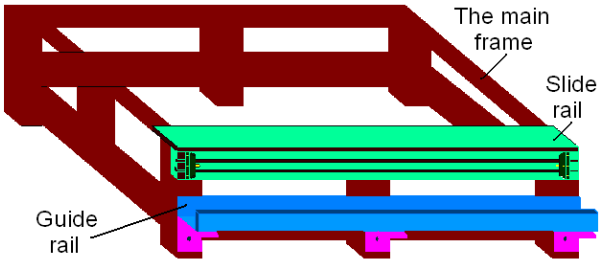

Fig.5. Bed of the unconventional machine

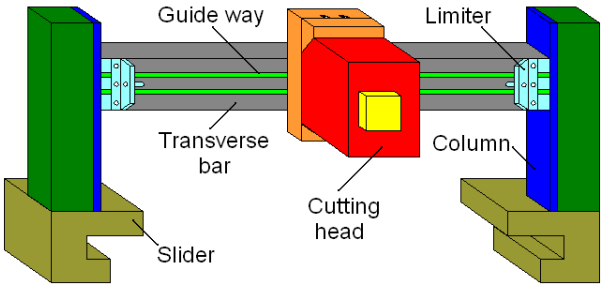

Fig.6. Modular motion system

Shown in Fig. 7 is possible variant of the modular design unconventional cutting machine with extended working table. This concept uses the flexible bed of the machine and a replaceable transverse bar with more cutting heads.

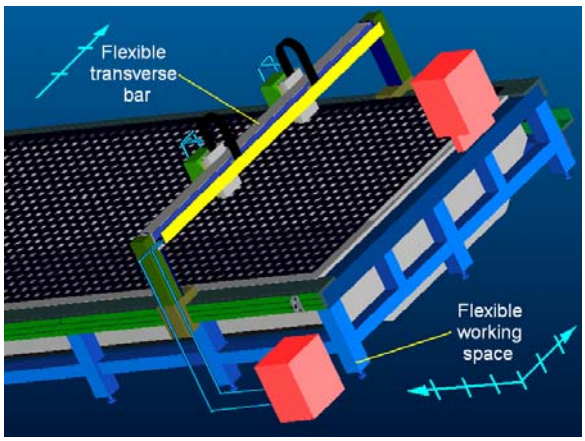

Fig.7. Unconventional machine with extended working table

The presented modular design of unconventional cutting machine allows that all standard options are easily installable as a module afterward and enabling a machine upgrade to the customer's wishes. This is a perfect example of how a modular design concept makes it possible to make small changes to existing designs to create an unconventional cutting machine with custom capabilities.

5. CONCLUSION

Modular design of machine tools is completely different substantially from traditional approaches to design. Historically, modular principle of design has been based on experience.

The modular design of unconventional cutting machine, because of the high price of equipment, economically is much approved procedure. The presented modular design of unconventional machine allows efficient construction of elements and systems to be ensured a good design. It is flexible machine which allows answering customer requirements for various options. This modular composition of the machine offers optimum value of technology for various types of machining sheet materials.

6. ACKNOWLEDGEMENTS

The paper is the result of the research within the project TR 35015 (2011/15) financed by the Ministry of Education, Science and Technological Development of the Republic of Serbia.

7. REFERENCES

[1] Star, M.K.: *Modular production - A new concept*, Harvard Business Review, Vol.43, No.6, pp. 131-142, 1965.
[2] Koenigsberger, F.: *Advanced in machine tool design and research*, Pergamon Press, Oxford, 1968.
[3] Ito, Y.: *Modular design for machine tools*, McGraw-Hill, New York, 2008.
[4] Bazrov, B.M.: *Modular design of machine tools*, Russian Engineering Research, Vol.31, No.11, pp. 1084-1086, 2011.
[5] Padayachee, J., Bright, G.: *Modular machine tools: Design and barriers to industrial implementation*, Journal of Manufacturing Systems, Vol.31, pp. 92-102, 2012.
[6] Peukerta, B., Saojia, M., Uhlmann, E.: *An evaluation of building sets designed for modular machine tool structures to support sustainable manufacturing*, Procedia CIRP 26, pp. 612-617, 2015.
[7] Kovac, P., Gostimirovic, M., Sekulic, M., Savkovic, B.: *A review of research related to advancing manufacturing technology*, Journal of Production Engineering, Vol.12, No.1, pp. 9-16, 2009.
[8] Gostimirovic, M., Kovac, P., Sekulic, M.: *An inverse heat transfer problem for optimization of the thermal process in machining*, Sadhana, Vol.36, No.4, pp. 489-504, 2011.
[9] Gostimirovic M., Sekulic M., Kopac J., Kovac P.: *Optimal control of workpiece thermal state in creep-feed grinding using inverse heat conduction analysis*, Strojniški vestnik - Journal of Mechanical Engineering, Vol. 57, No.10, pp. 730-738, 2011.
[10] Sekulic, M., Kovac, P., Gostimirovic, M., Kramar, D.: *Optimization of high-pressure jet assisted turning process by Taguchi method*, Advances in Production Engineering & Management, Vol.8, No.1, pp. 5-12, 2013.
[11] Krajny, Z.: *Vysokotlakovy vodny luc – WJM projects*, Slovenska technicka univerzita v Bratislave, Bratislava, 2011.
[12] Krajcarz, D.: *Comparison Metal Water Jet Cutting with Laser and Plasma Cutting*, Procedia Engineering, Vol. 69, pp. 838-843, 2014.
[13] Madic, M., Radovanovic, M., Gostimirovic M.: *ANN modeling of kerf taper angle in CO2 laser cutting and optimization of cutting parameters using Monte Carlo method*, International Journal of Industrial Engineering Computations, Vol.6, pp. 33-42, 2015.

Authors: **Prof. Dr. Marin Gostimirović[1], Prof. Dr. Pavel Kovač[1], Prof. Dr. Miroslav Radovanović[2], Dr. Miloš Madić[2], Ing. Dr. Zdenko Krajny[3]**
[1]University of Novi Sad, Faculty of Technical Sciences, Department of Production Engineering, Trg Dositeja Obradovića 6, 21000 Novi Sad, Serbia, Phone.: +381 21 450 366, Fax: +381 21 454 495.
[2]University of Niš, Faculty of Mechanical Engineering in Niš, Aleksandra Medvedeva 14, 18 000 Niš, Serbia, Phone: +381 18 500 626, Fax: +381 18 588 244.
[2]Slovak Technical University in Bratislava, Faculty of Mechanical Engineering, N. Slobody 17, 81231 Bratislava 1, Slovakia, Phone: +421 2 572 96 111, Fax: +421 2 52 925 749.
E-mail: maring@uns.ac.rs, pkovac@uns.ac.rs
mirado@masfak.ni.ac.rs
madic@masfak.ni.ac.rs
zdenko.krajny@stuba.sk
***Note*: This paper presents a part of researching at the CEEPUS project and Project number TR 35015.**

Journal of Production Engineering
Vol.18 No.1
JPE (2015) Vol.18 (1) Original Scientific Paper
Beňo, J., Tomáš, M., Ižol, P., Varga, J.

ANALYSIS OF THE FREE FORM SURFACE MILLING BASED ON A FRAGMENTATION APPROACH

Received: 18 May 2015 / Accepted: 15 June 2015

Abstract: *In this paper, authors performs analysis of the free–form surface milling based on the fragmentation of the design elements which create active surfaces in tool making. Their analysis is based on fragmentation approach which makes the most of combining CAD, modelling and testing objects in tool making as well as selecting of the fragments with parts of free/form surfaces. Examples being introduced in this paper point out that it is volume based fragmentation of free form surfaces which allows to associate CAD design of tooling parts, their modelling and producing in chosen scale as well as testing different milling strategies. Results also showed that it is the Lining strategy of ball end milling which denotes desired compromise between machining time and surface quality when ball end milling fragments with different signed curvature radius.*
Key words: *free form surface, fragmentation types, design elements, roughness parameters.*

Analiza glodanja slobodih površina baziran na pristupu fragmentacije. *U ovom radu, autori vrše analizu glodanja slobodnih površina na osnovu fragmentacije elemenata aktivnih površina koje se stvaraju pri glodanju. Analiza je zasnovana na pristupu fragmentacije koji čini najveći deo kombinovanja CAD-a, modeliranja i testiranja objektata pri izradi alata, kao i selektovanje fragmenata sa delovima slobodnih površina. Primeri koji se navode u ovom radu ukazuju na to da objekat zasnovan na fragmentaciji slobodnih površina omogućava da se poveže CAD dizajn delova alata, njihovog modeliranja i proizvodnje u izabranoj skali kao i testiranje različitih zahvata glodanja. Rezultati takođe pokazuju da obrada sa loptastim glodalom označava željeni kompromis između vremena obrade i kvaliteta površine kada su loptasti fragmenti različitih radijusa.*
Ključne reči: *slobodna površina, tipovi fragmentacije, elementi dizajna, hrapavost površine.*

1. INTRODUCTION

Tools for sheet or bulk forming and moulding have significant position in products innovation and reduction of their life cycle for determining product quality and accuracy. They include free–form elements and their active parts are produced by CNC milling which is the largest subject in this technology. State–of–the–art is very wide and can be categorised in six main fields:

1. The first field is surface design [1], [2] which employs basic features of free–form shape. Composition of the features allows generating complex surface being used in industry including tooling for forming dies and plastic moulding.
2. The second field is modelling and decomposition of free–form surfaces [3], [4] which applies division of product into fragments with parts of free–from surfaces. Fragments enable programming paths of ball end mill cutters which are based on orientation of any surfaces; such a methodology is applicable in design of moulds.
3. The third field includes milling strategies and directions of tool path [5], [6] which consider machining time and dimension accuracy. Milling strategies assume elimination of the surface inaccuracy by means of topology data [7] and by tool edge contact with workpiece [8].
4. The fourth subject is programming of tool path and it represents topology and combining of tool motion and so–called CC points in tool path and CL points of cutter position [5]. To check surface inaccuracy, programming considers deformation of the cutter body [9].
5. The fifth field is performance of milling cutters as end mill and ball end mill, their performance is given by forces, tool body deformation and machined surface [10]. In moulding of plastics, combination of strategies, cutter diameter and way of milling do affect active surface [11]. Technology to produce sheet forming tools consists of division of active surfaces into fragments [12].
6. The last field is quality checking of active surface and critical spots of produced tooling. In fact that field combines following approaches: programming variable data as feed and spindle revolutions [13], surface texture simulation [14] and texture analysis in two directions [15]. To check true machined surface, 3D measurement of texture being dependent on feed and infeed is used [16]; however, digital analysis of texture due to various forms of contact between ball end mill cutter and work piece is applied [17]. In analysis of quality of free–form surfaces, such approaches as 3D metrology [5], roughness figures [13], [14], surface texture and Abbot's curves [16], texture variation in two directions [10] etc., are employed. Performance of end mill cutters is expressed in terms of tool edge wear [10], [11] and cutting forces [9], [13].

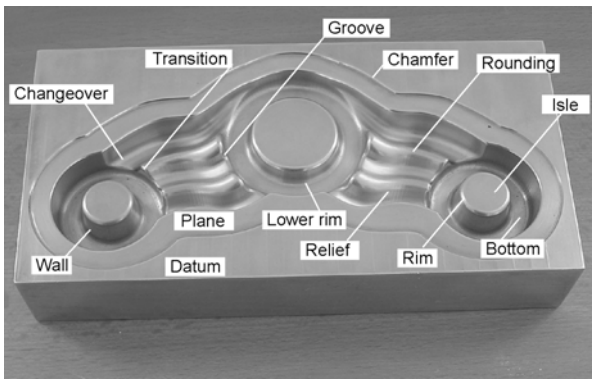

Fig. 1. An example of design elements when tool making the lower die

Tooling for sheet or bulk forming and moulding make form product through their active parts. Manufacturing of the tooling shape in Figure 1, though, consists of different milling strategies which are expressed through programming instructions; therefore, checking of the final shape gives lack of measurability. In order to secure proper checking of the machined surface quality, there is only way of securing such measurability, the measurable fragments. Fragments are supposed to bear all the significant attributes in the free–form surface whereas they must be capable of identifying and measuring the active surface of tooling. In order to achieve such a surface checking, the fragmentation is introduced to analyse the fragments of the whole relief surfaces.

2. TOOLING FRAGMENTATION VARIETES AND THEIR FEATURES

Basic idea of free–form surface fragmentation is that a pattern is taken from the tooling entity, which can be further studied as a fragment of the surface or as a sample being produced in laboratory. This approach offers study of wide scale of effects as formulation of the surface as for instance, radii, their transition, datum in Figure 1 which replaces the parts of planes as bottoms, walls, etc. Because of wide varieties in fragmentation, three ways of expressing fragment shape are introduced below.

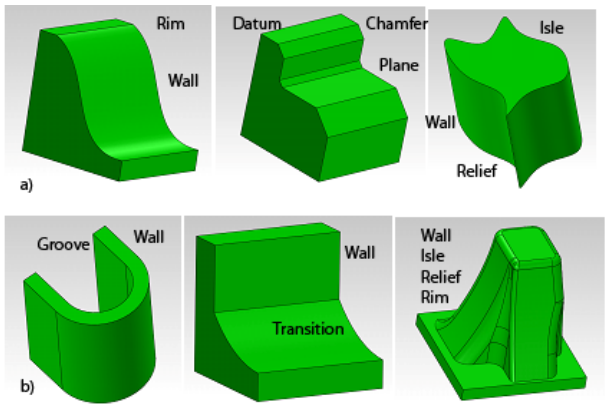

Fig. 2. CAD based fragmentation: attributes of the free form surface in tool making (a) Fragments based on measurability (b) Fragments based on combining of dimension

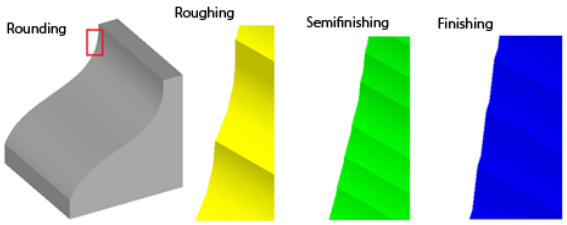

Fig. 3. CAD based fragmentation and sequence of producing resultant surface finish a case of the LINING strategy

2.1 CAD Based Fragmentation

CAD based fragmentation of the free–form surface seems to be the feasible tool to investigate end ball milling process. Main advantage in such a way is that any part of the free form surface is transferred into virtual volume (mainly 100^3 mm^3) in Figure 2 wherein such analyses as modelling and simulation of machining are used. Thus, CAD drawing of tooling part allows to take out the representatives of free form surfaces. Such way of free form surface fragmenting makes the most of applying calculation of the scallop heigh, the surface error in Figure 3, however, roughness models in Figure 4 are based on sequence of milling operations in LINING Milling Strategy. In modelling of cusp height, roughing applies ball–end–mill cutter of diameter D=16 mm; semi finishing is modelled with D=10 mm and finishing results from D=6 mm.

2.2 Object Based Fragmentation

While CAD based fragmentation allows to identify wide variety of milling strategies and their effect on surface finish, results always need verifying. In principle, object based fragmentation represents the art of selecting an object which is included in the design of tooling and subsequently such an object is modelled in terms of different milling strategies. Simple parabolic surface $y=30–0.048x^2$ was used to verify this approach whereas three kinds of milling strategy as SPIRAL, CONSTANT Z LEVEL and LINING were used to produce resultant surface finish. Commercial sintered carbide ball end milling cutter D=8 mm was used to machine AlCu4Mg alloy (feed per tooth f_z=0.03 mm, revolutions n=4900 1/min, side step a_e=0,5 mm, coolant: emulsion, machine tool EMCOMILL 155 with control unit Heidenhein TNC 426). Figure 4 illustrates an example of comparing CAD model with real machined object and data in Table 1, the parameters of surface roughness by ISO 4287, make distinguish suitability the Constant Z level as the strategy reducing subsequent grinding and polishing of this part of tooling, an isle/wall/transition according to the notation shown in Figure 1.

2.3 Volume Based fragmentation

Two main dimensions create the idea of the Volume Based Fragmentation. The first dimension is 100^3 mm^3, a volume of a part of the product, either a part of tooling in fact as e.g., a any die, or an entity as e.g., tooling in injection moulding. A volumetric segment,

which is supposed to be of 10^3 mm^3, represent a fragment to measure machined surface roughness, such a dimension allows to replace a part of relief surface by a circle.

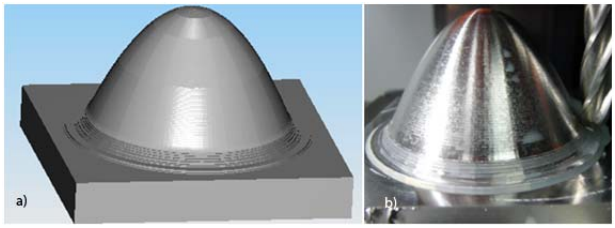

Fig. 4. An example of object based fragmentation: (a) CAD representation of the object; (b) applying of the Spiral Milling Strategy

Milling strategy	spiral	constant z level	lining
Ra [µm]	2.19	0.58	1.69
Rz [µm]	9.78	3.06	8.01
Rt [µm]	11.71	4.18	10.83
Rp [µm]	5.74	1.6	4.5
Rv [µm]	3.96	1.46	3.51

Table 1. Results of measuring surface texture parameters when ball end milling (Mitutoyo SJ 301)

Positioning of the machined surface in Vee block in Figure 6a) shows that stylus moves along ridge lines and valley lines of the machined surface while the former means position of stylus in that of Figure. If centre of a radius R, which defines a part of relief surface is located within a sample, it represents positive signed curvature radius which is taken as k=1/R, a convex case of the signed curvature. Otherwise, the ratio k=–1/R represents the negative signed curvature, a concave case of the measured fragment: in other words said, the centre of the circle radius is located outside machined surface. Such cases of the signed curvature radii are shown in Figure 6(b) and their combination produces final fragment of the machined surface. Now, different milling strategies are applicable to such a fragment, the whole Figure 6 gives evidence about how milling strategy LINING is being investigated.

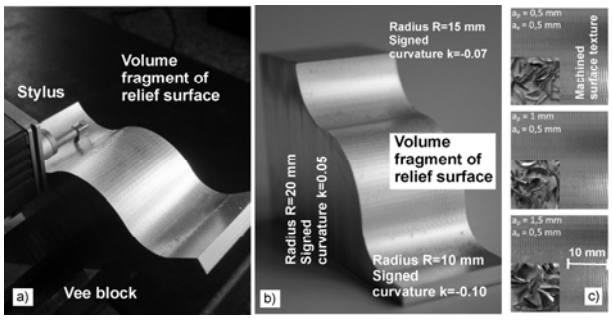

Fig. 6. Measurability of the relief surface fragment: (a) positioning of the fragment at the Vee block (b) volume fragment and related radii used in experimental measurements (c) surface texture and its changes as an effect of the depth of cut a_p (milling strategy LINING, signed curvature k=–0.10 mm, roughness range Ra=1.30–1.60 µm)

Experimental measurement were performed to identify effect of signed curvature k and cutting conditions on surface roughness parameters Ra and Rz. Commercial sintered carbide ball end milling cutter D=8 mm with number of flutes z=2 and helix angle 30 degree was used to machine AlCu4Mg alloy. The samples included radii and signed curvatures according to the Figure 6(b) while L27 Taguchi design was used in experiments. Identical range of depth of cut a_p and side step a_e (a_p=0.5 – 1.5 mm, a_e = 0.5 – 1.5 mm) were used in L27 Taguchi design while feed rate and spindle revolutions were v_f = 1500 mm/min and n = 5000 1/min; machine tool EMCOMILL 155 with control unit Heidenhein TNC 426. The L27 design was created by means of MiniTAB software and there is no need to explain its matrix here for returning evaluation instantly including relevance of results. The roughness parameters Ra and Rz were measured at the ridge/valley lines shown in Figure 6(a) and Taguchi L27 returned following statistical formulae:

$$Ra=0.58+k-1.71a_p+3.63a_e+12k^2+1.09a_p^2-0.50a_e^2+0.97k.a_p-1.69k.a_e-0.40a_p.a_e \quad (1)$$

$$Rz=0.33+2.10k-8.23a_p+22.7a_e+102k^2+4.43a_p^2-5.50a_e^2+6.97k.a_p-7.60k.a_e-0.57a_p.a_e \quad (2)$$

Meaning of the above mentioned formulae is contribution of the ball end milling factors to the resultant surface roughness. Though determination index is very high (R^2=0.94 and 0.91, respectively), contribution of the factors as a_e and a_e and k is quite different. Results of ANOVA (Analysis of variance) points out that the a_e bears the main effect on the resultant surface roughness which was found out to be about 90 – 91 per cent, while the a_p and k brought effects no greater than 2.1 – 2.5 percent. In other words said, the signed curvature of workpiece is rendered through the errors in models, thus final effect of a_e and a_p was found out as:

$$Ra=0.62-1.75a_p+3.71a_e+1.02a_p^2-0.50a_e^2-0.40a_p.a_e \quad (3)$$

$$Rz=0.27-8.51a_p+23.00a_e+4.43a_p^2-5.61a_e^2-0.57a_p.a_e \quad (4)$$

and they are shown in Figures 7(a) and b.

3. CONCLUSION AND PROSPECT

In this paper, authors introduce their results based on fragmentation of definite free–form surface in tool making. Their approach combines set of factors affecting design in tooling whereas simple notation of design shapes in tool making is introduced. Three ways of fragmenting active surfaces in tool making are proposed. There is limited field of application for CAD based fragmentation, it can be used to rapid creating of the fragments. Prospect of such an approach is that it will combine such quantities as models of surface fragment and their relationship to the kinematics of any milling strategy. The Object Based Approach represents definite part of tooling which can be produced in any scale to study effect of milling strategy on its resultant surface quality. It must be noted that roughness parameters are not only results assessing quality of free form milling, it is also dimension accuracy which implies surface metrology. Main

advantage of the Volume Based Fragmentation is combining of CAD, experiments and surface metrology, thus, it provides for verifiable results being tested in laboratory. The variable signed curvature and design of testing piece presented in this paper are one of the possible solutions which are offered by design of tooling. Because of large set of factors as art of milling strategy, diameter of end ball milling cutter and its geometry, tooling fragment designed as 2D or 3D, cutting conditions, etc., use of experimental design identifies all the relevant influences and in fact, design of experiment allow to optimize this process as such.

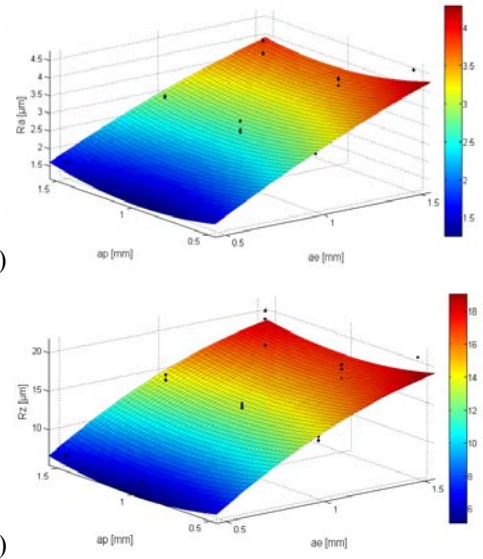

a)

b)

Fig. 7. Effect of cutting conditions a_p and a_e on surface roughness parameters based on L27 Taguchi design (a) mean arithmetic deviation Ra (b) average maximum height of the profile Rz

Acknowledgments

This work was supported by the project VEGA 1/0360/15 Research on Active Surface Preparation For Advanced Tooling Produced by CNC Form Milling and VEGA 1/0434/15 Research on Process Dependent Interface when Milling with Small Diameter of End Mill Cutters granted by Scientific grant agency VEGA of Ministry of Education, Science, Research and Sport. Authors express also their thanks Slovak Research and Development Agency under Contract No. DO7RP–0014–09

4. REFERENCES

[1] Van den Berg, E., et al.: Free form feature modelling: concepts and prospects. Computers in Industry. 49, 2012, 217–233.

[2] Pernot J.P. et al.: Incorporating free-form features in aesthetic and engineering product design. Computers in Industry 59 (2008) 626–637.

[3] Radzevich S.: Conditions of proper sculpture surface machining. Computer Aided Design, 34, 2002, 707–740.

[4] Quinn J.A. et al.: Generalized Anisotropic Stratified Surface Sampling. IEEE Transactions on Vizualization and Computer Graphics, 10, 2012, No. 10, 1–16.

[5] Lasemi A. et al.: Recent development in CNC machining of freeform surfaces. Computer–Aided Design 42 (2010) 641 – 654.

[6] Quinsat Y., Laurent S.: Optimal selection of machining direction for three–axis milling of sculptured parts. Int J Adv Manuf Technolology, (2006), DOI 10.1007/s00170–006–0515–5.

[7] Schützer, K. et al.: Using Advanced CAM–Systems for Optimized HSC–Machining of Complex Free Form Surfaces. Journal of the Brazil Society of Mechanical Science. & Engineering. 2007, Vol. 29, No. 3, 313–318.

[8] Toh C.K.: A study of the effects of cutter path strategies and orientations in milling. Journal of Mater. Process. Technology 152 (2004) 346-356.

[9] Lopez de Lacalle L.N, Lamikiz A, Sanchez J.A, Salgado M.A.: Toolpath selection based on the minimum deflection cutting forces in the programming of complex surfaces milling. International Journal of Machine Tools and Manufacture 2007;47(2):388-400.

[10] Urbanski J.P. et al.: High speed machining of moulds and dies for net shape manufacture. Materials and Design 21, 2000, 395-402.

[11] Vivancos J. et al.: Optimal machining parameters selection in high speed milling of hardened steels for injection moulds. Journal of Mater. Process. Technology 155–156 (2004) 1505–1512.

[12] Sun G. et al.: Operation decomposition for freeform surface features in process planning. Computer–Aided Design 33 (2001) 621 – 636.

[13] Vijayaraghavan A. et al.: Improving end milling surface finish by workpiece rotation and adaptive tool path spacing. International Journal of Machine Tools & Manufacture 49 (2009) 89–98.

[14] Ning Liu er al.: Surface finish visualisation in high speed, ball nose milling applications. International Journal of Machine Tools & Manufacture 45 (2005) 1152–1161.

[15] Ramos A.M. et al.: The influence of finishing milling strategies on texture, roughness and dimensio.nal deviations on the machining of complex surfaces. Journal of Materials Processing Technology 136 (2003) 209–216.

[16] Denkena B. et al.: Kinematic and Stochastic Surface Topography of Machined, TiAl6V4–Parts by means of Ball Nose End Milling. Procedia Engineering 19 (2011) 81 – 87.

[17] Weinert K. et al.: Simulation of Surface–Microstructures Resulting from Milling Processes. In: International Conference on Smart Machining Systems, National Institute of Standards and Technology (NIST) Files, 2007, Gaithersburg, Maryland, USA.

Authors: **Jozef Beňo, MSc. PhD., Miroslav Tomáš, MSc. PhD., Peter Ižol, MSc. PhD., Ján Varga, MSc. PhD.**, Technical University in Košice, Faculty of Mechanical Engineering, Institute of Technologies and Management, Mäsiarska 74, 040 01 Košice, Slovak republic, Phone.: +421 55 602 3527.
E-mail: jozef.beno@tuke.sk
peter.izol@tuke.sk
miroslav.tomas@tuke.sk

Journal of Production Engineering
Vol.18 No.1
JPE (2015) Vol.18 (1) Original Scientific Paper
Sekulić, S.

RELIABILITY WHICH CORRESPOND TO MEAN TIME TO FAILURE

Received: 16 December 2014 / Accepted: 02 March 2015

Abstract: *On the basic of large experimental date processing, mean time to failure related with reliability or unreliability 50% is not coincidence and we can on more directly way determine mean time to failure analytically or from graphics.*
Key words: *reliability, failure, mean time to failure, Weibull's distribution*

Pouzdanost koja odgovara srednjem vremenu bezotkaznog rada. *Na osnovu opsežnih ispitianja otkaza reznih alata uočeno je da srednjem vremenu bezotkaznog rada odgovara pouzdanost odnosno nepouzdanost od 50%. U radu je pokazano da to nije slučajno i da se na direktniji način može odrediti srednje vreme bezotkaznog rada analitički ili sa grafika.*
Ključne reči: *pouzdanost, otkaz, srednje vreme bezotkaznog rada, Weibullova raspodela*

1. INTRODUCTION

Starting with probability positions mean time to failure can be determined on the basis of observed failures in time [1-2].
Observed object in time can be described with simple state function

$$x(t)=\begin{cases} 1 & \text{object in available} \\ 0 & \text{object in failure} \end{cases}$$

The time in failure on observed object is not constant and present random value which we can prognose if it is known distribution function parameters and/or approximate - analytical or graphical [3-5].

For discrete systems if we observe N objects and if after time t is $N(t)$ objects in available and $n(t)$ in failure, the reliability can be expressed as

$$R(t) = N(t)/N = [N - n(t)]/N = n(t)/N \quad (1)$$

and unreliability

$$F(t) = 1 - R(t) = [1 - N(t]/N \ [N - n(t)]/N = 1 - n(t)/N \quad (2)$$

From previous equation follows

$$R(t) + F(t) = 1 \quad (3)$$

which indicates complementarities.
Frequency of failure is

$$f(t) = \Delta n/N \quad (4)$$

and intensity of failures

$$\lambda = \Delta n/N(t) = f(t)/R(t) \quad (5)$$

the mean time to failure is

$$T_m = (1/N)\ \Sigma\, \Delta n[(t_{i-1} + t_i)]/2 = \Sigma\, \Delta n\ t_{im}/N \quad (6)$$

where Δn is the number of failures in interval Δt and t_{i-1} is the time on beginning and t_i on the end of interval, and t_{im} the time in the middle of interval [6-8].
If the distribution function is known the reliability is

$$R(t) = 1 - F(t) \quad (7)$$

because it is

$$R(t) + F(t) = 1 \quad (8)$$

The frequency of failure as defined as

$$f(t) = dR(t)/dt \quad (9)$$

and failure intensity

$$\lambda = f(t)/R(t) \quad (10)$$

The mean time to failure by definition is

$$T_m = {}_0\int^{\infty} R(t)\, dt \quad (11)$$

and represent an area under a curve of reliability $R(t) = f(t)$.
When using Weibull's distribution function,

$$F(t) = 1 - \exp(-t/\eta)^{\beta} \quad (12)$$

which finds its application in analysis of reliability of technical systems, mean time to failure can be determined via gamma functions

$$T_m = \eta\, \Gamma(1 + 1/\beta) \quad (13)$$

whereby the gamma function table is used [9].

As shown in [10] mean time to failure correspond reliability, that is, unreliability $R(t) = F(t) = 0{,}5$ and can be determined directly analytically or from graphics on the basis of distribution function of failure (12), i.e., from graphics $R(t) = f_1(t)$ and/or $F(t) = f_2(t)$.

Staring from Weibull's distribution function (12), mean time to failure can be determined directly from Weibull's distribution function for $R(t) = F(t) = 0{,}5$

$$\boldsymbol{T_m = \eta\, C^{1/\beta} = \eta\, K}$$

where is $K = [-ln(1-0,5)]^{1/\beta} = f(\beta)$ (14)

2. RELIABILITY R(t) = 0,5 CORRESPOND TO MEAN TIME TO FAILURE

On the basis of large number of processed data to failures the mean time to failure correspond reliability i.e. unreliability *R(t) = F(t) = 0,5* (see Appendix on the end of paper). Starting from this fact the corresponding theoretical explanation is demanded.

On the *Fig.1* the changes of reliability *R(t)* and unreliability *F(t)* in time are proposed.

The mean time to failure, defined as

$$T_m = \int_0^\infty R(t)\,dt \quad (11)$$

and represent area under curve $R(t) = f_1(t)$. (*Fig. 2*)

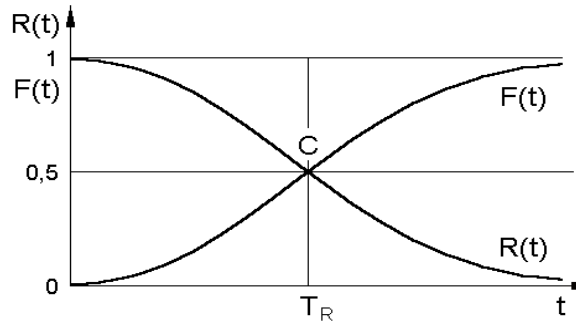

Fig. 1

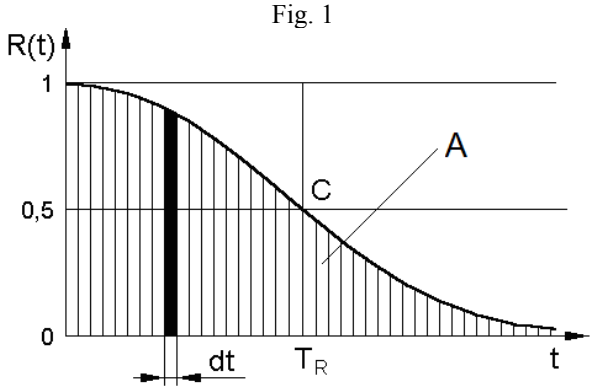

Fig. 2

If the supposition of the mean time to failure T_m correspond reliability or unreliability *R(t)=F(t)=0,5* is correct, the area A (*Fig. 2*) must be equal with area or rectangle (*Fig. 3*) $T_m = T_m$. *1* By them follow to estimate the complementarity condition $A_2=A_3$ and concluding equality $A_1=A_3$, $A_1=A_2=A_3$ (*Fig. 4*) [11].

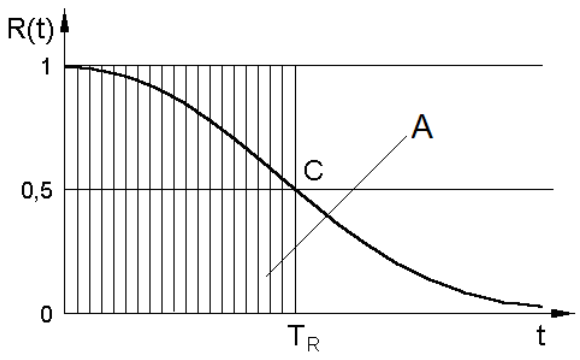

Fig. 3

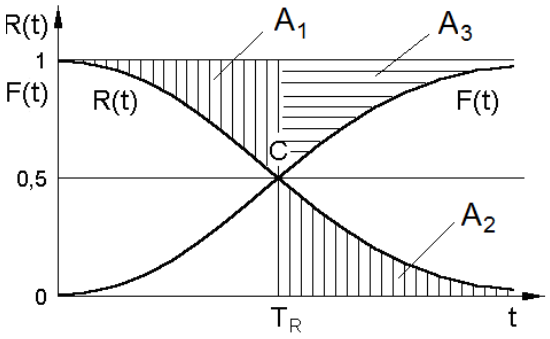

Fig. 4

Proof of the mean time to failure correspond *R(t) = =F(t) = 0,5* deduce on the claim $A_1=A_3$. From the *Fig. 5* follow

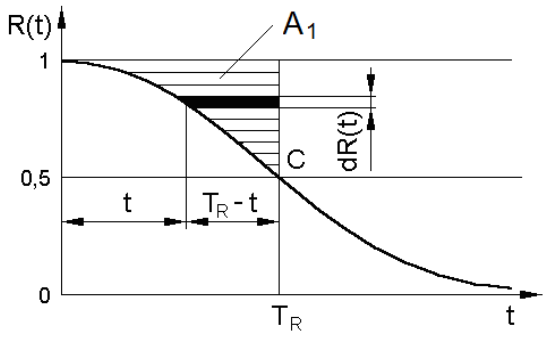

Fig. 5

$$\mathbf{A_1 = \int_{0,5}^{1} (T_m - t)\,dR(t))} \quad (15)$$

And from *Fig. 6*

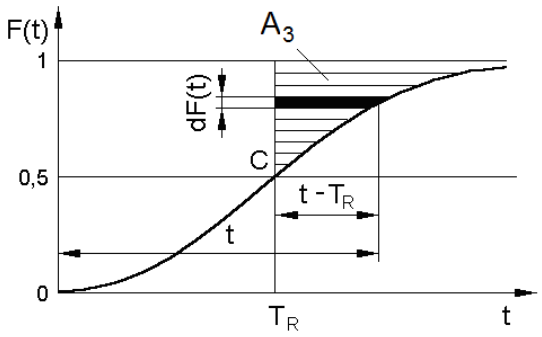

Fig. 6

$$A_3 = \int_{0,5}^{1} (t - T_m)\,dF(t) \quad (16)$$

From the condition of complementarity (8), after derivation follows

$$dF(t) = -\,dR(t) \quad (17)$$

and after substitution in (16) we have

$$\mathbf{A_3 = \int_{0,5}^{1} (t - T_m)\,(-dR(t)) = \int_{0,5}^{1} (T_m - t)\,dR(t)} \quad (18)$$

How integrals for A_1 (15) and A_3 (18) are identical we conclude.

$$\mathbf{T_{R=0,5} = T_m} \quad (19)$$

i.e.
mean time to failure correspond reliability or unreliability R(t) = F(t) = 0,5 [12].

On the above, mentioned mean time to failure can be determined analytically on the basis from distribution function (12) or from graphics $R(t) = f_1(t)$ and/or $F(t) = f_2(t)$, or from probability papers.
From (12) follows

$$t = \eta\,[-\ln(1 - F(t)]^{1/\beta} \qquad (13)$$

and for $F(t) = R(t) = 0,5$ is $t = T_{R=0,5} = T_m$ we have

$$T_m = \eta\,[-\ln(1 - 0,5)]^{1/\beta}$$

or finally

$$T_m = \eta\,(0,6931472)^{1/\beta} \qquad (13')$$

i.e.

$$T_m = \eta\, C^{1/\beta} = K\eta$$

where is $K = [-\ln(1-0,5)]^{1/\beta} = f(\beta)$ (13'')

If comparing terms

$$T_m = \eta\,\Gamma(1 + 1/\beta) \qquad (12)$$

and

$$T_m = \eta\, C^{1/\beta} \quad \text{where is} \quad C = 0,6931472 \qquad (13)$$

in both cases first part is proportional with position parameter η, and second parts of terms are functions of shape parameter β.

$$\Gamma(1 + 1/\beta) \quad \text{and} \quad K = C^{1/\beta}$$

3. CONCLUSION

On the basis of before mentioned we can conclude:

- The mean time to failure correspond to reliability and unreliability $R(t) = F(t) = 0,5$
- The mean time to failure can be determined analytically via distribution function and/or from graphics $R(t) = f_1(t)$ and/or $F(t) = f_2(t)$ and/or from probability papers, for $R(t) = F(t) = 0,5$

4. REFERENCES

[1] Todorovic, J., Zelenovic, D., *Effectiveness of Systems in Mechanical Engineering*, Naucna knjiga, Belgrade, 1981. (in Serbian).

[2] Kececioglu, D., *Reliability Engineering Handbook,* Vol. 1 & Vol. 2, PTR Prentice Hall, Englewood Cliffs, New Jersey, 1991

[3] Sekulic, S., *Statistical Formulation of a Cutting-tool Reliability in a Working Conditions,* Reports of the 21th Conference of the European Organizations for Quality Control EOQC - Varna 77, Bulgaria, Varna, 1977.

[4] Sekulic, S., *Methodologies for Determination of Cutting-tool Reliability*, Drugie medzynarodove Symozium NARZEDZIA '84, Krakow - Janovice - Tarnow, Poland, 1984.

[5] Sekulic, S., *Determination of Cutting-tool Reliability on Flexible Automatic Flow Lines,* Towardthe Factory of the Future, Proc. 8th ICPR, Aug., 1985, Springer-Verlag, Berlin- Heilderberg, New-York, okio, 1985.

[6] Sekulic, S., *Graphical Procedure for Prognosis of the Cutting-tool Reliability on Flexible Automatics Lines Based on the Number of Work Pieces Machined with Particular Tools.* Proc. INTRTRIBO '90, Sept. 1990, Budapest, 1990.

[7] Sekulic, S., Bogicevic, S., Dudic, S., *Methodologies for Determination of Cutting-tool Reliability Supported by Computer*, Proc. International Computer Science Conference Micro CAD '96, Febr. 1986, Miskolc, Hungary, pp 75-81.

[8] Sekulic, S., *Reliability which Correspond Mean Time to Failure,* CD-ROM Proc. XXX JUPITER Conference 17th Symposium CAD/CAM, 2004, Belgrade, Serbia, 2004; (in Serbian)

[9] Sekulic, S., Nikolic, B., *Influence of Cutting-Tool Condition elements on Cutting-Tool Reliability Function Parameters in Turning*, Proc.CD-ROM 16th International Conference on Production Research ICPR – 16, July. 2001, Prague, Czech Republic, 2001, Contribution No 0019, P097.

[10] Ivanovic, G., Stanivukovic, D., Beker, I.: *Reliability of technical systems,* Edition: Faculty of Technical Sciences, Novi Sad, 2010 (in serbian: Pouzdanost tehničkih sistema);

[11] Sekulić, S., Tasić, N., Bogojević, B.: "*Supporting Graphics for Determination of Mean Time to Failure of Technical Systems*", 5. Life Cycle Engineering and Management, Beograd: Research Center DQM, 27-28 Jun, 2014, Belgrade, Serbia, pp. 46-51, ISBN 978-86-86355-17-1.

[12] Sekulic, S. *About Mean Time to Failure Determination of Technical System*, Proc. XVI International Scientific Conference on Industrial Systems (IS'14), Andrevlje, Novi Sad, Serbia, 15-17 Oct. 2014,

APENDIX 1

In goal to determine the mean time to failure of cutting tool T_m and reliability $R(t)$, which corresponding the observation of cutting tool failure, by turning on the lathe, in real production conditions, by different cutting conditions, on operation turning, external, longitudinal, rough-finish, by machining cylinder head of engine "Perkins", type M3. The 25 different cutting conditions was varied (5 different cutting speeds v and 5 different feeds s, in combination each with everyone. By grapho-analytical data processing, the distribution function parameters, for Weibull's distribution function β and η, on the basis of that, the mean time to failure
$T_m = \eta\,\Gamma(1 + 1/\beta)$ *and* reliability which corresponding $R(T_m) = exp(-T_m/\eta)^{\beta}$ and $T_{R=0,5}$ which corresponding reliability or unreliability $R(t) = F(t) = 0,5$. are determined. Quoted data are classified in *Table T.1*. The table contains values of mean time to failure given from two equations $T_m = \eta\,\Gamma(1 + 1/\beta)$ and
$T_m = \eta\,[-\ln(1 - 0,5]^{1/\beta} = \eta\,(0,6931472)^{1/\beta}$ which relates on same experimental data.

	(n, rev/min)		(160)	(200)	(250)	(315)	(400)
	v, m/min		47,226	59,03	73,79	92,98	118,06
			1	2	3	4	5
	0,8	β η	3,0 600	3,1 320	3,3 158	2,9 70	3,65 38
		$\hat{T}_m$	535,8	286,1	141,7	62,4	34,3
		$R(T_m)$	0,49	0,49	0,50	0,49	0,50
		$\hat{T}_{R=0,5}$	531,0	284,3	141,4	61,7	31,0
			6	7	8	9	10
	1,0	β η	3,28 290	3,07 132	2,48 65	3,2 31,8	3,65 14
		$\hat{T}_m$	260,1	118,0	57,7	28,5	12,6
		$R(T_m)$	0,50	0,49	0,48	0,50	0,50
		$\hat{T}_{R=0,5}$	259,3	117,2	56,1	28,4	16,7
			11	12	13	14	15
s,	1,2	β η	2,72 170	2,76 80	2,72 37,5	2,75 19	1,6 8
mm/rev		$\hat{T}_m$	151,8	71,2	33,3	16,9	7,2
		$R(T_m)$	0,48	0,48	0,48	0,48	0,43
		$\hat{T}_{R=0,5}$	148,6	69,9	32,8	16,6	6,4
			16	17	18	19	20
	1,4	β η	2,91 118	3,0 57	3,0 28	3,0 12,5	1,9 5,5
		$\hat{T}_m$	105,0	50,9	25,0	11,2	4,9
		$R(T_m)$	0,49	0,49	0,49	0,49	0,45
		$\hat{T}_{R=0,5}$	104,0	50,5	25,8	11,1	4,5
			21	22	23	24	25
	1,6	β η	3,54 89	3,2 40	1,62 17	2,01 8	1,4 3.5
		$\hat{T}_m$	80,1	35,8	15,2	7,1	3,2
		$R(T_m)$	0,50	0,50	0,43	0,46	0,42
		$\hat{T}_{R=0,5}$	80,3	35,7	13,6	6,7	2,7

Table T.1. **Estimated values of and correspond mean time to failure $\hat{T}_m$ i $\hat{T}_{R=0,5}$**

APENDIX 2

How it is presented in the paper, mean time to failure, with two equation, in analytical form, can be determined

$$T_m = \eta\,\Gamma(1 + 1/\beta)$$

$$T_m = \eta\,(0{,}6931472)^{1/\beta} = \eta K \text{ where is } K = f(\beta)$$

By comparing this terms we can conclude that the mean time to failure T_m direct proportional with position parameter of Weibull's distribution function η. Values of gamma functions corresponds to values of K.

In *Table T.2*, differences between gamma function Γ and K values both in function of β shape parameter, are given.

β	Γ	K	Γ - K	%
0,2	120,00	10,160	-40,000	33,3
0,35	6,292	0,349	5,943	94.5
0,5	2,000	0,481	1,519	84,0
0,7	1,266	0,592	0,674	53,2
1,0	1,000	0,693	0,307	30,7
1,5	0,903	0,803	0,100	11,1
2,0	0,886	0,833	0,053	6,1
2,5	0,887	0,864	0,023	2,6
3,0	0,893	0,885	0,008	1,5
4,0	0,906	0,912	-0,006	0,7
5,0	0,918	0,929	-0,011	1,2
6,0	0,928	0,941	-0,013	1,2
7,5	0,938	0,952	-0,014	1,6
10,0	0,965	0,964	0,001	3,4

Table T.2

Authors: **Prof . dr. Sava St. Sekulić**
Department for Industrial Engineering and Management, Faculty of Technical Sciences, University of Novi Sad, 21000 Novi Sad, Dositej Obradović Square 7,
e-mail: nemanja.tasic@uns.ac.rs

Journal of Production Engineering
Vol.18 No.1
JPE (2015) Vol.18 (1) Original Scientific Paper
Madić, M., Radovanović, M., Kovačević, M.

MODELING AND OPTIMIZATION OF KERF WIDTH OBTAINED IN CO_2 LASER CUTTING OF ALUMINUM ALLOY USING DISCRETE MONTE CARLO METHOD

Received: 19 May 2015 / Accepted: 16 June 2015

Abstract: *In this paper, mathematical model for the establishing relationship between laser cutting parameters such as laser power, cutting speed and assist gas pressure, and kerf width obtained in CO_2 laser cutting of aluminum alloy ($AlMg_3$) was developed. To this aim, second order polynomial model was developed by using experimental data obtained in laser cutting experimentation planned as per standard full factorial experimental design. Statistically assessed as adequate, developed model was then used to investigate the effect of the laser cutting parameters on the kerf width angle by generating 3D plots. In addition to modeling, by applying discrete Monte Carlo method laser cutting parameter values that produce the minimal kerf width were identified.*
Key words: *CO2 laser cutting, aluminum-magnesium alloy, kerf width, discrete Monte Carlo method*

Modeliranje i optimizacija širine reza kod CO_2 laserskog sečenja legure aluminijuma primenom diskretne Monte Carlo metode. *U ovom radu je kreiran matematički model za uspostavljanje relacija između parametara laserskog sečenja kao što su snaga lasera, brzina sečenja i pritisiak pomoćnog gasa, i širine reza kod CO_2 laserskog sečenja legure aluminijuma ($AlMg_3$). U tom cilju koristeći eksperimentalne podatke, dobijene realizacijom punog faktornog eksperimenta, kreiran je polinomski model drugog reda. Nakon što je statistički ocenjen kao adekvatan, kreirani model je korišćen za istraživanje uticaja parametara laserskog sečenja na širinu reza kreiranjem 3D grafika. Pored modeliranja, primenom diskretne Monte Carlo metode određene su vrednosti parametara laserskog sečenja kojima se postiže minimalna širina reza.*
Ključne reči: *CO_2 lasersko sečenje, legura aluminijum-magnezijum, širina reza, diskretni Monte Carlo metod*

1. INTRODUCTION

Aluminum and its alloys are among the most versatile engineering materials in many industries such as the automotive, construction, and aerospace industry because of their unique properties [1]. Pure aluminum is soft and ductile, and it is often alloyed with small amounts of copper, magnesium, manganese, silicon, zinc or lithium to improve its techno-technological characteristics.

In industry for cutting of aluminum and its alloys nonconventional machining technologies are predominantly used, particularly laser cutting and abrasive waterjet cutting. CO_2 laser cutting of aluminum and its alloys is considered difficult because of high reflectivity and thermal conductivity of aluminum and its alloys. Therefore, it is a common practice to use Nd:YAG lasers for cutting aluminum alloys since higher absorptivity of the Nd:YAG laser enables its processing with relatively less laser power. On the other hand, the use of CO_2 lasers for cutting of aluminum alloys is not usual, however, from the industrial point of view, such a possibility would be very welcome [1].

To this aim, a number of research investigations were carried out each covering a specific aspect of laser cutting of aluminium and its alloys by using laser cutting technology. As already mentioned a number of of previous studies investigated laser cutting of aluminium and its alloys by using Nd:YAG lasers [2-4]. These and many other researches were focused on different aspect of laser cutting such as analysis of the effects of process parameters on kerf width, kerf deviation, kerf taper, dross formation, surface roughness etc. Modeling and single and multi-objective optimization problems were also solved by applying different methods such as Taguchi's robust design methodology, grey relational analysis and regression analysis. Regarding the use of CO_2 lasers for cutting of aluminum and its alloys the same modeling and optimization methods were used while investigating the effect of process parameters on kerf geometry, HAZ, surface roughness, dross formation, surface chemistry and microstructural examination [1, 5-7].

The scope of this paper is development of mathematical relationship between process parameters (laser power, cutting speed, assist gas pressure) and kerf width obtained in CO_2 laser cutting of aluminum alloy ($AlMg_3$). To this aim, full factorial experimental design was adopted for the purpose of experimentation and obtained data were used for the development of kerf width mathematical model by using second order polynomial. In addition to modeling, the kerf width mathematical model was optimized, i.e. an attempt has been made to determine process parameter values such that kerf width is minimized. To this aim, discrete Monte Carlo method was applied. To the authors' knowledge, little work has been reported in the literature on optimization using discrete Monte Carlo method, although it has many benefits such as high probability of success, parameter free optimization approach and fast computation.

2. EXPERIMENTAL DETAILS AND RESULTS

For conducting the experiment trials, CO_2 laser cutting machine (Prima Industry) with a maximal power of 4 kW was employed. Straight cuts performed with a Gaussian distribution beam mode (TEM_{00}) in continuous wave mode on 3 mm thick $AlMg_3$ sheet sheet. The laser beam was focused on the bottom surface of the sheet using a focusing lens with a focal length of 5 in (127 mm). The conical shape nozzle with 2 mm diameter was used. The nozzle–workpiece distance was set at 0.8 mm.

For the purpose of experimentation, the full factorial design was used in which the experiment trials were performed as per standard 3^3 full factorial design. Based on the pre-analysis and pilot experimentation, three laser cutting parameters were selected, i.e. laser power (P), assist gas pressure (p) and cutting speed (v). Since it was assumed that there exist a non-linear relationship between laser cutting parameters and kerf width, P, p and v were were varied at three levels: P = 3, 3.5, 4 kW; p = 6, 8, 10 bar; v = 3, 3.25, 3.5 m/min. Therefore, 27 experimental trials in total were performed (Table 1).

Rectangular specimens with dimensions 20 mm × 40 mm were cut in every experimental trial (Figure 1). Kerf width (w) was measured using optical coordinate measuring device Mitutoyo (type: QSL-200Z) with resolution of the length measuring system of 0.5 μm. The kerf width of each specimen was measured by analyzing pictures of the top (laser beam entry) and bottom surface (laser beam exit) of the specimens using Q-spark image processing software. The kerf width was measured at 3 equally distanced positions along the picture of the kerf.

Fig. 1. Plate with specimens obtained after laser cutting,

Kerf width is an important feature of the laser cutting process that provides the advantage of this technology compared to other methods of contour cutting. By focusing the laser beam and by flow stream of assist gas material is removed from the cutting zone and the kerf occurs with a certain width. Kerf width increases with the increase of material thickness, and depends on the size of the spot, laser power, cutting speed, the characteristics of the material, the wavelength, method of cutting, etc. When cutting with oxygen kerf width is largely affected by assist gas pressure. The dynamic nature of the exothermic reaction produces an irregular, non-uniform kerf width as well as periodic striations on the surface of the cut. When cutting with nitrogen a significantly better and more regular cut is obtained. Cutting width at the bottom "output" side of the sheet is usually smaller, and is somewhat larger than the diameter of a focused laser beam at optimum cutting conditions. In general, when using laser cutting technology the goal is to obtain the smallest possible kerf width because this minimizes the amount of removed material.

Trial	P (kW)	p (bar)	v (m/min)	Kerf width (mm)
1	3	6	3	0.41
2	3	6	3.25	0.40
3	3	6	3.5	0.40
4	3	8	3	0.47
5	3	8	3.25	0.39
6	3	8	3.5	0.42
7	3	10	3	0.43
8	3	10	3.25	0.41
9	3.5	10	3.5	0.47
10	3.5	6	3	0.41
11	3.5	6	3.25	0.44
12	3.5	6	3.5	0.48
13	3.5	8	3	0.52
14	3.5	8	3.25	0.48
15	3.5	8	3.5	0.50
16	3.5	10	3	0.54
17	3.5	10	3.25	0.51
18	4	10	3.5	0.47
19	4	6	3	0.39
20	4	6	3.25	0.43
21	4	6	3.5	0.45
22	4	8	3	0.46
23	4	8	3.25	0.36
24	4	8	3.5	0.51
25	4	10	3	0.54
26	4	10	3.25	0.53
27	4	10	3.5	0.42

Table 1. Experimental trials and results

3. KERF WIDTH MATHEMATICAL MODEL

Raw data are impractical for interpretation and analysis of experimental results. Therefore, for the purpose of the detailed analysis of the conducted experimentation, based on obtained data the mathematical model using regression analysis was developed. To include first, second order main effects and interaction effects of the laser cutting factors, full second order regression model was developed:

$$w = -0.81791 + 1.5983 \cdot P + 0.32929 \cdot p - 1.72637 \cdot v - 0.23837 \cdot P^2 - 0.00612 \cdot p^2 + 0.36 \cdot v^2 + 0.01072 \cdot P \cdot p + 0.00622 \cdot P \cdot v - 0.07778 \cdot p \cdot v \quad (1)$$

With mean average percentage error of about 5 % between experimentally measured kerf width values and predictions it can be concluded that developed mathematical model is quite accurate.

To analyze the effects of laser cutting factors on the kerf width Eq. (1) was plotted. Three 3-D surface plots (Figure 2) were generated by varying two factors of interest, while other the third was held constant at middle level.

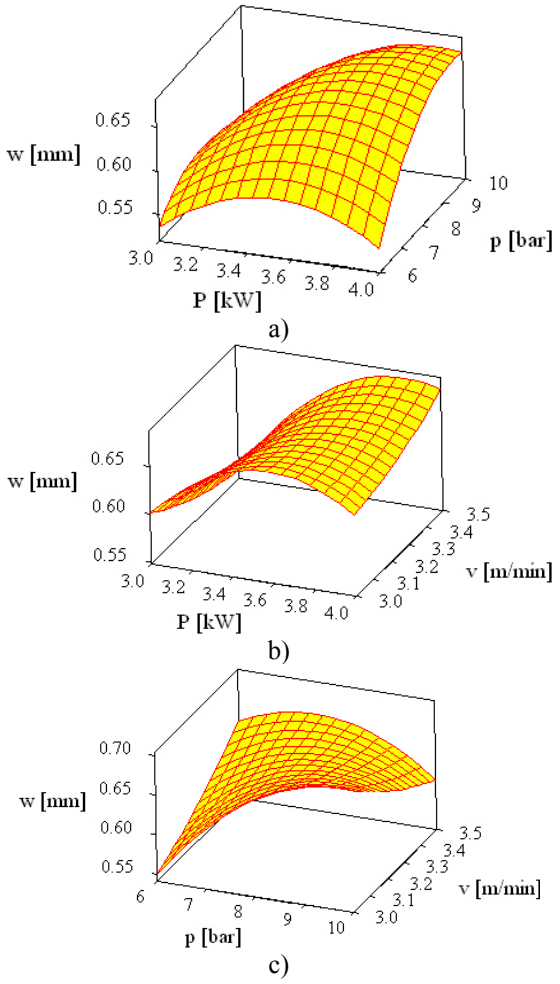

Fig. 2. Effect of laser cutting parameter interactions on kerf width [8]

As seen from Figure 2 the effect of the laser cutting parameters on the kerf width is nonlinear and variable.

As could be expected, low laser power and the higher cutting speed results in the low heat input during cutting operation so as lower kerf width is obtained (Figure 2). For higher laser power levels more material is being melted which results in larger kerf width. Similarly, when using higher levels of cutting speeds, there is lesser interaction time between laser beam and workpiece material, i.e. the material is heated within a relatively narrower zone around the laser beam thus forming a narrower kerf. These results are in agreement with those reported in literature.

Besides these, some unusual observations from Figure 2 are evident. Namely, it can be observed that for some specific combinations of laser cutting parameter values, kerf width decreases with the increase in laser power. Also, for certain laser cutting conditions, the increase in cutting speed results in an increase in kerf width. A more detailed analysis of the Figure 2 can reveal that these may be result of higher laser power levels or lower assist gas pressure levels used. Namely, in situations when greater proportion of material are evaporated and there is no sufficient gas pressure, one can expect the formation of surface plasma that reduces the amount of irradiated energy absorbed in the cutting region.

4. OPTIMIZATION OF KERF WIDTH

From Figure 2 it is obvious that achieving desired kerf width can be obtained by a set of different combinations of laser cutting parameter values. However, finding a set of the laser cutting parameter values to meet the desired kerf width, calls for the parameter optimization in three-dimensional laser cutting parameter hyperspace.

The goal of the optimization is to determine the optimal laser cutting parameter values at which the minimum kerf width is obtained. Mathematically, the optimization problem is as follows:

$$\begin{aligned} &\text{Find: } P_{opt}, v_{opt}, p_{opt} \\ &\text{to minimize: } w = \mathrm{f}(P, v, p) \\ &\text{subject to: } 3 \le P \le 4 \text{ [kW]} \\ &\qquad 6 \le p \le 10 \text{ [bar]} \\ &\qquad 3 \le v \le 3.5 \text{ [m/min]} \end{aligned} \quad (2)$$

The optimization problem in Eq. 2 was solved with discrete Monte Carlo method. The details about Monte Carlo method can be found in [9, 10]. This method was selected as it represents a parameter free approach that only requires performing a large number of simulations that are, however, executed very fast. Moreover, discrete Monte Carlo method takes into account techno-technological possibilities of machine tools and the determined solutions can be easily set on a given machine tool [9].

Before the actual application of discrete Monte Carlo method one needs to define the search step for each laser cutting parameter. This step defines the number of possible values that can take a given parameter within the given range. In order to create relatively dense search grid and by considering laser cutting machine technological characteristics, search steps for laser power, cutting speed and assist gas pressure were set to 0.01. This resulted in 2065551 parameter values combinations. The probability of finding a desire objective value (minimum) is only 1/2065551, but running it 10000000 times results in probability of finding optimal value over 99.99%. The

optimization problem formulated in Eq. 2 was solved using the developed software solution "Analysis VirtuoLab" which supports the application of exhaustive iterative search, continual and discrete Monte Carlo method for solving optimization problems with and without constraints [11]. Here it should be noted that optimization was performed within few seconds on desktop Intel Core i7-2600 CPU@3.4GHz with 12 GB RAM computer.

As a result of the application of discrete Monte Carlo method, the minimal value of kerf width of w = 0.497 mm was obtained. This solution corresponds to the following combination of the laser cutting parameter values: P = 3 kW, p = 6 bar, v = 3.02 m/min.

These values can be easily set for performing a given laser cutting operation.

5. CONCLUSION

In this paper, regression based mathematical model is developed in order to relate the laser cutting parameters i.e. laser power, cutting speed and assist gas pressure, and kerf width in CO_2 laser cutting of aluminum alloy. Experiment trials were performed according to full factorial design. By applying the discrete Monte Carlo method, the optimal laser cutting parameter settings, which minimize kerf width were determined. It was found that focusing the laser beam on the bottom surface of the sheet using assist gas pressure of 6 bar at combination of laser power of 3 kW and cutting speed of 3.11 m/min, produced an minimal kerf width.

The conclusions drawn can be summarized by the following points:

- the kerf width is highly sensitive to the selected laser cutting parameters and their interactions,
- the effect of a given laser cutting parameter on the kerf width must be considered through the interaction with other parameters,
- the discrete Monte Carlo approach is found to be very simple, easy to implement and efficient for the optimization.

6. ACKNOWLEDGEMENT

This work was carried out within the project TR 35034 financially supported by the Ministry of Education and Science of the Republic of Serbia.

7. REFERENCES

¶

[1] Stournaras, A., Stavropoulos, P., Salonitis, K., Chryssolouris, G.: *An Investigation of quality in CO_2 laser cutting of aluminum*, CIRP Journal of Manufacturing Science and Technology, Vol. 2, No. 1, p.p. 61-69, 2009.

[2] Pandey, A.K., Dubey, A.K.: *Multiple quality optimization in laser cutting of difficult-to-laser-cut material using grey–fuzzy methodology*, International Journal of Advanced Manufacturing Technology, Vol. 65, No. 1-4, p.p. 421-431, 2013.

[3] Leone, C. Genna, S., Caggiano, A., Tagliaferri, V., Molitierno, R.: *An investigation on Nd:YAG laser cutting of Al 6061 T6 alloy sheet*, Procedia CIRP, Vol. 28, p.p. 64-69, 2015.

[4] Dubey, A.K., Yadava, V.: *Robust parameter design and multi-objective optimization of laser beam cutting for aluminium alloy sheet*, International Journal of Advanced Manufacturing Technology, Vol. 38, No. 3-4, p.p. 268-277, 2008.

[5] Riveiro, A., Quintero, F., Lusquinos, F., Comesana, R., Pou, J.: *Parametric investigation of CO_2 laser cutting of 2024-T3 alloy*, Journal of Materials Processing Technology, Vol. 210, No. 9, p.p. 1138-, 2010.

[6] Araujo, D., Carpio, F.J., Mendez, D., Garcia, A.J., Villar, M.P., Garcia, R., Jimenez, D., Rubio, L.:. *Microstructural study of CO_2 laser machined heat affected zone of 2024 aluminum alloy*, Applied Surface Science, Vol. 208-209, No. 1, p.p. 210-217, 2003.

[7] Riveiro, A., Quintero, F., Lusquiños, F., Comesaña, R., Del Val, J., Pou, J.: *The role of the assist gas nature in laser cutting of aluminum alloys*, Physics Procedia, Vol. 12, No. 1, p.p. 548-554, 2011.

[8] Madić, M., Radovanović, M., Mladenović, S., Petković, D., Janković, P.*: An experimental investigation of kerf width in CO_2 laser cutting of aluminum alloy*, 12. International Conference on Accomplishments in Electrical and Mechanical Engineering and Information Technology – DEMI2015, May 29-30, Banja Luka, p.p. 85-90, 2015.

[9] Madić, M., Kovačević, M., Radovanović, M.: *Possibilities of using discrete Monte Carlo method for solving machining optimization problems*, 12. International Conference on Accomplishments in Electrical and Mechanical Engineering and Information Technology – DEMI2015, May 29-30, Banja Luka, p.p. 781-786, 2015.

[10] Pokorádi, L., Molnár, B.: *Monte-Carlo simulation of the pipeline system to investigate water temperature's effects*, U.P.B. Scientific Bulletin Series D: Mechanical Engineering, Vol. 73, No. 4, p.p. 223-226, 2011.

[11] http://www.virtuode.com/?page=SoftwareSolutions

Authors: **Dr. Miloš Madić, Prof. Dr. Miroslav Radovanović,** University of Niš, Faculty of Mechanical Engineering in Niš, Aleksandra Medvedeva 14, 18 000 Niš, Serbia, Phone: +381 18 500-687, Fax: +381 18 588-244;

MsC Marko Kovačević, University of Niš, Faculty of Electronic Engineering in Niš, Aleksandra Medvedeva 14, 18 000 Niš, Serbia, Phone: +381 64 2705028;

E-mail: madic@masfak.ni.ac.rs
mirado@masfak.ni.ac.rs
marko.kovacevic@elfak.ni.ac.rs

Journal of Production Engineering
Vol.18 No.1
JPE (2015) Vol.18 (1) Original Scientific Paper
Živanović, S., Milutinović, D., Slavković, N., Dimić, Z.

TESTING AND PROGRAMMING MINI LABORATORY AND DESKTOP 3-AXIS PARALLEL KINEMATIC MILLING MACHINE

Received: 26 January 2015 / Accepted: 22 March 2015

Abstract: *This paper describes testing and programming methods for parallel kinematic machine based on mini laboratory and desktop 3-axis parallel kinematic milling machine (PKMM). The paper presents the IDEF0 methodology for developmentally testing of new machine tools, with an example of application of this methodology. Several test workpieces are machined in order to verify the developed control and programming system.*
Key words: *testing, programming, parallel kinematic machine*

Programiranje i ispitivanje mini laboratorijske stone troosne glodalice sa paralelnom kinematikom. *U ovom radu se opisuje ispitivanje i metodi za programiranje mašina sa paralelnom kinematikom, na osnovu mini laboratorijske i stone troosne mašine sa paralelnom kinematikom. Prikazana je i IDEF0 metodologoja za razvojno ispitivanje novih mašina alatki, sa primerom primene. Obrađeno je nekoliko test radnih predmeta u cilju verifikacije razvijenog sistema za upravljenje i programiranje.*
Ključne reči: *ispitivanje, programiranje, mašina sa paralelnom kinematikom*

1. INTRODUCTION

Previous experience in the field of PKMM and successfully developed first industrial prototype of vertical milling machine based on newly developed parallel mechanism is shown in [1,2]. As a result of the experience in developing vertical milling machine industrial-size prototype, we come to the conclusion that, based on the same mechanism, a low-cost mini laboratory and desktop educational 3-axis parallel kinematic milling machine can be developed as a help in the process of acquiring basic experiences in the field of PKM [3-8].

Compared to the first experimental industrial-size prototype milling machine, scaling factor 5 is adopted for the desktop machine, because the machine would be real desktop and would have five times smaller overall sizes and five times smaller workspace overall sizes, retaining all advantages of parallel mechanism which is used. The structure of the parallel mechanism, modeling approach, solving of inverse and direct kinematics, workspace and singularity analysis and control system of developed mini laboratory and desktop 3-axis PKMM, have been described in previous research [1-8].

Based on adopted concept and design parameters, the first low-cost desktop educational 3-axis parallel kinematic milling machine has been built and tested in our laboratory [5-8]. The first low-cost desktop educational 3-axis PKMM presented in [3-5] was physically realized and was named pn101_st V1. This paper presents a testing of new version (pn101_st V1.5) with small modifications that includes the protection cover as well as trunk for chip, Fig. 1.

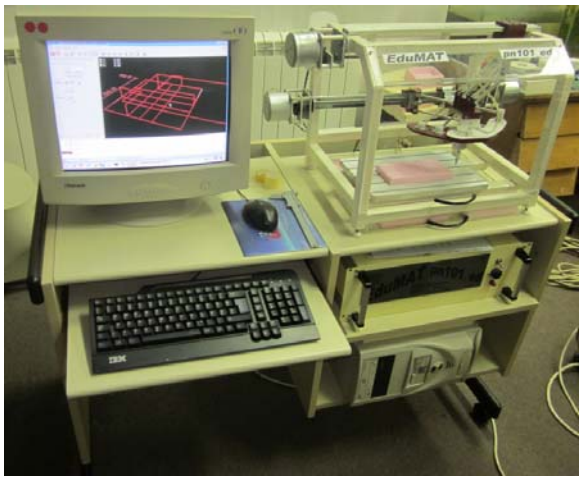

Fig. 1. Mini laboratory and desktop 3-axis PKMM

Control system of parallel kinematic machine is much more complex than control system of traditional machines with serial kinematics, because it is necessary to solve inverse and direct kinematic problems. Advantage of this parallel mechanism is in the fact that inverse kinematic problem can be solved in an easy way [5,8]. The control system, for our machine, is based on PC Linux platform with real time extension and EMC (Enhanced Machine Controller) software system [9]. EMC was created by NIST (the National Institute of Standards and Technology) [10] and is free software released under the terms of the GPL (General Public License).

The paper structured as follows. Section 2 gives an overview of the programming methods for realized machine. Section 3 gives the description of the methodology for testing mini laboratory and desktop 3-axis PKMM. Section 4 describes machining experiments and program verification during the machine testing.

2. PROGRAMMIMNG METHODS

Current situation of programming method is based completely on the G code. Numerical control machine tools have evolved from simple machines with controllers that had no memory, driven by punched tape to today's highly sophisticated Computer Numerically Controlled (CNC) machine tools. Machine tools have changed radically, but the programming language has remained the same with G code programming (ISO 6983) [11].

This paper also presents programming methods for mini laboratory and desktop 3-axis PKMM as well as programming system based on G code. Mini laboratory and desktop 3-axis PKMM can be programmed using several different methods, (i) Manually programming; (ii) Conversational programming; (iii) Programming using the CAD/CAM system; and (iv) New programming method using the software STEP-NC Machine [6,12,13].

An open challenge, in the field of machine tool programming is the new programming method using standard known as STEP-NC. The development of new programming method is running, but is still an unfinished work [12-19]. STEP-NC is a new interface that has developed for exchange of information between CAD/CAM systems and CNC controllers. The STEP-NC provides CNC controller new opportunities that enables controller to receive high level of information from workpiece design. It allows bi-directional flow of data between CAD/CAM and CNC Machine Tools without losing information. STEP-NC does not describe the tool trajectories for specific CNC machine tool as G code does, but it provides a feature based data model. A STEP-NC file is not machine tool specific and can be used on various machine tool controllers [15]. Now, this method of programming can't be completely used, because the resources for that development are owned by several research centers. There are possibilities for application through two possible scenarios (SC1, SC2) which are described in [13]. This approach is an indirect application of this programming method on existing machines and available software.

3. METHODOLOGY FOR TESTING MINI LABORATORY AND DESKTOP 3-AXIS PKMM

IDEF0 is the method designed to model the decisions, action, and activities of an organization or system. It is useful in establishing the scope of analysis, especially for a functional analysis. IDEF0 is used to produce a "function model". A function model is structured representation of functions, activities or processes within the modeled system or subject area[4].

In this paper, functions of testing mini laboratory and desktop 3-axis PKMM, are described by using the IDEF0 diagram. This is a part of methodology of configuring new machine tools, which is described in details in [4,8]. A full decomposition of the activities in configuring new machine tools with an example of application of this methodology for mini laboratory and desktop 3-axis PKMM is summarized in Table 1.

A1. Design machine pn101_st V.1 and the establishment of the necessary model
A11. Selection and design of machine components
A12. Project of a complete machine tool
A13. Configure family machine tools
A14. Techno-economics of machine tool
A2. Configuring Control for pn101_st V.1
A21. Control modeling for machine pn101_st V.1
A22. Integration of model control into EMC
A23. Simulation of CNC system in EMC
A24. Configuring virtual machine simulator
A25. Integration of control systems into EMC
A3. Analysis and simulation of the model
A31. Formation of the model for CAE and optimization
A32. CAE analysis
A33. Optimization of the model
A4. Make pn101_st V.1 and test work
A41. Development of special components and subcomponents
A42. Assembly of machine tool
A43. Calibration of machine tool
A44. Testing and trial work of machine tool

Table 1. A full decomposition of configuring activities [4]

According to the IDEF0 methodology, by analyzing diagram A44 in details, we get the basic flow of activities shown in Fig. 2. The basic activities are: A441 – Direct measurement, A442 – Indirect measurement, A443 – Rating and/or determination of quality indicators and A444 – Correction and setting up mini laboratory and desktop 3-axis PKMM.

The basic activities for testing in A44 diagrams, are very important for the final verification for control and programming system of mini laboratory and desktop 3-axis PKMM, throughout trial run. A detailed plan of methodology for developmentally testing is shown in Fig. 2, and special attention is paid to indirect methods of testing (A442), that is relating to the testing of the working accuracy.

Indirect testing methods were realized on the mini laboratory and desktop 3-axis PKMM during its trial work. These include verification of the workspace [5, 8], positions of referent points, and machining several test workpieces.

4. MACHINING EXPERIMENT

Several test workpieces are machined in order to verify the control and programming system. The main goal of the experiments was to test capabilities of the developed prototype of mini laboratory and desktop 3-axis PKMM.

The first test is done to verify the positioning of tool tip during the drilling of properly spaced holes, as an indirect testing method and is shown in Fig. 3a,b.

The second test is done to verify control and programming system based on G code using manually programming method. Linear interpolation is very serious test for parallel kinematic machine. A linear move is perhaps one of the most difficult motions that parallel kinematic machine can achieve. Therefore a non-standard test workpiece with grid of slots is chosen [6].

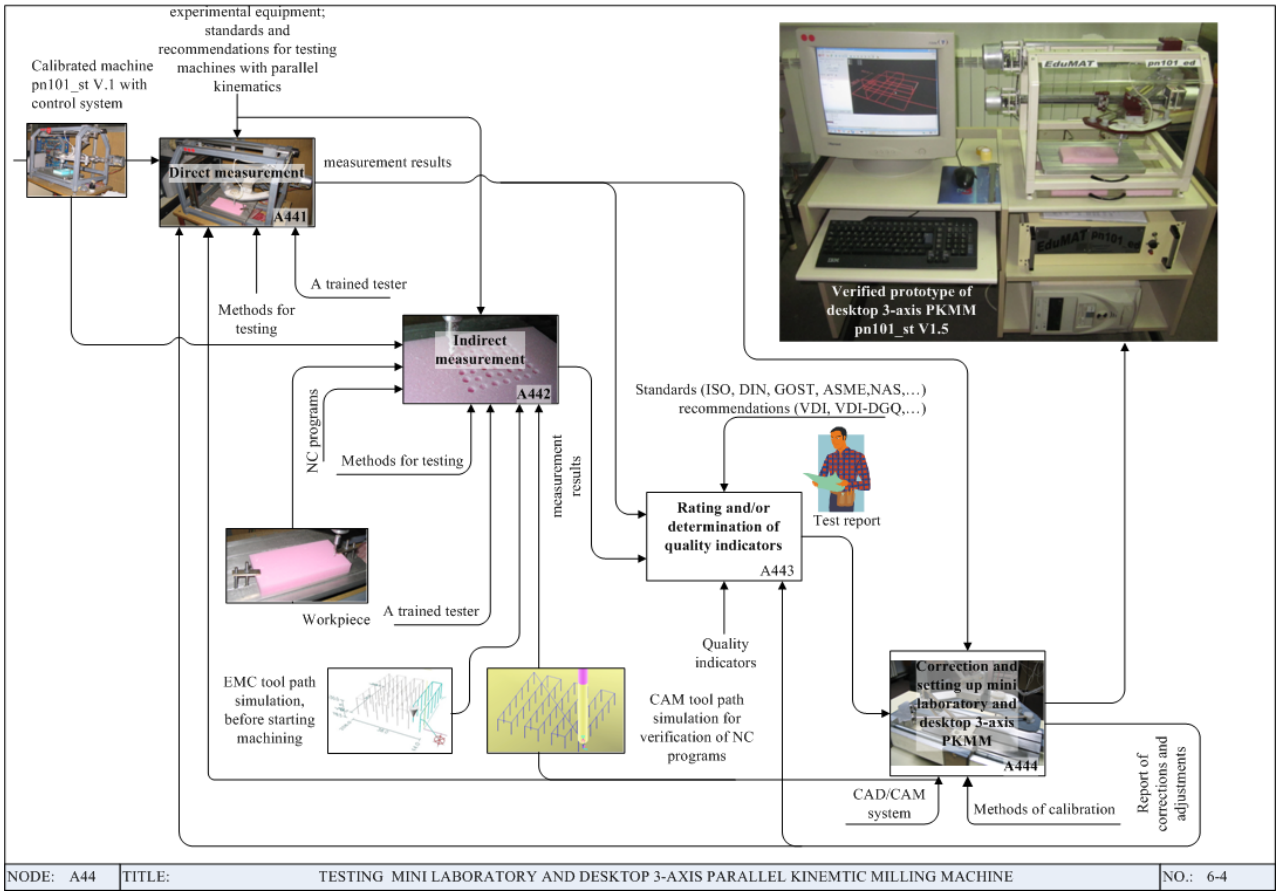

Fig. 2. The basic flow of activities for testing mini laboratory and desktop 3-axis PKMM

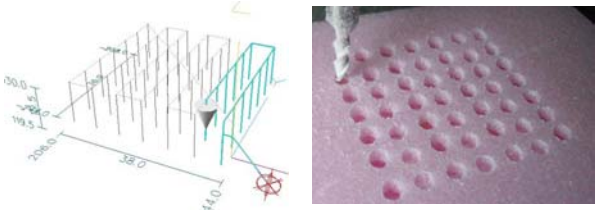

a) tool path simulation

b) drilling holes

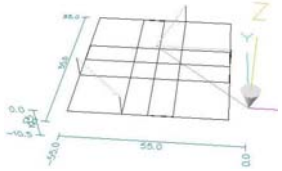

c) tool path simulation

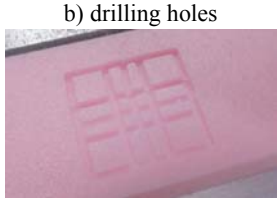

d) machined non-standard test workpiece with grid of slots

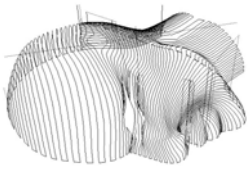

e) tool path simulation

f) machined workpiece having the shape of profile of human head

Fig. 3. First, second and third test workpiece machining

Tool path simulation and machined second test workpiece are shown in Fig. 3c,d. The third test is involved the machining of complex geometric esthetic surfaces, having the shape of profile of human head, using CAD/CAM system for programming. Fig. 3e,f shows 3 -axis machining of freeform surfaces having the shape of profile of human head.

The fourth test is done in order to verify current application of new method of programming based on STEP-NC. Figure 4 shows the example which refers to the machining benchmark workpiece based on the original STEP-NC program according to ISO 14649-11.

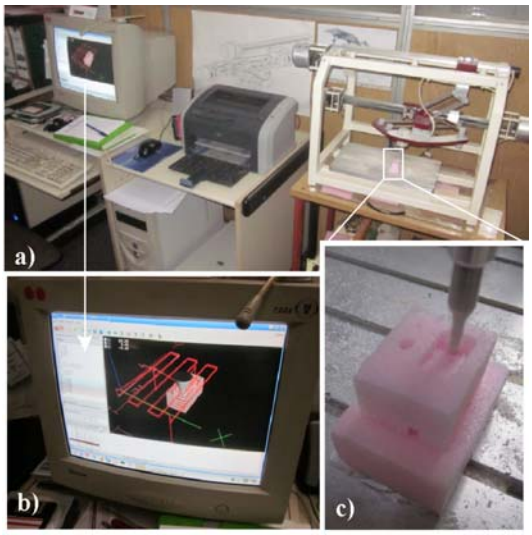

Fig. 4. Machining benchmark workpiece based on the original STEP-NC program according to ISO 14649-11

There are five machining working steps in this benchmark test. They are milling the top surface of the workpiece, drilling and reaming the hole, and rough and finish milling the pocket. Original STEP-NC program, according to ISO 14649-11 is translated using STEP-NC interpreter [20] in Canonical Machining Commands (CMCs), then these CMCs are translated into G code and then machining workpiece on the mini laboratory and desktop 3-axis PKMM is carried out.

Dimensions of workpieces are set according to the dimensions of machine workspace. Several test workpieces were made of styrofoam. In any considered case, a flat end mill tool (diameter 3 mm), was used.

For the prepared programs, the test workpieces are set in workspace boundaries correctly and workpieces are machined. We can state that these tests have successfully verified control and programming system of prototype of mini laboratory and desktop 3-axis PKMM.

5. CONCLUSION

This paper described the programming methods for mini-laboratory and desktop 3-axis PKMM in several different ways, such as manually programming, conversational programming, programming using the CAD/CAM system and new programming method using the software STEP-NC Machine. The methodology for developmentally testing of new machine tool and application of this methodology for testing of mini-laboratory and desktop 3-axis PKMM during its trial work were presented in this paper.

Developed desktop machine can machining soft materials, it is programmable in a common way, and it is fully safe for user-beginners, and represents a comprehensive and sophisticated educational machine tool.

Our future research will be focused on realized open architecture control system, that can download and directly execute programs in some of the STEP-NC formats for mini-laboratory and desktop 3-axis PKMM.

Acknowledgment
The authors would like to thank the Ministry of Education, Science and Technological Development of Serbia for providing financial support that made this work possible.

6. REFERENCES

[1] Milutinovic D., Glavonjic M., Kvrgic V., Zivanovic S.: *A New 3-DOF Spatial Parallel Mechanism for Milling Machines with Long X Travel*, Annals of the CIRP, vol. 54, no.1, p. 345-348, 2005.

[2] Glavonjic M., Milutinovic D.: *Parallel structured milling machines with long X travel*, Robotics and Computer-Integrated Manufacturing, vol. 24, p. 310-320, 2008.

[3] Milutinovic, D., Glavonjic, M., Zivanovic, S., Dimic, Z., Kvrgic, V.: *Mini educational 3-axis parallel kinematic milling machine,* Proceedings of 3rd Interanational Conference on Manufacturing Engineering ICMEN and EUREKA Brokerage Event, Kallithea of Chalkidiki, Greece, p.463-474, 2008.

[4] Zivanovic, S., Glavonjic, M., Dimic, Z.: *Methodology for Configuring Desktop 3-axis Parallel Kinematic Machine,* FME Transactions, vol. 37, no 3, p. 107-115, 2009.

[5] Glavonjic, M., Milutinovic, D., Zivanovic, S., Dimic, Z., Kvrgic, V.: *Desktop 3-axis parallel kinematic milling machine,* International Journal of Advanced Manufacturing Technology, vol.46, p.51-60, 2010.

[6] Zivanovic, S., Glavonjic, M., Milutinovic, D., Slavkovic, N.: *Programming methods for mini laboratory and desktop 3-axis parallel kinematic milling machine*, Proceedings of 5th International Conference on Manufacturing Engineering ICMEN, pp.153-162, 2014..

[7] Živanović, S., Glavonjić, M., Milutinović D., Slavković N., Dimić Z.: *Razvoj prototipa mini laboratorijske i edukacione stone troosne glodalice sa paralelnom kinematikom,* TEHNIKA: Časopis saveza inženjera i tehničara Srbije, Tehnika-Mašinstvo 62, Broj 3, Godina LXIX, str 438-445, 2014.

[8] Živanović S.: *Development of educational parallel kinematic machine*, Zaduzbina Andrejevic, University of Belgrade Faculty of Mechanical Engineering, Apollo Graphic Production, Belgrade, 2012 (in Serbian)

[9] EMC, Enhanced Machine Controller, http://www.linuxcnc.org

[10] NIST, (the National Institute of Standards and Technology) http://www.isd.mel.nist.gov/projects/rcslib/

[11] ISO 6983-1:1982 Numerical control of machines – Program format and definition of address words – Part 1: Data format for positioning, line motion and contouring control systems.

[12] STEP NC-MACHINE, Step Tools, Inc., from http://www.steptools.com/products/stepncmachine

[13] Živanović, S., Glavonjić, M.: *Methodology for implementation scenarios for applying protocol STEP-NC*, Journal of Production Engineering, vol.17, no.1, p.71-74, 2014.

[14] Zhao Y., Habeeb S., Xu X.: *Reserach into integrated design and manufacturing based on STEP*, International Journal of Advanced Manufacturing Technology, vol.44, p. 606-624, 2009.

[15] Rauch M., Laguionie R., Hascoet J.Y., Suh S.H.: *An advanced STEP-NC controller for intelligent machining processes*. Robotics and Computer-Integrated Manufacturing, vol. 28, p. 375–384, 2012.

[16] Randjelovic S., Zivanovic S.: *CAD-CAM Data Transfer as a Part of Product Life Cycle*, Facta Universitatis Series: Mechanical Engineering vol.5, no.1 p.87-96, 2007.

[17] STEP-NC Newsletter, Issue 2, July 2000. http://www.step-nc.org/data/newsletter2.pdf

[18] STEP-NC Newsletter, Issue 3, November 2000. http://www.step-nc.org/data/newsletter3.pdf

[19] STEP-NC Newsletter, Issue 5, September 2003. http://www.step-nc.org/data/newsletter5.pdf

[20] Toolkit for ISO 14649 / STEP-NC, http://code.google.com/p/iso-14649-toolkit/downloads/list

Authors: **Assist. Prof. Dr. Saša Živanović, Prof. Dr. Dragan Milutinović, Slavković Nikola,** University of Belgrade, Faculty of Mechanical Engineering, Production Engineering Department, Kraljice Marije 16, 11120 Belgrade, Serbia, Phone.: +381 (11) 33-02-423, Fax: +381 11 33-70-364.
Zoran Dimić, Lola Institut, Kneza Višeslava 70A, 11030, Belgrade, Serbia, Phone.:+381 (11) 25 46 423

E-mail: szivanovic@mas.bg.ac.rs
dmilutinovic@mas.bg.ac.rs
nslavkovic@mas.bg.ac.rs
zoran.dimic@li.rs

Journal of Production Engineering
Vol.18 No.1
JPE (2015) Vol.18 (1) Original Scientific Paper
Mlađenović, C., Zeljković, M., Košarac, A., Živković, A.

DEFINITION OF MACHINING SYSTEMS STABILITY LOBE DIAGRAM USING ANALYTICAL MODELS

Received: 16 March 2015 / Accepted: 02 June 2015

Abstract: *The occurrence of self-excited vibrations in machining can cause a number of problems, such as: tool wear or breakage, poor surface quality, increase energy consumption, increase of noise, etc. In order to avoid the consequences of self-excited vibration it is necessary to define those cutting regimes which can not cause the occurrence of these vibrations. For this purpose, it is necessary to define a stability lobe diagram of the observed machining system, which shows the boundary between stable and unstable zone of machining operations, depending on the number of revolutions of the spindle and cutting depth.*
This paper, presents the application of analytical methods for defining of stability lobe diagram, for the case of a milling machining center FM-38.
Key words: *dynamic behavior of the machining system; self-excited vibrations; frequency response function; stability lobe diagram*

Definisanje karte stabilnosti obradnih sistema primenom analitičkih modela. *Pojava samopobudnih vibracija pri obradi rezanjem može da izazove neželjene pojave pri procesu obrade, kao npr. habanje ili lom alata, loš kvalitet obrađene površine, povećanje potrošnje energije, povećanje bučnosti mašine, itd. Da bi se izbegle posledice samopobudnih vibracija, pri radu mašine alatke potrebno je definisati one režime rezanja pri kojima ne dolazi do pojave ovih vibracija. U tu svrhu, potrebno je definisati kartu stabilnosti posmatranog obradnog sistema, koja prikazuje granicu između režima stabilnog i nestabilnog rada mašina u zavisnosti od broja obrtaja glavnog vretena i od dubine rezanja.*
U radu je, na primeru obradnog centra za glodanje FM-38, prikazana primena analitičkih modela za definisanje karte stabilnosti.
Ključne reči: *dinamičko ponašanje obradnih sistema; samopobudne vibracije; funkcija frekventnog odziva; karta stabilnosti;*

1. INTRODUCTION

When the machine tool works, it may cause the emergence of various types of vibration wich have a significant impact on the machining process. These types of vibration are free, forced and selfexcited vibrations.

The most unfavorable vibrations that occur in machining processes, are selfexcited vibration, which draw the energy necessary for their creation and growth of amplitude from the cutting process itself. These vibrations can occur due to friction in the tool-workpiece system, due to thermo-mechanical effects, or as a result of the regenerative effect, ie. variation of cutting depth during machining. Selfexcited vibrations often lead to unstable operation of machine tools, and also reduce the quality of the machined surface, causing the appearance of noise, leads to rapid wear of the cutting tools and elements of machine tools, etc. [1].

In order to avoid the consequences of selfexcited vibrations, it is often not possible to use certain cutting regimes, because they cause unstable operation of the machine tool. Diagrams which show the stable and unstable area of machine tools operation, are called stability lobe diagrams (SLD), and they are defined according to the number of revolutions of the main spindle and the cutting depth. Stability lobe diagrams are usually defined analytically based on the modal parameters of a machining system and the parameters of the cutting process.

The first research on of mathematical modeling of selfexcited vibrations are conducted by *Tobias* [2, 3] and *Tlusty* [2, 4], which identified a regenerative mechanism of selfexcited vibration, and developed a mathematical model in the form of delay differential equations (DDE). The zeroth order approximation, ZOA, method of *Altintas* and *Budak* [5] suggest making stability predictions using the zeroth order Fourier term to approximate the cutting force variation and achieve reasonably accurate stability lobe diagrams predictions for processes, where the cutting force varies relatively little, i.e. considerable radial immersions and large number of teeth.

Besides the above mentioned, a number of researchers is also applied complicated mathematical expressions for modeling selfexcited vibrations in order to define stability lobe diagrams, and so *Insperger* and *Stephan* [6, 7] apply semi-discretization method (SD) to reduce a complicated DDE method to series of ordinary differential equations (ODE) with a known solution. *Gradišek* [8] compared the stability limit of milling process obtained by methods ZOA and SD, and concluded that the two methods yield very similar stability lobe diagrams for machining with relatively large values of radial immersions, while for small values of the radial immersions these two methods provides stability lobe diagrams with significant differences. The occurrence of selfexcited vibrations are also analyzed by *Milisavljević* and *Zeljković*

[9,10,11], who developed the two-dimensional model for prediction of selfexcited vibration, based on the Sokolovski oscillator.

The paper considers two analytical models for defining a stability lobe diagrams of machining systems, average tooth angle model, and Fourier series model. These models are then applied for analytical definition of stability lobe diagrams for milling machining center FM-38. In order to determine the modal parameters of a machining system, which are required as input data in defining a stability lobe diagrams, a series of impulse tests in order to obtain a frequency response function (transfer function) of the system is conducted, from which it is possible to determine its modal parameters. In order to determine the modal parameters of a machining system, as well as to perform the calculations necessary for defining the stability lobe diagrams, the MATLAB programming environment is applied, and in order to collect experimental data in the impulse tests, a software system LabVIEW is applied.

2. DEFINITION OF STABILITY LOBE DIAGRAMS USING ANALYTICAL MODELS

As noted above, the stability lobe diagram shows the boundary between the stable and unstable zone of the cutting process, depending on the axial cutting depth b_{lim}, and machine tools spindle rpm (Fig. 1). Defining of the stability lobe diagram will be carried out on the basis of the two previously mentioned models, *Tlustys* average tooth angle model, and *Altyintas* Fourier series model.

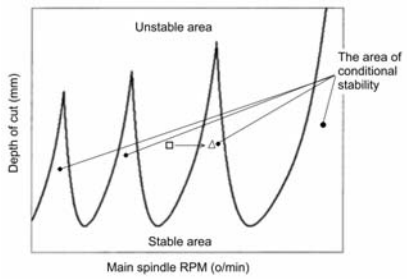

Fig. 1. Appearance of stability lobe diagram

2.1 Average tooth angle model

Tlustys average tooth angle model model was originally developed for orthogonal cutting operations, but the theory has been extended to include milling operations. For this purpose *Tlusty* adopted five assumptions [4, 12]:

- Oscillatory system is linear;
- Direction of variable cutting force component is constant;
- The variable component of the cutting forces depend only on the fluctuations in the direction perpendicular to the machined surface;
- Size of variable cutting force component varies proportionally and simultaneously with the change of the chip cross section;
- Although the position of the tool is variable in time, the system can be modeled as unchangeable in time by analyzing the stability of the system for a "average" angle of tool contact.

Taking into account the above assumptions, this model defines the axial depth of cut b_{lim} and the corresponding number of revolutions of the main spindle n, for frequency range in which one can expect the emergence selfexcited vibration. These values (b_{lim} and n) are entered into the stability lobe diagram relative to one another. The axial depth and number of revolutions of the main spindle are determined from the expression:

$$b_{\lim} = \frac{-1}{2K_S G_{orient} m'} \qquad (1)$$

$$n = \frac{f_c}{2\pi N\left(k + \frac{\varepsilon}{2\pi}\right)} \qquad (2)$$

Where:

G_{orient} i H_{orient} - real and imaginary part of the oriented transfer function

$k=0,1,2,3..$ - number of "waves" on the stability lobe diagram

f_c - frequency of selfexcited vibrations

Ks - specific cutting force

N - number of cutters teeth

$m' = N\frac{\phi_{ex} - \phi_{st}}{360}$ - the average number of tooth in contact with machined suface

$\varepsilon = 2\left[\pi - \tan^{-1}\left(\frac{G_{orient}}{H_{orient}}\right)\right]$ - phase shift between waves on machined surface after the passage of two successive tools teeth

2.2 Fourier series model

Altintas and *Budak* considered a milling tool with N teeth and helix angle 0º as a dynamic system with two degrees of freedom (Figure 2), and applied the method of Fourier series for solving complex equations of motion.

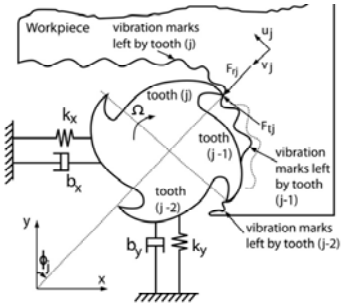

Fig. 2. Regeneration of waviness in a Fourier series model [5]

The axial depth and number of revolutions of the main spindle are determined from the expression:

$$b_{\lim} = \frac{2\pi\Lambda_R}{NK_t}\left(1+\kappa^2\right) \qquad (3)$$

$$n = 60 / NT \qquad (4)$$

Where:

Λ_R i Λ_I - real and imaginary part of the complex quadratic function which is defined on the basis of observed

system FRF, where: $\kappa = \Lambda_I / \Lambda_R$

$T = \dfrac{\varepsilon + 2k\pi}{\omega_c}$ - period between two successive tooth passage

$k=0,1,2,3,\ldots$ - number of "waves" on the stability lobe diagram

ω_c - angular velocity of sekfexcited vibration

$\varepsilon = \pi - 2\psi$ - phase shift between waves on machined surface after the passage of two successive tools teeth, where: $\psi = \tan^{-1}\kappa$

Ks - specific cutting force

N - number of cutters teeth

In order to define the stability lobe diagram by any of above-mentioned analytical models, it is necessary to know some of the dynamic characteristics of the observed system, or its modal parameters. In most cases the required information on the system dynamic characteristics are obtained from the transfer function (TF) or frequency response function (FRF) of the machine tool-tool holder-tool system.

In determining the TF of main spindle-tool system, the impulse tests are frequently applied. The machine tool structure is excited with a impulse hammer while the response was monitored by appropriate displacement, velocity or acceleration sensors.

3. STABILITY LOBE DIAGRAM OF MACHINING CENTER FM-38

To define the stability lobe diagram of a observed machining center, it is necessary to determine its modal parameters, ie. natural frequency, modal stiffness and damping coefficient, which is usually determined by the frequency response function (FRF) of the system.

As already noted, the frequency response function, of observed machining center can be identified experimentally using the impulse excitation force. The basic idea is to excite the machine structure by a impulse force at a certain place (tool tip), and to monitor the dynamic response of the system in the same or another place. Figure 3. shows an experimental model for the determination of a machining center FRF, consisting of triaxial acceleration sensor DYTRAN 3023A1 (1), which measures the oscillations of the tool tip, and the excitation hammer *Bruel & Kjaer Type 8206* (2). excitation hammer and accelerometer are connected to the *National Instruments cDAQ 9172* A/D converter *NI 9233* (3), which directly sends obtained information to the computer (4).

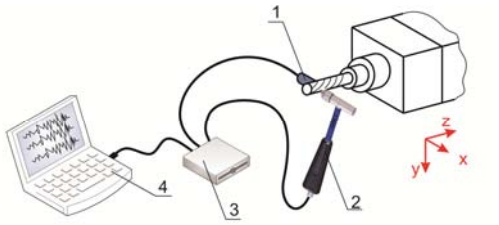

Fig. 3. The experimental model for determination of frequency response function machining

It should be noted that the HSS end mill with four cutting edges (teeth) and diameter ø10 is mounted in the machining center main spindle.

Accelerometer signal and the signal of the impact hammer are sent to the PC through the A/D converter, and stored in tabular form using the LabVIEW software. The application of program system MATLAB allows fast Fourier transform (FFT) of received signal and determining FRF of observed system, ie. its real and imaginary part. Figure 4 shows the real and the imaginary part of FRF for ø10 end mill mounted in the main spindle of machining center FM-38.

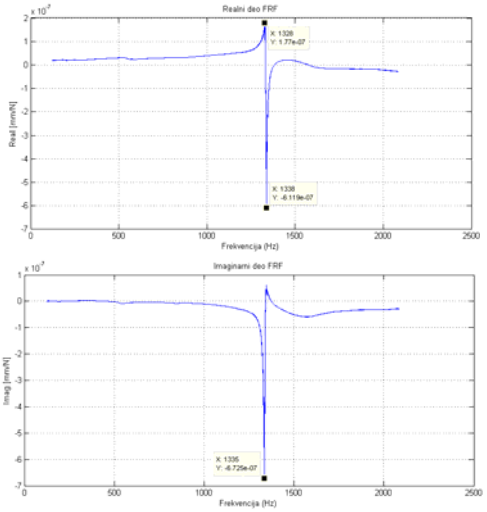

Fig. 4. Real and imaginary part of the FRF system

In addition to the calculated modal parameters for defining stability lobe diagram are also required parameters depend on the material of the workpiece and the machining process. These data, together with a defined modal parameters are shown in Table 1.

$f_n = 1335\ [Hz]$	- natural frequency of the system
$k = 1,9 \cdot 10^8\ [N/m]$	- modal stiffness of the system
$\zeta = 0,0037$	- damping coefficien
$d = 10\ [mm]$ $N = 4$	- diameter and number of tools teeth
$\beta = 60^\circ$	- angle of the cutting force
$K_{rc} = 0,07$ $K_{tc} = 800\ [N/mm^2]$	- corresponding coefficients of cutting force

Table 1. Parameters required for defining SLD

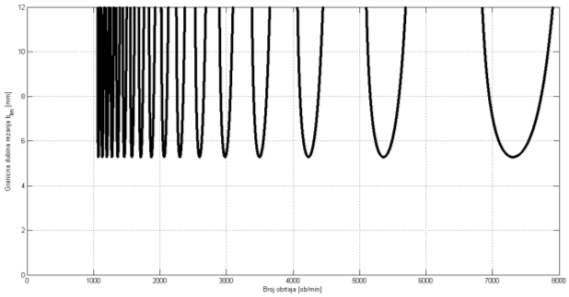

Fig. 5. Stability lobe diagram obtained by average tooth angle model

By applying MATLAB programming system, based on the parameters shown in Table 1 and using the two previously explained models, were defined two stability lobe diagrams as illustrated in (Fig. 5) and (Fig. 6).

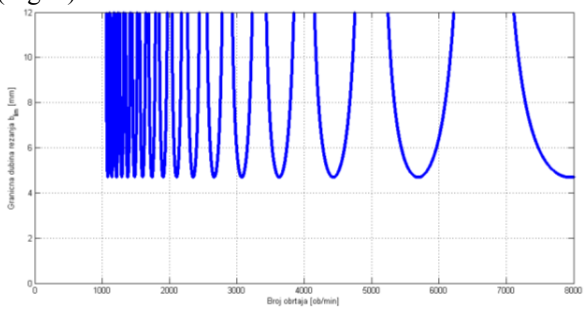

Fig. 6. Stability lobe diagram obtained by Fourier series model

4. CONCLUSION

The emphasis of this paper is placed on analysis and understanding of phenomena of selfexcited vibration in the milling process, through analytical models for defining the machining systems stability lobe diagram.

Defining of the stability lobe diagram was carried out on the basis of the two analitical models, *Tlustys* average tooth angle model [4], and *Altyintas* Fourier series model [5].

In order to determine the modal parameters of machining center FM-38, which are required for defining the stability lobe diagram, a series of experiments using modern diagnostic equipment was carried out.

By applying MATLAB programming system, based on the defined modal parameters and using the two analitical models, the two stability lobe diagrams were defined.

Analyzing the results, ie. stability lobe defined in this way, it is concluded that the average tooth angle model gives the limit depth of cut 5.28 mm, while model of Fourier series gives somewhat lower limit depth of cut 4.7 mm.

To analyze models for defining a stability lobe diagram of machining systems, which was conducted in this paper, it is necessary to experimentally define stability lobe diagrams of machining center FM-38, and then compare the obtained results with analytical data. This would assess the validity of the analytical models for stability lobe diagrams defining, and this task represents the direction of future research within the milling process stability analysis.

Acknowledgement: *This paper presents a part of the research results on the project "Contemporary Approaches in the Development of Special Solutions Bearing in Mechanical Engineering and Medical Prosthetics", TR 35025, financed by the Ministry of Education and Science of the Republic of Serbia.*

5. REFERENCES

[1] Quintana, G., Ciurana, J., Teixidor, D.: *A new experimental methodology for identification of stability lobes diagram in milling operations*, International Journal of Machine Tools and Manufacture, Vol. 48, Issue 15, pp. 1637–1645, 2008.

[2] Quintana, G., Ciurana, J.: *Chatter in machining processes: A rewiev*, International Journal of Machine Tools and Manufacture, Vol. 51, pp. 363–376, 2011.

[3] Tobias, S.A.; Fishwick, W: *Theory of regenerative machine tool chatter,* The engineer 1958, 258.

[4] Tlusty, J. Polacek, M.: The stability of machine tools against self-excited vibrations in machining, Proceedings of the ASME Production Engineering Research Conference, pp. 465–474, 1963.

[5] Altintas, Y., Budak, E.: *Analytical Prediction of Stability Lobes in Milling*, Annals of the CIRP, Vol. 44/1, pp. 357-362, 1995.

[6] Insperger, T., Stepan, G.: *Semi-discretization method for delayed systems*, International Journal for Numerical Methods in Engineering, Vol. 55, Issues 5, pp. 503–518, 2002.

[7] Insperger, T., Stepan, G.: *Updated semi-discretization method for periodic delay-differential equations with discrete delay*, International Journal for Numerical Methods in Engineering, Vol. 61, Issue 1, pp. 117–141, 2004.

[8] Gradisek, J., Kalveram, M., Insperger, T., Weinert, K., Stepan, G., Govekar, E.: *On stability prediction for milling*, International Journal of Machine Tools and Manufacture, Vol. 45, Issues 7-8, pp. 769–781, 2005/06.

[9] Milisavljević, B., Zeljković, M.: *Bifurkacije i samopobudne vibracije pri obradi rezanjem - dvodimenzionalni model*, Zbornik radova,VI medjunarodna naučno-stručna konferencija MMA '97 - Fleksibilne tehnologije, Novi Sad, 1997, str.103-108

[10] Milisavljević. B., Zeljković, M., Gatalo, R.: *The nonlinear model of a chatter and bifurcation*, Proceedings of the 5th engineering systems design and analysis conference - ESDA – ASME 2000, PD. Vol. 82, New York, 2000, pp 391 – 398

[11] Milisavljević, B., Zeljković, M.: *Bifurkacija ravnotežnog stanja pri obradi rezanjem: oscilator Sokolovskog*, Zbornik radova, 27. JUPITER konferencija - 23. simpozijum NU-ROBOTI-FTS, Beograd, 2001, str. 3.37 - 3.40

[12] Duncan, S. G.: *Milling Dynamics Prediction and Uncertainty Analysis Using Receptance Coupling Substructure Analysis*, Doctoral Thesis, University of Florida, 2006.

Authors: **MSc. Cvijetin Mladenović, Dr Milan Zeljković, Dr Aleksandar Živković**, University of Novi Sad, Faculty of Technical Sciences, Institute for Production Engineering, Trg Dositeja Obradovica 6, 21000 Novi Sad, Serbia, Phone.: +381 21 450-366, Fax: +381 21 454-495. **MSc. Aleksandar Košarac,** University of East Sarajevo, Faculty of Mechanical Engineering.
E-mail: mladja@uns.ac.rs, milanz@uns.ac.rs
acoz@uns.ac.rs, acosarac@gmail.com

Journal of Production Engineering
Vol.18 No.1
JPE (2015) Vol.18 (1) Original Scientific Paper
Brajlih, T., Kadivnik, Z., Paulic, M., Irgolic, T., Hadzistevic, M., Matin, I., Drstvensek, I.

COMPARISON OF SELECTIVE LASER SINTERING AND INJECTION MOULDING

Received: 20 May 2015 / Accepted: 22 June 2015
Abstract: *This paper presents a comparison between selective laser sintering and injection moulding technology for the production of small batches of plastic products. The comparison is based on analysing the time-cost efficiencies of each manufacturing process regarding the size of the series regarding the selected product sample. The presented analysis could be used as a general guideline for decision-making process regarding the more efficient manufacturing methods.*
Key words: *Additive Manufacturing; Selective Laser Sintering; Injection Moulding*

Poređenje selektivnog laserskog sinterovanja i injekcionog presovanja. *U radu se porede tehnologije selektivnog laserskog sinterovanja i injekcionog presovanja plastičnog proizvoda. Poređenje se zasniva na analizi vremena i troškova za svaku tehnologiju i tip proizvodnje. Predstavljena analiza se može koristi kao opšta smernica za izbor optimalnije tehnologije.*
Ključne reči: *aditivne tehnologije; selektivno lasersko sinterovanje; injekciono presovanje*

1. INTRODUCTION

For a long period additive manufacturing machines (AMM) were mainly used for Rapid Prototyping (RP). The parts made by these machines were used as various prototypes during different stages of product development. That meant that this was mainly individual or very low volume production at which AMM were generally more efficient than conventional manufacturing processes. Later, the Rapid Manufacturing (RM) term was established to describe cases of using AMM for producing end-user parts. Nevertheless, in the majority of these kinds of cases, it was individual, highly customised or very low volume production. Usually the search for the most appropriate manufacturing process was made amongst different additive manufacturing (AM) technologies. The most important decision criteria were usually the available material properties and achievable accuracy [1, 2], whilst manufacturing time and cost differences played only minor roles. The purpose of the research presented in this paper was to evaluate the efficiencies of AM regarding larger series. In such cases comparisons have to be made between conventional manufacturing processes that are usually used during high volume production.

2. STATE OF THE ART

The first research into the efficiencies of using AM was focused within the field of RP. These kinds of studies examined how AM performs compared to conventional workshop-based prototyping. The advantages shown by these studies, and proven by the quick expansion of AMM, enabled a new field of RM [3, 4]. Initial studies in this field mainly focused on comparing different additive technologies and machines between themselves [2, 4]. In addition, based on certain gained results, some decision making models were established [1, 3]. There have also been studies that compared AM to conventional manufacturing at high volume series but which usually also included some redesigning of the product itself by making it more adaptable to additive technologies [4].

3. RESEARCH APPROACH

At the beginning of the research a decision was made to limit the study to a single-product and the study was to be limited to the plastic part of the production. In order to obtain useful results, a real life example was needed of a part that would fit the description of a ‘standard usual mass-produced plastic part. A plastic cylindrical protective cover was chosen (Fig. 1).

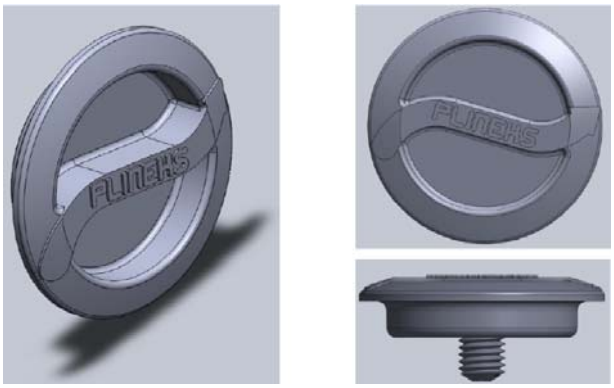

Fig. 1. Tested product

The larger diameter of the part was 55 mm and the part’s complexity was limited to company logo and an M10 thread on the part. In addition the company interested in producing the part was fairly unsure of

possible series volume, making the selected part even more appropriate for a planned study.

4. SELECTIVE LASER SINTERING

Selective laser sintering (SLS) is an AM technology that uses a laser as the power source to sinter powdered material, binding the material together to create a solid structure. The manufacturing procedure begins with CAD data preparation, orientation and placement in the machine's workspace, and layer and laser strategy definitions. In the next phase, the machine manufactures the parts. After the required cooling-down period, the parts can be cleaned.

Previous research has already proved that an individual part's cost depends largely on how efficiently the machines workspace is used during manufacturing [3]. The following analysis was made using selected product sample, a SLS machine with a workspace volume of 200 x 250 x 330 mm and 0.1 mm layer thickness when manufacturing. If we build just one part it takes the machine 2.05 hours to finish the manufacturing phase. If the entire level is filled (12 parts) manufacturing takes 2.65 hours. We can further increase the workspace yield by placing an additional 12 reoriented parts above the first level. In this case the manufacturing of 24 parts takes 4.65 hours.
The corresponding drop of in an individual part's required manufacturing time is presented by the following diagram (Fig. 2).

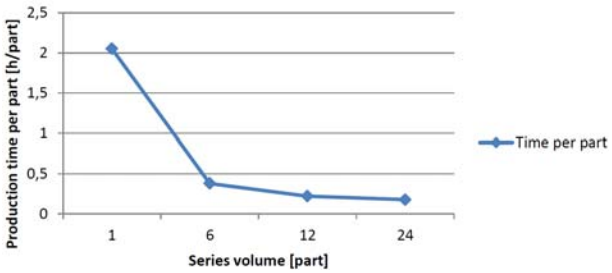

Fig. 2. Diagram of production time per part

If the entire workspace of the machine is filled by vertically adding this 24 parts setup, 192 parts are manufactured in 34.75 hours. Therefore, if serial production of the part is considered, it makes sense to continually manufacture parts with completely filled workspace volume jobs. Such production begins with initial data and machine preparation. Before manufacturing starts, a SLS machine has to be slowly preheated to the working temperature.

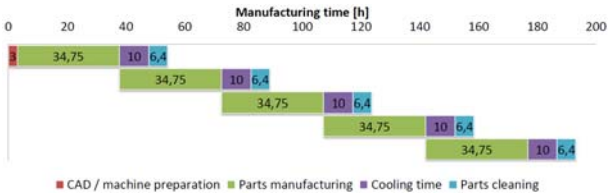

Fig. 3. Serial production workflow

During this time, CAD data and a controller program can also be prepared. When the manufacturing phase of the first job is finished the cooling down period begins. If the SLS machine has a removable workspace frame, this can be performed outside the machine. This means that the next process of manufacturing can start with the same program on an already preheated machine. When the cooling of the first process has finished, there is still enough time for all the parts to be cleaned before the next parts are completed on the same machine (Fig. 3).
In order to calculate the costs of serial production it was presumed that the SLS machine would be run 24 hour per day. The work runs over three shifts with one worker running and supervising the machine and also cleaning the finished parts, during each shift. The combined machine/worker hours was estimated at 25 €/hour. The cost must also be added, and was estimated at 2 € per part, presuming the previously presented workspace yield and recommended 50% used powder refresh rate. Now, the series volume dependent price part can be calculated (Fig. 4). The serial production runs in steps of 192 parts. The material and machine/worker's hourly costs during the required jobs are added to the costs of the initial CAD/machine preparation and final cooling-down and cleaning phases, when the serial production on the machine has already stopped.

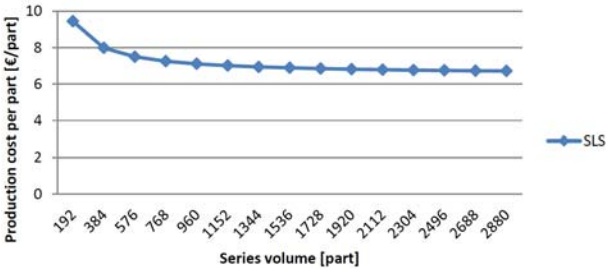

Fig. 4. Series volume dependand production costs per part

5. SELECTIVE LASER SINTERING

Injection moulding is a manufacturing process for producing parts by injecting the material into a mould. Injection moulding can be performed using a host of materials, including metals, glasses, elastomers, and most commonly thermoplastic and thermosetting polymers. After a product has been designed, by an engineer, moulds are made by a mouldmaker from metal, and precision-machined to form the features of the part.

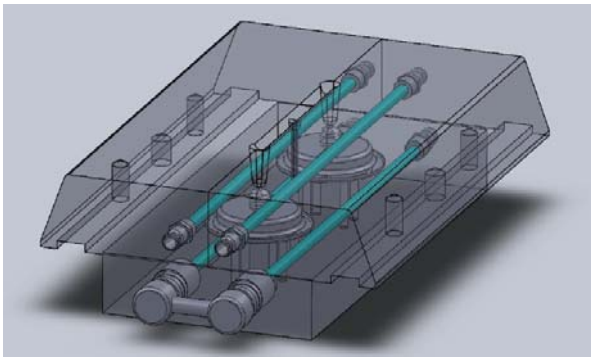

Fig. 5. Mould cavity design

In regard to the selected sample part, a two-nested cavity design was predicted in order to enable the removal of finished parts from the mould and a three-part cavity plate design was constructed (Fig. 5).

Besides the cavity part of the mould, other construction parts are also necessary when using the mould on a standard injection moulding machine (IMM). These parts are usually bought from standard mould parts' suppliers. The price of the standard parts necessary for tool assembly is usually a good indicator of the final mould price (often 50 % of the final price contributes to the standard parts). After consultation with a renowned mould making shop in Slovenia the final price of the selected injection mould design was estimated at 8,000 €.

Mould manufacturing time estimation was made under ideal circumstances, which meant that the mould making shop had free capacity to start each phase of the manufacturing process as soon as possible [2]. In such a case, 8 days were estimated to be required for presented the injection mould (Fig. 6).

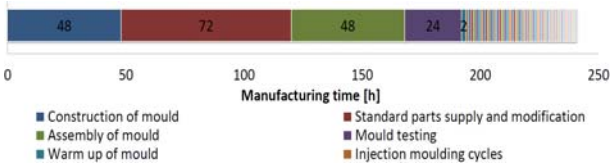

Fig. 6. Injection moulding serial production workflow

Next, a serial production on the IMM can begin. Again, a continual three-shift production was predicted. After 3 hour the initial mould/machine setup is performed 40 seconds (predicted by an injection moulding simulation software) sequential production of 2 parts begins. For the series number dependent price parts to be calculated, the costs of mould production, combined IMM/worker cost (20 €/h) and material costs (1 €/part) have to be considered (Fig. 7).

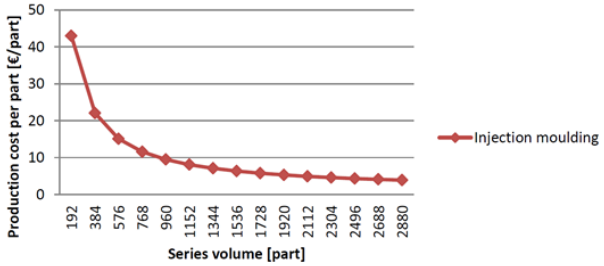

Fig. 7. Series volume dependand production costs per part.

6. SERIES VOLUME BASED COMPARISON

6.1 Production costs analysis

Production costs per part with SLS becomes almost constant for series volumes higher than 192 parts, due to only the initial CAD/machine preparation and final cooling-down and cleaning phase being distributed between more produced parts. In contrast, with injection moulding much higher mould production costs (per part) are quickly compensated by technology's much faster production rate.

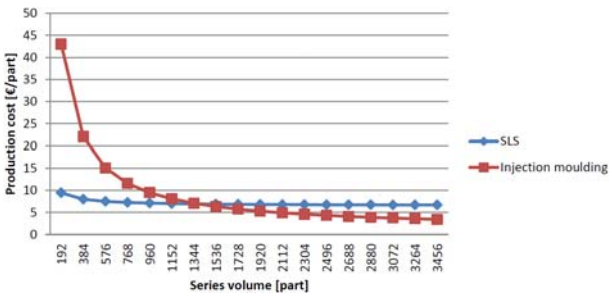

Fig. 8. Comparison of production costs per part

Naturally, a break-even point (a production volume at which the production costs per part are the same, regardless of the technology) is interesting (Fig. 8).

During the presented comparison an exact break-even point number could not be determined due to a lack of the necessary 192 parts cycle of SLS for the estimated production cost to be valid. However, a 192 interval value could be found after which the production costs per part of injection moulding fell below the almost constant costs per part of SLS. In the presented case this number was at 1344 parts at which the costs per part of SLS were 6.94 €/part whilst the injection moulded parts were at 7.09 €/part (Fig. 9).

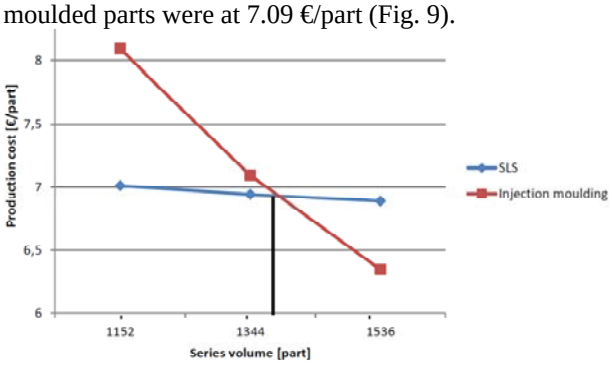

Fig. 9. Break-even point estimation

6.2 Production time analysis

The following production time analysis is also based on ideal circumstances that both technologies are available for any phase of production to start a soon as possible. With SLS production can start immediately and after 54 15 hours the first 192 parts were finished. Afterwards, each new batch of 192 parts was finished in 34.75 hours. With injection moulding technology an initial phase of mould production results in an 8 days waiting period for the first parts to be completed. Afterwards moulding production starts and quickly overtakes with 3150 parts already completed, when SLS would still be manufacturing the 192 part steps to 1152 series volume (Fig. 10). At that volume (3150 parts) the production costs per part of injection moulding would have already fallen to 3.6 €/part.

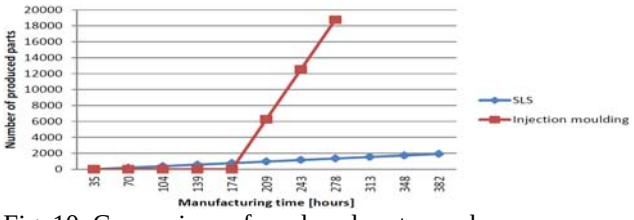

Fig. 10. Comparison of produced parts numbers

7. DISCUSSION

The presented results clearly show that SLS cannot compete with injection moulding regarding anything that could be considered as high volume production. The absolute numbers presented in this paper are only valid for the selected part's production, but general cost per part relationship between both technologies could be attributed to a general case. With injection moulding, there are always high initial costs for mould production that have to be compensated by larger series volume. Therefore, for any plastic part a certain lower limit of the series volume that is more cost-effective to be produced on SLS machine can be determined. This limit in a general case depends largely on how many parts are possible to be produced with maximal workspace volume yield within a single SLS machine run. This means that the part's maximal outer dimension and geometrical properties in connection with the particular machine's workspace have to be considered for each case. In a case when only single part serial production is considered and final CAD data is already available, an efficient workspace yield layout for that part can be quickly determined relatively. Once this is established, a predictively required manufacturing time can be obtained from a selective laser sintering machine's software.

8. REFERENCES

[1] Goffard, R., Sforza, T., Clarinval, A., Dormal, T., Boilet, L., Hocquet, S., and Cambier, F.: *Additive manufacturing of biocom-patible ceramics*, Advances in Production Engineering & Management, Vol. 8, no. 2, p.p. 96–106, 2013.

[2] Campbell, I., Bourell, D. and Gibson, I.: *Additive manufacturing: Rapid proto-typing comes of age*, Rapid Prototyping Journal, Vol. 18, no. 4, p.p. 255–258, 2012.

[3] Gracanin, D., Lalic, B., Beker, I., Lalic, D. and Buchmeister, B.: *Cost-time profile simulation for job shop scheduling decisions*, International Journal of Simulation Modelling, Vol. 12, no.4, p.p. 213–224, 2013.

[4] Evans, M. A. and Campbell R. I.: *A comparative evaluation of industrial design models produced using rapid prototyping and workshop-based fabrication techniques*, Rapid Prototyping Journal, vol. 9, no. 5, pp. 344–351, 2003.

Authors: **Dr. Tomaz Brajlih, B.Sc. Ziga Kadivnik, B.Sc. Matej Paulic, B.Sc. Tomaz Irgolic, Prof. Dr. Igor Drstvensek.,** University of Maribor, Faculty of Mechanical Engineering, Institute for Production Engineering, Smetanova ulica 17, 2000 Maribor, Slovenia, Phone.: +386 2 220 7596, Fax: +386 2 220 7996.

E-mail: tomaz.brajlih@um.si
ziga@ortotip.com
matej.paulic@gmail.com
tomaz.irgolic@gmail.com
igor.drstvensek@um.si

Prof. Dr. Miodrag Hadzistevic, Dr. Ivan Matin.,
University of Novi Sad, Faculty of Technical Sciences, Department for Production Engineering, Trg Dositeja Obradovica 6, 21000 Novi Sad, Serbia, Phone.: +381 21 450-366, Fax: +381 21 454-495.

E-mail: miodrags@uns.ac.rs
matini@uns.ac.rs

Journal of Production Engineering
Vol.18 No.1
JPE (2015) Vol.18 (1) Original Scientific Paper
Ocampo, L.

MEASUREMENT SYSTEM ANALYSIS OF WIREPULL TEST IN SEMICONDUCTOR WIREBONDING PROCESS: A CASE STUDY

Received: 6 April 2015 / Accepted: 4 May 2015

Abstract: *Wirebonding is a crucial process in semiconductor industry as bonding strength accounts for one of the major causes of yield loss. With this, the industry adopts a wirepull test (WPT) that measures the wirebond strength. It is thus important to evaluate the variability of the data obtained in WPT so that these approximate the actual wirebond strength and the variability caused by the measurement systems must be kept insignificant. Since, WPT involves procedures, intstruments and operators, measurement systems analysis (MSA) is a helpful tool in determining the validity of the measurement system. Thus, this paper presents a case study on the use of MSA in WPT of a wirebonding process in a leading semiconductor manufacturing firm in central Philippines. Results are reported in this work.*
Key words: *wirebonding, wirepull test, MSA, semiconductor*

Analiza sistema merenja testa kidanja pri procesu spajanja poluprovodnika: studija slučaja. *Spajanje je ključan proces u industriji poluprovodnika i kao vezivna snaga čini jedan od glavnih uzroka gubitaka. Zbog toga industrija usvaja test kidanja (VPT) koji meri vezivnu snagu spoja. Stoga je važno da se proceni promenljivost podataka dobijenih pri VPT tako da budu približni stvarnoj snazi spoja i promenljivost uzrokovanja mernih sistema mora da ostane beznačajna. Jer, VPT koji uključuje procedure, instrumente i operatere, analize mernih sistema (MSP) je korisna alatka u utvrđivanje valjanosti sistema za merenje. Tako da u ovom radu predstavlja studiju slučaja o korišćenju VBA u VPT pri procesu spajanja u vodećoj firmi koja se bavi proizvodnjom poluprovodnika u centralnim Filipinima. Rezultati su prikazani u ovovm radu.*
Ključne reči: *spajanje, test kidanja, MSA, poluprovodnik*

1. INTRODUCTION

In the semiconductor industry, wirebonding is a critical process that involves connecting the chips through contact pads, the substrates and the output pins [1] using Au, Al and Cu wires of high quality [2]. Technically, it is an electrical interconnection technique using thin wire and a combination of heat, pressure, and/or ultrasonic energy. This is where two metallic materials, i.e. wire and pad surface, are brought into intimate contact. Once the surfaces are engaged in intimate contact, electron sharing or interdiffusion of atoms happens, resulting in the formation of wire bond. Three types of wire bonding processes are known in the semiconductor industry: thermocompression bonding, ultrasonic bonding, and thermosonic bonding. A comprehensive discussion on the details of the wirebonding process can be found in Chauhan et al. [2].

Due to its wide applicability, this paper focuses on thermosonic wirebonding process. This process combines ultrasonic energy with the ball-bonding capillary technique of thermocompression. The process is practically similar, but in thermosonic bonding, the capillary is not heated and substrate temperatures are maintained typically between 120 to 220°. This is suitable for both ball-bonding and wedge-bonding which are two forms of wirebonding techniques. Servais and Bradenburg [3] claim that wirebonding may seem to be a simple process and is often taken for granted. In fact, wirebonding represents the highest yield loss which accounts to 42.5% relative to other processes in an integrated circuit assembly [1]. These failures can be attributed to various causes and insufficient bonding strength is one of the main causes [1].

There are many input variables in a wirebonding process and they are tightly monitored in a particular semiconductor firm. Two of the most important input variables directly related to a successful wirebond are the wire and the critical wirebond parameters such as the bond time, bond power, bond force and the heater block temperature [2]. Servais and Bradenburg [3] provided details on the evaluation of successful wirebonds. These two input variables highly impact the wirebond strength – an important key process output variable. To control wirebond strength, the semiconductor industry in general uses a destructive test method popularly known as wire pull test (WPT).

WPT or bond pull testing, is one of the several available time-zero tests for wirebond strength and quality. It is performed by applying an upward force under the wire to be tested, effectively pulling the wire away from the die. The greater upward force required to break the the wire, the better is the wirebond quality. Since WPT is crucial in determining wirebond test, semiconductor industry must ensure that the resulting values of the test really represent the actual wirebond strength with minimal variances. Failure to record these actual values would put the wirebonding process at

stake and may ultimately increase yield loss [1]. When actual values are recorded, process capability increases and defects related to the wirebonding process may be minimal. Since WPT involves the interfaces of equipment, methodology and operators, measuring the validity of this measurement system is a crucial task for process engineers and measurement system analysis (MSA) is the most appropriate approach.

This paper presents MSA of testing the validity of the measurement system used to conduct WPT. MSA is a methodology that quantifies a measurement error by examining various sources of variation in a process resulting from the measurement system, the operators and the parts [4]. MSA defines measurement quality in terms of bias, reproducibility, reliability and stability [5] although the term gauge repeatability and reproducibility has surfaced to represent bias, reproducibility, reliability [6]. A case study on a 2500 g-f WPT module in a leading semiconductor manufacturing firm in central Philippines is conducted to illustrate the methodology. The contribution of this paper is in presenting a case analysis on testing the capability of the measurement system used to perform wirepull test in determining wirebond strength.

This paper is organized as follows: Section 2 presents a literature review on wirebonding process and measurement system analysis. Section 3 details the methodology of the case study. Section 4 presents the results and discussion and Section 5 ends with a conclusion.

2. BACKGROUND OF THE STUDY

2.1 Wirebonding process

In the wirebonding process, the wire is usually made of gold (Au), aluminum (Al) or copper (Cu). Harmon [7], however details that Au thermosonic wirebonding has been used in the semiconductor industry for many decades. Because of the steep increase in prices of Au, the industry has shift to Cu although there are many issues that must be resolved in Cu wirebonding such as oxidation rate and hardness of Cu wire [8]. Although there are many benefits of Cu wirebonding including lower material cost, higher electrical and thermal conductivity; Goh et al. [8] highlight that cracking of the wirebond interface has been a problem due to high humidity and temperature. In fact, a number of studies have underscored the comparison between Au and Cu wirebonding technology. Zhaohui et al. [9] made such comparison in terms of bond force, stress and strain distribution of the bond pad and temperature evolution during the bonding process. It was found out Cu wirebonding induces much higher stress and strain to the electrode structure compared to Au wirebonding process. It was also found out that plastic and friction heating effect of Cu wirebonding is more significant than Au wirebonding as Cu wirebonding requires more bonding force and power. Goh et al. [8], on the other hand, made the same comparison in terms of their corrosion and oxidation behaviour under different environmental conditions. It was found out that Au wirebonding process produces good results.

Wire size must be compatible with the semiconductor pad area and therefore quite thin that commonly ranges from 15 to 25μm in diameter. There are two forms of wire bonding technique: wedge bonding and ball bonding. In ball bonding, the thin Au wire tip is melted with a small electrical spark which eventually forms metal ball at the end of the wire. Then the capillary from which the wire is fed presses the wire into the bonding pad on the chip. The capillary lifts and moves to the connection pad where it descends and attaches the wire to the metal pad. While the capillary is down, the wire is pulled back so that it breaks close to the bonding area. After, the capillary is lifted and a few microns of wire is fed in. At this stage, the capillary is ready to form a ball again for the next ball bonding process. In wedge bonding the wire is pressed into the semiconductor pad horizontally and attaches in that position. After the first bond, the wedge tool tip is lifted and moves to the connection pad position where the wire is attached horizontally. The wire is now pulled in order to break after the attachment near the bond area. The wedge tool is lifted and a few microns of wire are fed making it ready to the next wedge bond process. Figure 1 shows a ball bond attached to the wire pad and Figure 2 shows the mechanism of the wirebonding process. A thorough discussion on this process can be found in Chauhan et al. [2] and Su and Chiang [1].

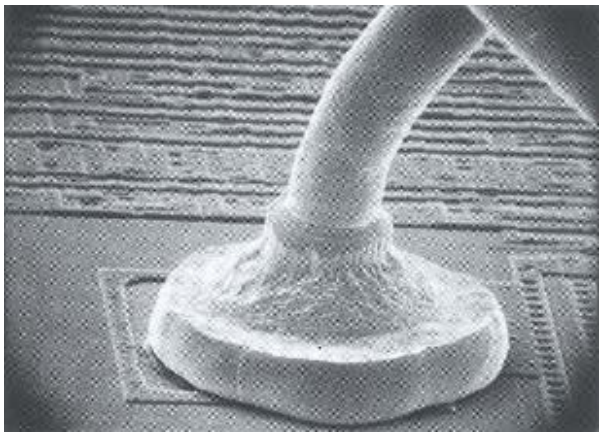

Fig. 1. Front view of the ball bond attached to a die pad [3]

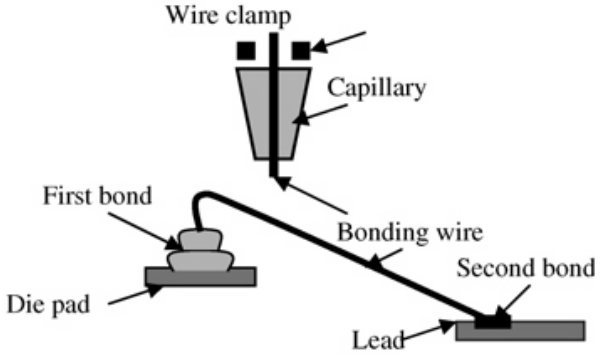

Fig. 2. The mechanism of wirebonding process [1]

Currently, three bondong methods are available: thermocompression, ultrasonic and thermosonic. Thermocompression consists of applying a relatively high force with the wire ball into the pre-heated or substrate operating at 250^0C up to 500^0C and the wire must be gold. Ultrasonic wirebonding consists of applying a relatively smaller force pressing the wire to the substrate at room temperature and applying vibrational energy in the form of ultrasounds with wire material can be either gold or aluminum. Thermosonic wirebonding on the other hand is the most preferred method which is a combination of thermocompression and ultrasonic methods operation at 100^0C up to 200^0C and wire material can be either Au, Al or Cu. Comprehensive discussion on almost all details of wirebonding process can be found in Chauhan et al. [2]. Nevertheless, wirebonding is a crucial process and quality of the bonding strength is one of the major causes of wirebonding failures [1].

2.2 Measurement system analysis (MSA)

Montgomery [10] claims that determining the capability of the measurement system is an important part of many quality and process improvement activities. However, Mukherjee et al. [11] argue that it may not be cost efficient to calibrate each measurement device daily, nor would it be beneficial to calibrate or test each device only once per decade. Thus, MSA provides a quantitative tool in determining the capability of the measurement system. MSA seeks to describe, categorize, and evaluate the quality of measurements, improve the usefulness, accuracy, precision, and meaningfulness of measurements [12]. It is experimental and statistical method that identifies the variations in the measurement system [10]. It is used to verify that the differences in the data are due to actual differences in what is being measured and not to variation in measurement system. In any measuring, some of the observed variability is due to variability in the process, whereas the rest variability is due to the measurement error or gauge variability. Smith et al. [13] detail the aspects of MSA in terms of analyzing bias, linearity, reproducibility, reliability and stability of the measurement system. Bias is the systematic error that is an indication of a measuring instrument. In statistical terms, bias is recognized when the averages of measurements have a different fixed value from the reference value [14]. Linearity ensures that measurement is true and/or consistent across the range of the gauge. Stability implies that measurements remain constant and predictable over time. Repeatability refers to the variation that occurs when repeated measurements are made of the same item under identical conditions, also known as the equipment variance and reproducibility refers to the variation that occurs when different conditions are used to make the same measurements, also know as the appraiser variance. The framework of MSA is shown in Figure 3 which implies that the measurement system consists of methods, the instruments and the operator. Thus, determining holistic capability of the measurement system require careful consideration of this interconnected system.

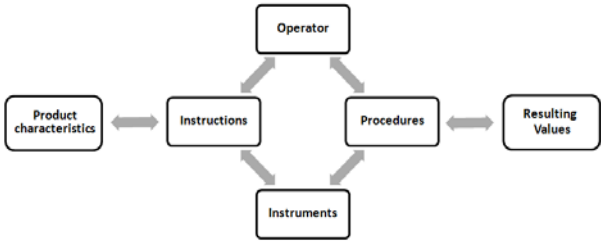

Fig. 3. Measurement system analysis process [15].

3. METHODOLOGY

3.1 Wirepull test (WPT)

WPT requires an equipment commonly known in the semiconductor industry as the wire pull tester or bond pull tester which consists of two major parts. The first part is a mechanism for applying the upward pulling force on the wire using a tool known as a pull hook and the second part is a calibrated instrument for measuring the force at which the wire eventually breaks. This breaking force is expressed in gram-force (g-f). Figure 4 shows a wirepull tester and pull hook used in this case study.

Figure 4. Wire pull tester stage (left) and a pull hook (right)

There exist various test conditions in performing WPT, however, the double-bond WPT is widely used for conventional wirebonded semiconductor devices. This procedure consists of applying the pull hook under a wire that is attached at both ends, i.e., one end to a bond pad on the die, and the other end to the bonding finger or bonding post of the device. The pull hook is usually positioned at the highest point along the loop of the wire, and the pulling force is applied perpendicular to the die surface (vertically if the die surface is horizontal). The wire pull tester measures the pulling force at which the wire or bond fails. The measured force is then recorded in gram-force (g-f). Aside from the bond strength reading, the operator must also record the bond failure mode. Failure mode in this case refers to one of the following: first bond (ball bond) lifting, neck break, midspan wire break, heel break, second bond (wedge bond) lifting. For this case study, only the wirebond strength reading is measured and analyzed for MSA. Figure 5 shows the schematic diagram of the WPT process. Force (F) is applied to the wire until it breaks. The dage machine or the wirepull tester as shown in Figure 6 records the force applied F at the break point.

3.2 Data gathering

For every measured WPT data, total variation can be expressed as:

$$\sigma_T^2 = \sigma_{AT}^2 + \sigma_{MS}^2 \quad (1)$$

where σ_T^2 is the total variability of the data, σ_{AT}^2 is actual variation of the wirebond strength data and σ_{MS}^2 is the variation due to the measurement system. Note that in MSA, σ_{MS}^2 must be insignificant to σ_T^2 so that $\sigma_{AT}^2 \rightarrow \sigma_T^2$. Data are gathered from the results of the WPT for a week time duration. For stability analysis, 125 readings of 1,500 g-f reference value are evaluated from 25 subgroups referring to 25-hour runs randomly selected from three shifts for one week. Five trials are gathered for each run. For bias, ten random samples of 500 g-f reference value are gathered. For linearity, 50 samples are evaluated of 50, 250, 500, 1,000, 2,500 g-f reference values. For gage reproducibility and repeatability (GR&R), three operators are analyzed each with three trials, corresponding to three days, and ten samples per trial. All statistical analysis were done through SAS JMP software v. 9.0.

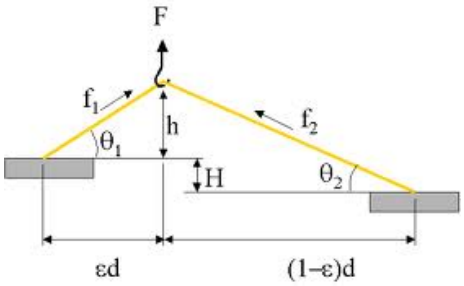

Fig. 5. Schematic diagram of the WPT.

Fig. 6. Wirepull tester used in the case firm

4. RESULTS AND DISCUSSION

4.1 Short-term stability

For a period of one week, 25-hour subgroups are gathered each with five trials. The reference value for this test is 1,500 g-f. For brevity, the data set is not presented here. Figure 7 shows the $\bar{x}$ and R control chart.

It can be observed in Figure 7 that as far as short term stability is concerned, the readings are within control limits and therefore, the readings are stable in the short run.

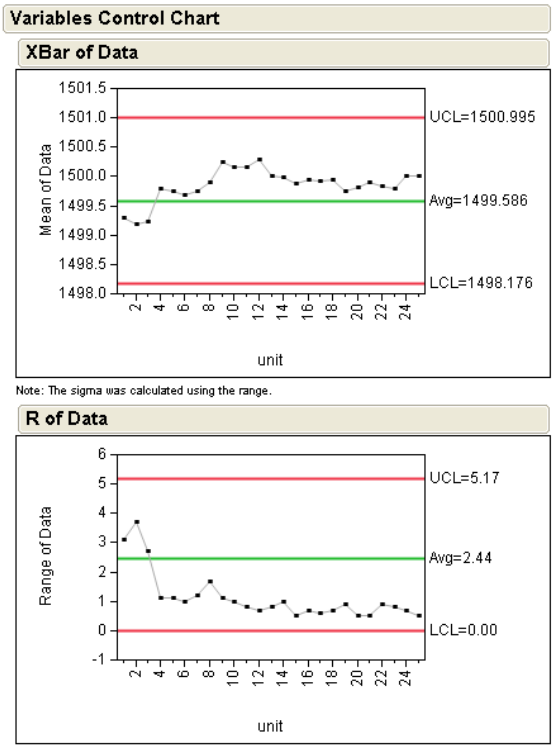

Fig. 7. $\bar{x}$ and R control chart using SAS JMP 9.0

4.2 Bias

Previous studies done in the case firm suggest that WPT data follows a normal distribution. Thus, from Central Limit Theorem, it is acceptable to gather less than 30 samples and then analyze bias from there. With this, ten samples were randomly picked from the 7-day, 24-hour per day operation for the WPT. For a measurement system to be valid, it must be accurate such that the mean μ of the error (referred herein as the bias) should be μ = 0. In this case, we can set the following hypothesis:

$$H_0 : \mu = 0 \quad (2)$$

$$H_1 : \mu \neq 0 \quad (3)$$

Using t-test for this hypothesis testing, the following analysis is shown in Figure 8.

Using $\alpha = 0.05$, the two-tailed t-test yields $p-value = 0.7976 > \alpha = 0.05$, therefore H_0 must be accepted and conclude that at 95% confidence level, $\mu = 0$ which shows that the readings are not bias. It can be also extended using at 95% confidence level, $-0.19129 \leq \mu \leq 0.15129$ which further implies that there is a probability that μ=0. Thus, the readings are not bias.

4.3 Linearity

For readings to be consistent across levels of the gage, the bias of each of the readings compared to the reference value of the wirebond strength should be consistent such that it exhibits linearity across reference

values. The linearity condition in MSA states that at a range of reference values, bias is consistent.

For the experiment, 10 readings for each of the 5 levels, i.e. 50, 250, 500, 1000, 2500 g-f are gathered in random for one week period. Figure 9 shows the results.

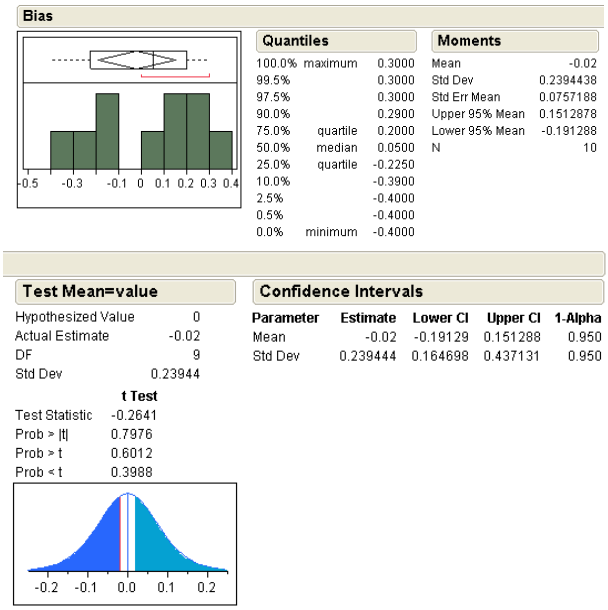

Fig. 8. t-test for bias

In Figure 9, bias values are plotted against reference values. For MSA, the slope of the regression fit should be close to zero. This can be explained as follows. When slope is close to zero, therefore bias is consistent throughout the reference values. To test if the regression fit is valid, SAS JMP displays t-test (two-tailed). Values are 0.9529 and 0.7389 for intercept and reference values respectively, which are greater than α = 0.05. Therefore, the slope of the regression is significantly zero. Further explanation of the linearity test can be done graphically. It is shown that the regression line is within the confidence band at level 95%. Thus, linearity is acceptable.

4.4 Gage Repeatability and Reproducibility

Three operators were taken into consideration. Each operator is given three days each at ten readings per day. Figure 10 shows the results.

From Figure 10, %GR&R = 3.958% which means that GR&R error is only taking up 3.958% of the total variation, less than the acceptable 10%. The number of distinct categories (NDC) as shown is also greater than 5. Thus, the gage is acceptable.

4.5 Summary of MSA

The following tables show the summary of the results of MSA.

Control Limits:	$\bar{x}$ - Chart	R - Chart
UCL	1500.9950 g-f	5.1700 g-f
CL	1499.5886 g-f	2.4400 g-f
LCL	1498.1760 g-f	0.0000 g-f
Short-Term Stable?	Yes	

Table 1. Short term stability summary

Standard Used	
True Value	500 g-f
$\bar{x}$	500.0200 g-f
Bias	- 0.0200
Prob>|t|	0.7976
Significant Bias?	Not significant

Table 2. Bias summary

Standards Used			
True Values	50 g-f 1000 g-f	250 g-f 2500 g-f	500 g-f
For Each Standard:			
$\bar{x}$	50.005 g-f 999.940 g-f	250.001 g-f 2499.990 g-f	500.020 g-f
Significant Linearity?	Not significant		

Table 3. Linearity summary

Estimate of Variance	Variation	% Tolerance	% Total	% Contribution
EV	1.0435	0.0400	0.0000	0.0000
AV	0.4541	0.0200	0.0000	0.0000
Interaction	0.2777	0.0100	0.0000	0.0000
GRR	1.1380	0.0500	0.0000	0.0000
PV	2875.5544	118.3400	100.0000	100.0000
TV	2875.5546	118.3400	100.0000	100.0000
P/T Ratio	0.00047			
NDC	3562			
Capable?	Yes			

Table 4. GR&R summary

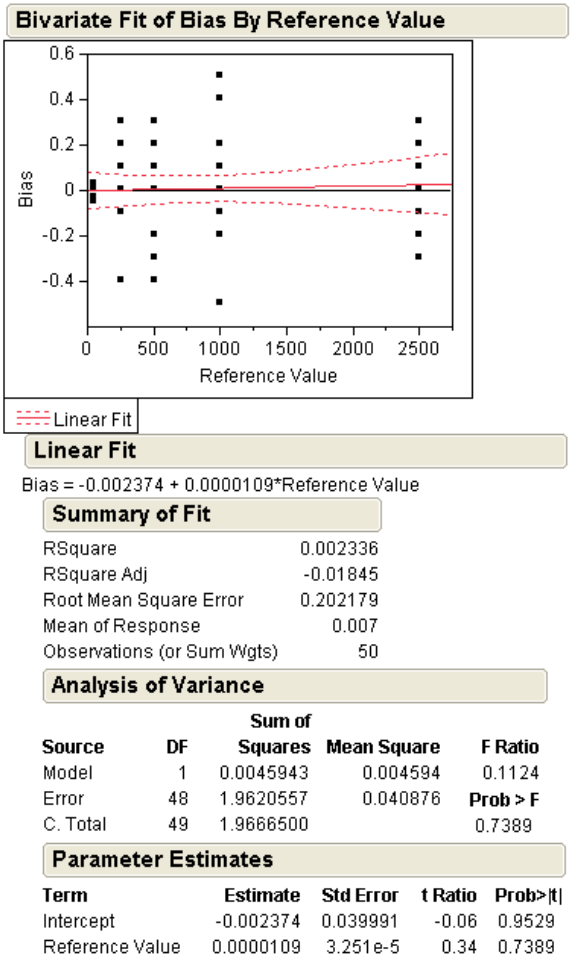

Fig. 9. Linearity analysis using SAS JMP v. 9.0

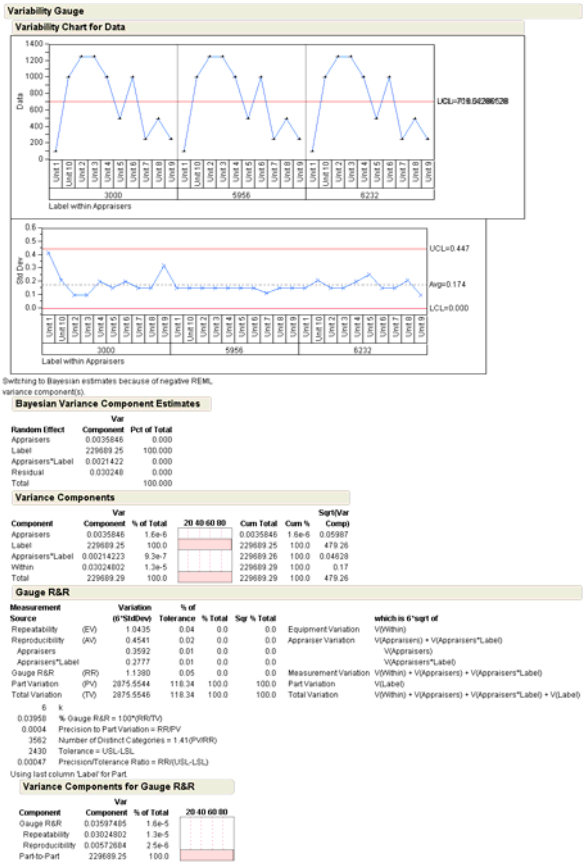

Fig. 10. GR&R analysis using SAS JMP

5. CONCLUSION

This study presents MSA of wirepull test in a semiconductor wirebonding process. Results show that 2500 g-f Wirepull Module has an acceptable measurement system based from stability, accuracy, linearity and GR&R analysis. In Repeatability and Reproducibility summary, almost 100% of the variation is taken by actual variation of readings of wirebond pull strength, not by the measurement system i.e. equipment, operator and the interaction of both. At 95% confidence level, $\sigma_{AT}^2 \rightarrow \sigma_T^2$. At this level, the 2500 g-f wirepull module can be used to measure wirebond strength for engineering and statistical analysis. The process presented using MSA can be used to evaluate other measurement systems of the case firm or of any manufacturing process.

6. REFERENCES

[1] Su, C.-T., Chiang, T.-L.: *Optimizing the IC wire bonding process using a neural networks/genetic algorithms approach*, Journal of Intelligent Manufacturing, Vol. 14, No. 2, pp. 229-238, 2003.

[2] Chauhan, P.S., Choubey, A., Zhong, Z., Pecht, M.G.: *Copper wire bonding*, Springer, New York, 2014.

[3] Servais, G.E., Brandenburg, S.D.: *Wire bonding – a closer look*, ISTFA'91: The 17th International Symposium for Testing & Failure Analysis, pp. 525-529, Los Angeles, California, 1991.

[4] Kazemi, A., Haleh, H., Hajipour, V., Rahmati, S.H.A.: *Developing a method for increasing accuracy and precision in measurement system analysis: a fuzzy approach*, Journal of Optimization in Industrial Engineering, Vol. 3, No. 6, pp. 25-32, 2010.

[5] AIAG: *Measurement systems analysis, reference manual*, 3rd ed., Automative Industry Action Group, Southfield, Michigan, 2002.

[6] Foster, S.T.: *Managing quality: an integrated approach*, 3rd ed., Prentice Hall, Upper Saddle River, New Jersey, 2006.

[7] Harmon, G.: *Wire bonding in microelectronics: materials, processes, reliability and yield*, 2nd ed.; McGraw-Hill, New York, 1997.

[8] Goh, C.S., Chong, W.L.E., Lee, T.K., Breach, C.: *Corrosion study and intermetallics formation in gold and copper wire bonding in microelectronics packaging*, Crystals, Vol. 3, No. 3, pp. 391-404., 2013.

[9] Zhaohui, C., Yong, L., Sheng, L.: *Comparison of the copper and gold wire bonding processes for LED packaging*, Journal of Semiconductors, Vol. 32, No. 2, pp. 024011-1- 024011-4, 2011.

[10] Montgomery, D.C.: *Introduction to statistical quality control,* 5th ed., JohnWiley & Sons, Inc., NY, 2005.

[11] Mukherjee, S., Paul, A.R., Roy, P.: *Mechanical sciences: Engineering mechanics and strength of materials*, PHI Learning Pvt. Ltd., New Delhi, India, 2005.

[12] Allen, M.J., Yen, W.M.: *Introduction to Measurement Theory*. Brooks/Cole, Monterey, California, 1979.

[13] Smith, R.R., McCrary, S.W., Callahan, R.N.: *Gauge repeatability and reproducibility studies and measurement system analysis: a multimethod exploration of the state of practice*, Journal of Industrial Technology, Vol. 23, No. 1, pp. 2-12, 2007.

[14] George, M.L., Maxey, J., Price, M., Rowlands, D.: *The lean six sigma pocket toolbook*, McGraw-Hill, New York, 2005.

[15] Ford, *General Motors and Chrysler MSA Reference Manual*, 1995.

Author: **Dr. Lanndon Ocampo, Lecturer,** University of San Carlos, Department of Mechanical Engineering, Cebu City, 6000 Cebu, Philippines
Phone.: +63 932 5101510
E-mail: don_leafriser@yahoo.com

Journal of Production Engineering
Vol.18 No.1
JPE (2015) Vol.18 (1) Original Scientific Paper

Kiss, F., Rajović, V.

LIFE CYCLE INVENTORY ANALYSIS OF LIGNITE-BASED ELECTRICITY GENERATION: CASE STUDY OF SERBIA

Received: 26 May 2015 / Accepted: 22 June 2015

Abstract: *The study provides updated life cycle inventory data of electricity generated in Serbian coal-fired power plants. The data refer to the situation in 2012 and cover the whole life cycle of electricity, including power plant emissions, and up- (e.g., coal mining and transportation, provision of auxiliary materials, etc.) and downstream (e.g., coal ash treatment) processes. In 2012, the global warming potential and the cumulative fossil energy requirements of electricity were 1.18 kg CO_{2eq}·kWh^{-1} and 11.64 MJ·kWh^{-1}, respectively.*
Key words: *Electricity, lignite, life cycle inventory, power plants, Serbia.*

Analiza inventara životnog ciklusa električne energije iz termoelektrana na lignit u Srbiji: studija slučaja. *Studija daje uvid u ažurirani inventar životnog ciklusa proizvedene električne energije u elektranama na ugalj u Srbiji. Podaci se odnose na situaciju 2012. i pokrivaju celokupan životni ciklus električne energije, uključujući emisije iz elektrana, proizvodni lanac električne energije (eksploatacija uglja, transport, dodatni materijali, itd) i tretiranje otpada (npr. pepeo nakon sagorevanja). Potencijal globalnog zagrevanja i kumulativne potrebe električne energije za energijom iz fosilnih goriva bio je 1,18 kg CO_{2eq}·kWh^{-1} i 11,64 MJ·kWh^{-1}, respektivno.*
Ključne reči: *Električna energija, lignit, inventar životnog ciklusa, elektrane, Srbija.*

1. INTRODUCTION

Without electricity, no industrial process would be achievable. Therefore, accurate life cycle inventory (LCI) of electricity system in life cycle assessment (LCA) study is crucial. Commercial LCI databases on Serbian electricity system are based on older information, often from the mid-1990s, which makes them uncompetitive. Updated Serbian electricity system LCI data would grant benefit to many LCA studies. In 2012, net electricity generation in Serbia was approximately 34,509 GWh [1]. 70.4% of electricity production in 2012 relied on lignite, most undesirable coal (low calorific value, high moisture and sulphur content). Hydroelectric power plants contributed 28.5% of the total, while other energy sources (mainly natural gas) have virtually negligible share in total electricity generation (about 1%) [1].

In 2013 the Electric Power Industry of Serbia *(Elektroprivreda Srbije – EPS)* published several reports [1, 2], which provided information on annual emissions, fuel consumption and the net electricity generation of each Serbian power plant. Information provided by EPS is very useful, but limited in LCA study for a few reasons. Data on upstream processes (e.g. extraction, fuel production, fuel transportation) is not provided and modest information on emissions is presented.

The aim of this study is to provide more accurate and comprehensive LCI information on electricity generated in the Serbian coal-fired power plants in 2012 by including flows associated with upstream processes (e.g., fuel extraction, fuel production, etc.) and other emissions not addressed in the EPS reports.

The assessment is limited to coal-fired power plants (i.e., thermal power-plants; TPPs). However, the results of this research are a good proxy for the total environmental impacts caused by electricity generation in Serbia, given the negligible environmental impacts arising from life cycle emissions associated with hydroelectricity [3] and small share of other fossil fuels (ca. 1%) in electricity generation [1].

2. METHODS AND MATERIALS

2.1 Coal-fired power plants in Serbia

LCI of six Serbian coal-fired power plants (operated by EPS) is presented in this study. 3,936 MW is their total net output capacity, which is 55% of total capacities [1]. Overview of power plants covered in this research is given in Table 1. More detailed data on the technical characteristics of Serbian coal-fired power plants are available on the webpage of the Electric Power Industry of Serbia.

2.2 Functional unit and system boundaries

The functional unit is defined as 1 kWh of electricity generated in Serbian coal-fired power plants in 2012. System boundaries include *i)* coal mining, *ii)* coal transportation, *iii)* coal combustion in TPPs, i.e. electricity generation, and *iv)* treatment of coal ash. Transmission and distribution of electricity and consequently the electric grid infrastructure and losses are not within the system boundaries.

2.3 LCI data and assumptions

Data on power plant emissions, fuel and material inputs of electricity generation are largely available from EPS reports [1, 2], while LCI data associated with these inputs is taken from the Ecoinvent v.2.2 LCI database [4] which is integrated in the SimaPro 8 LCA software used for calculations.

Name of the TPP	abbrev.	Net output electric capacity (MW)	Electricity generation ($GWh \cdot a^{-1}$)	Thermal energy generation ($GWh \cdot a^{-1}$)	LHW* of coal ($kJ \cdot kg^{-1}$)	Coal consumption (million Mg**)
TPP "Nikola Tesla A"	TENT A	1,502	10,581		7,448	15.34
TPP "Nikola Tesla B"	TENT B	1,160	6,725		7,448	9.54
TPP "Kolubara"	TEK	245	1,195		6,805	1.81
TPP "Morava"	TEM	108	651		8,757	0.83
TPP "Kostolac A"	TEK A	281	2,091	302	8,079	3.44
TPP "Kostolac B"	TEK B	640	3,032		8,079	4.12
Total		3,936	24,275	302		34.92

Table 1. Electric capacity and annual production of electricity and heat in Serbian coal-fired power plants in 2012 [1, 2, 3]

Concise description of life cycle subsystems and processes and implemented LCI datasets are provided below.

i) Coal mining. Total coal consumption of provided TPPs in 2012 (Table 1) was ca. 35 million Mg with energy content of 7.7 $MJ \cdot kg^{-1}$. The required quantities of coal are retrieved via opencast method in Kolubara and Kostolac lignite coal mines [1, 3]. The coal is obtained by surface mining, which involves fracturing and removing the overlying soil and rock, breaking the coal by blasting or mechanical means, and loading the coal for transport to its final destination.

Ecoinvent v.2.2 includes LCI data of coal excavation from opencast mines. „Lignite, at mine/RER“ is the respective process and refers to the excavation of 1 kg of coal from the average opencast lignite mine in Europe. In order to have more representative results, the flow describing lignite in the original dataset “Coal, brown” which has a calorific value of 9.9 $MJ \cdot kg^{-1}$ is changed into the “Coal, brown, 8 MJ per kg”.

ii) Coal transportation. Distances and transportation of coal are obtained from the EPS officials and they refer to the case in 2011. TPPs receive coal loads via conventional freight trains and/or conveyor belts. Due to assumed small environmental impact, conveyor belts are not taken in the calculation in this study. Our previous studies provide data on transportation distances from coal mines to TPPs [3, 5].

Ecoinvent database: „Operation, coal freight train, electricity/CN” describes LCI inventory data of coal electric train transport. It was necessary to adopt Serbian electricity system data, since the original process refers to coal transport with electric trains in China [3, 5].

iii) Electricity generation in power plants. Annual emission of pollutants (CO_2, SO_2, NO_x) and particles (PM) is available from the EPS report [2]. Information on other emissions, as well as information on particle size distribution is not available from the report. Since size of the particles is relevant due to their influence on life cycle impact assessment (LCIA) results, we followed recommendation of Röder et al. [6] who suggested the following size distribution of particles emitted from power plants equipped with electrostatic precipitators: 83.1% are particles with diameter bellow 2.5 µm ($PM_{2.5}$), 7.1% are particles with diameter bigger than 10 µm (PM_{10}) and the rest are particles with diameter between 2.5 µm and 10 µm ($PM_{2.5\text{-}10}$).

Required raw water (from rivers and underground aquifers) for cooling and steam generation processes in TPPs is provided in EPS report [2]. Ecoinvent v.2.2 database provides LCI of these processes.

Data inventory on emissions released during the construction, maintenance and demolition of TPPs equipment and infrastructure is contained and is taken from Ecoinvent database. Same database provided data on quantity and LCI of chlorine consumed in Serbian power plants (see Table 2).

iv) Coal ash treatment. Röder et al. [6] concluded that after each kg of burned lignite coal in Serbian TPPs, 0.189 kg of ash was formed. According to annual coal consumption (Table 1), annual ash produced is estimated to be around 7 million Mg. Environmental flows considering ash disposal in the Serbian TPPs are given in the Ecoinvent v.2.2 database. In this study we assumed that formed ash is recycled in form of backfilling material in opencast mines.

Table 2 gives an overview of environmental and product flows associated with the life cycle of electricity from Serbian TPPs and references to their respective LCI datasets.

3. RESULTS AND DISCUSSION

3.1 Life cycle inventory results

Selected results of LCI analyses are summarized in Table 3. Due to space limitation only selected environmental flows are presented here. However, the whole LCI and selected LCIA results of electricity generated in Serbian TPPs are available on-line (https://goo.gl/R2hGBj). The LCI data refer to the situation in 2012.

Life cycle CO_2 emissions of coal-based electricity in Serbia range from 1,125 to 1,426 g kWh^{-1} with 1,170 g kWh^{-1} as a weighted average value. Substantial difference between the results can be explained with different electric efficiencies of TPPs, and with differences in chemical composition and heating value of lignite used for electricity generation in different power plants. In 2012 the average heating value of lignite used by different power plants varied between 6.8 $MJ \cdot kg^{-1}$ and 8.7 $MJ \cdot kg^{-1}$ [3]. Relatively high life cycle SO_2 emissions of about 13.5 g kWh^{-1} characterize the Serbian TPPs. About 99% of total SO_2 emissions are released during the combustion of lignite in TPPs. Sulphur content in combusted lignite is main determinant of SO_x emissions. Other factors are: heating value, moisture and alkali concentration. Besides the

high sulphur content of the Serbian lignite (up to 1.58 wt.% on dry basis [7]), old abatement technology and the lack of treatment of flue gases in Serbian TPPs are also determining factors of the high SO_2 emissions.

	Life cycle phase	Unit	TENT A	TENT B	TEK	TEM	TEK A*	TEK B	Average	LCI data
I.	Coal mining									
	- lignite	kg	1.45E+0	1.42E+0	1.52E+0	1.27E+0	1.44E+0	1.36E+0	1.42E+0	(a)
II.	Coal transportation									
	- rail transport	Mg·km	9.28E-2	1.08E-1	1.52E-2	2.85E-1	0.00E+0	0.00E+0	7.78E-2	(b)
	- rail infrastructure	Mg·km	9.28E-2	1.08E-1	1.52E-2	2.85E-1	0.00E+0	0.00E+0	7.78E-2	(c)
III.	Power plant									
	- emissions									
	PM	kg	3.89E-4	3.18E-4	4.25E-3	6.96E-3	6.96E-4	1.41E-3	8.87E-4	
	$PM_{2.5}$	kg	3.24E-4	2.65E-4	3.53E-3	5.79E-3	5.78E-4	1.17E-3	7.37E-4	
	$PM_{2,5-10}$	kg	3.81E-5	3.11E-5	4.15E-4	6.80E-4	6.80E-5	1.38E-4	8.67E-5	
	PM_{10}	kg	2.77E-5	2.27E-5	3.03E-4	4.95E-4	4.95E-5	1.00E-4	6.31E-5	
	SO_2	kg	9.96E-3	1.40E-2	1.95E-2	2.63E-2	2.10E-2	1.27E-2	1.34E-2	
	NO_x	kg	1.91E-3	1.80E-3	2.80E-3	2.23E-3	1.28E-3	8.67E-4	1.74E-3	
	CO_2	kg	1.14E+0	1.10E+0	1.41E+0	1.25E+0	1.11E+0	1.20E+0	1.15E+0	
	- infrastructure	p.	1.18E-11	1.18E-11	1.18E-11	1.18E-11	1.18E-11	1.18E-11	1.18E-11	(d)
	- water for cooling	m^3	1.00E-1	1.27E-1	1.32E-1	1.28E-1	1.47E-1	1.58E-1	1.21E-1	(e)
	- water other	kg	8.07E-2	7.45E-2	1.30E-1	1.97E-1	1.30E-1	2.96E-1	1.03E-1	(f)
	- chlorine	kg	1.21E-4	1.21E-4	1.21E-4	1.21E-4	1.21E-4	1.21E-4	1.21E-4	(g)
IV.	Coal ash treatment									
	- coal ash	kg	2.74E-1	2.68E-1	2.87E-1	2.40E-1	2.72E-1	2.57E-1	2.69E-1	(h)

Notes: Life cycle inventory data from the Ecoinvent v.2.2 LCI database: (a) modified "Lignite, at mine/RER" see Section 2.3; (b) modified "Operation, coal freight train, electricity/CN", see Section 2.3; (c) modified "Transport, freight, rail/RER", only infrastructure related flows considered; (d) Lignite power plantl/RER; (e) Water, cooling, unspecified natural origin/m^3; (f) Water, completely softened, at plant/RER; (g) Chlorine, liquid, production mix, at plant/RER; (h) Disposal, lignite ash, 0% water, to opencast refill/CS. 13% of total flows related to TPP "Kostolac A"is allocated to heat co-product according to the principles of energy allocation.*

Table 2. Material and energy flows associated with electricity generation in the Serbian TPPs (per 1 kWh)

Life cycle phase	Unit	TENT A	TENT B	TEK	TEM	TEK A	TEK B	Average
Resources								
Coal (lignite)	kg	1.46E+0	1.43E+0	1.52E+0	1.28E+0	1.44E+0	1.36E+0	1.43E+0
Coal (hard)	kg	4.03E-3	4.00E-3	3.99E-3	4.11E-3	3.78E-3	3.60E-3	3.93E-3
Crude oil	kg	1.57E-3	1.58E-3	1.46E-3	1.84E-3	1.37E-3	1.31E-3	1.52E-3
Natural gas	m^3	1.69E-3	1.67E-3	1.68E-3	1.70E-3	1.58E-3	1.50E-3	1.64E-3
Water (all sources)	kg	2.67E+2	2.97E+2	2.70E+2	3.63E+2	2.73E+2	2.77E+2	2.79E+2
Emissions to air								
PM	kg	1.00E-3	9.21E-4	4.89E-3	7.52E-3	1.30E-3	1.98E-3	1.49E-3
$PM_{2,5}$	kg	3.36E-4	2.77E-4	3.54E-3	5.81E-3	5.86E-4	1.18E-3	7.49E-4
$PM_{2,5-10}$	kg	4.34E-5	3.67E-5	4.20E-4	6.88E-4	7.18E-5	1.41E-4	9.18E-5
PM_{10}	kg	6.25E-4	6.07E-4	9.24E-4	1.03E-3	6.38E-4	6.57E-4	6.48E-4
SO_2	kg	1.01E-2	1.41E-2	1.95E-2	2.64E-2	2.11E-2	1.27E-2	1.35E-2
NO_x	kg	1.98E-3	1.87E-3	2.86E-3	2.32E-3	1.34E-3	9.24E-4	1.81E-3
CO_2	kg	1.16E+0	1.13E+0	1.43E+0	1.28E+0	1.13E+0	1.22E+0	1.17E+0
NMVOC	kg	9.90E-6	9.93E-6	9.29E-6	1.13E-5	8.72E-6	8.32E-6	9.58E-6
CO	kg	4.33E-5	4.42E-5	3.75E-5	5.74E-5	3.53E-5	3.43E-5	4.17E-5
CH_4	kg	3.69E-4	3.62E-4	3.83E-4	3.31E-4	3.63E-4	3.43E-4	3.61E-4

Table 3. Selected results of LCI analyses of electricity generated in Serbian TPPs (per 1 kWh in 2012)

Variation of NOx and PM emissions within different TPPs can be explained with various fuel composition, boiler construction and combustion conditions, and different extension of installation and efficiency of emission control devices in the investigated TPPs.

CO_2, NO_x, SO_2, $PM_{2.5-10}$, and $PM_{2.5}$ emissions are mainly released during lignite combustion in the power plants, accounting for 94–99% of the total, whereas other emissions are mainly associated with up- and downstream processes.

Total annual CO_2 emissions associated with the lignite combustion in the Serbian TPPs are 28 Tg (Tg = million metric tons), accounting for 61% of the total CO_2 emissions in Serbia in 2012 (ca. 46 Tg). Serbian TPPs in 2012 released 0.33 Tg and 0.04 Tg of SO_2 and NO_x, respectively.

3.2 Comparison with Ecoinvent data

Results were compared with respective processes from Ecoinvent v.2.2 (Electricity, lignite, at power plant/CS) and Ecoinvent v. 3 (Electricity, high voltage {RS}|electricity production, lignite|Alloc Def) databases. Selected results of LCIA calculated with SimaPro 8 and the ReCePi Midpoint (H) v.1.10 and cumulative energy demand (CED) LCIA methods are shown on Fig. 1.

Ecoinvent processes show higher environmental impacts in most of the impact categories compared to our average process. This can be largely explained with older and more complete emission datasets used by Ecoinvent v.2.2 and v.3 and different heating values of lignite assumed in Ecoinvent. According to data on Fig. 1, in 2012, the global warming potential and cumulative fossil energy requirements of electricity generated in Serbian TPPs were 1.18 kg CO_{2eq} and 11.64 MJ, respectively.

4. CONCLUSIONS

Available Ecoinvent LCI datasets do not accurately describe the environmental impact of electricity produced in Serbian coal-fired power plants. Since most industrial processes directly (or indirectly) link to the electricity, it is paramount to provide up-to-date, accurate and comprehensive LCI datasets of electricity.

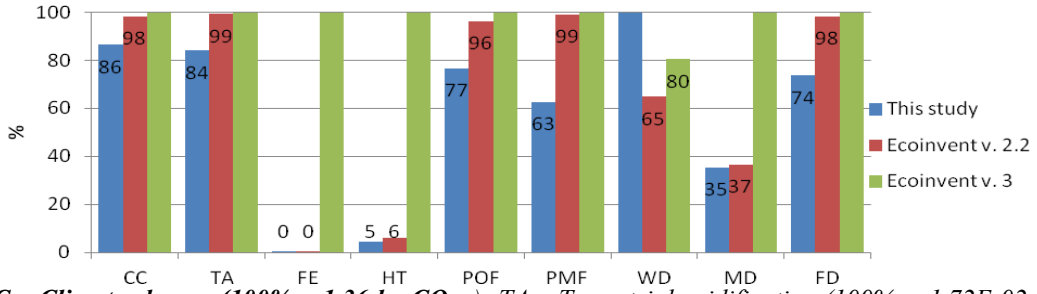

Notes: CC – Climate change (100% = 1.36 kg CO_{2eq}); *TA – Terrestrial acidification (100% = 1.72E-02 kg SO_{2eq}); FE – Freshwater eutrophication (100% = 3.58E-03 kg P_{eq}); HT – Human toxicity (100% = 2.43E+00 kg 1.4 DB_{eq}); POF – Photochemical oxidant formation (100% = 3.79E-03 kg NMVOC); PMF – Particulate matter formation (100% = 6.28E-03 kg PM_{10eq}); WD – Water depletion (100% = 2.74E-01 m^3); MD –Metal depletion (100% = 6.53E-03 kg Fe_{eq}); FD – Fossil depletion; i.e. cumulative fossil energy demand (100% = 15.7 MJ);*

Fig. 1. Comparable LCIA results of electricity generated in Serbian power plants according to the Ecoinvent database and this study.

Notes: This research was supported by the Hungarian Academy of Sciences within the framework of the Domus Program. This article was originally published in the Proceedings of the Scientific-Expert Conference ETIKUM 2015, Novi Sad: Faculty of Technical Sciences.

5. REFERENCES

[1] Electric Power Industry of Serbia: *Technical Report for 2012*, Belgrade, 2013.

[2] Electric Power Industry of Serbia: *Annual Report on the State of Environmental Protection for 2012*, Belgrade, 2013.

[3] Kiss, F.: *Real costs of electricity generation in Serbia – study on environmental and economic interdependencies (available in Hungarian from the author)*, Project financed by the Hungarian Academy of Sciences, 2014.

[4] Frischknecht, R. et al.: The ecoinvent database: Overview and methodological framework, *International Journal of Life Cycle Assessment*, 10, pp. 3–9, 2005.

[5] Kiss, F., Petkovič, Đ.: *Revealing the Costs of Air Pollution Caused by Coal-based Electricity Generation in Serbia*. Proceedings of the EXPRES 2015 Conference, pp. 96–101, Subotica, Serbia, 2015.

[6] Röder, A., Bauer, C., Dones, D.: *Kohle: Sachbilanzen von Energiesystemen*, Final report No. 6 ecoinvent data v2.0. Dübendorf and Villigen, Switzerland, 2008.

[7] Životić, D. et al.: *Petrological and geochemical composition of lignite from the D field, Kolubara basin (Serbia)*, International Journal of Coal Geology, 111, pp. 5-22, 2013.

Authors: **Dr. Ferenc Kiss, MSc. Vuk Rajović, PhD candidate**, University of Novi Sad, Faculty of Technology, Bul. cara Lazara 1, 21000 Novi Sad, Serbia,
E-mail: ferenc1980@gmail.com rajovic89@gmail.com

Journal of Production Engineering
Vol.18 No.1
JPE (2015) Vol.18 (1) Original Scientific Paper
Šokac, M., Budak, I., Ralević, N., Soković, M., Santoši, Ž.

ACCURACY ANALYSIS OF CLUSTERING ALGORITHMS FOR SEGMENTATION OF INDUSTRIAL CT IMAGES

Received: 25 January 2015 / Accepted: 18 March 2015

Abstract: *Image analysis today plays an important role in the field of industrial engineering for image processing. The use of different tools in order to extract important information from industrial CT images is an active field of research that attracts the attention of many researchers. In this paper two methods will be presented that are used for segmentation of CT images. Those methods are fuzzy C-means clustering and K-means clustering. Comparative analysis will be performed in the form of accuracy of segmented binary images. Presented analysis leads to the conclusion that fuzzy C-means clustering has greater accuracy than hard K-means clustering approach.*
Key words: *Segmentation, Industrial CT, fuzzy clustering, hard clustering*

Analiza tačnosti algoritama za klasterizaciju za segmentaciju industrijskih CT snimaka *Analiza slike danas ima važnu ulogu u oblasti industrijskog inženjerstva za obradu slike. Primena različitih alata kako bi se izvukle važne informacije iz industrijskih CT snimaka je danas aktivna oblast istraživanja koja privlači pažnju mnogih istraživača. U ovom radu su prikazane dve metode koje se koriste za segmentaciju CT snimaka. Ove metode su metoda klasterizacije fazi C-srednjih vrednosti i metoda klasterizacije K-srednjih vrednosti. Izvršena je komparativna analiza u vidu tačnosti segmentiranih binarnih slika generisanih primenom ove dve metode. Predstavljenom analizom se dolazi do zaključka da metoda fazi C srednih vrednoasti ima veću tačnost kod segmentiranih snimaka.*
Ključne reči: *Segmentacija, Industrijski CT, fazi klasterizacija, hard klasterizacija*

1. INTRODUCTION

The application of modern computer – aided technologies in different fields allows vast growth, large and increasing number of industrial applications of X-ray Computed Tomography (CT) in the manufacturing industry as well as in other industries such as such as aviation, railway, military industry and others [1,2].

CT technology is used to acquire two dimensional (2D) images of an object and then from these images a three dimensional (3D) model of the object's external and internal structure is reconstructed and which can then be analyzed. Therefore, CT became very popular for its use in material analysis because of its non-destructive testing (NDT) ability and the detection of flaws such as voids and cracks, and particle analysis in materials. CT is the only technology able to measure as well the inner as the outer geometry of a component without need to cut it through and destroy it. As such, it is very usefull for industrial quality control of workpieces having non-accessible internal features (e.g. components produced by additive manufacturing) or multi-material components (e.g. two-component injection molded plastic parts or plastic parts with metallic inserts) [3].

Many different methods for automatic extraction of important information from industrial CT images have been proposed. Feature extraction from CT images is mostly done through a preliminary segmentation step using methods such as region growing [4], fuzzy clustering [5] water shedding [6], morphological filter operations [7] and others. As a result, these methods provide a binary classification of individual volume voxels into segmented regions, meaning that a whole voxel either belongs to the region of a specific feature, or not.

2. METHODS

The segmentation process is widely spread and is applied in many applications such as algorithms for robot vision, registration of facilities, analysis of geographical areas and analysis of CT images [8,9]. In a more classical definition, segmentation is defined as a process of dividing image on non-overlapping, consistent homogenous regions, in accordance with certain characteristics such as intensity of grayscale or texture. As a result of the segmentation process a binary image is generated where the value 1 represents the region of interest, and 0 represents the background that has been excluded [10].

Cluster analysis is based on partitioning a collection of data points into a number of clusters, where the points inside a cluster show a certain degree of closeness or similarity. Clustering methods can be considered as either hard (crisp) or fuzzy, depending on whether a pattern belongs exclusively to a single cluster or to several clusters with different degrees of belongings. In hard clustering each point (voxel) of the dataset belongs to exactly one cluster, a membership value of zero or one is assigned to each pattern, whereas in fuzzy clustering, a value between zero and one is assigned to each point by a membership

function. [11].

K-means clustering method (also known as Lloyd's algorithm) is one of the most popular methods used for unsupervised classification of data. It is working on the principle of classification data in a predefined number of clusters (shown in figure 1) [11].

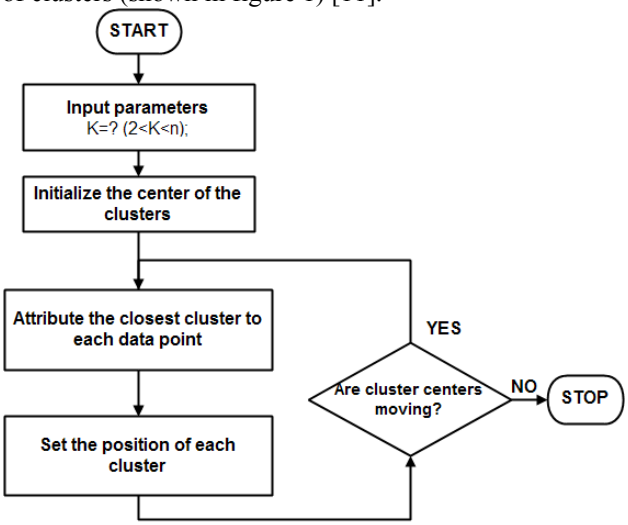

Fig. 1. K-means clustering algorithm

Fuzzy C-means clustering algorithm is widely used in the field of image processing. It is used for clustering, or grouping of data where each data belongs to a cluster with a certain degree of belonging, unlike hard clustering, where each data belongs to only one cluster [12]. In the clustering process of CT images the most common parameter that is taken into account is the pixels intensity displayed in grayscale. In this way the FCM objective function is minimized when high membership values are assigned to pixels whose intensities are close to the centroid of its particular class, and low membership values are assigned when the point is far from the centroid [13]. With fuzzy c-means, the centroid of a cluster is computed as being the mean of all points, weighted by their degree of belonging to the cluster. The degree of being in a certain cluster is related to the inverse of the distance to the cluster. By iteratively updating the cluster centers and the membership grades for each data point, FCM iteratively moves the cluster centers to the "right" location within a data set [12].

It is necessary to define input parameters such as the number of clusters C and weighted exponent m which defines the degree of fuzzification or affiliation of pixels to clusters. When the weighted exponent m is equal to 1 it is called a crisp clustering, and when $m>1$ the degree of fuzziness increases among points in the decision space. Figure 2 shows the basic scheme of fuzzy clustering [12].

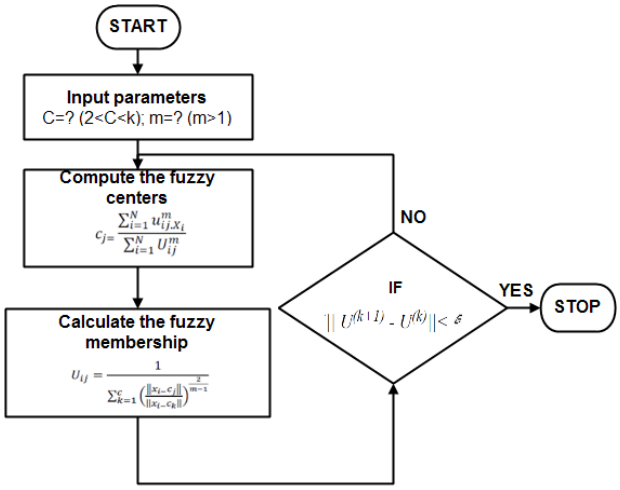

Fig. 2. Fuzzy C-means clustering algorithm

The main difference between fuzzy and hard clustering is that with fuzzy clustering any pixel in the image can belong to several clusters, but with a certain degree of belonging to a given cluster, which moves in the interval from 0 to 1. This is an important trait in image analysis in order to maximize sensitivity.

3. RESULTS

Experimental results were carried out on six CT images which were taken from a stack of CT images of a motor block [14] shown in figure 3 and figure 4. The two presented algorithm (named FCM and HARD) have been implemented in Matlab software, on a computer (Fujitsu CELSIUS M470-2) with Intel (R) Xeon (R) CPU E5645, 2.40GHz processor and 16 GB of RAM.

Fig. 3. 3D model of a motor block

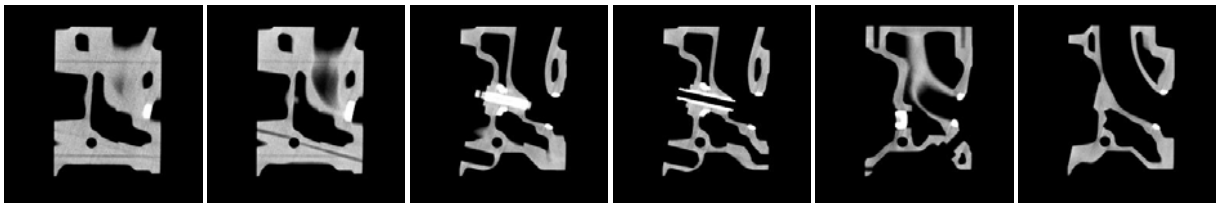

Fig. 4. CT images used for analysis

No additional postprocessing was carried out in order to show the real results in the application of these algorithms for processing of industrial CT images.

Input parameters that were used in these two algorithms are a number of clusters C which are defined by the user manually, termination criterion ε (accuracy), the maximum number of iterations and weighting exponent m (only FCM algorithm). In order to extract as much information from the images in both approaches, after a short experimental analysis, optimal segmentation parameters in each of these industrial CT images were considered.

Input parameters that were used in these two algorithms are a number of clusters C which the user enters manually, termination criterion ε (accuracy), the maximum number of iterations and weighted exponent m (only with FCM algorithm). In order to extract as much information from the images in both algorithms, after a short experimental analysis, optimal parameters were considered in each of these three industrial CT images.

In order to be able to perform accuracy analysis of the segmented images, each of these CT images was manually segmented. These manually segmented images were then used as reference images in relation to which were both fuzzy clustering and hard clustering segmented images compared (figure 5).

Parameters that are commonly used for the statistical analysis of segmented binary images are Jaccard index [15] and Dice coefficient [16]. They are used as evaluators of the segmented CT images. In these evaluators extent overlapping ranges from 0 to 1, where 1 defines a complete overlap of the segmented image with the reference image.

These evaluators are defined according to the following formula:

Jaccard index

$$JI = \frac{|A \cap B|}{|A \cup B|} \tag{1}$$

Dice coefficient

$$DK = \frac{2|A \cap B|}{|A| + |B|} \tag{2}$$

where A is the result of segmentation of the reference image, and B is the segmentation result of FCM/HARD algorithm that was compared with A.

Figure 5 shows the results of segmentation results by FCM and HARD algorithm.

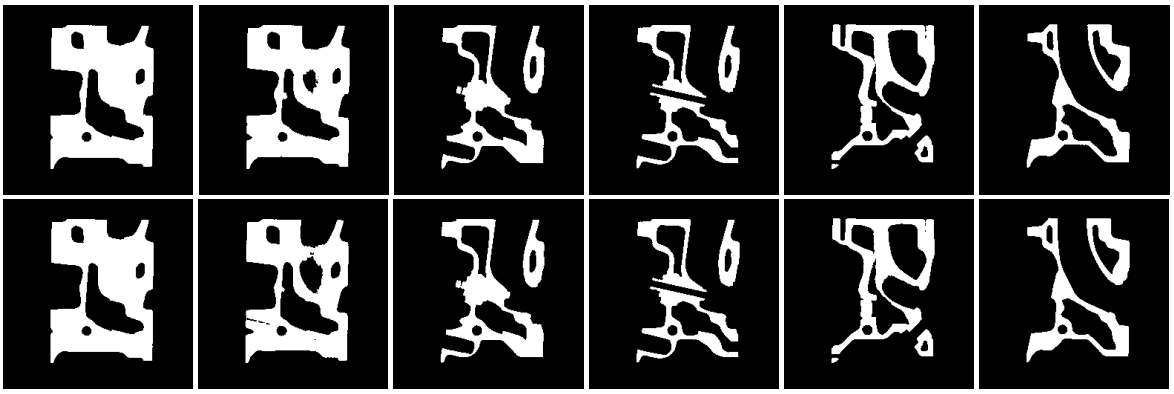

Fig. 5. Results from segmentation using FCM and HARD algoritm

On figure 6 and figure 7 are shown evaluation results by Jaccard index and Dice coefficient for all six CT images, segmented by both FCM and HARD algorithm, which were compared to their segmented reference images.

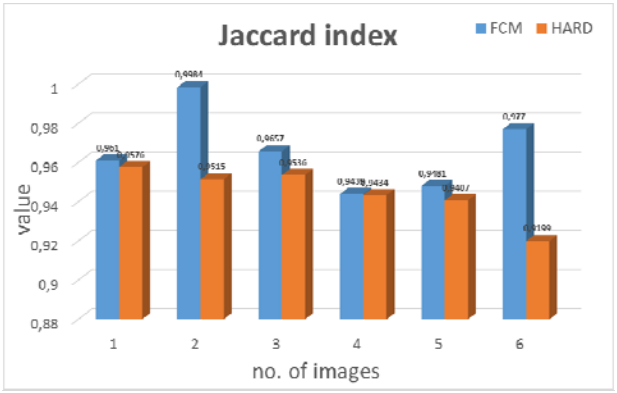

Fig. 6 Graph showing results obtained from Jaccard

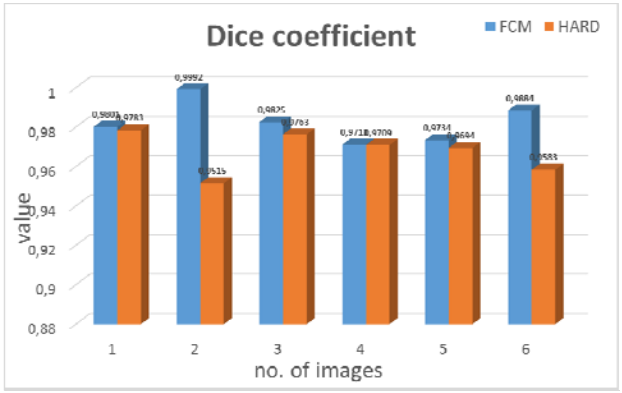

Fig. 7. Graph showing results obtained from Dice

4. DISCUSSION

Based on the presented results it can be seen that the segmentation results using the FCM algorithm show better results compared to the results obtained

using HARD algorithm. The results of evaluation by Jaccard index for all six CT images segmented by FCM algorithm are 0,961, 0,9984, 0,9657, 0,9439, 0,9481 and 0,977, respectively. And the results of evaluation by Jaccard index for all six CT images segmented by HARD algorithm are 0,9576, 0,9515, 0,9536, 0,9434, 0,9407 and 0,9199, respectively. Results of the evaluation by Dice coefficient for all six CT images with FCM algorithm are 0,9801, 0,9992, 0,9825, 0,9711, 0,9734 and 0,9884, respectively. And the results of evaluation for all six CT images segmented by HARD algorithm are 0,9783, 0,9515, 0,9763, 0,9709, 0,9694 and 0,9583, respectively. However, in cases 2 and 6 it can be seen that the results by Jaccard are much better for FCM than HARD algorithm. The reason why this could be is that by applying fuzzy clustering on these images, due to the vague areas on CT image, the FCM algorithm was able to extract more information from the images unlike HARD algorithm, which essencialy separates data by them either belonging to certain cluster on don't. This can be seen on results from both Jaccard and Dice.

5. CONCLUSION

In this paper is presented a comparative analysis of two different clustering methods for segmentation of industrial CT images. Segmentation was performed on six industrial CT images, and those results were compared with the results of the manual segmentation. As segmentation evaluators were used Jaccard index and Dice coefficient. Results for all six CT images segmented by FCM algorithm are showing very good results, thus showing the advantage of fuzzy clustering over hard clustering for segmentation of industrial CT images.

6. REFERENCES

[1] Kruth J.P., Bartscher M., Carmignato S., Schmitt R., De Chiffre L.,Weckenmann A.: *Computed tomography for dimensional metrology*, CIRP Annals - Manufacturing Technology, 60, p.p. 821–842, 2011.

[2] Huang R., Ma K., McCormick P., Ward W.: *Visualizing industrial CT volume data for nondestructive testing applications*, Proceedings of the 14th IEEE visualization 2003. IEEE Computer Society; p.p. 547–54, 2003.

[3] De Chiffre L., Carmignato S., Kruth J.P., Schmitt R., Weckenmann A.: *Industrial applications of computed tomography*, CIRP Annals - Manufacturing Technology, 63, p.p. 655–677, 2014.

[4] Adams R., Bischof L.: *Seeded region growing.,* IEEE Trans. Pattern Anal. Mach. Intell.,16, p.p. 641–647, 1994.

[5] Bezdek J: *A Convergence Theorem for the Fuzzy ISODATA Clustering Algorithms*, IEEE transactions on pattern analysis and machine intelligence, 2, p.p. 1-8, 1980.

[6] Sikandar Hayat Khiyal M., Khan A., Bibi A.: *Modified Watershed Algorithm for Segmentation of 2D Images*, Issues in Informing Science and Information Technology, 6, p.p. 877-886, 2009.

[7] Boutalis Y.S., Tsirikolias K., Metrtzios B.G., Andreadis I.T.: *Implementation of morphological filters using coordinate logic operations*, Pattern Recognition, 35, p.p. 187-198, 2002.

[8] Bezdek J., Hall L., Clarke L.: *Review of MR image segmentation techniques using pattern recognition*, Medical Physics., 20, p.p 1033–1048, 1993.

[9] Pham D., Xu C., Prince J.: *A survey of current methods in medical image segmentation*, Annual Review of Biomedical Engineering, 2, p.p. 315–337, 2000.

[10] Cai W., Chen S., Zhang D.: *Fast and Robust Fuzzy C-Means Clustering Algorithms Incorporating Local Information for Image Segmentation*, Pattern Recognition, 40, p.p. 825–838, 2007.

[11] El-Melegy M., Zanaty E., Abd-Elhafiez W. M., Fara A.: *On cluster validity indexes in fuzzy and hard clustering algorithms for image segmentation*, Image Processing, ICIP, IEEE International Conference, 6, p.p. 5-8,, San Antonio, TX, IEEE, 2007.

[12] Bezdek J.: *Pattern Recognition with Fuzzy Objective Function Algoritms*, Kluwer Academic Publishers Norwell, MA, USA, 1981.

[13] E.A. Zanaty: *Determining the number of clusters for kernelized fuzzy C-means algorithms for automatic medical image segmentation*, Egyptian Informatics Journal, 3, p.p. 39–58, 2012.

[14] -----:Scientific Computing and Imaging Institute, URL:http://www.sci.utah.edu/download/IV3DData.html (Accessed 10.06.2015.)

[15] Jaccard, P.: *Étude comparative de la distribution florale dans une portion des Alpes et des Jura*, Bulletin de la Société Vaudoise des Sciences Naturelles, 37, p.p. 547–579, 1901.

[16] Dice, L. R.:*Measures of the Amount of Ecologic Association Between Species*, Ecology, 26, p.p. 297–302, 1945.

Authors: **Assist. M.Sc. Mario Šokac, Assoc. prof. dr Igor Budak, Prof. dr. Ralević Nebojša, M.Sc. Željko Santoši,** University of Novi Sad, Faculty of Technical Sciences, Institute for Production Engineering, Trg Dositeja Obradovića 6, Novi Sad, Serbia, Phone.: +381 21 485 2332, Fax: +381 21 454-495.
E-mail: marios@uns.ac.rs
budaki@uns.ac.rs
nralevic@uns.ac.rs
zeljkos@uns.ac.rs

Prof. dr. Mirko Soković. University of Ljubljana, Faculty of Mechanical Engineering, Aškerčeva 6, 1000 Ljubljana, Slovenia, Phone: +386 1 4771214
E-mail: mirko.sokovic@fs.uni-lj.si.

Note: The part of results presented in this paper have been obtained in the framework of the project "Research and development of modeling methods and approaches in manufacturing of dental recoveries with the application of modern technologies and computer aided systems," TR - 35020, funded by the Ministry of Education, Science and Technological Development of Republic of Serbia.

Journal of Production Engineering
Vol.18 No.1
JPE (2015) Vol.18 (1) Original Scientific Paper
Tadić A., Mirković S., Puškar T., Šokac M., Budak I.

IMPLANT PLANNING THERAPY BASED ON CBCT IMAGES OF THE RADIOSENSITIVE TEETH

Received: 06 May 2015 / Accepted: 22 June 2015

Abstract: *The loss of one, several or all teeth reduces the quality of life. Modern dentistry offers many options for the rehabilitation of such patients. The planning and preimplantation diagnostics and preparation take an important place in oral implantology. In the process of planning and preparation for implantation, radiography occupies a central place.This paper presents the case of 60 year old patient, edentulous, who came to the Dentistry Clinic of Vojvodina in order to get fixed dental restorations carried by dental implants. Both upper and lower acrylate complete dentures were made, using radiosensitive teeth and a CBCT scan was made with the dentures in the mouth of the patient. Analyzing scans obtained in this manner , the final treatment plan was made.*
Key words: *Implantology, CBCT, radiosensitive teeth*

Planiranje implantološke terapije na bazi CBCT snimaka sa radiosenzitivnim zubima *Nedostatak jednog, više ili svih zuba smanjuje kvalitet života. Savremena stomatologija pruža brojne mogućnosti za rehabilitaciju ovakvih pacijenata. Planiranje i preimplantacijska dijagnostika i priprema zauzimaju posebno važno mesto u oralnoj implantologiji. U procesu planiranja i pripreme implantacije centralno mesto zauzima rendgenološka dijagnostika. U radu je prikazan slučaj pacijenta starog 60 godina, totalno bezubog, koji se javio na Kliniku za stomatologiju Vojvodine zbog izrade zubnih nadoknada nošenih dentalnim implantima. Pacijentu je izrađena gornja i donja totalna proteza, uz upotrebu radiosenzitivnih zuba, te načinjen CBCT snimak sa ovim protezama u ustima. Analizom ovako dobijenih snimaka napravljen je konačan plan terapije.*
Ključne reči: *Implantologija, CBCT, radiosenzitivni zubi*

1. INTRODUCTION

The teeth and oral cavity, as the initial part of the digestive system, have an important physiological role in the organism, as well as their role in the function of speech, they have an impact on the appearance of a person, so they have a large affect the psychology of a person and its identity. The loss of one, several or all teeth has multiple consequences, reducing the quality of human life [1].

Modern dentistry offers many options for the rehabilitation of such patients. In last two decades especially dental implantology has developed, enabling us to make fixed and removable dental restorations carried by dental implants.

In everyday clinical practice, we meet with a relatively large number of patients who require implant treatment, and where the loss of one, several or all teeth led to a significant bone loss of the alveolar ridge [2].

Alveolar ridge of the jaw carries the teeth in the dental alveoli and the formation of this ridge begins simultaneously with the eruption of teeth, and its atrophy and reduction is caused by their loss. This means that the alveolar bone has the function to receive and distribute the forces of chewing on the bones of the skull [3].

In these situations it is necessary to compensate the lost bone in order to ensure optimal conditions for placement of dental implants and prosthodontics [2].

Loss of alveolar bone may occur prior to tooth extraction because of periodontal disease, periapical pathology or trauma to teeth and bone [4]. The tooth extraction can also result in a significant bone loss.

All of the above, can cause the appearance of unevenly resorbed ridges of different shape, height and width, which creates serious problems if we want to obtain the quality prosthetic rehabilitation of these patients [3].

The problem of rehabilitating partially or totally edentulous patients is not only related to underdeveloped countries. More than 60% of the population in the highly industrialized countries requires treatment with dental implants, which is the reason for the annual growth of implants market of about 15% [5]. It is estimated that in the US alone, according to current data, there are about 36 million edentulous people [3].

The planning and preimplantation diagnostics and preparation take special important place in oral implantology. Planning is mostly teamwork involving professionals of different specialties. In the process of planning and preparation of implant therapy radiological diagnostics occupies a central place [3].

2. APPLICATION OF CBCT WITH RADIOSENSITIVE TEETH

CT and CBCT (Cone beam computerized tomography) technology provides clinicians with new methods to view patient anatomy exceeding conventional two-dimensional radiology. Interactive software applications allow for improved interpretation of the CT scan data. The enhanced capability of innovative software applications that allow clinicians to interpret and maneuver through various three-dimensional images has far- reaching implications when interactive treatment planning software is combined with computer-aided design and manufacturing [6]. Cone beam CT (CBCT) permits finely detailed visualization of the osseous architecture with high contrast and without burn out. By offering tomographic slices download to 0.08 mm, a true volumetric presentation of the arch is obtained [7]. Information obtained from cone beam computed tomographic scans permits the measurement of the density, height, and buccolingual with of the alveolar bone at any jaw location, as well as visualization of the pathology, inclination of the bone, and anatomic vital structures [8].

In everyday clinical practice use of CBCT is a standard today, and it is crucial in planing of the implant position. If a patient lost only one or a small number of teeth, only CBCT scan is sufficient, but with totally edentulous patients it does not provide us with enough data so that we can accurately determine the exact position of the implants. CBCT scan with a model of a tooth restoration using radiosensitive markers in the mouth is one way to overcome this problem, because it gives us information about the teeth position in the final prosthesis. As markers, unlike in conventional radiographic methods, in making CBCT images metal can't be used, but takes into account the use of gutta-percha points or radiosensitive acrylate [3].

Making the temporary prosthesis with radiosensitive acrylic teeth is just a method that enables us to overcome the above problems and limitations of CBCT in the planning of implant treatment in edentulous patients. Software analysis of the recorded images thus gain us insight into the dental-alveolar relations, and we can accurately determine the position and inclination of the implant and to plan augmentation procedures on residual alveolar ridge if there is a need.(Figure 1.)

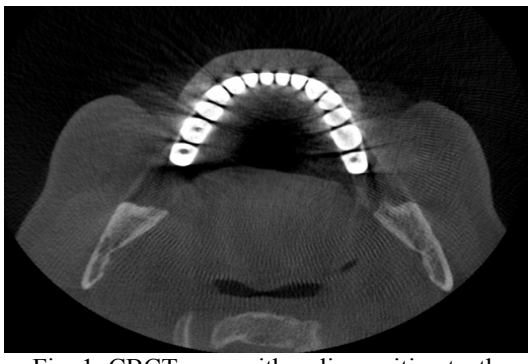

Fig. 1. CBCT scan with radiosensitive teeth

CT and computerized systems have brought revolutionary changes in implantology and in the future will certainly have a key importance in the development of this discipline [3].

3. IMPLANT PLANNING THERAPY - CASE REPORT

This paper presents the case of a 60 year old patient, totally edentulous, responding to the Dentistry Clinic of Vojvodina in order to get fixed dental restorations carried by dental implants . His medical history data were obtained and showed that the patient is in a good general state of health, does not take any treatment and is not allergic to food, medicines nor dental materials. Teeth have been extracted successively for several years, and he had never had dentures. It also states that in the upper jaw he had surgery twice on the roots of the front teeth.

Clinical intraoral examination shows significant degree of bone resorption in the residual alveolar ridges, which is especially pronounced in the upper jaw (Figures 2. And 3.)

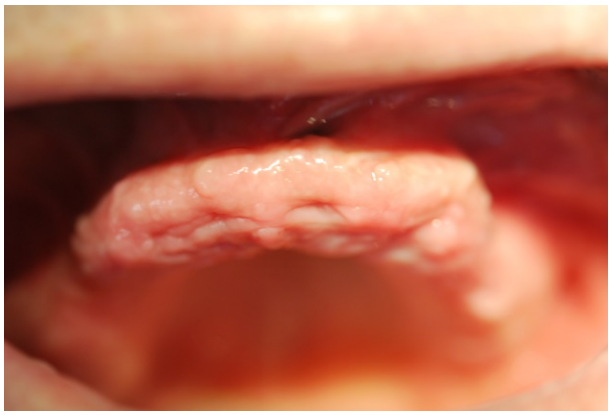

Fig. 2. Upper jaw

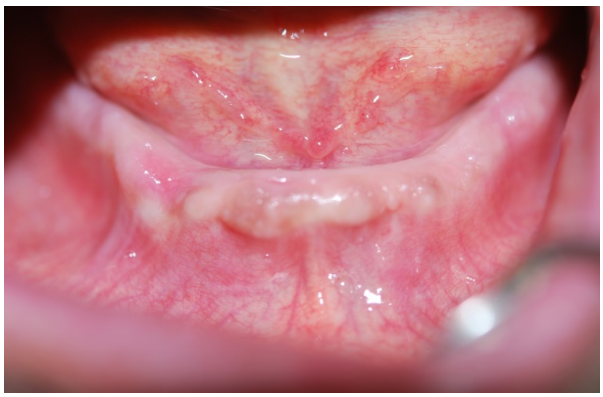

Fig.3. Lower jaw

By making an analysis and X-ray OPT footage a considerable loss of bone in both jaws was noticed , as well as enhanced pneumatisation of both maxillary sinuses.

It was decided that prior to definitive treatment plan, the patient should be provided with a temporary upper and lower total acrylic prosthesis, but conventional acrylic teeth should be replaced with radiosensitive teeth (Figure 4).

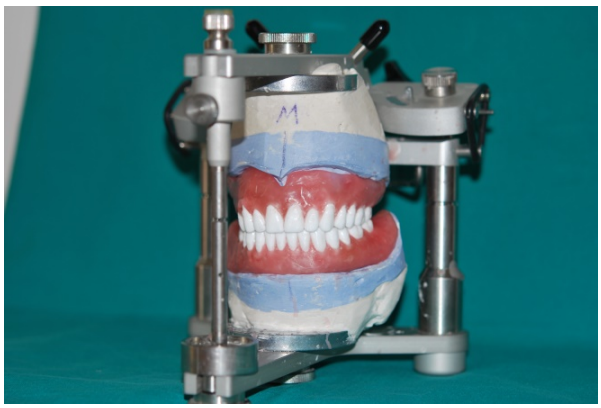

Fig.4. Making of the denture

Fig. 5. The lower denture in the mouth

Next step would be making of a CBCT scan with these dentures and placing them in the patients mouth. (Figure 5)

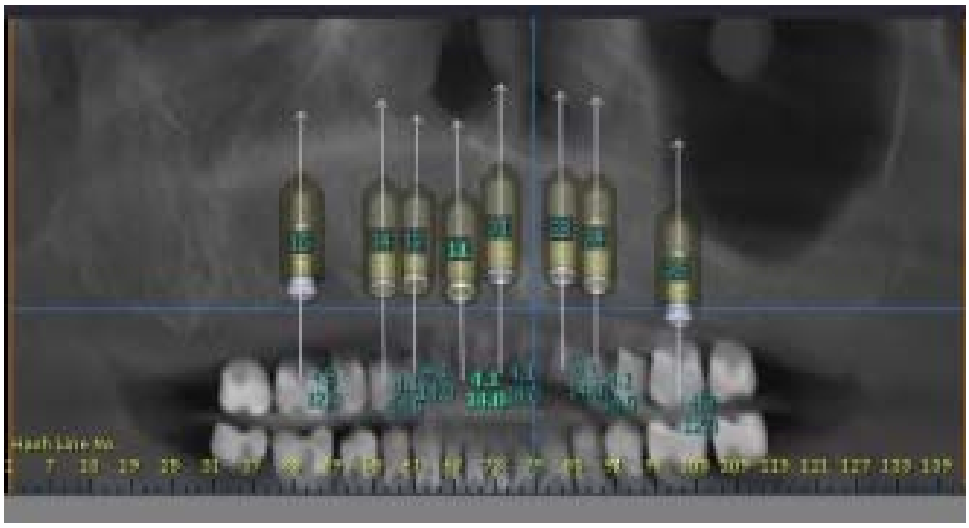

Fig.6. Planning in the upper jaw

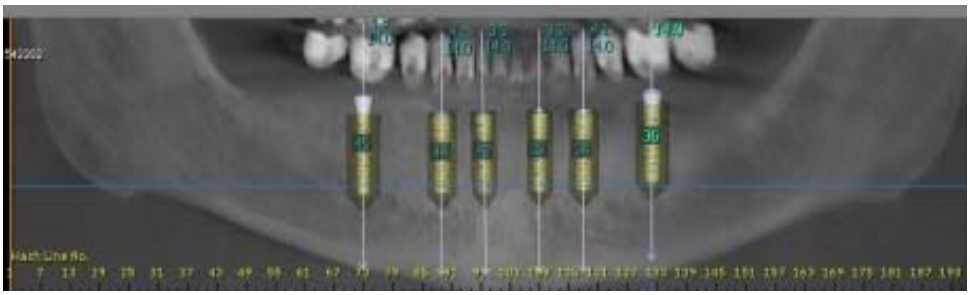

Fig. 7. Planning in the lower jaw

After the analysis of the obtained images, it was possible to make a definitive treatment plan (Figures 6., 7. and 8.). Number, positions and dimensions of the dental implants that will carry dental restorations was established , as well as the amount of bone tissue that must be compensated prior to the implant placement. In the upper jaw, since the atrophy of the ridge was far more progressive, a two-phase intervention was planned, whereby in the first act alveolar ridge augmentation should be carried out, and in the second insertion of the implants. In the lower jaw it was possible to implement therapy in one act, i.e. implants will be placed with simultaneous compensation of smaller amount of bone loss. After such a developed treatment plan, we started its implementation.

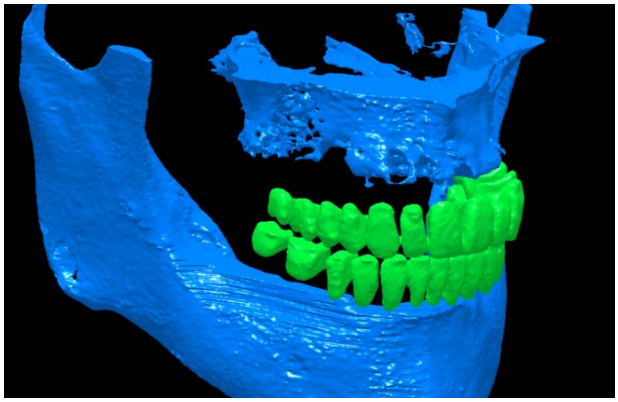

Fig. 8. Software analysis of dental-alveolar relationship

4. CONCLUSION

Tooth loss and its consequences in modern society represent a serious medical, social and economic problem and, therefore, it is not surprising that a large number of scientists of medical and technical sciences are dealing with it. The development of science and technology in the last 20 years puts dental implantology in the front row, as a branch of dentistry that largely solves this problem. Particular progress has been made in terms of preimplantation diagnostics and planning of implant therapy.

Today, dental implantology is not possible without the use of CBCT devices and a software support for these machines, in the form of a number of programs aimed at analyzing, planning, virtual implant placement into the desired position, and all other processes that allow us to implement optimal therapy in each case. The introduction of radiosensitive teeth in treatment planning of edentulous patients greatly improve the accuracy and reliability, and reduces the possibility of error when making teeth restorations. The very simplicity of the procedure to make dentures with the teeth is giving it an advantage over some other procedures that have been used in practice.

Although this procedure extends a treatment and makes it more expensive, benefits which it brings exceeds its disadvantages, and the authors of this paper suggest that the this protocol should be included in the regular protocols in implant treatment of edentulous patients.

5. REFERENCES

[1] Mirković S.: *Mini dentalni implanti*, Univerzitet u Novom Sadu, medicinski fakultet, 2013.

[2] Mirković S., Đurđević Mirković T., Puškar T.: *Application of concetrated growth factors in reconstruction of bone defects after removal of large jaw cyst-report of two cases*. Vojnosanit Pregl, 2014 (accepted for publishing)

[3] Jurišić M., Stamenković D., Marković A., Todorović A., Leković V., Dimitrijević B.: *Oralna implantologija*, 1st ed. Beograd: Stomatološki fakultet Beograd, 2008.

[4] Mohammad M., Farzad M.: *Guided bone regeneration, A literature review,* J Oral Health Oral Epidemiol, 1, p.p. 3-18, 2012.

[5] Peterson K., Pamenius M., Eliasson A., Narby B., Holender F., Palmqvist S. Hakansson J.: *20-year follow-up of patients receiving high-cost dental care within the Swedish Dental Insurance System, 1977-1978 to 1998-2000*, Swed Dent J. 30, p.p. 77-86, 2006.

[6] Ganz SD.: *Computer-aided Design/Computer-aided Manufacturing Applications Using CT and Cone Beam CT Scanning Technology*, Dent Clin Nor Am, 52, p.p. 777-808, 2008

[7] Eshak M., Brooks S., Abdel-Wahed N., Edwards PC.: *Cone beam CT evaluation of the presence of anatomic accesory canals in the jaws*, Dentomaxillofacial Radiology, 43, 2014.

[8] Egbert N., Cagna DR., Ahuja S., Wicks RA.: *Accuracy and reliability of stitched cone-beam computed tomography images,* Imaging Science in Dentistry, 45, p.p. 41-47, 2015.

Authors: **Dr. stom. Ana Tadic, Assoc. prof. dr Sinisa Mirkovic, Assoc.prof. dr Tatjana Puškar,** University of Novi Sad, Faculty of Medicine, Hajduk Veljkova 3, 21000 Novi Sad, Serbia, Phone.: +381 21 420-677, Fax: +381 21 662-4153.
E-mail: tadic.ana76@gmail.com
sinisa.mirkovic021@gmail.com
tatjanapuskar@yahoo.com

Assoc. prof. dr Igor Budak, MS.c Mario Sokac University of Novi Sad, Faculty of Technical Sciences, Institute for Production Engineering, Trg Dositeja Obradovica 6, 21000 Novi Sad, Serbia, Phone.: +381 21 485 2255, Fax:+381 21 454-495.
E-mail: budaki@uns.ac.rs
marios@uns.ac.rs

Note: The part of results presented in this paper have been obtained in the framework of the project "Research and development of modeling methods and approaches in manufacturing of dental recoveries with the application of modern technologies and computer aided systems," TR - 35020, funded by the Ministry of Education, Science and Technological Development of Republic of Serbia.

Journal of Production Engineering
Vol.18 No.1
JPE (2015) Vol.18 (1) Preliminary Note
Lapčević, A., Jevremović, D., Trifković, B., Santoši, Ž., Vukelić, Đ.

APPLICATION OF CAD/CAM TECHNOLOGY IN THE DESIGN AND CREATION OF FULL ANATOMIC BRIDGE FORM ZIRCONIUM DIOXIDE

Received: 20 May 2015 / Accepted: 15 June 2015

Abstract: *Daily progress of dentistry, especially in the field of prosthodontics is introducing new materials and technologies. With the increasing need for aesthetically acceptable and non-metal materials, it came to development and improvement of ceramic materials and computer based systems (CA). The patient came in order to compensate the missing left lateral incisor. Since the adjacent teeth are brushed and the print was taken, casted model has been scanned using 3Shape D800 laboratory scanner. Dental restoration has been designed using 3Shape DentalSystem Premium software and the available tools. After completing the virtual design, the data are sent to the program responsible for CAM Zenotec® mini CAD/CAM device. As a result, the compensation with the full morphology was obtained without the need for finishing works.*
Key words: *CAD/CAM, zirconium dioxide, dental restorations*

Primena CAD/CAM tehnologije u projektovanju i izradi mostova pune anatomske forme na bazi cirkonijum-dioksida. *Stomatologija, posebno stomatološka protetika svakodnevno napreduje uvođenjem novih materijala i tehnologija. Kako se javlja sve veća potreba za estetski prihvatljivim i bezmetalnim materijalima, došlo je do razvoja i unapređenja keramičkih materijala i računarima podržanih sistema (CA). Pacijent se javio radi nadoknade nedostajućeg levog bočnog sekutića. Pošto su susedni zubi zbrušeni i uzet otisak, izliven je model koji je skeniran pomoću 3Shape D 800 laboratorijskog skenera. Zubna nadoknada je dizajnirana pomoću 3Shape DentalSystem Premium softvera korišćenjem raspoloživih alata. Nakon završenog dizajna virtuelni podaci su poslati u program odgovoran za CAM Zenotec® mini CAD/CAM uređaja. Kao rezultat, dobijena je nadoknada pune morfologije bez potrebe za doradivanjem.*
Ključne reči: *CAD/CAM, cirkonijum-oksid, zubne nadoknade*

1. INTRODUCTION

By introducing new materials and technology in the filed of dentistry, especially in prosthodontics, it is rapidly progressing. With increasing popularity of intraosealnih implants, there was an expansion of fixed dental restorations [1]. With the increasing need for aesthetically acceptable non-metal materials, developments and improvements of ceramic materials and computer supported systems (CA) progressed. In CA systems, wich have the greatest application in the field of dentistry, are including 3D digitization systems, computer aided design (CAD) with reverse engineering (RE) and computer aided manufacturing (CAM) [2].
CAD / CAM systems enable efficient creation of high-quality dental restorations with high precision and accuracy in one visit [3]. On the other hand, the main disadvantage of such restorations is aesthetics that was not at a high level. The blocks of compensation was made, and it is obtained with the use of rototillings cut method, they had been uniform and could not fully imitate tooth structure that differ in color and translucency without finishing by dental technicians. In this way the time needed for tooth reparation is extended which is increasing the costs of their production. For this reason, for a long time CAD/CAM system was only used as a method for making metal-free base compensation, then the dental technician inflict the veneers ceramics. Zirconium oxide ceramic has excellent biocompatibility and mechanical characteristics compared to conventional ceramics [4]. However, the main disadvantage of this ceramic system states breaking a part of veneering ceramic layer [5-8]. The solution of this problem is the creation of one-piece restoration using CAD/CAM system. From zirconium-oxide ceramics it is possible to produce a single large compensation with the full range of the morphology, which has no need for veneering.

2. CASE STUDY: CAD/CAM APPLICATION IN THE DESIGN AND CREATION OF FULL ANATOMIC BRIDGE

The patient sought to compensate the missing left lateral incisor. After examination and discussion he suggested that the missing tooth compensate with the bridge of zirconium. In the next visit the adjacent teeth are milled, left central incisor and canine and prints are taken.

2.1 3D Digitization

After taking impressions, models are casted of special plaster for scanning (Fujirock EP OptiXscan, GC, Japan). The model was scanned using 3Shape D800 laboratory scanner (Fig. 1) supported with 3Shape DentalSystem Premium software. This scanner has two cameras with resolution of 5.0 Mpix, red light laser technology and accuracy of 20 microns.

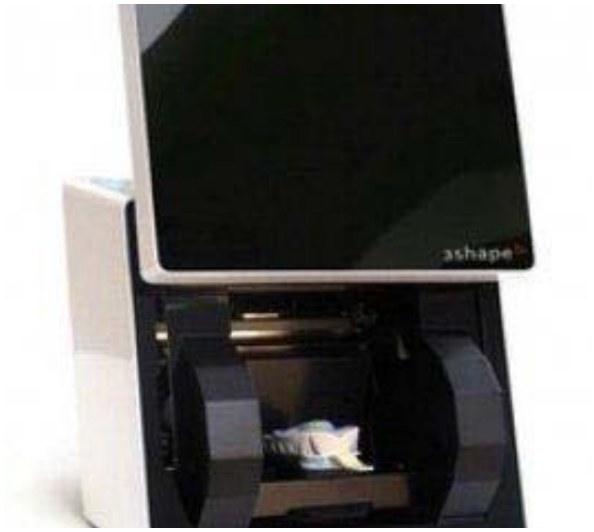

Fig. 1. 3Shape D800 labaratory scanner

After the 3D digitization is complete, the virtual model appeared on the screen (Fig. 2).

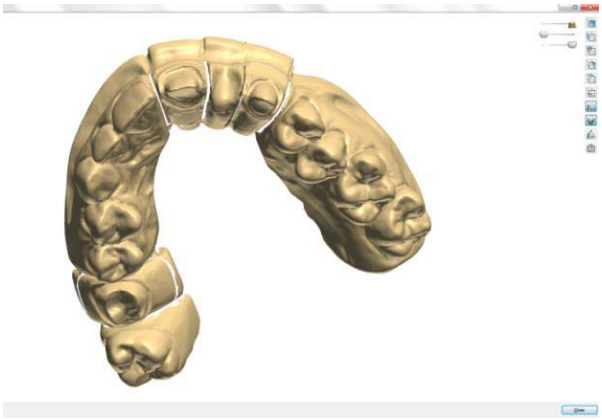

Fig. 2. The result of 3D digitizing

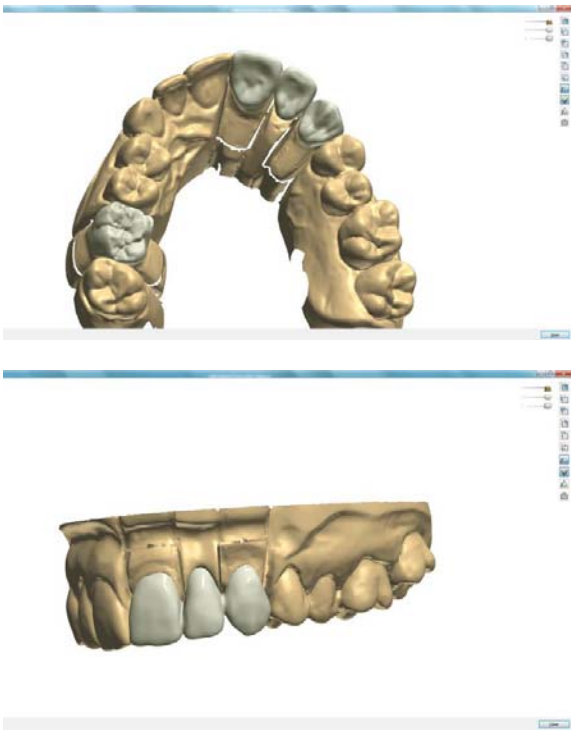

Fig. 3. Finished compensation design

2.2 Restorations CAD design

The begining of designing compensation involves determining the lines of demarcation. The computer automatically gives the proposal of the demarcation line, but the user interface allows for manual corrections. The next phase is the determination of entering way of compensation. Then, from the data base are choosen cheapest morphological files. The files vary in height and number of nodules, fissure complex, and ridge morphology. Further adjustments are allowing compensation of group movement, correction of individual teeth axis or correction of individual zones with tools for adding or removing material (Fig. 3).

2.3 CAM compensation

Virtual project is automatically converted into the STL file and then electronically sent to the program responsible for the CAM process. In this case, STL file is imported into the program rototillings Zenotec® mini CAD/CAM (Wieland Dental) (Fig 4). The compensations are then milled from non-ferrous single-zirconium discs (color T1). Usually, coloring requires a separate working step which is comprising to application of the liquid coloring matter based on metal oxide, dipping or by using the brush technique before sintering. For colored discs, the colors are added to the zirconium powder and are homogenized during the industrial production process.

Fig. 4. Zenotec® mini CAD/CAM device

As a result the compensation of highly homogeneous color was obtained (Fig. 5). The need for manual veneering can exist in extremely attimis works, while more simple aesthetic forms can simply paint the surface and is additional advantage when creating compensation which is time saving. The consistency of color is another advantage that should not be ignored. Contact points in the zirconium dioxid ceramics should be highly polished, thus preventing abrasion of antagonist.

Fig. 5. Final compensation

3. CONCLUSION

Displayed zirconium oxide ceramic has excellent mechanical characteristics, aesthetic performance, excellent biocompatibility and as well as the abrasion resistance, as compared to conventional ceramics. In contrast to the glass-ceramics, which are less stable in the mouth, they are limited to restoration of individual or small bridges [4], from zirconium - oxide ceramics and it can make long-span bridges with full morphology. Thanks to the materials and painted homogenized discs, finishing work by dental technicians can be minimized, and the finished work can be obtained quickly, easily and reliably using CAD/CAM technology.

4. REFERENCES

[1] Miyazaki,T., Nakamura, T., Matsumura, H., Ban, S., Kobayashi, T. Current status of zirconia restoration, Journal of Prosthodontic Research 57, pp 236–261, 2013.

[2] Williams, R.J., Eggbeer, D., Lapcevic, A., Trifkovic, B., Puskar, T., Budak, I., Jevremovic, D. RE-CAD-CAM approach in design and manufacturing of dental ceramic crowns in combination with manual individualization. 11th International Scientific Conference "MMA 2012-advanced production 24 technologies", September 20-21., 2012. Novi Sad, Serbia

[3] Mörmann, W.H. The evolution of the CEREC system, The Journal of the American Dental Association, 137, p.p.7S-13S, 2006.

[4] Hmaidouch, R., Muller, W.D., Lauer, H.C.,Weigl, P. Surface roughness of zirconia for full-contour crowns after clinically simulated grinding and polishing, International Journal of Oral Science 6, pp 241–246, 2014.

[5] Raigrodski, A.J., Yu, A., Chiche, G.J. Clinical efficacy of veneered zirconium dioxidebased posterior partial fixed dental prostheses: fiveyear results, J Prosthet Dent 108(4), pp214– 222, 2012.

[6] Kokubo, Y., Tsumita, M., Sakurai, S. et al: Five-year clinical evaluation of In-Ceram crowns fabricated using GN-I (CAD/CAM) system. J Oral Rehabil, 38(8), pp 601–607, 2011.

[7] Ortorp, A., Kihl, M.L., Carlsson, G.E. A 3-year retrospective and clinical follow-up study of zirconia single crowns performed in a private practice, J Dent 37(9), pp 731–736, 2009.

[8] Etman, M.K., Woolford, M.J. Three-year clinical evaluation of two ceramic crown systems: a preliminary study, J Prosthet Dent 103(2), pp 80–90, 2010.

Authors: **Assist. dr Ana Lapčević, Prof. dr Danimir Jevremović,** University Business Academy, Faculty of Stomatology, Clinic for Prosthodontics, Žarka Zrenjanina 179, 26000 Pančevo, Republic of Serbia, tel. +381 13 235-1292.
E-mail: dranalapcevic@gmail.com
dr.danimir@sbb.rs

Assist. dr Branka Trifković, University of Beograd, School of Dental Medicine, Clinic for Prosthodontics, Rankeova 4, 11000 Beograd, Republic of Serbia, tel. +381 11 243-3433
E-mail: trifkovicbranka1011@gmail.com

Prof. dr Đorđe Vukelić, M.Sc Željko Santoši, University of Novi Sad, Faculty of Technical Sciences, Department of Production Engineering, Trg Dositeja Obradovica 6, 21000 Novi Sad, Republic of Serbia, Tel: +381 21 485 2306, Fax: +381 21 454-495.
E-mail: vukelic@uns.ac.rs
zeljkos@uns.ac.rs

ACKNOWLEDGMENT

The part of results presented in this paper have been obtained in the framework of the project "Research and development of modeling methods and approaches in manufacturing of dental recoveries with the application of modern technologies and computer aided systems," TR - 35020, funded by the Ministry of Education, Science and Technological Development of Republic of Serbia.

Journal of Production Engineering
Vol.18 No.1
JPE (2015) Vol.18 (1) Preliminary Note

Kádárová J., Kalafusová Ľ.

GLOBAL DISTRIBUTION NETWORK AND RISK MODELING

Received: 28 April 2015 / Accepted: 28 May 2015

Abstract: *The paper discusses the current gaps and future directions of global supply chain defined by the literature. The basic terminology and classification of supply chain create the base for the future analysis. In the paper the current factors influencing basic supply chain model are analyzed and defined in the individual and global viewpoint. The most used research methods in the field of supply chain were identified by their quantitative occurrence in the literature. According to the review provided by various companies, the future directions of supply chain risk management were defined and pointed in the map. Developing the future supply chain require time, insight and input from a wide range of industry players (e.g. retailers, consumer products, manufacturers, industry standards organizations, technology companies, etc.) so it is necessary to start with the collaboration between them to become more prosper in this dynamic environment.*
Key words: *Risk modeling, distribution network, future directions, gaps*

Globalna distributivna mreža i modelovanje rizika. *U radu su prikazani trenutni nedostaci i budući pravci globalnog lanca snabdevanja definisani literaturom. Osnovna terminologija i klasifikacija lanca snabdevanja stvaraju osnovu za buduće analize. U ovom radu aktuelni faktori koji utiču na osnovni model lanca snabdevanja su analizirani i definisani sa individualnog i globalnog stanovišta. Metode istraživanja iz oblasti lanca snabdevanja koje se najviše koriste identifikovane su po njihovim kvantitativnim pojavama prema literaturi. Prema pregledima raznih kompanija, budući pravci upravljanja rizicima lancem snabdevanja su definisani i ukazni na karti. Razvoj budućeg lanaca snabdevanja zahteva vreme, uvid i ulaz iz širokog spektra industrijskih subjekata (npr. trgovci, potrošači proizvode, proizvođači, industrijske standarde organizacije, tehnološke kompanije, itd.), tako da je neophodno da se počne saradnja između njih da bi više napredovali u ovom dinamičnom okruženju.*
Ključne reči: *modelovanje rizika, distributivna mreža, budući pravci, nedostaci*

1. INTRODUCTION

Supply Chain Risk Management (SCRM) is one aspect of Enterprise Risk Management (ERM) which start with the risk identification. Many different definitions of risk in a supply chain (SC) context are provided in literature.

According to Jüttner et al. supply chain risk (SCR) can be defined as "the variation in the distribution of possible supply chain outcomes, their likelihoods, and their subjective values"[1]. This definition highlights two risk dimensions, namely: (1) impact and (2) likelihood of occurrence.

The supply chain may be divided into four dimensions: (1) traditional, (2) lean, (3) agile and (4) leagile supply chain [2]. Chopra and Sodhi classified supply chain risks as disruptions, delays, systems, forecast, intellectual property, receivables, inventory, and capacity [3].

According to Sinha et al. the most important supply chain risk areas are standards, supplier, technology, and practice [4]. Finch mentioned three levels of risk coverage, namely: (1) application level; (2) organizational level; and (3) inter-organizational level [5]. Norrman and Jansson, categorized all types of SC risk into three categories: (1) operational accidents; (2) operational catastrophes; and (3) strategy uncertainty [6]. According to Tang there are two kinds of risks in SC: (1) operational risk; and (2) disruption risk [7]. Kleindorfer and Saad divided risk in two categories as: (1) risks arising from the problems of coordinating supply chain and demand; (2) risks arising from disruptions to natural activities [8]. Companies usually manage supply chain risks at the strategic (long term) or at the tactical (medium term) level [9].

2. LITERATURE REVIEW

Managing risks in a global supply chain requires lot of information sharing, close relationships and trust on the partners, alignment of incentives and knowledge about risks [2]. The literature suggests that proactive approaches at supply chain level should be implemented in order to effectively manage disruptions [10]. Research community has developed numerous supply chain design models. To confront the challenges of a complex and unstable competitive environment and to gain long-term benefits, it is necessary to include resilience and robustness considerations into supply chain design [10].

Dynamic supply chain models under uncertainty are needed, as well as tools able to consider interactions characterizing supply chain factors and risk sources. Nevertheless, very complex interactions among supply chain factors make the supply chain inherently vulnerable to disruptions. That is the reason why only the most relative risk factors of SC should be considered.

This creates a challenge for managers to choose the most relevant risk factors in their models.
Many researchers analyzed supply chain risks through different influence factors pointed in below (Tab. 1).

	INFLUENCE	DESCRIPTION	PREVIOUS RESEARCH
DELIVERY	Capacity	Supplier is near or at full capacity	Lee et al. [11]; Chopra and Sodhi, [3]; Norrman and Jansson [6]
	Cycle Time	Unreliable cycle times of suppliers	Zsidisin [12]
	Material availability	Unreliable raw material sources	Norrman and Jansson [6]; Noordewier et al. [13]; Hillman [14]
	Logistic	Unreliable logistics infrastructure of suppliers	Chopra and Sodhi, [3]; Hillman [14]
	Natural Disaster	Suppliers are located in areas prone to natural/political disruptions	Chopra and Sodhi, [3]; Zsidisin [12]; Norrman and Jansson [6]
COST	Market strength	Suppliers are to strength or to weak to dictate the price	Kraljic [15]
	Currency	Suppliers common currency is volatile	Hillman [14]
	Financial	Supplier is financially weak	Chopra and Sodhi, [3]; Babich [16]
	Cost management	Poor management skills of suppliers	Hillman [14]; Zsidisin [12]
QUALITY	Quality system	Substandard control quality methods of suppliers	Hillman[14]; Zsidisin [12]
	Legal Standards	Supplier is unaware/unconcerned with legal / environmental standards	Hillman [14]; Huang et al. [17]
FLEXIBILITY	R&D	Poor product development methods of suppliers	Droge et al. [18]; Noordewier et al. [13]; Laseter and Ramdas [19]
	Flexibility	Suppliers have processes which don´t allow significant changes in volume	Chopra and Sodhi, [3]; Noordewier et al. [13]; Norrman and Jansson [6]; Zsidisin [12]
CONFIDENCE	Management	Lack of clear management vision or expertise	(Hillman, 2006)[14]
	Market characteristics	The market in which the supplier operates is volatile	Chopra and Sodhi [3]; Noordewier et al. [13]
	Information	Unreliable information system of suppliers	Chopra and Sodhi [3]; Hillman [14]
	Product type	The supplier may not be able to handle the complexity or sensitivity of product requirements	Chopra and Sodhi, [3]; Hillman [14]
	Relationship	It is difficult to manage the relationships with suppliers (communication barriers)	Noordewier et al. [13]; Hillman [14]

Table 1. Factors of failure pointed in the literature

We believe that empirically grounded research supports the development of quantitative modelling using empirical studies and conceptual models.

WEF 2011, presented triggers of global supply chain disruptions with the top external disruptions highlighted in the Table 2 [20].

According to their research the initial event may results in a cascading disruption or failure across regions or industries.

ENVIRONMENTAL	GEOPOLITICAL
Natural disasters Extreme weather Pandemic	Conflict and political unrest Export/import restrictions Terrorism Corruption Illicit trade and organized crime Maritime piracy Nuclear/biological/chemical weapons
ECONOMIC	**TECHNOLOGICAL**
Sudden demand shocks Extreme volatility in commodity prices Border delays Currency fluctuations Global energy shortages Ownership/investment restrictions Shortage of labor	Information and communications disruptions Transport infrastructure failures

Table 2. Triggers of global supply chain disruptions [20]

Modeling the critical point of failure within a SC network is un-attempted and demands further research [5]. We believe that disruption impact evaluation in terms of cost, duration, and service will provide better transparency for effective SCR modelling.

According to Musa the percentage of publications by types of research methods were analyzed [21]. In the literature review process were identified four types of research approaches pointed below:

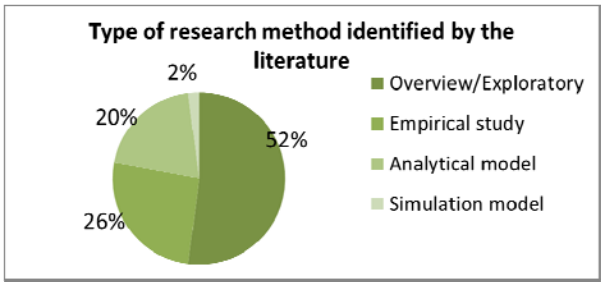

Fig. 1 Percentage of publications by types of research method in the field of Global Supply Chain

According to Colicchia and Strozzi it is necessary to analyze how key concepts and performance measures from other disciplines can be incorporated into SCR models [10]. Also there is a need to

investigate – through empirically based research – how companies assess their supply chain risk exposure and how they develop mitigation capabilities in collaboration with their supply chain partners.

3. SCRM RESEARCH GAPS

Using literature review, main six research gaps in the field of SCRM were determined:

1. According to the research, the holistic SCRM approach is lacking in the current literature. Williams et al. claims that studying dyadic relationships are extremely important for the holistic understanding of SCRM [22]. These holistic "system of systems" approach is expected to bring fresh thinking for current SC problems [23].
2. There is a need to develop novel quantitative as well as qualitative methods to quantify the risk propagation and create an effective quantitative modelling approach to solve SCRM problems. There are many quantitative tools, like mathematical programming and simulation models Rao and Goldsby [24] or graph theory Colicchia and Strozzi [10], which are not developed to solve SCRM problems. According to Khan et al. it is necessary to develop well-grounded quantitative models which could consider other interdisciplinary research approaches [25]. Quantitative tools and theories which could be used to the dynamic behavior of the complex SC system might be: (1) System Dynamics using causal loops diagrams and flow diagrams, (2) Real Option Valuation, and (3) Simulation modelling.
3. According to Jüttner et al. there is an increasing importance to identify risk drivers and their potential impact to SC processes [1]. Bryson et al. forced the need for creating an effective recovery system to mitigate the effect of disasters [26]. Only some authors like Khan and Burnes [27] and Natarajarathinamet al. [28] examined the effects of risk disruption and recovery planning. For these reason, the robust contingency/recovery planning strategies for potential future disruption are needed. We believe that create an appropriate risk recovery model will require proactive planning combining appropriate information and human intervention.
4. The global compliance standards and environmental thinking become more important in recent years. This environmental awareness force logistics activities to be more effective. Also there is a pressure to use natural resources and recycle. Many companies are aware of this recent trend and take into consideration the interrelationship between risks and sustainability perspective to become more successful in the current competitive global market.
5. Companies need to be able to monitor real time logistics networks. Low information and communication technology make the visibility of SC performance almost insignificant. According to Tang [7] and Rao and Goldsby [24] current technologies such Radio Frequency Identification (RFID), Enterprise Resource Planning (ERP) or General Packet Radio Service (GPRS) will become important information tools for management of supply chain risks in terms to improve SC performance. Nevertheless, the recent technology used to analyze risk management demands needs to be investigated more extensively.
6. Network information communication and sharing avoids defaults and generate trust between shareholders. Nevertheless, long-terms contracts for disruption are still lacking in the literature. Only few research papers were focused on contracts relating to price and demand fluctuations.

Other additional gaps which might be considered are the lack of understanding of the nature of complexity among many supply chain researchers and the low effectiveness of risk management[29].

4. FUTURE DIRECTIONS OF SCRM

Each supply chain should follow 5 steps of improvement provided by Logisitics [30], namely: (1) Analyze the entire supply chain, (2) Connect Electronically, (3) Anticipate Issues, (4) Set up Alternative Plans, (5) Manage by Exception (Fig. 2).

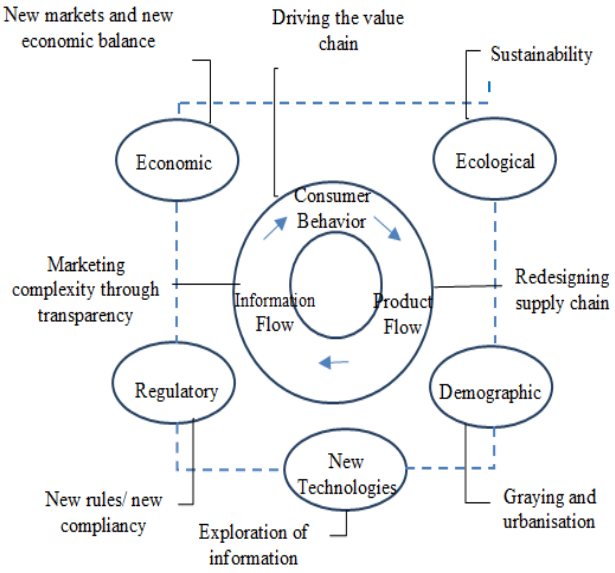

Fig. 2 Future SC proposed by CapGemini [31]

4.1 Case study

Global supply chain suffers many breakdowns in recent years. Many of them were related to natural disasters, e.g. Japan tsunami (2011), Hurricane Katrina in US (2005), Indian ocean tsunami (2004), etc.

These natural disaster caused cascading effect of disruptions pointed below (Tab. 3).

According to our study, future directions of global supply chain should be oriented on scenario planning, quantitative risk metrics and data/information sharing.

The most important directions of Global Supply Chain are also pointed below (Fig. 3).

The importance of the selected areas was measured by their key words occurrence in the literature. The importance of individual areas was numerically and graphically classified.

CAUSE	EFFECT
PHYSICAL /INFRA-STRUCTURE DISRUPTION	All major ports were closed with intense effect on the global logistic services. The spilling effect of the earthquake and tsunami led to a nuclear power plant breakdown in fukushima. Nuclear crisis and electricity shutdown forced companies to shut down their plants.
FINANCIAL DISRUPTION	After the japan tsunami, three sectors, namely: (1) automotive; (2) steel industry; (3) electronics, were identified by global supply chain analysts as most affected business areas (hike in prices of all affected products).
TECHNO-LOGY DISRUPTION	Impact on stability and integrity of e-services, loss of intellectual property.
INFORMA-TION DISRUPTION	Massive impact on information security (lack of communication due to a complete shutdown of the supply network).
HUMAN RESOURCE DISRUPTION	Loss of lives. Remove of employees (affect productivity).
SOCIAL AND ECOLOGI-CAL DISRUPTION	Corruption, organized crimes, global imbalance, etc.

Table 3. Cascading effect of disruptions

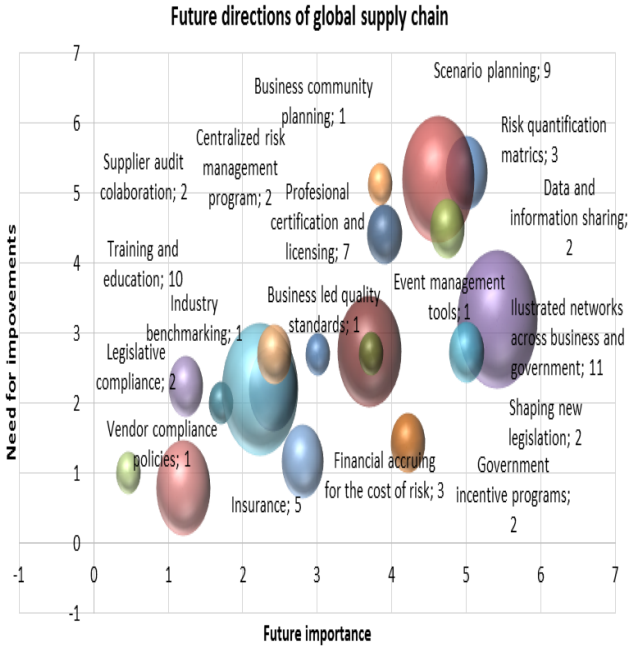

Fig. 3 Potential future directions of global supply chain identified by the literature

5. CONCLUSION

The common challenge for the future of global supply chain might be the (1) collaboration between consumers and shoppers which should be informed about the sustainability impact of their shopping choices, (2) collaboration and standardization between retailers in order to be profitable and achieve sustainable growth, (3) collaboration between manufacturers and suppliers with the aim to manufacture, market and supply the products that consumers need in a cost-efficient manner, (4) facilitate the distribution process from supplier to consumer using longer-term contracts with logistics service providers. Developing the future supply chain require time, insight and input from a wide range of industry players (e.g. retailers, consumer products, manufacturers, industry standards organizations, technology companies, etc.) so it is necessary to start with the collaboration between them to become more prosper in this dynamic environment.

6. REFERENCES

[1] Jüttner, U., Peck, H., & Christopher, M. (2003). SUPPLY CHAIN RISK MANAGEMENT: OUTLINING AN AGENDA FOR FUTURE RESEARCH. International Journal of Logistics: Research & Applications, 6(4), 197-210.

[2] Faisal, M. N., Banwet, K. D., & Shankar, R. (2006). Mapping supply chains on risk and customer sensitivity dimensions. (Emerald, Ed.) Industrial Management & Data Systems, 106(6), 878-895. Dostupné na Internete: http://www.emeraldinsight.com/doi/pdfplus/10.1108/02635570610671533

[3] Chopra, S., & Sodhi, M. S. (2004). Managing risk to avoid supply-chain breakdown. (Fall, Ed.) MIT Sloan Manage, 46, 53–61.

[4] Sinha , P. R., Whitman, L. E., & Malzahn, D. (2004). Methodology to mitigate supplier risk in an aerospace supply chain. (Emerald, Ed.) Supply Chain Management: An International Journal, 9(2), 154-168.

[5] Finch, P. (2004). Case study: Supply chain risk management. (Emerald, Ed.) Supply Chain Management: An International Journal, 9(2), 183-196.

[6] Norrman, A., & Jansson, U. (2004). Ericsson's proactive supply chain risk management. (E. G. Publishing, Ed.) 34(5), 434-456. doi:10.1108/09600030410545463

[7] Tang, C. S. (2006). Perspectives in supply chain risk management. (Elsevier, Ed.) Int. J. Production Economics, 103(2006), 451–488. doi:10.1016/j.ijpe.2005.12.006

[8] Kleindorfer, P. R., & Saad, G. H. (2005). Managing Disruption Risks in Supply Chains. (POMS, Ed.) PRODUCTION AND OPERATIONS MANAGEMENT, 1-16. Dostupné naInternete:http://opim.wharton.upenn.edu/risk/downloads/05-08-PK.pdf

[9] Tang, C., & Tomlin, B. (2008). The power of flexibility for mitigating supply chain risks. (Elsevier, Ed.) Int. J. Production Economics, 116(2008), 12–27. doi:10.1016/j.ijpe.2008.07.008

[10] Colicchia, C., & Strozzi, F. (2012). Supply chain risk management: a new methodology for a systematic literature review. (Emerald, Ed.) Supply Chain Management: An International Journal, 17(4), 403–418.

[11] Lee, H. L., Padmanabhan, V., & Wang, S. (1997). Information distortion in a supply chain: The bullwhip effect. Management Science, 43, 546–558. Dostupné na Internete:

http://www.ie.bilkent.edu.tr/~ie571/lee%20et%20al%20(1997),%20ms.pdf
[12] Zsidisin , G. A. (2006). Managerial Perceptions of Supply Risk. Journal of Supply Chain Management: A Global Review of Purchasing and Supply Copyrigh, 39(4), 14-26. Dostupné na Internete: http://onlinelibrary.wiley.com/doi/10.1111/j.1745-493X.2003.tb00146.x/pdf
[13] Noordewier, T. G., John, G., & Nevin, J. R. (1990). Performance outcomes of purchasing arrangement in industrial buyer-vendor relationships. (A. M. Associacion, Ed.) Journal of Marketing, 54(4), 80-93. Dostupné na Internete: http://part-timemba.carlsonschool.umn.edu/marketinginstitute/research/documents/John_PerformanceOutcomesofPurchasing_1990.pdf
[14] Hillman, M. (2006). Strategies for managing supply chain risk. Supply Chain Management Review(10), 11–13.
[15] Kraljic, P. (1983). Purchasing must become supply management. Harvard Business Review, 61, 109–117.
[16] Babich, V. (2004). Vulnerable Options in Supply Chains: Effects of Supplier Competition. Michigan: Department of Industrial and Operations Engineering, University of Michigan. Dostupné na Internete: http://www.realoptions.org/papers2004/BabichVulnerable.pdf
[17] Huang, A.; Yen, D. C.; Chou, D. C.; Xu, Y.;. (2003). Corporate Applications Integration: Challenges, Opportunities, and Implementation Strategies. Journal of Business and Management(9), 137–145.
[18] Droge, C., Jayaram, J., & Vickery, S. K. (2004). The effects of internal versus external integration practices on time-based performance and overall firm performance. (Elsevier, Ed.) Journal of Operations Management, 22, 557–573. doi:10.1016/j.jom.2004.08.001
[19] Laseter, T. M., & Ramdas, K. (2002). Product Types and Supplier Roles in Product Development: An Exploratory Analysis. IEEE TRANSACTIONS ON ENGINEERING MANAGEMENT, 2, 107-118. Dostupné na Internete: http://strategy.sauder.ubc.ca/nakamura/iar515p/laseter_product_types.pdf
[20] WEF. (2011). New Models for Addressing Supply Chain and Transport Risk: An Initiative of the Risk Response Network In collaboration with Accenture. Geneva, Switzerland.
[21] Musa , S. N. (2012). Supply Chain Risk Management: Identification, Evaluation and Mitigation Techniques. Linköping, SWEDEN : Linköping University . Dostupné na Internete: http://liu.divaportal.org/smash/get/diva2:535627/FULLTEXT01.pdf
[22] Williams, Z., Lueg, J. E., & LeMay, S. A. (2008). Supply chain security: an overview and research agenda. (Emerald, Ed.) The International Journal of Logistic Management, 19(2), 254-281. doi:10.1108/09574090810895988
[23] Mingers, J., & White , L. (2010). A review of the recent contribution of systems thinking to operational research and management science. (Elsevier, Ed.) European Journal of Operational Research, 207(2010), 1147–1161. doi:10.1016/j.ejor.2009.12.019
[24] Rao, S., & Goldsby, T. J. (2009). Supply chain risks: a review and typology. (Emerald, Ed.) The International Journal of Logistics Management, 20(1), 97-123.
[25] Khan, O., Christopher, M., & Burnes, B. (2008). The impact of product design on supply chain risk: a case study. (Emerald, Ed.) International Journal of Physical Distribution & Logistics Management, 38(5), 412-432.
[26] Bryson, K. M.; Millar, H.; Joseph, A.; Mobolurin, A.;. (2002). Using formal MS/OR modeling to support disaster recovery planning. (Elsevier, Ed.) European Journal of Operational Research, 141, 679–688.
[27] Khan, O., & Burnes, B. (2007). Risk and supply chain management: creating a research agenda. (Emerald, Ed.) The International Journal of Logistics Management, 18(2), 197-216.
[28] Natarajarathinam, M., Capar, I., & Narayanan, A. (2009). Managing supply chains in times of crisis: a review of literature and insights. (Emerald, Ed.) International Journal of Physical Distribution & Logistics Management, 39(7), 535-573. doi: 10.1108/09600030910996251
[29] Kern, D., Moser, R., Hartmann, E., & Moder, M. (2012). Supply risk management: model development and empirical analysis. (Emerald, Ed.) International Journal of Physical Distribution & Logistics Management, 42(1), 60-82.
[30] Logisitics. (2010). How to Enable a Proactive Supply Chain: 5 Steps to Supply Chain Empowermen. (Thomas, Ed.) NY. Dostupné na Internete: http://www.inboundlogistics.com/cms/article/how-to-enable-a-proactive-supply-chain/
[31] CapGemini. (2008). Future Supply Chain 2016: Serving customers in a sutable way. Dostupné na Internete: http://www.slideshare.net/BCLadd/future-supply-chain-2016?related=2

ACKNOWLEDGMENTS

The contribution has been developed according to The Grant Project No. 1/0669/13 “Proactive crisis management in industrial enterprises based on the concept of controlling”.

Authors: **doc. Ing. Jaroslava Kádárová, PhD.; Ing. Lenka Kalafusová.** Technical University of Košice, Department of Industrial Engineering and Management, Němcovej 32, 042 00, Košice, Slovak Republic, Phone.: +421 55 602 3242
E-mail: jaroslava.kadarova@tuke.sk
lenka.kalafusova@tuke.sk

Journal of Production Engineering
Vol.18 No.1
JPE (2015) Vol.18 (1) Preliminary Note

Nayak, N.C., Ray, P. K.

FLEXIBILITY AND QUALITY ASPECTS OF INDIAN MANUFACTURING MANAGEMENT PRACTICES: AN EMPIRICAL INVESTIGATION

Received: 11 December 2014 / Accepted: 10 March 2015

Abstract: *There appears an argument that flexibility and quality are two elements that compete with each other and that firms need to make a trade-off decision between the two. This research suggests that certain flexibility dimension practiced in firms for better quality products enhances performance. Using a case study of a leading alloy steel manufacturing firm in India, the hypothesized relationships are validated. The relationship between flexibility and quality appears to be limited, especially with respect to specific measures. However, future research will focus on empirically testing the practices presented in order to develop a more complete and rigorous list of flexibility measures for achieving quality.*
Key words: *manufacturing flexibility, product quality, case study, path model*

Aspekti fleksibilnosti i kvaliteta prakse industrijskog menadžmenta u Indiji: empirijsko istraživanje. *Često se pojavljuje argument da su fleksibilnost i kvalitet dva elementa koja se međusobno nadmeću i da kompanije moraju napraviti kompromis između njih. Ovaj rad sugeriše da određena dimenzija fleksibilnosti, upotrebljavana u firmama za pospešivanje kvaliteta proizvoda, povećava performanse. Korišćenjem studije vodećeg proizvođača legiranog čelika u Indiji hipotetičke teze su validovane. Zavisnost između fleksibilnosti i kvaliteta čini se da je ograničena, pogotovo u pogledu određenih mera. Buduća istraživanja će se fokusirati na testiranje iznetih praksi u cilju razvoja kompletnije i rigoroznije liste mera za postizanja kvaliteta.*
Ključne reči: *fleksibilnost proizvodnje , kvalitet proizvoda , studija slučaja , putanja modela*

1. INTRODUCTION

Unlike some of the industrial countries in Asia (Japan and China), India has basically relied on its manufacturing firms to compete in international market [1]. Evolving manufacturing environment offers new pressures to be confronted by the manufacturing firms, such as customized products with on-time delivery along with underlying requirements of quality and competitive cost [2]. Flexibility has brought about significant advantages by reducing the work-in-process levels of inventory and improving utilization of resources, reduction of space, reduction of scrap/rework, reduction of cycle time [3]. Quality has appeared two different meanings to researchers [4]. First the specification of a good/service and second how well its producer actually delivers to that specification [5]. Delivery to specification encompasses reliability and robustness, ease of purchase or access, ability to deal with complaints and after-sales service. As reported by Park and Son [6], improved product quality is the key factor in advanced manufacturing systems and plays an important role in improving the market share and profit margin of a manufacturing firm by decreasing the total manufacturing cost.

The interrelationship between dimensions of flexibility and basic characteristics of product quality is complex [7]. As there is a constant need of producing products with acceptable level of quality in a production system, the influence of flexibility on the level of quality of such products need to be modelled [8].

2. REVIEW OF LITERATURE

2.1 Production system flexibility

Flexibility has been classified according to approach/logic and interpretation in different aspects, e.g. supply, customer and manufacturing [9]. Among the vastness of publications, the study focused on eight basic flexibility dimensions with their definitions [10, 11, 12]. *Machine flexibility* is defined as the capability of production system to perform varying operations, in switching from one operation to another allowing small batch sizes, less inventory cost and higher machine utilization. *Process flexibility* is defined as the capability of performing several operations by the production system while reducing batch and inventory costs. *Routing flexibility* is defined as the ability of production system to produce a part by alternative routes using different machines, different set of process plans and operations. *Volume flexibility* is defined as the range of output levels a production system can economically produce to adjust the production upward or downward. *Operation flexibility* is defined as the number of alternative ways in which a part can be produced. *Part mix flexibility* is defined as the time it takes to add or substitute new products into the system. *Expansion flexibility* is defined as the ease at which capacity may be added to the system.

Material handling flexibility is defined as the capability of a production system to move different part types through the manufacturing system and to accommodate different parts of different sizes for proper positioning.

2.2 Product quality

Product quality is the degree to which the product conforms to the design specifications [13]. The concept of flexible manufacturing represents a strategy to improve quality. There appears two general approaches to quality in organizations: total quality control and TQM [14].

Product quality may be characterized with six basic functions [15]. *Performance* refers to the primary operating characteristics of a part/product.

Feature refers to the secondary characteristics that supplement the products basic functioning.

Reliability reflects the probability of a product's failing within a specified period of time.

Conformance refers to the degree to which a product's design and operating characteristics match pre-established standards.

Durability is a measure of product life having both economic and technical dimensions.

Serviceability refers to the speed, courtesy and competence of repair.

2.3 Flexibility and quality relationship

Constantly changing provides customers with more choices and manufacturers with more ways to compete [16, 17]. A few investigators have reported relationships between specific types of flexibility and quality. Li and Huang [18] established the impact of flexibility on product quality. Garg et al. [19] studied the relationships between flexibility and quality in Indian manufacturing organizations.

3. OBJECTIVES AND METHODOLOGY

The objective of present research is to explore the possible relationship between flexibility and quality and

i) flexibility dimensions are to be characterized and quantified

ii) quality parameters are to be decided and quantified

iii) flexibility quality relationship models are to be developed and the effect to be studied. For high production volume and high variety, whether the quality of product would be maintained? What happens to the performance of the firm due to flexibility?

A case study approach was decided to investigate the effect of flexibility on quality [20]. Sample in this study includes various sections/departments (forging, rolling, annealing, cutting and inspection) within an Alloy manufacturing firm. Table 1 provides an overview of the firm.

Attributes	Response
Year of establishment	1981
Turnover (million **$**)	85
Nature of product	Alloy steels
Number of employees	750
Domestic market share	17 %

Table 1. An overview of firm under study

4. CASE STUDY

4.1 Reasons for selecting the firm

Ferro alloy industry is chosen for several reasons. First, it is the world's largest manufacturing activity. Second, the history of this industry is fairly well disseminated. Third, the alloy industry has been explored within the context of specific countries. Finally, this industry offered the potential to simultaneously examine eight dimensions of flexibility and six parameters of quality considered in this research. The firm considered in this study is located at Odisha in which the company has maximum number of product variants. The firm aims to improve production system flexibility and maintain acceptable level of product quality to achieve better performance.

4.2 Operations at the firm

The division has many production modules for a large market share. Each module though automated, requires setup time for every variety change in operations. The firm produces alloys using any of the modules keeping scrap rate almost zero. The operating sequence at the manufacturing firm: Casting, Forging and Rolling, Annealing, Cutting, Quality check and Dispatch.

4. 3 Data collection from the firm

Field study coupled with both quantitative methods (document examination) and qualitative methods (questionnaire survey, personal discussions), was considered appropriate for the complex nature of the study and was used as data collection technique. Data required to compute the variables considered for various factors is drawn from various sources, such as, daily production report files, strategic plans for new part/products, review committee meeting reports, company presentations for customers/suppliers, bill-of-materials, financial statements and their sources.

Quality and flexibility parameter values for a period of more than sixty months are collected from the concerned firm using nominal group technique. Data pertaining to each parameter are collected from experts (manufacturing, quality control, sales and marketing, finance). Data represent the average figures for corresponding variables during a particular month on 0 to 1 scale. One aspect is discussed with more than one respondent [21]. Table 2 provides information regarding the informants.

Position	Percentage
Departmental heads	13
Departmental managers	41
Foreman & others	46

Table 2. Details of Informants

5. DATA ANALYSIS

Flexibility of production system is characterized with eight dimensions and quality of product six. Various dimensions of flexibility (FLX) and quality (QUA) considered in this study are: machine (MC), material handling (MH), volume (VO), process (PR), part mix (PD), routing (RO), expansion (EX) and operation (OP) flexibility. Quality has six parameters: performance (PE), feature (FE), reliability (RE), conformance (CO), durability (DU) and serviceability (SE). Data pertaining to each of these dimensions are collected from the group of experts. All the dimension of flexibility and quality possess Cronbach alpha values more than 0.6, which is the boundary for reliability. Path models relating flexibility and quality to observe the effect of one upon another are developed. In a multi-product manufacturing firm, there exist four situations of production system / machine-product combinations: many machines produces many product types (M-M-M-P), many machines produce one product type (M-M-1-P), one machine produces one product type (1-M-1-P) and one machine produces many product types (1-M-M-P). Path diagrams relating flexibility and quality are developed using AMOS software package. The details of the model and the corresponding path values are explained in the following subsections.

5.1 M-M-M-P production system

In this category of production system, there are finite numbers of machines in series producing finite number of part/products. The hypothesized relationship between FLX and QUA is shown in Fig. 1. The coefficients indicating the association between the variables of flexibility and quality are provided in Table 3. From the *p*-values, it is concluded that some of the relationships are quite significant (bold entries), while other relationships although they exist are statistically insignificant at 95% confidence interval.

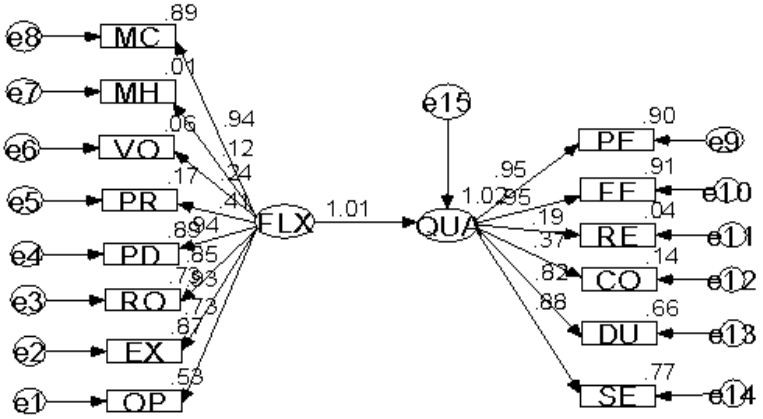

Fig. 1. Path diagram relating flexibility and quality

	Estimation	*Std. error*	*p-value*
QUA-FLX	1.01	0.125	*0.001*
CO-QUA	0.37	0.092	*0.025*
DU-QUA	0.81	0.065	*0.007*
SE-QUA	0.87	0.121	*0.006*
RE-QUA	0.19	0.025	*0.231*
FE-QUA	0.95	0.113	*0.003*
PE-QUA	0.95	0.066	*0.102*
PD-FLX	0.94	0.105	*0.003*
PR-FLX	0.4	0.125	*0.025*
RO-FLX	0.85	0.032	*0.011*
EX-FLX	0.93	0.21	*0.003*
OP-FLX	0.72	0.107	*0.015*
VO-FLX	0.24	0.182	*0.192*
MH-FLX	0.11	0.223	*0.257*
MC-FLX	0.94	0.102	*0.003*

Table 3. Path estimates of M-M-M-P system

In *M-M-M-P* model, dimensions such as part mix, process, routing, expansion, operation and machine flexibility affects significantly the system flexibility. Feature, serviceability, durability and conformance factors significantly affect part quality. The error values for all the variables are within the acceptable range, indicating that a good amount of variance of these variables is explained through the model.

5.2 M-M-1-P production system

In this category, path diagram (as in Fig. 1) is drawn whose path coefficients associating the variables of flexibility and quality are provided in Table 4. In *M-M-1-P* model, it is observed that process, routing, operation, volume and machine flexibility significantly affects system flexibility whereas performance, feature, serviceability and conformance factors significantly affect product quality.

Parameter	*Estimation*	*Std. Error*	*p-value*
QUA-FLX	1.12	0.098	*0.002*
CO-QUA	0.45	0.048	*0.025*
DU-QUA	0.05	0.063	*0.762*
SE-QUA	0.66	0.123	*0.021*
RE-QUA	0.14	0.078	*0.321*
FE-QUA	0.44	0.086	*0.025*
PE-QUA	0.56	0.046	*0.022*
PD-FLX	0.74	0.094	*0.026*
PR-FLX	0.41	0.084	*0.025*
RO-FLX	0.84	0.106	*0.016*
EX-FLX	0.14	0.097	*0.411*
OP-FLX	0.72	0.102	*0.018*
VO-FLX	0.91	0.112	*0.005*
MH-FLX	0.1	0.225	*0.501*
MC-FLX	0.83	0.078	*0.015*

Table 4. Path estimates of M-M-1-P system

5.3 1-M-1-P production system

Relationship between flexibility and quality is modelled using a path diagram (as in Fig. 1) where one machine produces one particular type of part/product. Path coefficients are provided in Table 5. From *1-M-1-P* model, it is observed that process, routing, operation, and volume flexibility significantly affects system flexibility whereas performance, feature, durability and conformance factors significantly affect product quality.

Parameter	*Estimation*	*Std. error*	*p-value*
QUA-FLX	1.03	0.173	*0.003*
CO-QUA	0.5	0.102	*0.022*
DU-QUA	0.82	0.196	*0.011*
SE-QUA	0.19	0.125	*0.317*
RE-QUA	0.12	0.107	*0.352*
FE-QUA	0.7	0.06	*0.015*
PE-QUA	0.67	0.272	*0.023*
PD-FLX	0.59	0.113	*0.026*
PR-FLX	0.37	0.108	*0.025*
RO-FLX	0.91	0.242	*0.003*
EX-FLX	0.63	0.051	*0.026*
OP-FLX	0.86	0.121	*0.012*
VO-FLX	0.8	0.098	*0.011*
MH-FLX	0.25	0.221	*0.195*
MC-FLX	0.43	0.134	*0.051*

Table 5. Path estimates of 1-M-1-P system

5.4 1-M-M-P production system

The relationship between flexibility and quality is found out with the help of a path diagram (as in fig. 1) where one particular machine produces variety of part types. Path coefficients are provided in Table 6. In *1-M-M-P model*, it is seen that dimensions such as part mix, routing, and operation flexibility significantly affects system flexibility whereas performance, feature, durability, serviceability and conformance factors significantly affects part quality.

Parameter	*Estimation*	*Std. error*	*p-value*
QUA-	0.93	0.109	*0.003*
CO-QUA	0.41	0.281	*0.025*
DU-QUA	0.84	0.056	*0.011*
SE-QUA	0.98	0.045	*0.001*
RE-QUA	0.14	0.215	*0.395*
FE-QUA	0.78	0.054	*0.017*
PE-QUA	0.95	0.074	*0.002*
PD-FLX	0.79	0.165	*0.017*
PR-FLX	0.28	0.198	*0.128*
RO-FLX	0.76	0.121	*0.023*
EX-FLX	0.73	0.124	*0.026*
OP-FLX	0.71	0.128	*0.024*
VO-FLX	0.84	0.106	*0.026*
MH-FLX	0.15	0.224	*0.375*
MC-FLX	0.34	0.201	*0.212*

Table 6. Path estimates of 1-M-M-P system

All the four estimated models show a good fit with the data. The ratio of χ^2 to dof is within 3.0. Fit indices for the models corresponding to all the combinations are provided in Table 7. For all the models, goodness-of-fit index (GFI) is greater than 0.9 indicates that the model is saturated due to hypothesized relationships between the parameters. Other fit indices for all the models are greater than 0.9. Achieved normed-fit-index (NFI) is within acceptable range. The values in table indicate fair amount of model fit, thus obtaining a satisfactory result.

Model	$\chi 2$	*dof*	*GFI*	*NFI*	*RMSEA*
1-M-1-P	226	76	.925	.902	.057
M-M-1-P	218	76	.933	.917	.069
1-M- M-P	169	76	.901	.936	.072
M-M-M-P	138	76	.924	.928	.068

Table 7. Fit indices for the relationships between flexibility and quality

6. RESULTS AND DISCUSSION

•In *M-M-M-P* system - part mix, routing, process, expansion, operation, and machine flexibility make significant contributions (at 0.05 confidence interval, *p*-value is less than 0.025) to system flexibility, i.e., increase in coefficients of these dimensions increases the system flexibility and product quality. Material handling and volume flexibility are not making significant contributions. Quality factors such as

conformance, durability, feature, and serviceability make significant contributions to product quality i.e., increase in coefficients of these functions increases quality of product. However, performance and reliability do not have any significant contribution to quality. Thus, flexibility bears a significant relationship with quality.

•In *M-M-1-P* system - part mix, process, routing, operation, volume, and machine flexibility make significant contributions to system flexibility. Material handling and expansion flexibility are not making significant contributions. Conformance, serviceability, and feature of the part make significant contributions to product quality. However, dimensions such as performance, durability and reliability do not have any significant contribution to quality. There exists a significant relationship between flexibility and quality.

•In *1-M-1-P* system - process, routing, operation, and volume flexibility make significant contributions to system flexibility. Machine, material handling, expansion and part mix flexibility are not making significant contributions. Conformance, durability, and feature make significant contributions to product quality. However, performance, serviceability and reliability do not have any significant contribution to quality. There exists a significant relationship between flexibility and quality.

•In *1-M-M-P* system - routing, process, and operation flexibility make significant contributions to system flexibility. Machine, material handling, expansion, part mix and volume flexibility are not making significant contributions. Conformance, durability, feature, and performance of the part make significant contributions to product quality. However, serviceability and reliability do not make any significant contribution to quality. Flexibility bears a significant relationship with product quality.

Results of path diagrams indicate that increase in certain flexibility dimension increases quality. Greater the path coefficient value better is the relationship/effect. There are specific flexibility dimensions which do not significantly affect product quality. In specific terms, increase in process, routing and operation flexibility increases the product quality. Moreover, material-handling flexibility has no effect on product quality.

7. CONCLUSIONS

Although the models developed in this research are tested in multi-product manufacturing firms, it is recommended that the firms practicing mass production may also find these models applicable. There exists a positive relationship between flexibility and quality and thus system flexibility contribute directly and indirectly to product quality. This research developed educational materials for use in academic and professional training purposes. Developing greater awareness and competence among manufacturing professionals is a critical step toward improving product quality and the case study approach helps achieve that goal. The findings suggest that the linkage between flexibility and quality is more complex than suggested by previous research and thus emphasize the need for additional studies using multivariate research designs.

It would be an important research direction to examine the impact of other dimensions, such as, worker flexibility, material flexibility, market flexibility, supplier flexibility on quality. Empirical research using a survey questionnaire would allow the researchers to test the generalisability of the practices, as well as identify any industry or regional differences.

8. REFERENCES

[1] Parka,J., Leea,J., Leea,H., Truex,D. Exploring the impact of communication effectiveness on service quality, trust and relationship commitment in IT services, Int. Jou. of Information Management, vol. 32, pp. 459- 468 (2012).

[2] Chan, F.T.S., Bhagwat, R. and Wadhwa, S. 'Flexibility performance: Taguchi's method study of physical system and operating control parameters of FMS', *Robotics and Computer Integrated Manufacturing*, vol. 23, no. 1, pp.25-37 (2007) .

[3] Gunasekaran, A., Martikainen, T. and Olli, P.Y. 'FMS: an investigation for research and applications', *European Jou. of Operations Research*, vol. 66, no. 1, pp.1–26 (1993).

[4] Lee, H., Kim, C. Benchmarking of service quality with data envelopment analysis, Expert Systems with Applications, 41, 3761–3768 (2014).

[5] Saleh, B., Hacker, M. and Randhawa, S. 'Factors in capital decisions involving advanced manufacturing technologies', *Int. Jou. of Operations and Production Management*, vol. 21, no. 10, pp.1265–1288 (2001).

[6] Park, C.S. and Son, Y.K 'An economic evaluation model for advanced manufacturing systems', *The Engineering Economist*, vol. 34, no. 1, pp.1–26 (1988) .

[7] Georgoulias, K., Papakostas, N., Chryssolouris, G., Stanev, S., Krappe, H. and Ovtcharova, J. 'Evaluation of flexibility for the effective change management of manufacturing organizations', *Robotics and Computer Integrated Manufacturing*, vol. 25, no. 6, pp. 888–893 (2009).

[8] Jitpaiboon, T. and Rao, S.S 'A meta-analysis of quality measures in manufacturing systems', *Int. Jou. of Quality and Reliability Management*, vol. 24, no. 1, pp.78–102 (2007).

[9] Chang, S.C., Yang, C.L., Cheng, H.C. and Sheu, C. 'Manufacturing flexibility and business strategy – an empirical study of SMEs', *Int.*

Jou. of Production Economics, vol. 83, no. 1, pp.13–26 (2003).
[10] Sethi, A. and Sethi, S. 'Flexibility in manufacturing: a survey', *Int. Jou. of Flexible Manufacturing Systems*, vol. 2, no. 4, pp. 289–328 (1990).
[11] Toni, A.D. and Tonicha, S. 'Performance measurement systems, models, characteristics, and measures', *Int. Jou. of Operations & Production Management*, vol. 21, nos. 1/2, pp.46–60 (2001).
[12] Nayak, N.C. and Ray, P.K. 'Flexibility and performance relationships: evidence from Indian bearing manufacturing firm', *Int. Jou. of Modelling in Operations Management*, Vol. 1, No. 1, pp.67–82 (2010).
[13] Hsua,T.H, Hungb,L.C, Tangc,J.W. A hybrid ANP evaluation model for electronic service quality, Applied Soft Computing, 12, pp. 72–81 (2012).
[14] Thai, V.V., Tay, W.J., Tan, R. Lai, A. Defining Service Quality in Tramp Shipping: Conceptual Model and Empirical Evidence,The Asian journal of shipping & Logistics, vol. 30, no. 1, pp. 1-29 (2014).
[15] Tsenga,M.L., Chena,Y.H. Gengb,Y. Integrated model of hot spring service quality perceptions under uncertainty, Applied Soft Computing, vol. 12, pp. 2352–2361 (2012).
[16] Yee, R.W.Y , Yeung,A.C.L., Cheng,T.C.E., An empirical study of employee loyalty, service quality and firm performance in the service industry, Int. Jou. Of Production Economics, vol. 124, pp. 109–120 (2010).
[17] Dangayach, G.S. and Deshmukh, S.G. 'Advanced manufacturing technologies: evidences from Indian automobile companies', *Int. Jou. of Manufacturing Technology and Management*, vol. 6, no. 5, pp. 426–433 (2004).
[18] Li, J. and Huang, N. 'Quality evaluation in flexible manufacturing systems: a Markovian approach', *Mathematical Problems in Engineering*, vol. 2, no. 1, pp. 124–148 (2007).
[19] Garg, S., Vrat, P., Kanda, A. and Dua, B.B. 'Aspects of flexibility and quality in Indian manufacturing management practices: a survey', *Int. Jou. of Manufacturing Technology and Management*, vol. 5, nos. 5/6, pp. 443–458 (2003).
[20] Calabrese,A. Flexibility and service quality: A necessary trade-off?, Int. Jou. of Production Economics, vol. 135, pp. 800–812 (2012).
[21] Stiglingh, M. Service quality framework for the South African Revenue Service from the perspective of the tax practitioner, Public Relations Review, vol. 40, pp. 240–250 (2014).

Authors:

Ph D Narayan C. Nayak, Mechanical Engineering Department, Indira Gandhi Institute of Technology, Sarang, Odisha, India. Mail ID: nayak.iem@gmail.com

Ph D Pradip. K. Ray, Industrial Engineering & Management Department, Indian Institute of Technology, Kharagpur, Kolkata, India. Mail ID: pkr@vgsom.iitkgp.ernet.in

Journal of Production Engineering
Vol.18 No.1
JPE (2015) Vol.18 (1) Preliminary Note
Ocampo, L., Carreon, R., Carvajal, J.A., Galagar, K.J., Gialolo, D.M., Gulayan, M., Indig, D., Nuñez, D.M., Tagsip, W.C., Vallecera, J.M., Villegas, Z.

MATRIX-BASED LIFE CYCLE ASSESSMENT (MLCA) ON POLYSTYRENE AND RECYCLED PAPER EGG TRAY PACKAGING

Received: 26 April 2015 / Accepted: 30 May 2015

Abstract: *Product packaging has been drawing interests in domain literature brought about by its economic, social and environmental contexts. Recently, there has been increasing number of works focusing on food product packaging due to its higher production volumes. Much of these interests focus on the design and selection of materials that address issues on sustainability. With this, life cycle assessment (LCA) is widely regarded as a tool that quantifies the environmental impacts of product systems. This paper presents a case study of a matrix-based LCA on the comparisons of polystyrene and recycled paper egg tray. Results of the LCA are reported in this work.*
Key words: *matrix-based LCA, egg tray, packaging*

Matrična procena životnog ciklusa polistirena i recikliranog kartonskog pakovanja za jaja. *Pakovanje proizvoda privlači interes u domenu literature zbog svog ekonomskog, socijalnog i ekološkog konteksta. U zadnje vreme se javlja sve više radova usmerenih na pakovanje pojedinih proizvoda zbog povećanja njihove proizvodnje. Mnogo tema se orijentišu na projektovanje i odabir materijala koji zadovoljavaju uslov održivosti. Procena životnog ciklusa (LCA) je opšte prihvaćen alat koji kvantifikuje ekološki uticaj proizvodnog sistema. U ovom radu je predstavljena studija poređenja matrične procene životnog ciklusa polistirena i recikliranog kartonskog pakovanja za jaja. Rezultati procene su navedeni u ovom radu.*
Ključne reči: *matrična procena životnog ciklusa, karton za jaja, pakovanje*

1. INTRODUCTION

Product packaging has been an interesting topic in domain literature in the context of economic, social and environmental issues [1]. From the standpoint of sustainability in general and sustainable manufacturing in particular [2], product packaging must adopt environmentally-conscious design with materials and processes that conform to sustainability. With this, life cycle assessment (LCA) provides a quantitative and logical approach in providing salient inputs to the design process. This has been a motivating research area which is evidenced by a number of works dedicated to this problem domain, e.g. Sanyé-Mengual et al. [3], Madivala et al. [4] among others. This is inherently due to the presence of product packaging in all industrial sectors and marketplace [3]. A general overview of product packaging in the context of LCA can be found in Lee and Xu [5].

Among various areas in product packaging, food product packaging draws interests in literature. For instance, Levi et al. [6] presented a comparative LCA of disposable and reusable packaging in distributing fruits and vegetables. Siracusa et al. [7] conducted an LCA on multilayer polymer bag for food packaging and preservation. Raheem [8] provided an overview on the applications of plastics and paper as food packaging materials. Arvanitoyannisab and Bosneab [9] presented status and perspectives on recycling of polymeric materials for food packaging. The highly-cited reference for food packaging is the work of Robertson [10] and an excellent exposition of the various issues in this domain including its environmental issues is done by Marsh and Bugusu [11].

This paper presents a matrix-based LCA on the comparison between polystyrene egg tray and recycled paper egg tray used in egg packaging. This paper embarks on the early work of Zabaniotou and Kassidi [12]. The main departure of this work is the application of the matrix-based framework originally developed by Heijungs and Suh [13]. In 2002, an estimated 53.4 million tonnes of eggs were produced and this figure eventually grows steeper as significant growth in the use of egg products was observed [14]. The Netherlands and the U.S. are the largest egg exporting countries and Germany is also the largest importer of eggs. Thus packaging of this product is important as well as the environmental issues associated with this packaging. The polystyrene, popularly known as styrofoam, egg tray and recycled paper egg tray were considered as the widely used egg packaging [12]. Since global awareness on environmental issues is increasing sharply over the last two decades following the Brundtland report [15], reuse and disposal of products have been important issues in literature. This study aims to determine, evaluate and compare the environmental burdens and impacts associated with each product packaging using a matrix-based LCA with an attempt to determine which packaging is more environmentally-benign. The contribution of this work lies in applying matrix-based LCA on the comparison of two egg packaging materials.

2. MATRIX-BASED LIFE CYCLE ASSESSMENT

2.1 Life Cycle Assessment (LCA)

LCA is a process for evaluating the environmental impacts associated with a product or process by identifying and quantifying energy and materials used and wastes released to the environment, assessing the impact on the environment of those energy and material uses and waste releases, and identifying ways for reducing the environmental impacts [16]. By definition, LCA covers the entire life cycle of a product or a system which is from extraction of raw materials, manufacturing, distribution and use, final disposal. This is termed as a cradle to grave analysis. In general, LCA is capable of identifying opportunities to improve the environmental aspects of products at various points in their life cycle, supporting decision-making in strategic planning, priority setting, product or process design or redesign, assisting selection of relevant indicators of environmental performance, and in marketing of products [17].

LCA as a methodology is widely used in environmental assessment and the specific activities in the methodology have been agreed by scholars and practitioners in the field with particular focus on the international standards for LCA – ISO 14040-14043. [17-19]. The general framework of LCA is composed of four phases: goal and scope definition, inventory analysis, impact assessment, and interpretation [20-21] and the International Standard ISO 14040 series [17], as shown in Figure 1.

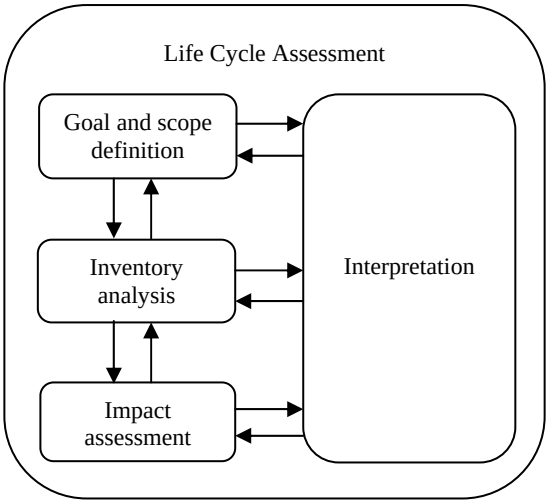

Fig. 1. Phases of life cycle assessment [17]

2.1.1 Goal and Scope Definition

The goal and scope of an LCA study shall be clearly defined which must be consistent with the intended application [17]. The goal of an LCA study must clearly state the intended application, the reasons for carrying out such study and its intended audience. In defining the scope of an LCA study, the functional unit, the system boundary and data requirements must be clearly described. As an iterative methodology, LCA allows modifications of the scope of the study while the study is being conducted as more additional information is obtained.

2.1.2 Life Cycle Inventory (LCI)

Life cycle inventory analysis involves data collection and calculation procedures to quantify relevant inputs and outputs of the product system. Inventoriable items of the LCA study must be declared in the goal and scope definition. These items may include the use of resources and emissions to land, water and air associated with the system. Likewise, inventory analysis is iterative. Thus, as data are collected and more is known about the system, new data requirements or limitations may be identified so that the goals of the study will still be met. Oftentimes, issues may be identified that require revisions of the goal or scope of the study.

2.1.3 Life Cycle Impact Assessment (LCIA)

This phase of LCA is aimed at evaluating the significance of potential environmental impacts using the results of the LCI. The impact assessment phase may include the following: assigning of inventory data to impact categories popularly known as classification, modeling of inventory data within impact categories which is known as characterization and possible aggregation of results.

2.1.4 Interpretation

Interpretation is the phase of LCA in which the findings from the inventory analysis and the impact assessment are combined together consistent with the goal and scope definition in order to reach conclusions and recommendations.

2.2 Matrix-based LCA

The matrix-based LCIA method was first introduced to LCI computation by Heijungs [22]. This method utilizes a system of linear equations to solve an inventory problem. Arranging the economic and environmental flows in matrix forms, the final cumulative environmental loads are calculated by some matrix algebra operations. Later, Heijungs developed the detailed computational methods were developed by Heijungs and Suh [13] and is considered the fundamental textbook of matrix-based LCA. A set of definitions of the matrix-based LCI and LCIA model is provided in this section which is lifted from the discussion of Heijungs and Tan [23]. More detailed discussion can be found in Heijungs and Suh [13].

Definition 1. The flow of economic goods within the life cycle system is balanced such that the net system output corresponds to the functional unit

$$As = f \tag{1}$$

where A is the technology matrix, s is the scaling vector, and f is the functional unit vector. The form of (1) can be written as

$$s = A^{-1} f \tag{2}$$

provided that A is invertible and A^{-1} exists.

Definition 2. The equation for balances of flows of resources and emissions of the life cycle is

$$Bs = g \tag{3}$$

where B is the intervention matrix and g is the inventory vector. The relationships provided in (2) and (3) may then be combined to give the generalized LCI model

$$g = BA^{-1}f \quad (4)$$

Every column in A or B represents a process within the life cycle system, each with a corresponding scaling vector s. The elements of f and g correspond to specific economic goods or environmental streams. Conventionally, positive values in A, B, f, or g represent outflows, while negative values denote inflows [13].

Definition 3. The environmental impact vector h is defined as

$$h = Qg \quad (5)$$

where Q is the characterization matrix that describes equivalence of $g_i \in g$ to $h_k \in h$. Combining (4) and (5) gives

$$h = QBA^{-1}f \quad (6).$$

Definition 4. If weighting of environmental impacts is applicable and logical, then the total environmental impact EI can be written as

$$EI = w^T h \quad (7)$$

where w^T is obtained by some prioritization method.

3. GOAL AND SCOPE DEFINITION

Shown in Figure 2 is the life cycle of polystyrene egg tray considered in this study. After several processes, the egg trays will be shaped and a total of 50,000 Polystyrene egg trays will be produced ready for packing and shipping to their specific destinations. The egg trays will be used by different consumers and is disposed afterwards.

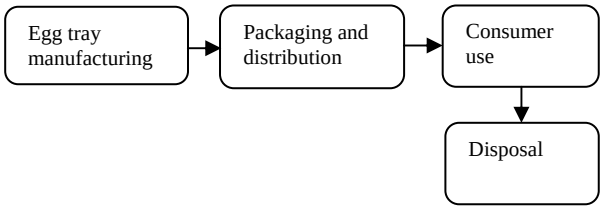

Fig. 2. Polystyrene egg tray and recycled paper egg tray processes

The manufacturing process of recycled waste paper will undergo on several processes using the pulping and egg tray maker machine. The water used in the process of making of trays is recycled thus no water is put into waste. A Dissolved Air Floatation is the one that treats and clarifies the water that will be used throughout the process. The manufacturing process ends in drying the formed egg tray. Afterwards, the egg trays will be packed and are ready for delivery at specific destinations. The trays will be delivered to different consumers. After the egg trays are used, these will be disposed.

In this study, the functional unit was based from the previous gathered date given 50,000 egg trays of six eggs each. Closed egg trays have been considered. In fifty thousand egg trays require for their production, a quantity of 680 kg of waste Polystyrene and 998 kg waste recycled paper, respectively after consumer use them. The chosen system boundary for this study is "gate-to-grave", which encompasses from the manufacturing to the disposal process of both Polystyrene and Recycled paper egg trays. Through this system boundary, this can help in the identifying the different energy, materials and releases of the two products through their life stages which can be candidates of environmental impact and purpose in further studies.

Table 1. Polystyrene egg tray list of economic and environmental flows

Process	Description	Economic Inflows	Economic Outflows	Environmental inflows	Environmental outflows
1	Egg Tray Manufacturing	0.45 kg Iron Mine 0.22 kg $CaCO_3$ 1.6 kg Bauxite 12 kg Mine Salt 718 m^3 fuel 715 m^3 Natural Gas	680 kg Egg tray	71298 MJ Energy consumption	3.44 kg CH_4 32.67 kg NO_x 2952 kg CO_2 0.011 kg N_2O 94.95 kg SO_x 1.959 kg CO
2	Packaging and Distributing	680 kg egg tray 866.66 kWh	680 kg packed egg tray		682 kg CO_2
3	Consumer Usage	680 kg packed egg tray	680 kg waste egg tray		-
4	Disposal	680 kg waste egg tray 51 kWh	680 kg solid waste		40.188 kg CO_2

The assumptions and limitations of this study are: (1) accidental pollution and environmental impacts caused by personnel at the site of production and delivery are neglected, (2) both egg packaging products produced are all used and disposed throughout the life cycle, (3) the use of diesel (combustion) and fuel (combustion) in truck deliveries were focused on the Carbon dioxide (CO2), Mono-nitrogen Oxides (NOx), and Carbon Monoxide (CO) emissions alone, and (4) all egg trays were all utilized by the consumer, thus the waste egg tray are the same quantity as of the produced egg trays on both life cycles

Table 2. Recycled paper egg tray list of economic and environmental flows

Process	Description	Economic Inflows	Economic Outflows	Environmental inflows	Environmental outflows
1	Egg Tray Manufacturing	1500 kg Recycled Paper	680 kg Egg tray	71298 MJ Energy consumption	3.44 kg CH_4 32.67 kg NO_x 2952 kg CO_2 0.011 kg N_2O 94.95 kg SO_x 1.959 kg CO
2	Packaging and Distributing	0.8kg Dye Solution	680 kg packed egg tray		682 kg CO_2
3	Consumer Usage	0.442kg Anti-Foaming	680 kg waste egg tray		-
4	Disposal	20kg Paraffin Solution	680 kg solid waste		40.188 kg CO_2

Table 3. Environmental impact categories: characterization

Impact category	CO_2	NO_x	CH_4	SO_x	CO	N_2O	Energy
Global Warming Potential	1 CO_2eq/kg	0	35 CO_2eq/kg	0	0	0	0
Acidification Potential	0	0.70 NO_x eq/kg	0	0	0	0	0
Energy Consumption	0	0	0	0	0	0	1 MJ

4. LIFE CYCLE INVENTORY

The matrices A and B together with vectors f and s for both type of egg trays are shown in Appendix A. Only vectors g are shown in this section. Using equations (1) to (4), amount of each inventory item is obtained.

$$g_{polystyrene} = \begin{pmatrix} CO_2 \\ NO_x \\ CH_4 \\ SO_x \\ CO \\ N_2O \\ Energy \end{pmatrix} = \begin{pmatrix} 3674.19 \\ 32.67 \\ 3.44 \\ 94.95 \\ 1.96 \\ 0.011 \\ -71298 \end{pmatrix}$$

$$g_{recycledpaper} = \begin{pmatrix} CO_2 \\ NO_x \\ CH_4 \\ SO_x \\ CO \\ N_2O \\ Energy \end{pmatrix} = \begin{pmatrix} 2513.25 \\ 4.16 \\ 1.55 \\ 5.85 \\ 0.92 \\ 0.016 \\ -25088 \end{pmatrix}$$

Based on the calculated values, g g1 to g6 are all positive since they are the emissions of the whole life cycle. The negative value g7 represents the use of the energy.

5. LIFE CYCLE IMPACT ASSESSMENT

Vector Q is given by

Q	CO2	NO_x	CH4	SO_x	CO	N2O	Energy
GWP	1	0	35	0	0	0	0
AP	0	0.7	0	0	0	0	0
Energy consumption	0	0	0	0	0	0	1

For h of polydstyrene egg trays,

	h
h1	3794.588
h2	22.869
h3	-71298

For h of recycled paper egg trays,

	h
h1	2567.5
h2	2.90934
h3	-25088

6. INTERPRETATION

Based on the results, the inventory indexes of Polystyrene Egg Tray on CO2, NOx, CH4, SOx, CO and N2O accumulated the greater values than the recycled paper egg tray life cycle. It can be concluded that the processes or stages through the Polystyrene Egg tray life cycles emits greater amount of harmful chemicals in the air than of the recycled paper egg tray processes. The obtained result for GWP got the highest value among the three impact categories being focused. It matches with the graph for emissions that CO2 has the highest value compared to other emissions.

7. CONCLUSION

The application of Life Cycle Assessment Procedure was made possible through the use of Matrix-Based method in assessing Life Cycle Assessment upon comparing the two products. The results obtained do not provide a clear-cut answer in defining the eco-friendly product but the goals were answered and compared using this method. The

obtained results have revealed that the Polystyrene Egg Tray, during its life cycle has higher environmental impacts than the recycled paper one. The Polystyrene Egg Tray in all of the degrees emits more due to its manufacturing inflows and outflows. The conclusion and data of this study can be used as a reference and database for further study. This study can also serve as a comparison purposes on both products. This study can only be used by the Polystyrene and Recycled paper egg tray manufacturers and those who transport raw materials from a supplier wherein transportation is needed. The machines used in the manufacturing until the disposal stage of both products are automatic machines.

8. REFERENCES

[1] Verghese, K., Crossin, E., Jollands, M.: Packaging materials, In: Verghese, K., Lewis, H., Fitzpatrick, L.: Packaging for sustainability, Springer, London, 2012.

[2] Joung, C.B., Carrell, J., Sarkar, P., Feng, S.C.: Categorization of indicators for sustainable manufacturing, Ecological Indicators, Vol. 24, pp. 148-157, 2013.

[3] Sanyé-Mengual, E., Lozano, R.G., Oliver-Solà, J., Gasol, C.M., Rieradevall, J.: Eco-design and product carbon footprint use in the packaging sector, In: Subramanian, S.M.: Assessment of carbon footprint in different industrial sectors, Vol. 1, EcoProduction 2014, Springer, Singapore, pp. 221-245.

[4] Madivala, S., Aurasa, R., Singha, S.P., Narayanb, R.: Assessment of the environmental profile of PLA, PET and PS clamshell containers using LCA methodology, Journal of Cleaner Production, Vol. 17, No. 13, pp. 1183–1194, 2009.

[5] Lee, S.G., Xu, X.: Design for the environment: life cycle assessment and sustainable packaging issues, International Journal of Environmental Technology and Management, Vol. 5, No. 1, pp. 14-41, 2005.

[6] Levi, M., Cortesi, S., Vezzoli, C., Salvia, G.: A comparative life cycle assessment of disposable and reusable packaging for the distribution of Italian fruit and vegetables, Packaging Technology and Science, Vol. 24, No. 7, pp. 387–400, 2011.

[7] Siracusaa, V., Ingraob, C., Giudicec, A.L., Mbohwac, C., Rosad, M.D.: Environmental assessment of a multilayer polymer bag for food packaging and preservation: An LCA approach, Food Research International, Vol. 62, pp. 151–161, 2014.

[8] Raheem, D.: Application of plastics and paper as food packaging materials – an overview, Emirates Journal Food Agriculture, Vol. 25, No. 3, pp. 177-188, 2012.

[9] Arvanitoyannisab, I.S., Bosneab, L.A.: Recycling of polymeric materials used for food packaging: current status and perspectives, Food Reviews International, Vol. 17, No. 3, pp. 291-346, 2001.

[10] Robertson, G.L.: Food packaging: principles and practice, 3rd ed., CRC Press Taylor & Francis Group, Boca Rotan, Florida, 2014.

[11] Marsh, K., Bugusu, B.: Food packaging—roles, materials, and environmental issues, Journal of Food Science, Vol. 72, No. 3, pp. 39–55, 2007.

[12] Zabaniotou, A., Kassidi, E.: Life cycle assessment applied to egg packaging made from polystyrene and recycled paper, Journal of Cleaner Production, Vol. 11, No. 5, pp. 549–559, 2003.

[13] Heijungs, R., Suh, S.: The computational structure of life cycle assessment, Kluwer, Dordrecht, 2002.

[14] International Egg Commission: Accessed April 20, 2015, https://www.internationalegg.com/corporate/eggindustry/details.asp?id=18

[15] Brundtland, G.H.: Report of the world commission on environment and development: our common future, Oxfor University Press, Oxford, U.K., 1987.

[16] Perriman, R.J.: A summary of SETAC guidelines for life cycle assessment, Journal of Cleaner Production, Vol. 1, No. 3-4, pp. 209-212, 1993.

[17] ISO 14040, Environmental management – Life cycle assessment – Principles and framework, International Standard Organization, 1997.

[18] ISO 14041, Environmental management – Life cycle assessment – Goal and scope definition and life cycle inventory analysis, International Standard Organization, 1998.

[19] ISO 14043, Environmental management – Life cycle assessment – Life cycle interpretation, International Standardization Organization, Geneva, 2000.

[20] A Technical Framework for Life-Cycle Assessment, SETAC Foundation for Environmental Education, Florida, 1991.

[21] Guidelines for Life-Cycle Assessment: A Code of Practice, SETAC Foundation for Environmental Education, Florida, 1993.

[22] Heijungs, R.: A generic method for the identification of options for cleaner products, Ecological Economics, Vol. 10, No. 1, pp. 69-81, 1994.

[23] Heijungs, R., Tan, R.: Rigorous proof of fuzzy error propagation with matrix-based LCI, International Journal of Life Cycle Assessment, Vol. 15, No. 9, pp. 1014-1019, 2010.

Authors: **Dr. Lanndon Ocampo, Lecturer,** University of San Carlos, Department of Mechanical Engineering, Cebu City, 6000 Cebu, Philippines, Phone.: +63 932 5101510
E-mail: don_leafriser@yahoo.com
Carreon, R., Carvajal, J.A., Galagar, K.J., Gialolo, D.M., Gulayan, M., Indig, D., Nuñez, D.M., Tagsip, W.C., Vallecera, J.M., Villegas, Z., Undergraduate Students, University of San Carlos, Department of Industrial Engineering, Cebu City, 6000 Cebu, Philippines

INSTRUCTIONS FOR CONTRIBUTORS

No. of pages:	4 DIN A4 pages
Margins:	left: 2,5 cm
	right: 2 cm
	top: 2 cm
	bottom: 2 cm
Font:	Times New Roman
Title:	Bold 12, capitals
Abstract:	Italic 10
Headings:	Bold 10, capitals
Subheadings:	Bold 10, small letters
Text:	Regular 10
Columns:	Equal column width with 0,7 cm spacing
Spacing:	Single line spacing
Formulae:	Centered and numerated from 1 in ascending order. Equations must be typed in Equation Editor, with following settings: Style>Math – Times New Roman Size>Full 12pt, Subscript/Superscript 7pt, Symbol 18 pt
Figures:	High quality, numerated from 1 in ascending order (e.g.: Fig.1, Fig. 2 etc.); Figures and tables can spread over both two columns, please avoid photographs and color prints
Tables:	Numerated from 1 in ascending order (e.g..: Tab. 1, Tab. 2, etc.)
References:	Numerated from [1] in ascending order; cited papers should be marked by the number from the reference list (e.g. [1], [2, 3] ...)
Submission:	**Papers prepared in MS Word format should be e-mailed to: pkovac@uns.ac.rs, savkovic@uns.ac.rs**
Notice:	**Papers are to be printed in Journal of Production Engineering** Sample paper with detailed instructions can be found at: **http://www.jpe.ftn.uns.ac.rs/**

FOR MORE INFORMATION, PLEASE CONTACT:

Prof. Pavel Kovač, PhD, MEng.
Borislav Savković, *MSc. Assistant*
FACULTY OF TECHNICAL SCIENCES
Department for Production Engineering
Trg Dositeja Obradovica 6
21000 Novi Sad
Serbia
Tel.: (+381 21) 485 23 24; 485 23 20 ; 450 366;
Fax: (+381 21) 454 495
E-mail: pkovac@uns.ac.rs, savkovic@uns.ac.rs
http://www.jpe.ftn.uns.ac.rs/